ISSN 0021-9673

VOL. 673 NO. 1 JULY 1, 1994

JOURNAL OF CHROMATOGRAPHY A

INCLUDING ELECTROPHORESIS AND OTHER SEPARATION METHODS

ELSEVIER

JOURNAL OF CHROMATOGRAPHY A

INCLUDING ELECTROPHORESIS AND OTHER SEPARATION METHODS

Scope. The *Journal of Chromatography A* publishes papers on all aspects of **chromatography, electrophoresis** and related methods. Contributions consist mainly of research papers dealing with chromatographic theory, instrumental developments and their applications. In the *Symposium volumes*, which are under separate editorship, proceedings of symposia on chromatography, electrophoresis and related methods are published. *Journal of Chromatography B: Biomedical Applications* —This journal, which is under separate editorship, deals with the following aspects: developments in and applications of chromatographic and electrophoretic techniques related to clinical diagnosis or alterations during medical treatment; screening and profiling of body fluids or tissues related to the analysis of active substances and to metabolic disorders; drug level monitoring and pharmacokinetic studies; clinical toxicology; forensic medicine; veterinary medicine; occupational medicine; results from basic medical research with direct consequences in clinical practice.

Submission of Papers. The preferred medium of submission is on disk with accompanying manuscript (see *Electronic manuscripts* in the Instructions to Authors, which can be obtained from the publisher, Elsevier Science B.V., P.O. Box 330, 1000 AH Amsterdam, Netherlands). Manuscripts (in English; *four* copies are required) should be submitted to: Editorial Office of *Journal of Chromatography A*, P.O. Box 681, 1000 AR Amsterdam, Netherlands, Telefax (+31-20) 5862 304, or to: The Editor of *Journal of Chromatography B: Biomedical Applications*, P.O. Box 681, 1000 AR Amsterdam, Netherlands. Review articles are invited or proposed in writing to the Editors who welcome suggestions for subjects. An outline of the proposed review should first be forwarded to the Editors for preliminary discussion prior to preparation. Submission of an article is understood to imply that the article is original and unpublished and is not being considered for publication elsewhere. For copyright regulations, see below.

Publication information. *Journal of Chromatography A* (ISSN 0021-9673): for 1994 Vols. 652–682 are scheduled for publication. *Journal of Chromatography B: Biomedical Applications* (ISSN 0378-4347): for 1994 Vols. 652–662 are scheduled for publication. Subscription prices for *Journal of Chromatography A*, *Journal of Chromatography B: Biomedical Applications* or a combined subscription are available upon request from the publisher. Subscriptions are accepted on a prepaid basis only and are entered on a calendar year basis. Issues are sent by surface mail except to the following countries where air delivery via SAL is ensured: Argentina, Australia, Brazil, Canada, China, Hong Kong, India, Israel, Japan, Malaysia, Mexico, New Zealand, Pakistan, Singapore, South Africa, South Korea, Taiwan, Thailand, USA. For all other countries airmail rates are available upon request. Claims for missing issues must be made within six months of our publication (mailing) date. Please address all your requests regarding orders and subscription queries to: Elsevier Science B.V., Journal Department, P.O. Box 211, 1000 AE Amsterdam, Netherlands. Tel.: (+31-20) 5803 642; Fax: (+31-20) 5803 598. Customers in the USA and Canada wishing information on this and other Elsevier journals, please contact Journal Information Center, Elsevier Science Inc., 655 Avenue of the Americas, New York, NY 10010, USA, Tel. (+1-212) 633 3750, Telefax (+1-212) 633 3764.

Abstracts/Contents Lists published in Analytical Abstracts, Biochemical Abstracts, Biological Abstracts, Chemical Abstracts, Chemical Titles, Chromatography Abstracts, Current Awareness in Biological Sciences (CABS), Current Contents/Life Sciences, Current Contents/Physical, Chemical & Earth Sciences, Deep-Sea Research/Part B: Oceanographic Literature Review, Excerpta Medica, Index Medicus, Mass Spectrometry Bulletin, PASCAL-CNRS, Referativnyi Zhurnal, Research Alert and Science Citation Index.

US Mailing Notice. *Journal of Chromatography A* (ISSN 0021-9673) is published weekly (total 52 issues) by Elsevier Science B.V., (Sara Burgerhartstraat 25, P.O. Box 211, 1000 AE Amsterdam, Netherlands). Annual subscription price in the USA US$ 4994.00 (US$ price valid in North, Central and South America only) including air speed delivery. Second class postage paid at Jamaica, NY 11431. **USA POSTMASTERS**: Send address changes to *Journal of Chromatography A*, Publications Expediting, Inc., 200 Meacham Avenue, Elmont, NY 11003. Airfreight and mailing in the USA by Publications Expediting.

See inside back cover for Publication Schedule, Information for Authors and information on Advertisements.

0021-9673/94/$07.00

Printed in the Netherlands

CONTENTS

(Abstracts/Contents Lists published in Analytical Abstracts, Biochemical Abstracts, Biological Abstracts, Chemical Abstracts, Chemical Titles, Chromatography Abstracts, Current Awareness in Biological Sciences (CABS), Current Contents/Life Sciences, Current Contents/Physical, Chemical & Earth Sciences, Deep-Sea Research/Part B: Oceanographic Literature Review, Excerpta Medica, Index Medicus, Mass Spectrometry Bulletin, PASCAL-CNRS, Referativnyi Zhurnal, Research Alert and Science Citation Index)

REGULAR PAPERS

Column Liquid Chromatography

Gas Chromatography

Planar Chromatography

(Continued overleaf)

Electrophoresis

SHORT COMMUNICATIONS

Column Liquid Chromatography

JOURNAL OF CHROMATOGRAPHY A

VOL. 673 (1994)

JOURNAL OF CHROMATOGRAPHY A

INCLUDING ELECTROPHORESIS AND OTHER SEPARATION METHODS

ELSEVIER

Amsterdam – Lausanne – New York – Oxford – Shannon – Tokyo

0021-9673/94/$07.00

ELSEVIER

Journal of Chromatography A, 673 (1994) 1–10

JOURNAL OF CHROMATOGRAPHY A

Retention prediction for β-adrenergic blocking drugs in normal-phase liquid chromatography

T. Hamoir, D.L. Massart*

Vrije Universiteit Brussel, Pharmaceutical Institute, Laarbeeklaan 103, B-1090 Brussels, Belgium

(First received December 24th, 1993; revised manuscript received March 2nd, 1994)

Abstract

The slope–intercept and the convergence model were used for describing the normal-phase retention data for a set of β-adrenergic blocking drugs obtained on a cyanopropyl column using various proportions of hexane–2-propanol–0.1% propylamine as mobile phase. Moreover, a quantitative structure–retention relationship with log *P* as descriptor was derived. The normal-phase retention data were also found to be rather strongly correlated with the data obtained for the same β-adrenergic blocking drugs in reversed phase. This allowed to derive an equation for the prediction of normal-phase retention data from reversed-phase data and vice versa.

1. Introduction

Reversed-phase liquid chromatography (RPLC) is the most commonly used chromatographic mode. However, for some applications normal-phase liquid chromatography (NPLC) has been shown to be very useful, such as for group separations and the separation of isomeric compounds [1].

Several models have been proposed to explain the retention mechanism in normal phase. Scott and co-workers [2–5] have considered solute–mobile phase and solute–stationary phase interactions for silica gel. The Snyder–Soczewinski adsorption model is based on the displacement of solvent molecules from the column surface by solute molecules [6–11]. Another model considering hydrogen bonding and other interactions was proposed by Chang and co-workers [12,13] for an aminopropyl column. At present, the Snyder–Soczewinski model can be considered to be the most useful model for describing solute retention in NPLC. A critical review of the Scott–Kucera and the Snyder–Soczewinski model has been presented by Snyder and Poppe [14]. In general, these models introduce several physical parameters which, however, are unknown or very difficult to ascertain. This, of course, limits the practical application of these models for retention prediction purposes. For this reason, more empirical models have been developed. Jandera [15] as well as Cooper and Hurtubise [16] proposed a so-called slope–intercept relationship for predicting solute retention in normal-phase chromatography. Kowalska [17] developed an approach based on the quantification of the efficiency of intermolecular interactions among the components of the mobile phase.

For retention prediction in RPLC we recently proposed a quantitative structure–retention relationship [18] and a model based on the conver-

* Corresponding author.

0021-9673/94/$07.00
SSDI 0021-9673(94)00213-S

gence concept [19]. Both models relate the change in retention (log k') to the volume percentage of the organic modifier in the mobile phase, on the one hand, and the structure of the compound, reflected by the calculated log P value, on the other hand. These models were successfully applied for retention prediction of a heterogeneous set of acidic, basic and neutral compounds. The parameter log P, which reflects the hydrophobic–lipophilic character of a molecule, has been extensively used for investigating structure–retention relationships, generally in RPLC [20]. However, some studies have shown that retention data obtained in normal-phase thin-layer chromatography (NP-TLC) can also be correlated with log P values [21,22].

In this work the chromatographic behaviour of β-adrenergic blocking drugs on a cyanopropyl column is investigated. These compounds belong to a class of clinically important drugs, which are generally associated with poor chromatography. Good separations for basic compounds on such a column were obtained in the presence of 0.1–0.5% (v/v) propylamine in the mobile phase [23] and for this reason this tailing suppressor will be used in this study. Another important characteristic of this group is that it covers a wide range in polarity, which is necessary to investigate the usefulness of log P for retention prediction purposes in NPLC.

The aim of this work is firstly to investigate the validity of the slope–intercept and the convergence model and afterwards to derive a quantitative structure–retention relationship (QSRR) using the descriptor log P in NPLC. Secondly, we will compare the retention data obtained for the β-adrenergic blocking drugs in NPLC with the retention data for the same drugs in RPLC [24] to investigate the feasibility to transfer retention data between both chromatographic systems.

2. Experimental

2.1. Standards and reagents

All standards were of pharmaceutical grade and donated by their manufacturers. The stock solutions (500 μg/ml) were prepared in 2-propanol and diluted to the final concentration with hexane. Both solvents were of analytical grade (Merck, Darmstadt, Germany). Propylamine (PA) was obtained from Fluka (Buchs, Switzerland).

2.2. High-performance liquid chromatography equipment

The chromatographic system consisted of a Varian 5000 gradient pump equipped with a Rheodyne injector (sample loop of 100 μl), a Merck–Hitachi L-4200 variable wavelength detector, operating at 0.05 A.U.F.S. and 220 nm, and a Varian CDS 401 data system. An Ultrasphere CN column (250 × 4.6 mm I.D., particle size 5 μm) was used. The mobile phase consisted of various proportions of hexane and 2-propanol, which both contained 0.1% PA. The flow rate was set at 2.0 ml/min. All experiments were performed in duplicate at 30°C. The capacity factors (k') were calculated as follows:

$$k' = (t_r - t_o)/t_o \quad (1)$$

where t_o represents the dead time of the system. The dead time was determined as the first distortion of the baseline after injection of 2-propanol, which, contrary to other methods investigated for the determination of t_o, more specifically the solvent disturbance peak, injection of pure hexane or toluene, was found to be independent of the mobile phase composition.

2.3. Computer

The regression calculations were performed using the Statistical Package for Social Sciences SPSS (Windows version 5.0.1) on an IBM PC or compatible computers.

3. Results and discussion

The retention data obtained for the β-adrenergic blocking drugs are listed in Table 1. For describing NPLC data Scott and Kucera [2] derived an equation accounting for the solute

Table 1
Chromatographic data (log k') and log P values for the β-adrenergic blocking drugs

No.	Name	log P [a]	log k' in % (v/v) 2-propanol				
			20	30	40	50	60
1	practolol	1.62	1.042	0.781	0.570	0.424	0.244
2	penbutolol	5.18	0.076	−0.034	−0.062	−0.088	−0.148
3	carazolol	3.24	0.759	0.534	0.389	0.284	0.137
4	atenolol	0.75	1.123	0.914	0.712	0.573	0.381
5	bupranolol	4.11	0.202	0.101	0.064	0.021	−0.034
6	mepindolol	2.95	n.a.[b]	0.637	0.484	0.358	0.223
7	metipranolol	3.33	0.441	0.267	0.198	0.128	0.027
8	prenalterol	1.89	0.785	0.548	0.395	0.291	0.128
9	metoprolol	2.36	0.418	0.279	0.215	0.152	0.061
10	oxprenolol	3.20	0.457	0.331	0.251	0.208	0.120
11	tertatolol	4.19	0.466	0.347	0.294	0.223	0.159
12	pindolol	2.42	n.a.	0.649	0.485	0.343	0.197
13	nadolol	1.85	0.814	0.655	0.481	0.367	0.191
14	bunitrolol	2.55	0.635	0.482	0.402	0.332	0.252
15	alprenolol	3.63	0.136	0.023	−0.014	−0.051	−0.115
16	acebutolol	2.31	n.a.	0.791	0.612	0.459	0.308
17	propranolol	3.66	0.262	0.193	0.144	0.098	0.017

Column, Ultrasphere CN; mobile phase, 2-propanol–hexane–0.1% propylamine
[a] Log P value calculated according to the Rekker fragmental method [35,36].
[b] n.a. = not available.

interactions in chromatography. One form of the equation is:

$$1/k' = A' + B' \cdot c_p \quad (2)$$

where A' and B' are constants for a particular solute and polar solvent, and c_p represents the concentration of the polar solvent in the binary mobile phase.

Considering only solute–adsorbent and solvent–adsorbent interactions, Snyder and Poppe [14] proposed another equation for NPLC with binary mobile phases:

$$\log k'_2 = \log k'_1 - (A_s/n_b) \cdot \log X_s \quad (3)$$

where k'_1 represents the capacity factor for a solute eluted with the pure strong solvent, k'_2 is the capacity factor for a solute eluted with the binary mobile phase, A_s represents the molecular area of the solute, n_b is the molecular area of the strong solvent, and X_s is the mole fraction of the strong solvent.

Soczewinski and Matysik [25] and Jandera and co-workers [26] have shown that the more convenient volume percentage of the more polar organic solvent can be used. In a first step, the dependence of log k' as a function of the mobile phase composition was investigated. As can be observed in Fig. 1, these plots are quite similar to those observed in RPLC [13], which indicates

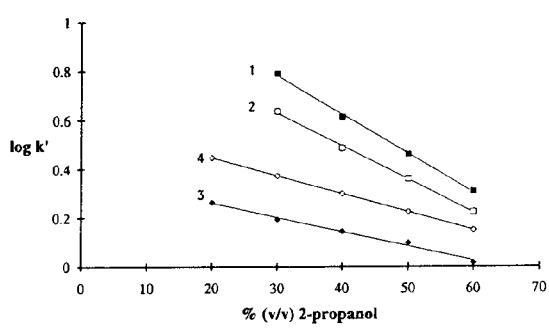

Fig. 1. Plot of log k' *vs.* the volume percentage 2-propanol in the mobile phase for the β-adrenergic blocking drugs acebutolol (1), mepindolol (2), propranolol (3) and tertatolol (4).

that the data can also be described using the model currently used in RPLC [27]:

$$\log k' = \log k'_w - S \cdot X_m \quad (4a)$$

where $\log k'_w$ represents the logarithm of the capacity factor for a solute in pure water and X_m is the volume fraction of the organic modifier in the binary mobile phase. To avoid confusion, in the NPLC context $\log k'_x$ is used instead of $\log k'_w$, as shown in Eq. 4b:

$$\log k' = \log k'_x - S \cdot X_m \quad (4b)$$

where $\log k'_x$ represents the logarithm of the capacity factor in pure hexane. The feasibility to apply Eq. 4b to our data would permit comparison of NPLC data with RPLC data for the β-adrenergic blocking drugs.

The values for the slopes (S), the intercepts ($\log k'_x$) in Eq. 4b and the corresponding correlation coefficient (r) are listed in Table 2. Since the linearity of the plots of $\log k'$ *vs.* the percentage of 2-propanol in the mobile phase was not investigated in the region below 20% of 2-propanol, the $\log k'_x$ values represent hypothetical extrapolated values. In Fig. 1 the regression lines for several β-adrenergic blocking drugs are presented. One can note that the results are in accordance with the convergence concept. Indeed, the lines for these β-adrenergic blocking drugs converge towards a single point (see below). Moreover, these plots showed quite good linearity over a rather wide range of 2-propanol compositions. As in RPLC, there seems to be a slight departure from the model. This was verified through analysis of the residuals. The pattern observed showed no indication of a violation of the linearity assumption. This will also be shown in a later part of this paper (see Eq. 11). Finally, the regression coefficients were used to calculate the standard error of estimate (*i.e.*, the standard deviation of the residuals) for the $\log k'$ prediction. This statistic demonstrates the practical value of the retention prediction. For the complete set of β-adrenergic blocking drugs a value of 0.0210 was obtained, which shows that this model provides rather accurate retention prediction. Overall, the results demonstrate that Eq. 4b can be applied for describing retention data for β-adrenergic blocking drugs in a system CN–hexane.

Table 2
Slopes (S), intercepts ($\log k'_x$) and correlation coefficients (r) for the relationship of $\log k'$ *versus* the volume fraction of the organic modifier in the mobile phase

No.	Slope (S)	Intercept ($\log k'_x$)	r
1	−1.9533	1.3936	−0.9941
2	−0.5015	0.1496	−0.9602
3	−1.4929	1.0178	−0.9907
4	−1.8262	1.4713	−0.9978
5	−0.5543	0.2927	−0.9818
6	−1.3679	1.0408	−0.9992
7	−0.9668	0.5990	−0.9823
8	−1.5702	1.0573	−0.9902
9	−0.8403	0.5611	−0.9878
10	−0.7975	0.5924	−0.9862
11	−0.7384	0.5933	−0.9898
12	−1.4986	1.0929	−0.9995
13	−1.5344	1.1154	−0.9983
14	−0.9859	0.7868	−0.9859
15	−0.5764	0.2265	−0.9741
16	−1.6012	1.2629	−0.9991
17	−0.5841	0.3765	−0.9954

Column, Ultrasphere CN; mobile phase, 2-propanol–hexane–0.1% propylamine. Numbering of the compounds as in Table 1

The occurrence of convergence indicates that the slope and intercept values for the different β-adrenergic blocking drugs are correlated, as can be seen in Fig. 2. Using linear regression

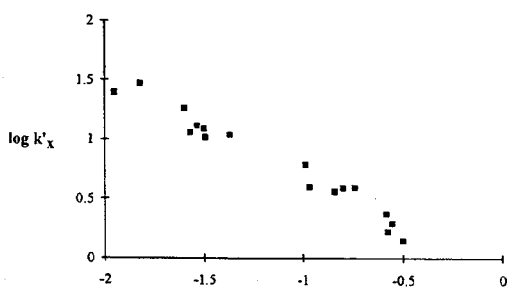

Fig. 2. Graph of slope (S) and intercept ($\log k'_x$) values for the set of β-adrenergic blocking drugs in NPLC.

analysis the following results were obtained for the straight line:

$$S = -1.1515(\pm 0.1281) \cdot \log k'_x - 0.2173(\pm 0.1149) \quad (5)$$
$$n = 17 \; s = 0.099 \; r = 0.980 \; F(\text{eq.}) = 367 \; p < 0.00005$$

The number of data points (n), the standard deviation of the residuals (s), the correlation coefficient (r), the calculated F value of the derived equation and its significance level (p) are provided. These results indicate a very good correlation between the slope and intercept values. Such significant correlations in RPLC were also observed by Schoenmakers [27], Braumann *et al.* [28], Hafkenscheid and Tomlinson [29], Jandera [30], Cooper and Hurtubise [31], and Baty and Sharp [32]. To our knowledge such correlations in NPLC have only been described by Jandera [15] and Cooper and Hurtubise [16].

Cooper and Hurtubise [16] used this so-called slope–intercept relationship for retention prediction for structurally related compounds. These authors also proposed a similar retention prediction model in RPLC [31]. The Cooper–Hurtubise NPLC model requires the calculation of the total solubility parameter values for the mobile phase [33,34], whereas in the RPLC model the volume fraction of the organic modifier is directly related to log k'. Considering the applicability of Eq. 4b to our data we investigated the usefulness of the RPLC slope–intercept model to predict the retention of β-adrenergic blocking drugs in NPLC:

$$\log k' = (1 - p \cdot X_m) \cdot \log k'_x - q \cdot X_m \quad (6)$$

where p and q represent the slope and intercept value for the plot of S *vs.* $\log k'_x$ (from Eq. 4b), respectively. This equation can be obtained by substituting Eq. 5 into Eq. 4b. Eq. 6 was used to predict the retention data for the set of β-adrenergic blocking drugs. As can be observed in Fig. 3, the predicted values (calculated by Eq. 6) correspond very well with the experimental values:

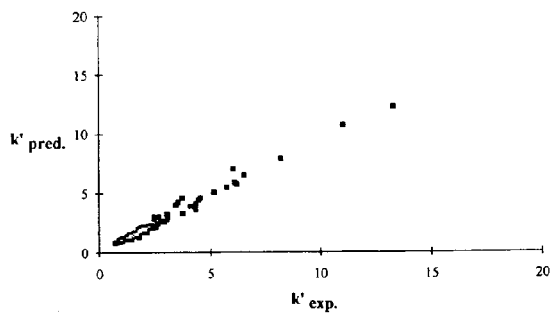

Fig. 3. Correlation of the predicted (calculated using Eq. 6) and experimental k' values for the set of β-adrenergic blocking drugs.

$$k'_{\text{pred.}} = 0.9597(\pm 0.0501) \cdot k'_{\text{exp.}} + 0.0863(\pm 0.0347) \quad (7)$$
$$n = 82 \; s = 0.293 \; r = 0.990 \; F(\text{eq.}) = 4036 \; p < 0.00005$$

The regression coefficients are accompanied by their 95% confidence intervals according to the t-test. Since 1 falls into the first and 0 into the second confidence interval, this is consistent with the equation $k'_{\text{pred}} = k'_{\text{exp}}$.

One must be aware that this retention prediction method presents a major disadvantage, namely for a new substance it requires an experimental k' value at a particular mobile phase composition for the calculation of the log k'_x value. Only then can k' values at other mobile phase compositions be predicted for an unknown compound. This, of course, limits the application of Eq. 6 for retention prediction purposes. Still, the results indicate that p and q values can be very useful for retention prediction in NPLC.

A way to extend the applicability of Eq. 6 is to consider not only the relationship of log k' *vs.* the volume fraction of the organic modifier in the mobile phase, but also to incorporate a parameter which characterizes or reflects the structure of the compound. Recently, we proposed a model based on theoretical considerations for retention prediction in RPLC [19]:

$$\log k'_i = \frac{(\Gamma \cdot \sum f + C' - \log k'_{cv})}{(0\%\text{MPS} - x_{cv}\%\text{MPS})} \cdot \%\text{MPS} + \Gamma \cdot \sum f + C' \quad (8)$$

where Σf represents the log P value of the solute calculated according to the Rekker hydrophobic fragmental system [35,36], x_{cv}%MPS and log k'_{cv} are the values for the convergence point (see below), %MPS represents the volume percentage of the organic modifier in the mobile phase, and Γ and C' are the slope and intercept values for the relationship of Σf *vs.* log k'_w.

Eq. 8, which relates the change in retention (log k') to the volume percentage of the organic modifier in the mobile phase, on the one hand, and the structure of the compound, reflected by the calculated log P value, on the other hand, was applied to predict the retention of the set of β-adrenergic blocking drugs in NPLC. The calculated log P values for the different drugs are listed in Table 1.

In a first step the convergence point was determined as described previously [19]. The lines for the β-adrenergic blocking drugs were found to converge towards the point with x-coordinate 83 (in % 2-propanol) and y-coordinate −0.145. The latter value corresponds to the mean log k' value at that percentage of 2-propanol for all the β-adrenergic blocking drugs. The x-coordinate and the y-coordinate represent x_{cv}%MPS and log k'_{cv}, respectively. The occurrence of convergence can also be observed in the data published by Soczewinski and Kuczmierczyk [37].

To obtain the values for the constants Γ and C' one has to consider the relationship between the calculated log P values and the extrapolated log k'_x values (Fig. 4). The following equation was derived by linear regression:

$$\log k'_x = -0.3249(\pm 0.1064) \cdot \log P + 1.7429(\pm 0.3284) \quad (9)$$
$$n = 17 \; s = 0.219 \; r = 0.859 \; F(\text{eq.}) = 42$$
$$p < 0.00005$$

The statistics for Eq. 9 indicate a significant correlation between both parameters. Numerous publications described the usefulness of log k'_w as a means for the estimation of the hydrophobicity–lipophilicity of a drug in RPLC [19]. Contrary to RPLC, in NPLC retention as reflected by the log k'_x value decreases as the compound becomes more lipophilic.

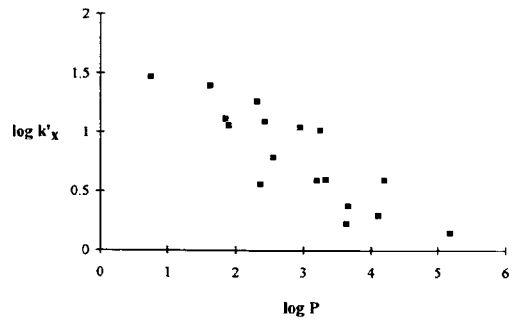

Fig. 4. Relationship between the estimated log P value and the log k'_x values for the set of β-adrenergic blocking drugs in NPLC.

The calculated log P values, the values for the convergence point and the constants Γ and C' were then used to predict the retention of the β-adrenergic blocking drugs in NPLC. From Fig. 5 and from the statistics one can conclude that the predicted values (calculated by Eq. 8) correspond rather well with the experimental values:

$$k'_{\text{pred.}} = 0.8526(\pm 0.0635) \cdot k'_{\text{exp.}} + 0.3435(\pm 0.2164) \quad (10)$$
$$n = 82 \; s = 0.618 \; r = 0.948 \; F(\text{eq.}) = 715$$
$$p < 0.00005$$

Eq. 8 has been shown to correspond with

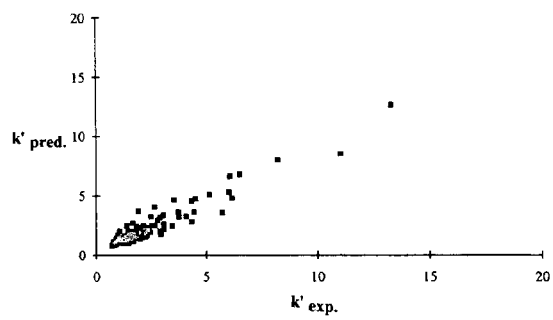

Fig. 5. Correlation of the predicted (calculated using Eq. 8) and experimental k' values for the set of β-adrenergic blocking drugs.

another model developed by multiple linear regression [34]. This frequently used statistical method for the analysis of chromatographic data, and more specifically for QSRR studies, has also been applied in this study for the interpretation of the NPLC retention data. Multiple linear regression was carried out by considering the dependent variable log k' and the independent variables log P, %MPS, the interaction term and the quadratic terms. The following equation was derived with the stepwise method (values of p-to-enter and p-to-remove 0.05 and 0.10, respectively):

$$\log k' = -0.0208(\pm 5.55.10^{-3}) \cdot \%\text{MPS} - 0.3150(\pm 0.0756) \cdot \log P + 0.0035 (\pm 1.777.10^{-3}) \cdot \%\text{MPS} \cdot \log P + 1.6791(\pm 0.2371) \quad (11)$$

$n = 82$ $s = 0.123$ Mult.$R = 0.896$ Adj.$R^2 = 0.796$ F(eq.) $= 106$ $p < 0.00005$

The terms %MPS, log P and the interaction term were found significant at $p < 0.00005$. The quadratic terms were found insignificant. The latter results justify the application of Eq. 4b in this study, *i.e.* the assumption of linearity of log k' *vs.* the volume fraction of the organic modifier.

From Eq. 11 one can note that the log k' values decrease as a function of the volume percentage of the organic modifier in the mobile phase and also in function of the hydrophobicity–lipophilicity of the compound.

Some authors [38–40] have claimed that cyanosilica behaves much like a deactivated silica when less polar mobile phases, such as dichloromethane are used. This means that the cyanopropyl groups show little participation as adsorption sites. However, it has been shown that as the polarity of the solvent increases, for instance with alcohols as mobile phase component, the effect of the residual silanol group is masked, leaving the cyanopropyl groups to function as the principal adsorption sites. Since log k' values obtained on a CN stationary phase are correlated with log P it can be concluded that the β-adrenergic blocking drugs interact with the propyl chains of the stationary phase. It is important to mention that the Ultrasphere CN column contains residual silanol groups. The β-adrenergic blocking drugs have been shown to interact strongly with the silanol groups resulting in a mixed retention mechanism [24]. However, Weiser *et al.* [40] suggested that 2-propanol deactivates the silanol groups. Moreover, in this study the attachment of solute to the strong adsorption sites (the residual silanol groups) is eliminated by the addition of 0.1% (v/v) propylamine to the mobile phase [23]. Overall, one can conclude that the cyanopropyl groups constitute the adsorption sites in these packings. One must be aware that as a result of the strong adsorption of 2-propanol onto the surface silanol groups and the addition of an alkylamine to the mobile phase, these chromatographic conditions are not favorable for isomeric separations, since one then needs localization effects (*i.e.* interaction with residual silanol groups) to play an important role.

Since the retention data for the β-adrenergic blocking drugs in NPLC were found to be correlated with the descriptor log P, we compared the retention data in NPLC with data obtained in RPLC [24]. In a first step, the slope and intercept values for the log k' *vs.* X_m relationships in RPLC were calculated (Table 3). Since these plots manifest curvature these values were determined within a limited methanol range. For all compounds the log k' for 40 and 50% methanol were used, except for penbutolol. For this compound only log k' values for 50 and 60% methanol were available. One must be aware that, firstly, the log k'_w obtained in this manner represent hypothetical extrapolated intercepts, and, secondly, that these values depend on the concentrations of methanol used for the linear regression [20]. At both levels acceptable k' values (*i.e.*, k' values situated between 0.5 and 15) were obtained for most of the β-adrenergic blocking drugs investigated. As can be observed in Fig. 6, the slope and intercept values for the different β-adrenergic blocking drugs in RPLC are strongly correlated. Using linear re-

Table 3
Slopes (S), intercepts ($\log k'_w$) and correlation coefficients (r) for the relationship of $\log k'$ *versus* the volume fraction of the organic modifier in the mobile phase [24]

No.	Slope (S)	Intercept ($\log k'_w$)
1	−2.0400	0.4670
2	−3.8300	3.1910
3	−4.6800	2.4390
4	−1.6900	0.2450
5	−4.1400	2.7980
6	−2.9700	1.2470
7	−5.1500	2.9690
8	−1.4300	0.1540
9	−3.3400	1.6840
10	−4.1900	2.3540
11	−4.8000	2.9980
12	−1.9400	0.6300
13	−2.3900	0.8970
14	−3.4400	1.6280
15	−4.5700	2.8880
16	−3.4300	1.6330
17	−4.3600	2.7250

Column, Nova-Pak RP18; mobile phase, methanol–phosphate buffer (pH 4.0, $\mu = 0.1$). Numbering of the drugs as in Table 1.

gression analysis the following results, including statistics, were obtained for the straight line:

$$S = -1.0605(\pm 0.1883) \cdot \log k'_w - 1.5041(\pm 0.3936) \quad (12)$$
$$n = 17 \; s = 0.374 \; r = 0.952 \; F(\text{eq.}) = 144$$
$$p < 0.00005$$

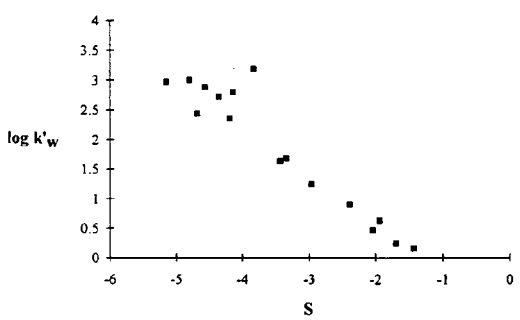

Fig. 6. Graph of slope (S) and intercept ($\log k'_w$) values for the set of β-adrenergic blocking drugs in RPLC.

These results indicate a very good correlation between slope and intercept values.

For the relationship between the calculated log P values and the extrapolated $\log k'_w$ values (Fig. 7) the following results were obtained:

$$\log k'_w = 0.8708(\pm 0.2309) \cdot \log P - 0.7018(\pm 0.7125) \quad (13)$$
$$n = 17 \; s = 0.475 \; r = 0.901 \; F(\text{eq.}) = 65$$
$$p < 0.00005$$

The extrapolated $\log k'_w$ values are strongly correlated to the log P values. These chromatographically obtained values can hence be used to provide an estimation of the lipophilicity of a drug.

The intercept values obtained in NPLC and RPLC were then compared. As can be observed in Fig. 8 and from the statistics for Eq. 14, the intercept values in both modes are inversely correlated:

$$\log k'_w = -2.1675(\pm 0.7458) \cdot \log k'_x + 3.5582(\pm 0.6689) \quad (14)$$
$$n = 17 \; s = 0.580 \; r = 0.848 \; F(\text{eq.}) = 38$$
$$p < 0.00005$$

Some β-adrenergic blocking drugs show a particular behaviour in NPLC, for instance the compounds metoprolol (no. 9) and acebutolol (no. 16). In RPLC these solutes do not show special properties, but are retained as one would expect from their hydrophobic properties. Con-

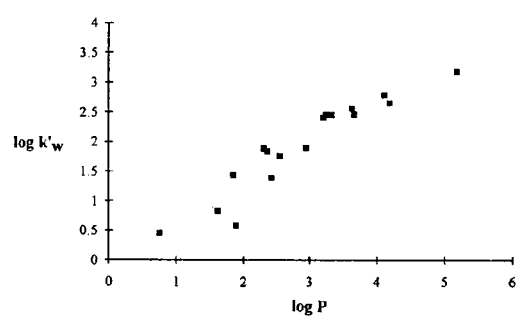

Fig. 7. Relationship between the estimated log P value and the log k'_w values for the β-adrenergic blocking drugs in RPLC.

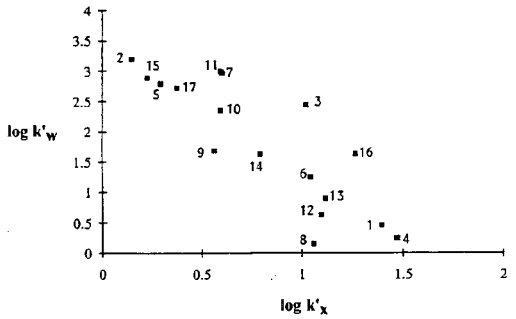

Fig. 8. Correlation between the intercept values obtained in NPLC (log k'_x) and RPLC (log k'_w) for the set of β-adrenergic blocking drugs.

sequently, other specific interactions occur in NPLC. Metoprolol (no. 9) possesses an aliphatic–O–fragment, whereas acebutolol (no. 16) contains two other functional groups, namely–CONH and–$COCH_3$ (Table 4). The latter functions can lead to strong polar interactions with the cyanopropyl groups of the stationary phase (1).

Since the retention data in both chromatographic systems were found to be correlated, an equation was derived by multiple regression to transfer the retention data for β-adrenergic blocking drugs obtained in RPLC [24] to NPLC:

$$\log k'_{NP} = -0.2922(\pm 0.0570) \cdot \log k'_{RP} - 0.0224(\pm 2.517.10^{-3}) \cdot \%MPS + 1.4051(\pm 0.1212) \quad (15)$$

$$n = 65 \; s = 0.114 \; \text{Mult.}R = 0.917 \; \text{Adj.}R^2 = 0.836 \; F(\text{eq.}) = 164 \; p < 0.00005$$

All terms were found significant at $p < 0.00005$. Since the retention data were compared at the same level, *i.e.* the same percentage of the organic modifier in the mobile phase, Eq. 15 can also be used to transfer NP retention data to RP data. This equation can therefore be very useful for HPLC method development.

The analogy between the RP system (with aqueous eluents) and the NP system (with non-aqueous eluents) is somewhat unexpected. This phenomenon could be related to the weakly polar properties of a CN type of column. It would therefore be most interesting to investigate the applicability of this approach on more polar adsorbents, such as pure silica.

Table 4
Overview of the functional groups (corresponding with Rekker fragments) present in the different β-adrenergic blocking drugs

No.	–NHCO (ar.)	–NH– (ar.)	$-CONH_2$ (al.)	–Cl (ar.)	–COO (ar.)	–OH (ar.)	–O– (al.)	$-CH{=}CH_2$ (al.)	–O– (ar.)	–S– (al.)	–OH (al.)	–CN (ar.)	–CONH (ar.)	$-COCH_3$ (ar.)
1	*													
2														
3		*												
4			*											
5				*										
6		*												
7					*									
8						*								
9							*							
10								*	*					
11										*				
12		*												
13											**			
14												*		
15								*						
16													*	*
17														

Numbering of the compounds as in Table 1.

4. Conclusions

The experimental data presented in this work indicate that the slope–intercept and convergence model can be used for describing the retention data of the β-adrenergic blocking drugs for this chromatographic system, *i.e.* an Ultrasphere CN column and a mobile phase composed of hexane–2-propanol–0.1% (v/v) propylamine.

The retention mechanism of the β-adrenergic blocking drugs in NPLC is governed by two types of interactions, namely hydrophobic–lipophilic interactions, on the one hand, and polar interactions, on the other one.

One can also observe that a CN–hexane system is less useful for the analysis of less polar compounds, in which these possess weak retention. However, the chromatographic conditions used in this study are particularly suitable for the more polar β-adrenergic blocking drugs, which show insufficient retention in RPLC.

Acknowledgement

The authors acknowledge the financial assistance of NFWO and FGWO.

References

[1] L.R. Snyder and J.J. Kirkland, *Introduction to Modern Liquid Chromatography*, Wiley-Interscience, New York, 2nd ed., 1979.
[2] R.P.W. Scott and P. Kucera, *Anal. Chem.*, 45 (1973) 749.
[3] R.P.W. Scott and P. Kucera, *J. Chromatogr.*, 112 (1975) 425.
[4] R.P.W. Scott, *J. Chromatogr.*, 122 (1976) 35.
[5] E.D. Katz, K. Ogan and R.P.W. Scott, *J. Chromatogr.*, 352 (1986) 67.
[6] L.R. Snyder, *J. Chromatogr.*, 46 (1974) 1384.
[7] L.R. Snyder and H. Poppe, *J. Chromatogr.*, 184 (1980) 363.
[8] L.R. Snyder, in Cs. Horváth (Editor), *High-Performance Liquid Chromatography–Advances and Perspectives*, Vol. 3, Academic Press, New York, 1983, pp. 157–223.
[9] E. Soczewinski, *Anal. Chem.*, 41 (1969) 179.
[10] E. Soczewinski, *J. Chromatogr.*, 130 (1977) 23.
[11] E. Soczewinski, *J. Chromatogr.*, 388 (1987) 91.
[12] C.A. Chang and C.S. Huang, *Anal. Chem.*, 57 (1985) 997.
[13] C.A. Chang and L.T. Tan, *J. Liq. Chromatogr.*, 8 (1985) 995.
[14] L.R. Snyder and H. Poppe, *J. Chromatogr.*, 184 (1980) 363.
[15] P. Jandera, *Chromatographia*, 26 (1988) 417.
[16] H.A. Cooper and R.J. Hurtubise, *J. Chromatogr.*, 360 (1986) 327.
[17] T. Kowalska, *J. High Resolut. Chromatogr.*, 12 (1989) 474.
[18] T. Hamoir, B. Bourguignon, H. Hindriks and D.L. Massart, *J. Chromatogr.*, 633 (1993) 43.
[19] T. Hamoir, W. King, S. Kokot, K. Douglas and D.L. Massart, *J. Chromatogr. Sci.*, 31 (1993) 393.
[20] R. Kaliszan, *Quantitative Structure-Chromatographic Retention Relationships*, Wiley-Interscience, New York, 1987.
[21] M. Bachrata, M. Blesova, A. Schultzova, L. Grolichova, Z. Bezakova and A. Lucas, *J. Chromatogr.*, 171 (1979) 29.
[22] K. Dadakova, J. Hartl and K. Waisser, *J. Chromatogr.*, 254 (1983) 276.
[23] D.L. Massart and M.R. Detaevernier, *J. Chromatogr. Sci.*, 18 (1980) 139.
[24] T. Hamoir, Y. Verlinden and D.L. Massart, *J. Chromatogr. Sci.*, 32 (1994) 14.
[25] E. Soczewinski and G. Matysik, *J. Chromatogr.*, 32 (1968) 458.
[26] P. Jandera, M. Janderová and J. Churáček, *J. Chromatogr.*, 115 (1975) 9.
[27] P.J. Schoenmakers, *Optimization of Chromatographic Selectivity–A Guide to Method Development*, Elsevier, Amsterdam, 1986.
[28] T. Braumann, G. Weber and L.H. Grimme, *J. Chromatogr.*, 261 (1983) 329.
[29] T.L. Hafkenscheid and E. Tomlinson, *J. Chromatogr.*, 264 (1983) 47.
[30] P. Jandera, *J. Chromatogr.*, 314 (1984) 13.
[31] H.A. Cooper and R.J. Hurtubise, *J. Chromatogr.*, 360 (1986) 313.
[32] J.D. Baty and S. Sharp, *J. Chromatogr.*, 437 (1988) 13.
[33] R. Tijssen, H.A.H. Billiet and P.J. Schoenmakers, *J. Chromatogr.*, 122 (1976) 185.
[34] B.L. Karger, L.R. Snyder and C. Eon, *J. Chromatogr.*, 125 (1976) 71.
[35] R.F. Rekker, *The Hydrophobic Fragmental Constant–Its Derivation and Application*, Elsevier, Amsterdam, 1977.
[36] R.F. Rekker and H.M. de Kort, *Eur. J. Med. Chem. Chim. Ther.*, 14 (1979) 479.
[37] E. Soczewinski and J. Kuczmierczyk, *J. Chromatogr.*, 150 (1978) 53.
[38] G. Jones, *J. Chromatogr.*, 276 (1983) 69.
[39] G. Ostvold, *J. Chromatogr.*, 282 (1983) 413.
[40] E.L. Weiser, A.W. Salotto, S.M. Flach and L.R. Snyder, *J. Chromatogr.*, 303 (1984) 1.

ELSEVIER

Journal of Chromatography A, 673 (1994) 11–19

JOURNAL OF CHROMATOGRAPHY A

Studies of physicochemical and chromatographic properties of mixed amino-alkylamide bonded phases☆

B. Buszewski☆☆, M. Jaroniec, R.K. Gilpin*

Department of Chemistry, Kent State University, Kent, OH 44242, USA

(First received September 28th, 1993; revised manuscript received March 4th, 1994)

Abstract

Mixed amino-alkylamide chemically bonded phases have been prepared via two-step reaction which involved the initial modification of silica with aminopropyldimethylsilyl groups under environmentally sealed conditions followed by a secondary derivatization with different acid chlorides (*i.e.*, acetyl, hexanoyl and stearoyl chlorides). In addition, for comparative purposes two conventional C_{18} phases with different coverage densities have been prepared. Subsequently, the physical properties of the mixed phases have been studied by liquid chromatography as well as by elemental analysis and solid-state nuclear magnetic resonance spectrometry. The resulting data have provided information about how the hydrophobic chains and the specific interaction sites in the bonded phases influence solute retention under reversed-phase conditions. A potentially important application of the mixed amino-alkylamide materials is for separating basic compounds such as amines and amides.

1. Introduction

Chemically bonded phases (CBPs), especially materials with alkyl ligands, are important in various areas of analytical chemistry including high-performance liquid chromatography (HPLC), filtration, solid-phase extraction, etc. [1–4]. Their general use and popularity are due to their hydrophobic character as well as good chemical, mechanical and thermal stabilities [3,5–8]. In addition, many analytical separations require more selective phases which contain simple polar functionalities such as amino and nitrile groups [1–4,8–12] to more complex chiral selective materials such as immobilized cyclodextrins, proteins and Pirkle-type phases [1,2,8,13–15].

Recently, the preparation of CBPs with a specific interaction site localized in the interior region of hydrophobic ligands (*i.e.*, bonded alkylamide groups) has been described [3,16,17]. In preliminary studies, the packings were found to be useful for separating polar compounds, particularly, those which contain basic functionalities [3,16,17]. Under such conditions enhanced peak symmetry was obtained compared to more conventional alkyl-bonded phases. A possible explanation for this enhanced behavior is via an internal masking mechanism [18].

In the current work mixed amino-alkylamide

* Corresponding author.

☆ Presented at the *17th International Symposium on Column Liquid Chromatography, Hamburg, May 9–14, 1993.* The proceedings of this symposium were published in *J. Chromatogr. A*, Vols. 660 + 661 (1994).

☆☆ Permanent address: Department of Chemical Physics, Faculty of Chemistry, M. Curie-Skłodowska University, Pl-20 031 Lublin, Poland.

0021-9673/94/$07.00
SSDI 0021-9673(94)00224-W

phases have been synthesized and their chromatographic properties evaluated. Emphasis has been placed on developing a better understanding of how changes to and the interplay between the terminal alkyl groups, the specific interaction site in the bonded alkylamide ligands, and the underlying amino groups used for attachment, influence the retention and separation of various solutes. In doing this, alkylbenzene and alkylaniline homologues, as well as phenol and nitrobenzene have been chromatographed as a function of temperature under reversed-phase conditions using mixed hydro–organic eluents. For reference purposes comparative measurements have been carried out on two conventional C_{18} phases with low and high coverage densities. In addition to the chromatographic studies, the surface properties of the mixed amino-alkylamide phases have been characterized by solid-state nuclear magnetic resonance spectrometry (NMR).

2. Experimental

2.1. Materials

The two types of 5-μm spherical silica used to prepare the bonded phases were Separon SGX (Tessek, Prague, Czech Republic) and LiChrospher Select B (SB; E. Merck, Darmstadt, Germany). These materials had nitrogen BET surface areas of 347 and 570 m^2/g, respectively.

The surface modification reagents, octadecyldimethylchlorosilane and γ-aminopropyldimethylmethoxysilane, were from Huls (Bristol, PA, USA) and the acetyl, hexanoyl and stearoyl chlorides as well as morpholine were from Aldrich (Milwaukee, WI, USA). The remaining chemicals used in the synthetic procedure, methanol, toluene and *n*-hexane (reagent grade) were also purchased from Aldrich.

The chromatographic solvents, methanol and acetonitrile (HPLC grade) were from Fisher Scientific (Fairlawn, NJ, USA) and the deionized water was purified in the laboratory using a Millipore (El Paso, TX, USA) Milli-Q reagent water system.

2.2. Synthesis

The preparation of the two C_{18} phases were as follows. A 3-g amount of silica was placed in a environmentally isolated glass reactor [3] and then heated to 185°C under vacuum (10^{-2} Pa) for 10 h. In addition, thermogravimetric studies of the silica sample showed that its heating up to 185°C primarily eliminates adsorbed water and does not affect significantly the surface silanols. Materials with high ($^hC_{18}$) and low ($^lC_{18}$) density coverages were prepared by varying the molar ratio of the octadecyldimethylchlorosilane and morpholine [3,20].

Similarly the mixed amino-alkylamide phases were synthesized in a sealed glass reactor by a two-step process [17], in which an initial aminopropyldimethylsilyl phase was prepared under environmentally isolated conditions [3,11] and subsequently reacted with either acetyl, hexanoyl or stearoyl chlorides [3,17,18].

2.3. Spectroscopic and elemental analysis

The ^{29}Si and ^{13}C cross-polarization magic-angle-spinning (CP-MAS) NMR spectra were obtained by using a General Electric (Fremont, CA, USA) Model GN-300 spectrometer and acquisition parameters similar to those reported previously [17]. The elemental analysis was performed on a Perkin-Elmer (Norwalk, CT, USA) Model 240B CHN analyzer and these results used to calculate the coverage density of the groups bonded to the surface during the silanization reactions [*i.e.*, for the octadecyl (α_{RP}) and the amino (α_{NH2}) phases] using Eq. 1 and the subsequent degree of amidization in the case of the mixed amino-alkylamide surfaces (α_{AA}) using Eq. 2.

$$\alpha_{RP} \text{ or } \alpha_{NH2}\,(\text{mol/m}^2) = \left[\frac{P_c}{1200n_{c(1)} - P_c(M_1 - 1)}\right]/S_{BET} \quad (1)$$

$$\alpha_{AA}\,(\text{mol/m}^2) = \left[\frac{P_{c(AA)} + P_{c(AA)}N_1(M_1 - 1) - 1200N_1n_{c(1)}}{1200n_{c(2)} - P_{c(AA)}(M_2 - 1)}\right]/S_{BET} \quad (2)$$

where P_c = carbon percentage for the bonded phase prepared via one-step reaction (*e.g.*, phases with octadecyl or amino ligands); $P_{c(AA)}$ = carbon percentage for the mixed amino-alkylamide phase; N_1 = concentration of the ligands bonded in the initial silanization; in the current work N_1 denotes the concentration of amino ligands in mol/g, which can be calculated from the carbon or nitrogen percentages for the NH_2 phase according to Eq. 1 (*cf.* Table 1); $n_{c(1)}$ = number of carbon atoms in the bonded ligand from the initial silanization; $n_{c(2)}$ = number of carbon atoms added in the second-step amidization reaction; M_1 = molecular mass of the bonded ligand from the initial silanization; M_2 = molecular mass of the added group in the second-step amidization reaction; and S_{BET} = BET specific surface area in m^2/g.

The coverage density of unreacted aminopropyl groups following the second-step amidization was calculated by subtracting the concentration of alkylamide ligands from the initial concentration of aminopropyldimethylsilyl groups calculated for the NH_2 phase.

2.4. Chromatographic studies

Chromatographic measurements were carried out on an IBM (Danbury, CT, USA) Model 9560 ternary gradient liquid chromatograph equipped with an LDC (Riviera Beach, FL, USA) Model III UV detector set at 254 nm, and a Rheodyne (Berkeley, CA, USA) Model 7100 sampling valve with 10-μl injection loop. The eluent was pre-equilibrated to the correct temperature before it reached the column. The column temperature was controlled to ± 0.1 K in in a Hotpack (Philadelphia, PA, USA) refrigerated water bath. The flow-rate of the mobile phase was monitored with a Phase Separations (Queensferry, UK) Model FLOSOA1 flow meter connected to the detector outlet.

2.5. Column packing

About 1.2 or 2.2 g of the modified silicas were packed, respectively, into 60 mm × 4.6 mm I.D. or 125 mm × 4.6 mm I.D. stainless-steel column blanks which were purchased from Supelco (Bellefonte, PA, USA). Prior to packing a slurry was prepared using 35 ml of 2-propanol and sonicating the mixture for 5 min. Subsequently, the columns were packed using a Haskel (Burbank, CA, USA) Model DST-52 pump at a pressure of 50 MPa and methanol as the carrier solvent.

3. Results and discussion

The non-specific and specific interactions which occur in the stationary layer of chemically bonded phases are a complex function of the residual silanols, the bonded ligands, and intercalated solvent molecules. Various approaches have been used to characterize these including

Table 1
Surface coverages of the octadecyl and mixed amino-alkylamide monomeric phases studied

Silica support	Phase	n_C	P_c	P_N	α_{RP}	α_{NH2}
Separon SGX	$^bC_{18}$	20	23.4	–	4.03	–
LiChrospher SB	$^1C_{18}$	20	23.2	–	2.42	–
	NH_2	5	6.9	1.6	–	2.33
	AA_1	7	8.3	1.7	1.38	0.96
	AA_2	12	9.9	1.6	0.98	1.35
	AA_3	24	19.7	1.6	1.59	0.74

n_C = Total number of carbon atoms in the bonded ligands; α_{RP} and α_{NH_2} denote the surface concentrations (in μmol/m^2) of the alkyl-ended and amino ligands, respectively. P_N = nitrogen percentage for a chemically bonded phase.

the measurement of ln k' *vs.* $1/T$ dependencies as well as variations in these relationships as a function of solvent composition [21–26]. Such procedures have been used in the current work in order to examine how differences in mixed amino-alkylamide phases effect both the specific and non-specific interactions of the solute molecule with the surface layer, as well as, the interaction of the immobilized amine and amide groups with the underlying residual silanols.

Listed in Table 1 are the coverage densities for three mixed amino-alkylamide phases with differing terminal chain lengths, the initial amino phase used to prepare these materials, and for comparative purposes two conventional C_{18} phases. As has been reported elsewhere [3,17,18], the amino-alkylamide phases were prepared via two-step synthesis which involved an initial silanization reaction using 3-aminopropyldimethylmethoxysilane (NH_2) followed by a secondary amidization using either acetyl chloride (AA_1), hexanoyl chloride (AA_2) or stearyl chloride (AA_3). During the initial silanization more than 70% of the accessible silanols were converted to aminopropyldimethylsilyl groups. In the subsequent step the extent of conversion of these groups to the alkylamide moiety ranged from approximately 40% for the AA_2 phase to about 60–70% for the AA_1 and AA_3 phases. Based on a statistical analysis of the nitrogen data listed in Table 1 the overall variations in the estimated coverages are approximately 10%. Thus, the small differences in alkylamide coverage (α_{AA}) for the AA_1 and AA_3 phases are within expected statistical variations. However, in contrast to these phases, the AA_2 material contained more unreacted aminopropyl groups (*i.e.*, see the α_{NH2} values in Table 1). Based on reactivity and steric considerations these latter results are unexpected and presumable reflect experimental differences in the reaction conditions used [18,19].

For both C_{18} phases the total amount of bound carbon was greater than 23%. However, the estimated surface densities (*i.e.*, the α_{RP} values in Table 1) which are based on the specific surface area of the unmodified silicas, were significantly different (*i.e.*, 4.03 μmol/m^2 for the Separon SGX material compared to 2.42 μmol/m^2 for the LiChrospher SB material). The density of the Separon material was about 1.7 times that of the LiChrospher material. It should be noted that although the coverage density depends on the synthetic procedure, it also is controlled by the nature of the native silica in terms of its porosity, specific surface area, type and distribution of surface silanols, etc. [1,3]. The surface area of the Separon SGX silica is smaller than that of the LiChrospher SB silica; however, it has been reported to contain a greater density of free silanols accessible for modification [3]. Thus, the lower coverage densities of both the $^1C_{18}$ and NH_2 which are statistically similar (*i.e.*, within 4% of each other) are consistent with reported reactivity differences of the native silicas [3].

For illustrative purposes a ^{13}C CP-MAS NMR spectrum for the AA_1 phase is shown in Fig. 1. The spectrum is consistent with previously published work [3,17,18] and contains six resonances at $\delta = -2.5$, 15.9, 21.5, 43.4, 50.9 and 171.9 ppm which are due to the dimethylsilyl, C1, C2, C5, C3 and C4 carbons. Spectra for the AA_2 and AA_3 phases contained additional resonances for the interior chain carbons and they were similar to those published elsewhere [3,17–19].

Variations in solute retention as a function of temperature were measured for benzene, toluene, aniline, nitrobenzene and phenol using binary mixtures of methanol–water (40:60, v/v) as mobile phases over a range from 263 to 313 K. These measurements were made in order to evaluate the physicochemical properties of the

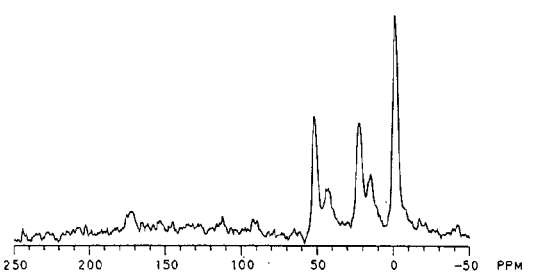

Fig. 1. ^{13}C CP-MAS NMR spectrum for the monomeric AA_1 phase.

three mixed AA materials *vs.* those of conventional C_{18} phases. Shown in Fig. 2 are the experimental dependencies of ln k' *vs.* $1/T$ in K for the solutes chromatographed on the AA_2, AA_3 and $^{1}C_{18}$ phases. Since almost all of the

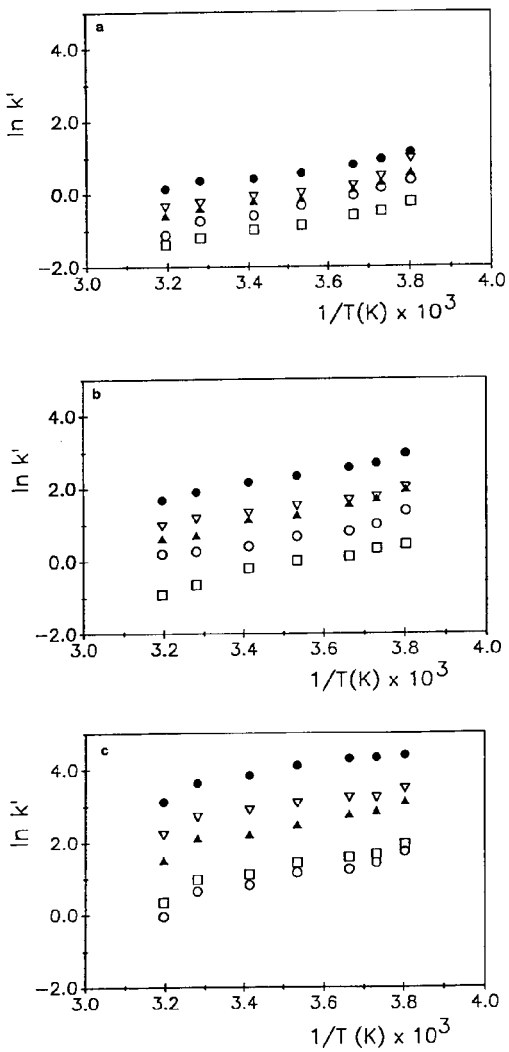

Fig. 2. Linear dependencies of the ln k' on the inverse temperature ($1/T$) measured for phenol (□), aniline (○), nitrobenzene (▲), benzene (△) and toluene (●) on the columns with the AA_2 (a), AA_3 (b) and $^{1}C_{18}$ (c) packings using the methanol–water (40:60, v/v) mobile phase. Chromatographic conditions: flow-rate 1 ml/min and UV detection at 254 nm.

capacity factors for the solutes on the AA_1 phase were smaller than unity, they were not considered to be accurate enough to be used in further calculations.

A comparison of the dependencies presented in Fig. 2 shows that the values of k' obtained on the $^{1}C_{18}$ phase are higher than those on the amino-alkylamide phases and that they decrease with decreasing length of terminal alkyl portion for the amino-alkylamide phases. Further, the data in Fig. 2 demonstrate that while the elution order for toluene, benzene and nitrobenzene was the same for the $^{1}C_{18}$ and amino-alkylamide packings, this was not the case for phenol and aniline. Phenol was retained longer on the $^{1}C_{18}$ column than aniline, however, on the amino-alkylamide material the elution order was reversed (*cf.* Fig. 2b and c).

Another feature of the dependencies shown in Fig. 2 are their significant deviations from linearity at lower temperatures which appears to be associated with degrading peak shapes. For all phases, the peak asymmetry increased with decreasing temperature. These same trends were also observed when acetonitrile–water was used as the eluent as is illustrated later. This was especially apparent for both of the conventional octadecyl materials. At temperatures below 269 K the peaks merged into highly convoluted irregular shaped profiles. However, in the case of the mixed amino-alkylamide phases, even at the lowest temperature studied, 263 K, the elution profiles although asymmetrical were less convoluted.

Enthalpy values (ΔH) were estimated on the basis of the linear regions of the ln k' *vs.* $1/T$ dependencies (*i.e.*, from 273 to 305 K) as illustrated in Fig. 3. This was done for the test solutes as a function of eluent composition using Eq. 3 [23,24]:

$$\ln k' = \frac{\Delta S}{R} + \ln \phi - \frac{\Delta H}{RT} \qquad (3)$$

where ϕ is the phase ratio. For the octadecyl phase, the values of ΔH were between −14 and −15 kJ/mol for aniline, phenol and nitrobenzene compared to approximately −13 kJ/mol for toluene and −10 kJ/mol for benzene. The slight-

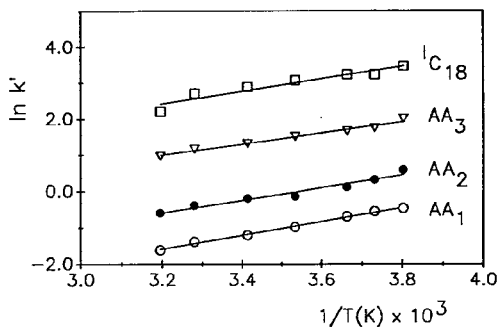

Fig. 3. Comparison of the linear dependencies of ln k' on the inverse temperature ($1/T$) for benzene on the amino-alkylamide and $^{1}C_{18}$ phases listed in Table 1. Chromatographic conditions as in Fig. 2.

ly larger heats of adsorption for the aromatic solutes containing polar substituents are consistent with increased specific interactions of the polar substituents with the residual silanols. Assuming an initial silanol concentration of 5.2 μmol/m^2 for unmodified LiChrospher SB [3,20], the concentration of residual surface silanols on the $^{1}C_{18}$ material after modification was about 2.8 μmol/m^2. Similarly, for the amino surface (*i.e.*, the NH_2 phase), as well as for the mixed amino-alkylamide materials the residual silanols were 2.8 μmol/m^2. These values were obtained by subtracting the concentration of bonded groups given in Table 1 from 5.2 μmol/m^2. In the case of the mixed amino-alkylamide phases, only the aminopropyldimethylsilyl ligands reacted with the acid chlorides and thus the number of remaining silanols was identical to the starting amino phase. In addition, the mixed amino-alkylamide phases contained unreacted aminopropyldimethylsilyl groups, as well as alkylamide groups. The concentration of each on the three mixed amino-alkylamide materials is given in Table 1. Thus, the chromatographic properties of the mixed amino-alkylamide materials should reflect interactions of the solute with the residual silanols, the unmodified amino groups, and the alkylamide ligands. However, since the number of residual silanols was the same for all of the phases, it seems reasonable to assume that the observed differences in retention behavior should be attributable to differences in the concentration of amino and alkylamide groups. Unfortunately, a direct comparison between the phases is complicated by the fact that the midrange AA_2 phase contained a different degree of amidization than the AA_1 and AA_3 materials. Although reproducibility of the amino-alkylamide phases under controlled conditions is good, further studies need to be done in order to specify experimental conditions for achieving the same degree of amidization for various alkylamide phases. Thus, the current data are limited in terms of developing a detailed description of the mechanisms controlling separation on the mixed amino-alkylamide surface. However, they are significant in that they demonstrated improved symmetry for polar solutes on the new mixed phases compared to more conventional alkyl type materials, *e.g.*, the values of the asymmetry factor for aniline on the $^{1}C_{18}$ and AA_3 phases were, respectively, 1.1 and 1.0. This improved performance is believed to be due to amino–silanol and amide–silanol interactions which act to mask or attenuate unwanted solute–silanol interactions.

Although large variations in solute retention were observed between the $^{1}C_{18}$ and AA_3 phases, differences in ΔH were not as significant. These trends suggest that the dominant interactions on both materials were hydrophobic and that the reduced retention volumes on the mixed amino-octadecylamide phase were due to the reduced density of the terminal alkyl groups. However, differences in the underlying polar groups between the AA_3 and conventional $^{1}C_{18}$ materials were manifested in the observed variations in solute selectivity for the polar solutes.

The chromatographic properties of the $^{1}C_{18}$ and AA_3 phases are compared further in Fig. 4 which contains plots of ln α *vs.* $1/T$. In each case, the selectivity values were calculated using benzene as the reference solute. The line for toluene/benzene, which lies above zero because toluene was retained longer on both phases than benzene, provides information about the non-specific (methylene) selectivity of the phases. The relative magnitude of the data are consistent with the reduced alkyl density on the AA_3 phase compared to the $^{1}C_{18}$ phase. The remaining α-

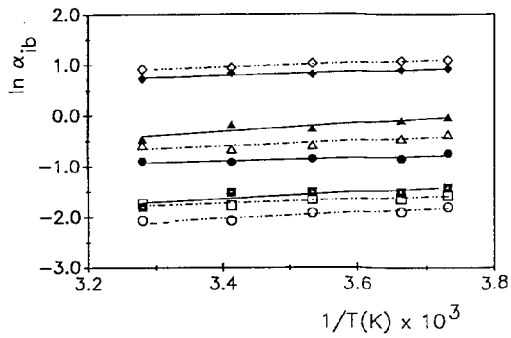

Fig. 4. Comparison of the temperature-dependent selectivities for the following pairs: aniline/benzene (□, ■); phenol/benzene (○, ●); nitrobenzene/benzene (△, ▲) and toluene/benzene (◇, ◆) on the $^{l}C_{18}$ (dashed line with open sympols) and AA_3 (solid line with filled sympols) phases; α_{ib} denotes selectivity for the i-th solute with respect to benzene.

plots in Fig. 4 lie below zero because benzene was retained longer on the $^{l}C_{18}$ and AA_3 phases than either phenol, aniline or nitrobenzene. These latter plots clearly demonstrate differences in the chromatographic behavior between the $^{l}C_{18}$ and AA_3 phases with respect to some of the polar compounds. This is illustrated by comparing the selectivity plots for aniline/benzene on the $^{l}C_{18}$ and AA_3 phases, which are similar to the lines for phenol/benzene, which are separated to a significant degree indicating that the OH group interacts differentially with the $^{l}C_{18}$ and AA_3 phases. Similarly the same effect was observed for the NO_2 group, but to a smaller degree.

In addition to the above studies, the hydrophobic interactions on the $^{h}C_{18}$, $^{l}C_{18}$ and AA_3 phases were examined further by measuring the methylene selectivity for alkylbenzene homologues using methanol–water (60:40) as the mobile phase. Shown in Fig. 5 is a plot of ln k' *vs.* the number of carbon atoms in the terminal alkyl portion of the mixed amino-alkylamide phases. The slopes of these plots (*i.e.*, methylene selectivity) for both the $^{l}C_{18}$ and AA_3 phases are similar and equal to about 0.57 which is also consistent with the idea that when the dominant mechanism controlling retention is based on hydrophobic interactions both materials behave similarly.

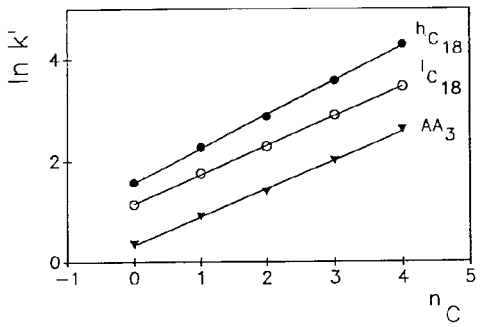

Fig. 5. Linear relationships between ln k' and the number of methylene groups (n_C) in alkylbenzenes measured on the $^{l}C_{18}$, $^{h}C_{18}$ and AA_3 packings (*cf.* Table 1) using the methanol–water (60:40, v/v) mobile phase. Other chromatographic parameters as in Fig. 2.

In addition to the above measurements, the $^{h}C_{18}$, $^{l}C_{18}$ and AA_3 phases were evaluated using acetonitrile–water (60:40) as the mobile phase. Shown in Fig. 6 are plots of ln k' *vs.* $1/T$ for benzene over a temperature range from 263 to 333 K. A cursory look at these data would seem to indicate that linearity was observed over a narrower range for the high-density octadecyl phase (293–323 K) compared to either the lower-density octadecyl or the AA_3 phases. As noted previously, a significant feature of the lower-temperature measurements were dramatic changes in peak symmetry and shape as illustrated in Fig. 7. Although these differences may

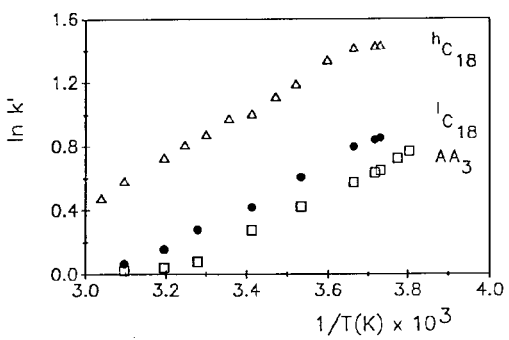

Fig. 6. The ln k' *vs.* $1/T$ plots for benzene measured on the AA_3 and C_{18} packings (*cf.* Table 1) using the acetonitrile–water (60:40, v/v) mobile phase. Chromatographic conditions as in Fig. 2.

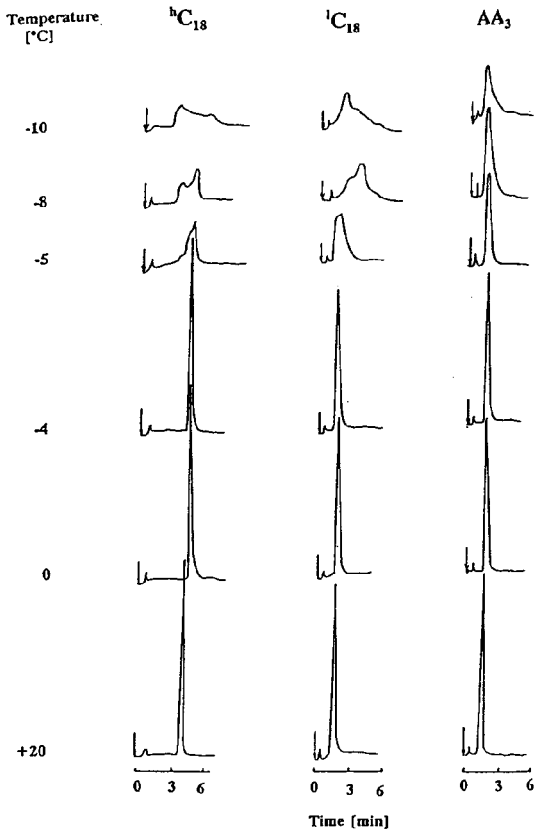

Fig. 7. Chromatograms for benzene recorded at different temperatures on the $^{h}C_{18}$, $^{l}C_{18}$ and AA_3 phases. Chromatographic conditions as in Fig. 6. The injected amount of benzene was equal to 40 ng.

be significant [27–29], based on the limited data obtained in the current study, it does not seem prudent to extract too much from them at the present time. However, additional work is now in progress to further elucidate the non-linear behavior and degradation of peak shape observed at the lower temperatures studied. The higher-temperature regions of the data shown in Fig. 6 were linear with slopes consistent with the methanol–water studies discussed above.

4. Conclusions

Comparative studies of mixed amino-alkylamide and conventional C_{18} bonded phases have shown that the specific interaction sites in the amino-alkylamide phases have a significant influence on solute retention and selectivity under reversed-phase conditions. In addition, improved peak symmetry was observed for polar solutes such as amines which makes these phases attractive for carrying separation of base type solutes. Systematic studies are now in progress to examine how differences in amidization influence solute retention. In addition, spectrometric investigations are being carried out in order to examine possible ligand–silanol interactions and their influence on peak symmetry.

5. Acknowledgements

The authors are grateful to Dr. M. Gangoda for some CP-MAS NMR measurements and the US Army Research Office for supporting this work (grant No. DAAL 03-90-G-0061).

6. References

[1] L.C. Sander and S.A. Wise, *CRC, Crit. Rev. Anal. Chem.*, 18 (1987) 299.
[2] C.F. Poole and S.K. Poole, *Chromatography Today*, Elsevier, Amsterdam, 1991.
[3] B. Buszewski, *Sc.D. Thesis*, Slovak Technical University, Bratislava, 1992 (in Slovak).
[4] J.G. Dorsey, J.P. Foley, W.T. Cooper, R.A. Barford and H.G. Barth, *Anal. Chem.*, 64 (1992) 324A.
[5] G.E. Berendsen, K.A. Pikaart and L. de Galan, *J. Liq. Chromatogr.*, 3 (1980) 1437.
[6] H.A. Claessens, C.A. Cramers, J.W. de Haan, F.A.H. den Otter, L.J.M. van de Van, P.J. Andree, G.J. de Kong, N. Lammers, J. Wijma and J. Zeeman, *Chromatographia*, 20 (1985) 582.
[7] J.J. Kirkland, J.L. Glajch and R.D. Farlee, *Anal. Chem.*, 61 (1989) 2.
[8] K.K. Unger (Editor), *Packings and Stationary Phases in Chromatographic Techniques*, Marcel Dekker, New York, 1990.
[9] B. Buszewski and R. Nasuto, *J. Anal. Chem. USSR, (Engl Transl.)*, 45 (1990) 1547.
[10] B. Buszewski and R. Lodkowski, *J. Liq. Chromatogr.*, 14 (1991) 1185.
[11] S.B. Ehtesham and R.K. Gilpin, *Chromatographia*, 32 (1991) 79.
[12] R.K. Gilpin, M. Jaroniec and S. Lin, *Anal. Chem.*, 63 (1991) 2849.

[13] S.G. Allenmark, *Chiral Separations by HPLC*, Ellis Horwood, Chichester, 1989.
[14] D.W. Amastrag, M. Hilton and L. Coffin, *LC·GC*, 9 (1991) 646.
[15] W.H. Pirkle and R.S. Readnour, *Chromatographia*, 31 (1991) 129.
[16] B. Feibush and C. Santasania, *J. Chromatogr.*, 544 (1991) 41.
[17] B. Buszewski, J. Schmid, K. Albert and E. Bayer, *J. Chromatogr.*, 552 (1991) 415.
[18] B. Buszewski, R.K. Gilpin and M. Jaroniec, presented at the *44th Pittsburgh Conference, Atlanta, GA, 1993*, Extended Abstracts, p. 477bP.
[19] K. Albert and E. Bayer, *J. Chromatogr.*, 544 (1991) 345.
[20] B. Buszewski, *Chromatographia*, 34 (1992) 573.
[21] B. Buszewski, J. Garaj, I. Novák and D. Berek, *Chem. Listy*, 81 (1987) 552.
[22] E. Grushka, H. Colin and G. Guiochon, *J. Chromatogr.*, 248 (1982) 325.
[23] H.J. Issaq and M. Jaroniec, *J. Liq. Chromatogr.*, 12 (1989) 2067.
[24] M. Jaroniec, *J. Chromatogr. A*, 656 (1993) 37.
[25] L.A. Cole and J.G. Dorsey, *Anal. Chem.*, 64 (1992) 1317.
[26] L.A. Cole, J.G. Dorsey and K.A. Dill, *Anal. Chem.*, 64 (1992) 1324.
[27] D. Morel and J. Serpinet, *J. Chromatogr.*, 200 (1980) 95.
[28] D. Morel and J. Serpinet, *J. Chromatogr.*, 214 (1981) 202.
[29] L.C. Sander and S.A. Wise, *J. Chromatogr.*, 61 (1989) 1749.

ELSEVIER

Journal of Chromatography A, 673 (1994) 21–29

JOURNAL OF CHROMATOGRAPHY A

Comparison of various extraction and clean-up methods for the determination of polycyclic aromatic hydrocarbons in sewage sludge-amended soils ☆

G. Codina, M.T. Vaquero, L. Comellas*, F. Broto-Puig

Secció de Cromatografia, CETS Institut Químic de Sarrià (Universitat Ramon Llull), Institut Químic de Sarrià s/n, 08017-Barcelona, Spain

(First received December 6th, 1993; revised manuscript received February 23rd, 1994)

Abstract

Different extraction and clean-up methods for the determination of polycyclic aromatic hydrocarbons (PAHs) in sewage sludge-amended soil were investigated. Soxhlet plus saponification extraction and silica gel clean-up provided the best results. HPLC with a programmable fluorescence detector performed accurate identification and quantification of PAHs. The initial PAH concentrations in sewage sludge-amended soil ranged from 8 ng/g for benzo[a]fluoranthene to 93 ng/g for phenanthrene, with a total PAH concentration of 417 ng/g. The weathering of PAHs in sludged soil was monitored for a 141-day period. The results indicated that low-molecular-mass PAHs were susceptible to abiotic and biotic loss processes.

1. Introduction

Polycyclic aromatic hydrocarbons (PAHs) are a group of organic compounds that are principally formed during the incomplete combustion of organic material such as coal, petrol, oil and wood. Wastewater catchments receive PAHs from two main sources: industrial and domestic fossil fuel spillages and urban runoff inputs that flush the hydrocarbons deposited on the ground surface from vehicles or heating systems. As a result of their very low aqueous solubility, PAHs are efficiently removed from the water during sedimentation in the wastewater treatment. This results in the formation of sewage sludges that typically contain between 1 and 10 mg/kg of each individual PAH [1–4].

A significant proportion of the generated sewage sludge is applied to land as an organic fertilizer or amendment. Because some PAHs are known or suspected carcinogens, the fate of these compounds in the soil environment is critical in assessing their potential hazard risk [5,6]. However, there is little information about the persistence or loss of PAHs in sewage sludge-amended soil and the mechanism of their biodegradation [7].

A prerequisite to determining the evolution of PAHs in sludged soils is to develop sensitive and effective analytical methods to measure their concentration. Their extraction and isolation from complex samples, where PAHs are only a minor fraction of the organics present, require

* Corresponding author.

☆ Presented at the *22nd Annual Meeting of the Spanish Chromatography Group, Barcelona, October 20–22, 1993.*

0021-9673/94/$07.00
SSDI 0021-9673(94)00190-K

accurate protocols. Several procedures have been described [8].

This paper discusses the use of Soxhlet or Soxhlet plus saponification extractions, and compares silica gel clean-up according to the EPA 3630B method with the specific PAH clean-up with XAD-2 [9, 10]. An HPLC method with both UV and fluorescence detection was also developed. Using the method developed, the weathering of PAHs from sewage sludge-amended soil was also studied for a 141-day period in a laboratory experiment.

2. Experimental

2.1. Experiment design and details

Anaerobically digested sewage sludge was obtained from DARGISA, a sewage aerobic treatment plant in Girona (Spain). The sludge was air-dried and ground to less than 0.4 mm before soil addition. Limey soil from Bellaterra (Barcelona, Spain) was ground and sieved to less than 2 mm.

High doses of sewage sludge (15%) were mixed with soil and were placed in 6-kg polyethylene containers. Three different treatments were adopted in duplicate: (a) control sewage sludged soil amended with 15% of sewage sludge (CON A, CON B), (b) sludge-amended soil to which hydrocarbons were added at twice the control concentration (PAH 2A, PAH 2B) and (c) sludged soil to which hydrocarbons were added at ten times the control concentration (PAH 10A, PAH 10B). Experimental soils were watered when necessary to maintain a moisture content of 20% in order to ensure half the water-holding capacity, which was appropriate to obtain the best microbiological activity [11]. Soils were sampled after 0, 4, 8, 15, 22, 32, 44, 60, 81 and 141 days. Homogeneous samples were guaranteed by sampling and mixing through all the container depth. The samples were preserved with formaldehyde (0.4%) and were stored in the dark at 4°C. Simultaneously two other experiments were applied: (a) sludge-amended soil with twice the hydrocarbon concentration of the control to which mercury(II) chloride ($HgCl_2$) (2% by mass) was added to ensure complete sterilization (PAH 2Hg) and (b) sludged soil with ten times the control concentration with the addition of 2% of $HgCl_2$ for sterilization (PAH 10Hg). These soils were sampled after 0 and 20 days.

2.2. Reagents and materials

Dichloromethane, hexane and pentane (Pestipur) were obtained from SDS (Peypin, France). Methanol and acetonitrile of HPLC grade and isooctane for residue analysis were supplied by Merck (Darmstadt, Germany). Toluene (purissimum grade) was purchased from Panreac (Barcelona, Spain) and was glass distilled prior to use. Deionized water was produced with a Millipore Milli-Q system from Waters (Milford, MA, USA). Anhydrous sodium sulphate (analytical-reagent grade) was supplied by Merck and was treated at 300°C for 12 h before analysis. Potassium hydroxide (analytical-reagent grade) and formaldehyde (35–40%) (purissimun grade) were obtained from Panreac. Silica gel 60 (63–200 μm) was supplied by Merck. XAD-2 from Alltech (Deerfield, IL, USA) was used.

Naphthalene (Na), fluorene (Fl), phenanthrene (Pa), anthracene (An), fluoranthene (Fa), pyrene (Pyr), chrysene (Chry), benzo[b]fluoranthene (BbFa), benzo[k]fluoranthene (BkFa) and benzo[a]pyrene (BaPyr) were obtained in pure form from Supelco (Bellefonte, PA, USA). Solid PAHs were dissolved in toluene in order to spike sludged soils. A 610-M commercial PAH mixture from Supelco, containing the previous PAHs and also acenaphthylene (Aci), acenaphthene (Ace), benz[a]anthracene (BaAn), dibenzo[*a,h*]anthracene (diBahAn), indenopyrene (I-P) and benzo[*ghi*]perylene (BghiPer), was used in appropriate dilutions with acetonitrile to study the chromatographic system and used as an external standard.

2.3. Soxhlet extraction

About 1 g of sewage sludge or 10 g of sludge-amended soil, thoroughly mixed with 10 g of anhydrous sodium sulphate, was Soxhlet extracted with 200 ml of dichloromethane for 6 h at

a rate of 4–6 cycles/h. The extract was then dried over 0.5 g of anhydrous sodium sulphate. The decanted extract was evaporated at 40°C in a rotary evaporator under reduced pressure to near dryness, dissolved in 1 ml of isooctane or acetonitrile for silica gel or XAD-2 clean-up, respectively, and re-evaporated to less than 1 ml.

2.4. Soxhlet and saponification extraction

Soxhlet extraction was carried out with 200 ml of dichloromethane for 6 h. The solvent was concentrated to 5 ml in a rotary evaporator under reduced pressure. A 100-ml volume of 0.5 *M* potassium hydroxide in methanol was added and the mixture was refluxed for 4 h in a water-bath at 80°C. After cooling 20 ml of Milli-Q-purified water were added and extraction was performed with hexane (3 × 50 ml). The combined organic extracts were dried over 0.5 g of anhydrous sodium sulphate. The decanted extract was evaporated at 40°C in a rotary evaporator under reduced pressure to near dryness, dissolved in 1 ml of isooctane or acetonitrile for silica gel or XAD-2 clean-up, respectively, and re-evaporated to less than 1 ml.

2.5. Silica gel clean-up

Silica gel was activated at 130°C for 16 h. The glass column (1.2 cm I.D.) was slurry packed in dichloromethane with silica gel (10 g) and a top layer of anhydrous sodium sulphate (0.5 g). The column was rinsed with 40 ml of hexane before use. The extract was transferred on to the column and sequentially eluted with 25 ml of hexane and 30 ml of hexane–dichloromethane (60:40) to give fractions enriched in alkanes and PAHs, respectively. The second eluate was evaporated under reduced pressure to near dryness and replaced with exactly 1 ml of acetonitrile.

2.6. XAD-2 clean-up

The glass column (10.4 × 1.2 cm I.D.) was slurry packed in methanol with XAD-2. The column was rinsed with 15 ml of pentane, 32 ml of toluene and 25 ml of methanol before use. The extract was transferred on to the column and sequentially eluted with 25 ml of methanol, 15 ml of pentane and 32 ml of toluene to give fractions enriched in polar compounds, alkanes and PAHs, respectively. The third eluate was evaporated under reduced pressure to near dryness and replaced with exactly 1 ml of acetonitrile.

2.7. Chromatographic instruments and conditions

A Tracer-Spherisorb ODS analytical column (5 μm, 243 mm × 4 mm I.D.) and a Spherisorb ODS guard column (4 mm I.D. cartridge), both from Teknokroma (Sant Cugat, Spain), were used. The chromatographic system consisted of a Waters Model 600E pump with a Rheodyne (Cotati, CA, USA) 20-μl loop injector. A Model 991 photodiode-array detector with integration software from Waters, a Model 470 fluorescence detector from Waters and a Model D-2000 integrator from Merck–Hitachi (Tokyo, Japan) were also used.

Acetonitrile and water were used as eluent components at a flow-rate of 1 ml/min. Linear gradient elution from 50% acetonitrile at 0 min to 100% acetonitrile at 25 min was applied, followed by isocratic elution with acetonitrile for 17 min.

The UV detector was set at 254 nm in combination with the diode-array detector to identify PAHs in the samples. The fluorescence excitation and emission wavelengths were changed during the chromatographic separation in order to obtain better sensitivity. The excitation/emission wavelengths were set as follows: 280/340 nm at 0 min, 250/376 nm at 16 min, 286/460 nm at 18 min, 305/430 nm at 19.5 min and 296/425 or 305/425 nm at 28 min to detect BghiPer or I-P, respectively.

3. Results and discussion

3.1. High-performance chromatography

The precision of the retention time within one day ranged from 0.2 to 0.8%; analyses from

day-to-day produced only a slight decrease in precision. The peak-height precision within one day ranged from 2.5 to 6.7% for the fluorescence detector and from 1.7 to 4.0% for the UV detector. The peak area precision was poorer, from 2.7 to 8.7% and from 2.3 to 3.7% for the fluorescence and UV detectors, respectively. The reproducibility from day-to-day of peak heights produced only a slight decrease in precision. Therefore, PAH determinations were performed by comparison of the peak heights with those of an external standard injected daily.

HPLC with fluorescence detection provided a linear response from 64 to 0.002 g/ml for each PAH and detection limits between 9 ng/ml for Na and 0.1 ng/ml for BkFa. HPLC with UV detection (254 nm) was also linear from 64 to 0.002 g/ml, but had higher detection limits between 62 ng/ml for Aci and 1 ng/ml for An. The detection limits calculated with a signal-to-noise ratio of 3 (IUPAC criteria) were decreased between 2- and 15-fold using fluorescence detection compared with UV detection.

3.2. Analytical procedure

A sample of sewage sludge-amended soil was submitted to the above-described extraction and clean-up methods. The subsequent PAH fractions were analysed by HPLC with photodiode-array and programmable fluorescence detection. The chromatograms are displayed in Fig. 1.

According to their retention times and UV spectra, several PAHs could be identified in the sludged soil: Pa, An, Pyr, Chry/BaAn, BbFa and BaPyr. Interferences from most other compounds in the extract were greatly reduced with fluorescence detection, resulting in the additional identification by retention times of Fl/Ace, Fa, BkFa and BghiPer. Moreover, HPLC with fluorescence detection is more selective and sensitive than HPLC with UV detection for the determination of PAHs and, therefore, is more suitable for determining them in sewage sludge-amended soils.

XAD-2 clean-up split the PAHs into two fractions: the low-fused PAHs were eluted with pentane and the high-fused PAHs with toluene. The silica gel column provided all PAHs in the second fraction together with alkylbenzenes, but these monoaromatic hydrocarbons did not interfere with HPLC analysis. Further, the concentration of low-fused aromatic hydrocarbons, namely Na and Fl/Ace, isolated with XAD-2 clean-up was lower than that obtained with silica gel clean-up. Losses were probably due to irreversible interactions of PAHs with the XAD-2 polymer and volatilization during toluene evaporation. Moreover, chromatograms of XAD-2 extracts presented more interferences, probably owing to the elution of monomers and oligomers of the polymer together with PAHs, although XAD-2 had been carefully cleaned. Hence the use of silica gel to clean up extracts appeared more suitable for PAH determinations.

Saponification improved the fluorescence profiles and enhanced the determination of PAHs. Associations between minor PAHs and lipid sludge fraction are reduced when the raw extract is submitted to a basic treatment, and liquid–liquid partitioning allows fatty acid removal and, therefore, extract clean-up is made easier.

The effectiveness of the methods was assessed with the analysis of a sludged soil spiked with PAHs. The recoveries were better for Soxhlet plus saponification extraction with silica gel clean-up (Table 1). Again, fluorescence detection was shown to perform better than UV detection in HPLC analyses. When the recoveries were calculated with UV chromatograms, Fa, Pyr and BkFa presented anomalous values, probably owing to difficulties in the quantification. In conclusion, Soxhlet plus saponification, silica gel clean-up and HPLC with fluorescence detection are suitable for PAH identification and quantification in sewage sludge-amended soil.

The precision of the selected procedure was studied with the analysis of a sludged soil sample in quadruplicate. The repeatability of analyses within one day was 17–31% with the exception of BghiPer (56%). The reproducibility of analysis from day-to-day was 25–37% with the exception of Na (81%). The accuracy of the method was tested by a standard addition analysis. Three different levels of addition were made in order to

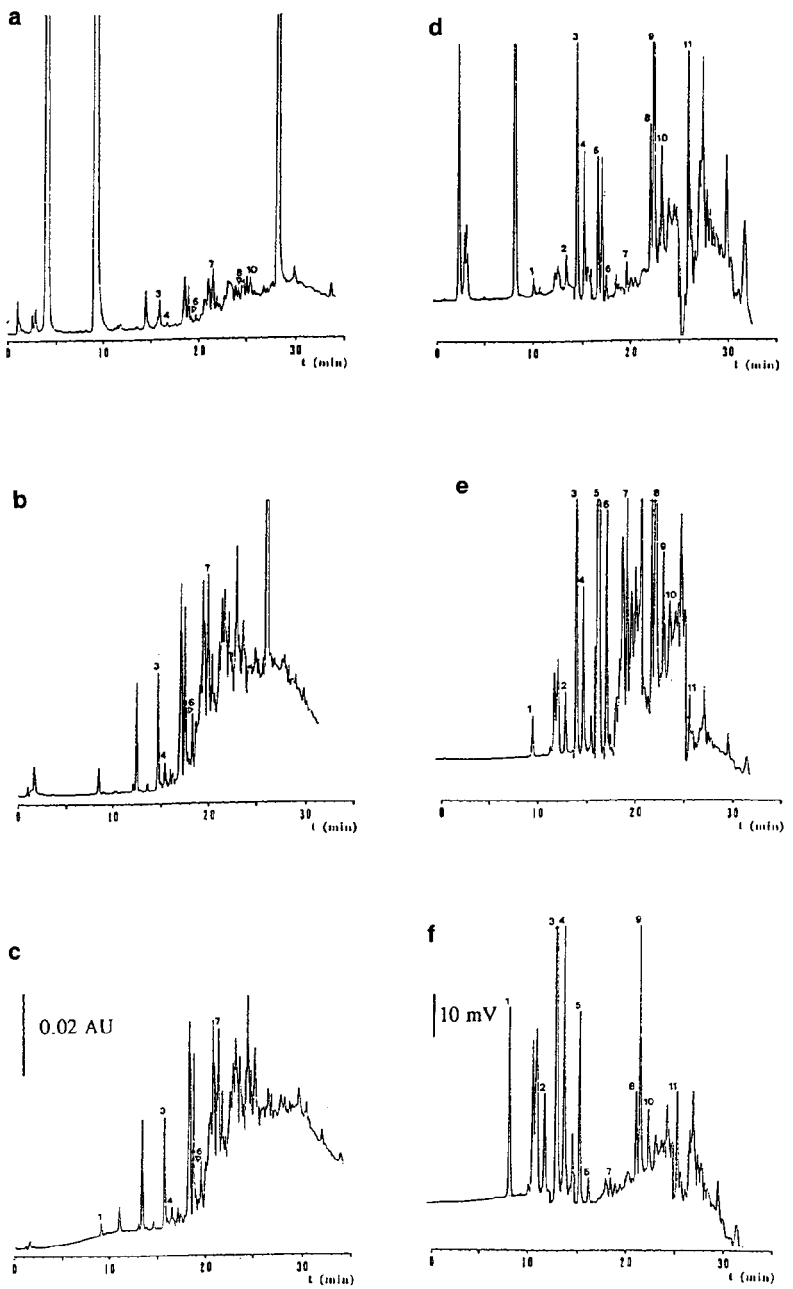

Fig. 1. (a–c) HPLC–UV and (d–f) HPLC–fluorescence detection of PAHs isolated from sewage sludge-amended soil by both extraction and clean-up methods: (a and d) Soxhlet with XAD-2 clean-up; (b and e) Soxhlet with silica gel clean-up; (c and f) Soxhlet plus saponification with silica gel clean-up. Identified PAHs: 1 = Na; 2 = Fl/Ace; 3 = Pa; 4 = An; 5 = Fa; 6 = Pyr; 7 = Chry/BaAn; 8 = BbFa; 9 = BkFa; 10 = BaPyr; 11 = BghiPer.

Table 1
Recoveries (%) of PAHs added to sewage sludge-amended soil obtained with different analytical methods

PAH	Soxhlet				Soxhlet + saponification			
	XAD-2		Silica gel		XAD-2		Silica gel	
	UV	Fluorescence	UV	Fluorescence	UV	Fluorescence	UV	Fluorescence
Na	0	0	46	41	0	2	74	80
Aci	7	–[a]	48	–[a]	21	–[a]	106	–[a]
Fl/Ace	63	8	64	53	42	21	128	119
Pa	70	70	40	46	117	115	108	102
An	41	41	50	50	96	95	106	106
Fa	159	65	240	61	162	124	256	108
Pyr	7	62	−9	212	79	107	−19	89
Chry/BaAn	76	61	43	52	146	132	95	96
BbFa	63	71	59	63	140	148	94	105
BkFa	111	65	174	59	185	142	233	106
BaPyr	59	50	80	41	107	120	121	82
diBahAn	44	62	0	56	120	148	108	101
I-P	0	–[a]	0	–[a]	172	–[a]	119	–[a]
BghiPer	0	54	46	54	145	114	103	93

[a] Do not have fluorescence at the programmed wavelengths.

increase the PAH concentration in the sewage sludged soil by two, five and ten times. The mean recoveries obtained were over 85%, except for Na (60%), Fl/Ace (44%), BaPyr (21%) and BghiPer (70%).

3.3. PAH losses from sewage sludge-amended soil

Significant losses of PAHs from sewage sludge-amended soil were achieved over the whole experimental period. Fig. 2 shows the results for HPLC with fluorescence detection at days 0, 8 and 141 for sample extracts taken from treatment CON B.

The losses of Na, Fl, Pa, An, Fa and Pyr were statistically different from zero, according to an analysis of variance at the $\alpha = 0.1$ level of confidence. Moreover, differences between loss percentages of these PAHs were very important. The low-molecular-mass PAHs appeared to be eliminated faster than the high-molecular-mass PAHs. The compound structure seems to influence PAH losses strongly. Losses of PAHs with the highest molecular mass, *i.e.*, Chry, BbFa, BkFa, BaPyr and BghiPer, were not statistically different from zero ($\alpha = 0.1$). These observations were consisted with other reported findings [12–14].

Fig. 3 shows the evolution of the total PAH concentration during the experimental period. This concentration also decreased statistically ($\alpha = 0.1$ level of confidence).

Half-lives were calculated for individual and total PAHs, as shown in Table 2. The expected increase in half-life with increasing molecular mass was observed in all the experiments. Further, half-life derived for experiments with the highest initial concentration of PAHs (PAH 10) are lower than those for the experiments with lower initial concentrations (CON and PAH 2). Losses of PAHs were statistically more rapid when the initial concentration was higher. Overall, PAHs added to the sludged soil appeared to be more susceptible to loss mechanisms and did not mimic the behaviour of sludge-applied PAHs.

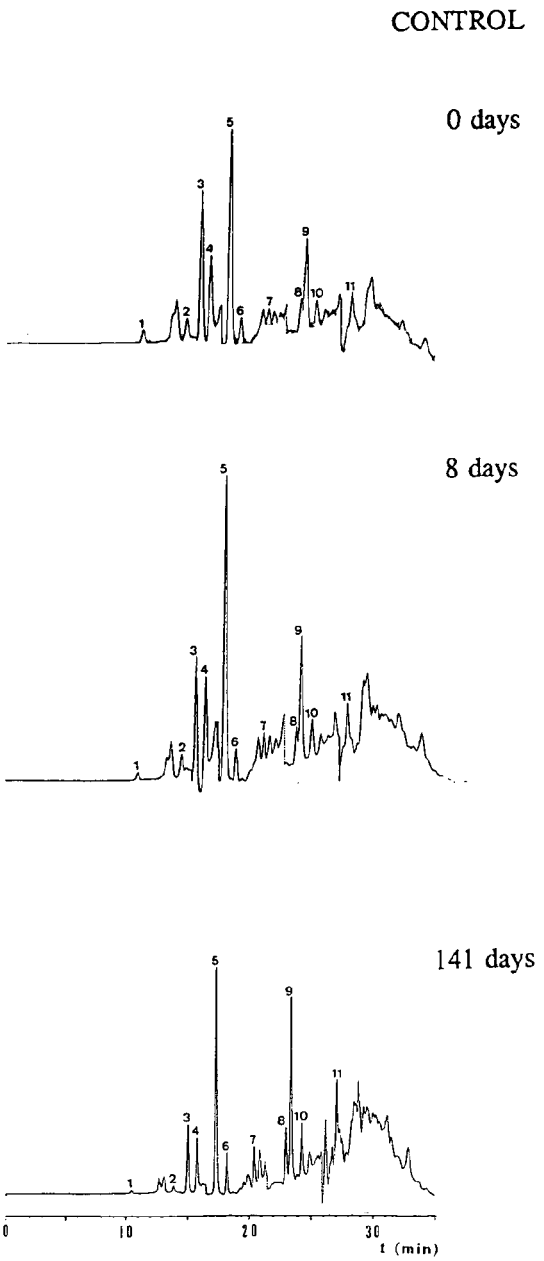

Fig. 2. HPLC–fluorescence detection of PAHs from CON experiment (sewage sludge-amended soil without addition) after 0, 8 and 141 days of evolution. Identified PAHs: 1 = Na; 2 = Fl/Ace; 3 = Pa; 4 = An; 5 = Fa; 6 = Pyr; 7 = Chry/BaAn; 8 = BbFa; 9 = BkFa; 10 = BaPyr; 11 = BghiPer.

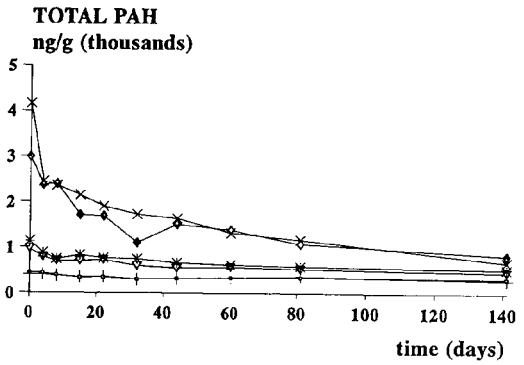

Fig. 3. Variation of total PAH concentration in sewage sludge-amended soil for each experiment *versus* time elapsed from the start of the experiment. □ = CON A; + = CON B; * = PAH 2A; ▽ = PAH 2B; × = PAH 10A; ◇ = PAH 10B.

3.4. Biotic and abiotic losses

Losses of PAHs from the sludged soils biologically inactived with $HgCl_2$ (2%) were due to abiotic mechanisms (mainly volatilization), whereas losses from the sludge-amended soil were due to the combination of both abiotic and biotic mechanisms. Biotic losses were then calculated by subtracting the abiotic losses from inactive soils from the total losses from biologically active soils. Fig. 4 shows the estimated abiotic and biotic loss percentages of PAHs in the experiment with double addition (PAH 2 and PAH 2Hg).

Biological loss processes were significant for some of the low-molecular-mass PAHs (Na, Fl, Pa and An). Losses for all PAHs occurred partially due to non-biological processes, and these were the main mechanisms of losses for Fa and Pyr.

As expected, the rate of biodegradation decreased with increasing number of benzene rings in the PAH molecules, probably owing to changes in the aqueous solubility, bioavailability and structural stability with increasing molecular mass. In literature it is reported that low-molecular-mass PAHs, such as naphthalene and phenanthrene, can act as the sole carbon/energy sources for microbes, while the multi-ringed

Table 2
PAH half-life derived for sewage sludge-amended soils

PAH	$t_{1/2}$ (days)					
	CON A	CON B	PAH 2A	PAH 2B	PAH 10A	PAH 10B
Na	3	3	3	3	2	2
Fl	16	13	7	11	3	7
Pa	14	18	6	7	4	7
An	24	29	20	2	4	14
Fa	260	175	100	102	46	69
Pyr	n.d.[a]	n.d.[a]	189	383	68	78
PAH	623	648	107	131	17	25

[a] Not determined.

species cannot act as sole sources, but may be degraded slowly in the environment by co-oxidation processes [7,14].

On the other hand, the percentage of abiotic losses decreased only slightly with increasing molecular mass. Other studies have shown greater differences between abiotic PAH losses, due to decreasing volatilization with increasing molecular mass [14].

Biodegradation seems to be an important process leading to the loss of low-molecular-mass PAHs in the soil system. This is feasible because the application of sludge to soil causes a period of enhanced microbial activity due to the addition of an available substrate and essential nutrients.

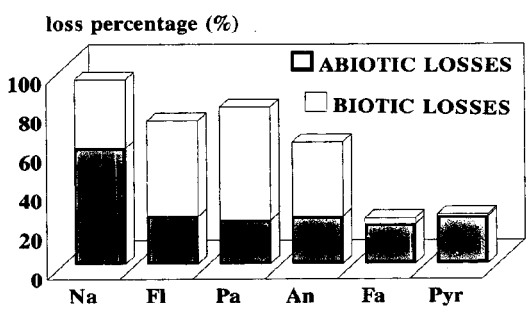

Fig. 4. Estimated abiotic and biotic loss percentages of some PAHs in 20 days from the experiment with double addition of PAHs (HID 2 and HID 2Hg).

4. Conclusions

Soxhlet plus saponification and HPLC with fluorescence detection are suitable for assessing PAH weathering in sewage sludge-amended soil. Losses of low-molecular-mass PAHs were significant over the experimental period, but high-molecular-mass PAHs were persistent. Moreover, the loss rates were faster for PAHs added at high concentrations to the sludged soil. The results suggested that biological degradation and abiotic processes were important for some of the low-molecular-mass PAHs.

Acknowledgements

We thank the CICYT, Spain, for financial support (NAT91-0340 project) and M.T.V. gratefully acknowledges the support of the CIRIT, Generalitat de Catalunya.

References

[1] M.T. Bomboi and A. Hernández, *Water Res.*, 25 (1991) 557.
[2] P.W.W. Kirk and J.N. Lester, *Environ. Technol.*, 12 (1990) 13.
[3] M.D. Webber and S. Lesage, *Waste Manag. Res.*, 7 (1989) 63.
[4] S.R. Wild, S.P. McGrath and K.C. Jones, *Chemosphere*, 20 (1990) 703.

[5] *Polynuclear Aromatic Compounds. Part 1. Chemical, Environmental and Experimental Data (IARC Monographs on the Evaluation of Carcinogenic Risks to Humans*, Vol. 32), IARC, Lyon, 1984.
[6] I.C.T. Nisbet and P.K. LaGoy, *Regul. Toxicol. Pharmacol.*, 16 (1992) 290.
[7] S.K. Mahmood and P. Rama Rao, *Bull. Environ. Contam. Toxicol.*, 50 (1993) 486.
[8] I. Blankehorn, D. Meijer and R.J. van Delft, *Fresenius' J. Anal. Chem.*, 343 (1992) 497.
[9] *Test Methods for Evaluating Solid Waste*, US Environmental Protection Agency, Washington, DC, 2nd revision, 1990, EPA Method 8310 (3630B).
[10] T. Spitzer and S. Kuwatsuka, *J. Chromatogr.*, 643 (1993) 305.
[11] J.M. Alcañiz, personal communication, 1992.
[12] S.R. Wild, M.L. Berrow and K.C. Jones, *Environ. Pollut.*, 72 (1991) 141.
[13] S.R. Wild, J.P. Obbard, C.I. Munn, M.L. Berrow and K.C. Jones, *Sci. Total Environ.*, 101 (1991) 235.
[14] S.R. Wild and K.C. Jones, *Environ. Toxicol. Chem.*, 12 (1993) 5.

ELSEVIER

Journal of Chromatography A, 673 (1994) 31–35

JOURNAL OF CHROMATOGRAPHY A

Quantitative analysis of mixtures of symmetric and mixed anhydrides

Abraham J. Domb*

Department of Pharmaceutical Chemistry, School of Pharmacy, Faculty of Medicine, Hebrew University of Jerusalem, Jerusalem 91120, Israel

(First received December 21th, 1993; revised manuscript received February 24th, 1994)

Abstract

HPLC and GC methods were developed for the determination of symmetrical and mixed anhydrides. Both symmetrical and mixed anhydrides and their respective acids were determined in a single reversed-phase HPLC run using acetonitrile–water as the mobile phase. GC was useful for the quantitative analysis of a mixture of mixed anhydrides symmetric anhydrides. Similar results were obtained from the HPLC and GC analyses of mixtures containing mixed anhydrides of fatty acids with benzoic acid and their corresponding symmetrical anhydrides and acids. These methods are useful in the investigation of anhydride chemistry, the routine analysis of raw materials and the quality control and purity determination of polymers and other compounds containing anhydrides.

1. Introduction

Acid anhydrides are among the most important classes of reagents used in organic synthesis. In the last few years, anhydride materials have been of great interest for use as polymeric drug carriers [1] and as prodrugs [2], to improve administration and bioavailability of drugs. They find widespread use in the formulation of resin systems for advanced composites [3]. Despite their importance, very little has been reported on the determination of anhydrides, particularly mixed anhydrides.

Direct determination of anhydrides is often difficult owing to their susceptibility to hydrolysis. Most published procedures for direct measurements use spectrophotometric techniques, *e.g.*, IR [4] and ^{1}H NMR spectrometry [5], to monitor functional groups. Indirect techniques such as titration [6], spectrophotometry [7], gas chromatography [8] and liquid chromatography [9] involve hydrolysis and derivatization; these are often multi-step and time-consuming methods. A direct normal-phase HPLC method for the determination of a few commercially important cyclic anhydrides was reported recently [10]. These methods are useful for the determination of total anhydride content, but not for the quantitative analysis of mixtures of symmetrical and mixed anhydrides.

We report on two methods for the quantitative analysis of mixtures of various anhydrides and their corresponding acids in a single step. The methods involve reversed-phase HPLC using

* Corresponding author.

* Affiliated with The David Bloom Center for Pharmacy.

SSDI 0021-9673(94)00242-2

acetonitrile–water as the mobile phase and GC using a methylphenylsilicone column.

2. Experimental

2.1. Chemicals and reagents

Acetic, propionic, butyric, pivalic, hexanoic, octanoic, lauric, palmitic, stearic, benzoic, phthalic, succinic and maleic anhydride, 1,2,5-benzenetricarboxylic anhydride (BTrCA), 1, 2, 4, 5 - benzenetetraboxylic dianhydride (BTCA), 1,2,3,4-tetrahydrofuranetetracarboxylic dianhydride (THFTCA) and their respective acids and acid chlorides were purchased from Aldrich (Milwaukee, WI, USA). Mixed anhydrides were prepared by the reaction between acids and acid chlorides (1.1:1 molar ratio) in dichloromethane in the presence of poly(4-vinylpyridine) (Reillex 402; Reilly Industries, NJ, USA) as acid acceptor. After 1 h at 0°C, the solvent was evaporated to dryness and the liquid residue was weighed and analysed for anhydride formation by IR and ^{1}H NMR spectrometry. HPLC-grade acetonitrile and dichloromethane were purchased from Lab-Scan (Dublin, Ireland). Tritiated water (1 mCi/ml) was purchased from New England Nuclear (Boston, MA, USA) and was diluted to 10 μCi/ml using deionized water. Scintillation solution was obtained from Lumax (Landgraaf, Netherlands).

2.2. Apparatus and assay conditions

The HPLC apparatus consisted of an HP 1050 (Hewlett-Packard, Palo Alto, CA, USA) modular system including a diode-array UV detector and an HPCHEM IBM-compatible data system with a ThinkJet printer. A Rheodyne (Cotati, CA, USA) injection valve equipped with a 20-μl loop was used, and the samples (10 μl in acetonitrile) were eluted through a C_8 column (Supelcosil LC-8, 100 Å, 5 μm) (250 × 4.6 mm I.D.) (Supelco, Bellefonte, PA, USA). Normal-phase analysis was conducted using a silica column (Supelcosil LC-Si, 100 Å 5 μm) (250 × 4.6 mm I.D.) (Supelco) and hexane–tetrahydrofuran mixtures as mobile phase.

GC analysis was conducted on a HP5890 gas chromatograph (Hewlett-Packard) with an HP 3396A integrator and a flame ionization detector. An HP Ultra 2 (25 m × 0.2 mm × 0.11 μm) column packed with methyl–5% phenylsilicone was used. The following conditions were employed: detector and injector temperatures, 260°C; column temperature constant at 150°C; and helium, air and hydrogen flow pressures 40, 60 and 40 p.s.i., respectively (1 p.s.i. = 6894.76 Pa). IR spectrometry was performed on a Perkin-Elmer (Norwalk, CT, USA) Model 1310 spectrophotometer. Samples were cast on to NaCl plates. Acids and solid samples were either pressed into KBr pellets or dispersed in Nujol on to NaCl plates. ^{1}H NMR spectra were obtained on a Varian (Palo Alto, CA, USA) 300-MHz spectrometer using 1% (w/v) solutions in $CDCl_3$ containing tetramethylsilane (TMS) as internal reference. Radioactivity counting was conducted on a Model 1211 RackBeta liquid scintillation counter (LKB–Wallac, Finland).

2.3. Anhydride stability in mobile phase

The hydrolytic stability of the anhydride molecules in the HPLC mobile phase mixtures was determined using 1 mg/ml solutions of benzoic and hexanoic anhydride in acetonitrile–water mixtures (50:50 and 70:30, v/v) maintained at 25°C. Samples taken from the solution every 10 min for 60 min were analysed by HPLC (see above). The 60-min aliquots were freeze-dried and the solid residue was dissolved in deuterated chloroform and analysed for anhydride by IR and ^{1}H NMR spectrometry.

In a second experiment, 1 mg/ml solutions of benzoic and lauric anhydride in a radioactive mixture of acetonitrile–water (7:3, v/v; ^3H_2O 10 μCi/mL) were maintained at 25°C for 30 min. The radioactive mixtures were prepared from acetonitrile and 10 μCi/ml tritiated water. After 30 min, the solutions were freeze-dried and dissolved in Lumax scintillation solution and the radioactivity was determined.

3. Results and discussion

3.1. Recovery and stability of anhydrides in the HPLC mobile phase

Initial work was directed at determining the stability of the anhydride molecules towards hydrolysis in acetonitrile–water mixtures. Two experiments were conducted. In the first, solutions of benzoic and hexanoic anhydride in acetonitrile–water (50:50 and 70:30, v/v) were followed for 60 min at 25°C. Samples removed from the solutions were freeze-dried and the residue was analysed by HPLC and IR and ^{1}H NMR spectrometry. HPLC analysis (see above) of the samples removed from the acetonitrile–water mixtures showed the peaks of the anhydrides with no emergence peaks of benzoic or hexanoic acid. IR and ^{1}H NMR analyses of the residual materials after freeze-drying gave similar spectra to those of the starting anhydride molecules. In the second experiment, the potential formation of acidic degradation products from the reaction with the water component of the mobile phase was investigated using radiolabelled water. Benzoic and lauric anhydride isolated from acetonitrile–^3H_2O (7:3, v/v) after 30 min at room temperature did not contain any radioactivity (the dpms were similar to the background). These experiments prove that the anhydride molecules dissolved in the mobile phase do not undergo hydrolysis during the course of analysis.

3.2. Determination of anhydrides by HPLC

Aliphatic and aromatic anhydrides were determined by reversed-phase HPLC (Table 1 and Fig. 1). Short-chain aliphatic and aromatic anhydrides were separated at retention factor (k') of 0.20–0.80, using water–acetonitrile (50:50, v/v) and UV detection at 237 nm. Long-chain anhydrides were eluted at $k' = 2.70$–4.93, using pure acetonitrile. The corresponding mixed an-

Table 1
HPLC of anhydrides

Anhydride (RCOOCOR)	R	k'	Mobile phase (acetonitrile–water)
Acetic	CH_3	0.18	50:50
Propionic	CH_3CH_2	0.35	50:50
Butyric	$CH_3(CH_2)_2$	0.47	50:50
Hexanoic	$CH_3(CH_2)_4$	0.70	50:50
Heptanoic	$CH_3(CH_2)_5$	0.79	50:50
Decanoic	$CH_3(CH_2)_8$	3.74	70:30
Lauric	$CH_3(CH_2)_{10}$	4.02	70:30
Palmitic	$CH_3(CH_2)_{14}$	4.37	70:30
Stearic	$CH_3(CH_2)_{16}$	4.66	70:30
Succinic	$-CH_2CH_2-$	2.18	50:50
Maleic	$-CH{=}CH-$	0.48	50:50
Benzenetricarboxylic anhydride		0.44	50:50
Phthalic	$-C_6H_4-$	1.11	50:50
Benzoic	C_6H_5	0.27	30:70
THF-tetracarboxylic anhydride		0.56	50:50
Benzenetetracarboxylic anhydride		0.63	50:50
Benzoic acid		0.18	30:70
THF-tetracarboxylic acid		0.19	50:50
Benzenetetracarboxylic acid		0.19	50:50
Aliphatic acids	$CH_3(CH_2)_{0-10}$	0–0.20	30:70

Analysis using a C_8 column, acctonitrile–water as mobile phase at a flow-rate of 1 ml/min and UV detection at 237 nm. The retention factor, k', was calculated from $k' = (t_R - t_0)/t_0$, where $t_0 = 2.70$ min.

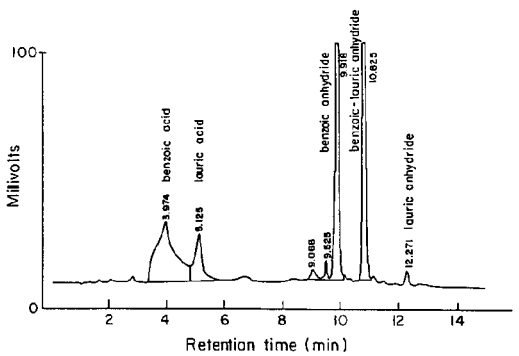

Fig. 1. Chromatogram of the symmetrical and mixed anhydrides of benzoic and lauric acid, obtained by HPLC using a C_8 column with acetonitrile–water (30:70, v/v) as the mobile phase.

hydrides of aliphatic and aromatic acids were eluted at intermediate times. For example, benzoic anhydride, benzoic–lauric mixed anhydride and lauric anhydride were eluted with acetonitrile–water (70:30, v/v) at $k' = 2.67$, 3.00 and 3.54, respectively (Fig. 1). Linear relationships between anhydride concentration and peak area were found with detection limits of 1 and 10 μg/ml for aromatic and aliphatic anhydrides, respectively.

Several cyclic anhydrides of commercial importance as curing agents and plasticizers in polymer composites and precursors for polyimide formation were studied (Table 1). The cyclic anhydrides were eluted at $k' = 0.48$–1.96 and their corresponding acids at $k' = 0.20$–0.48.

For comparison we followed the normal-phase method described by Patterson and Escott [10] using a normal-phase silica column with a mixture of anhydrous hexane and tetrahydrofuran as the mobile phase. Both aromatic and aliphatic anhydrides were eluted at close retention times with $k' < 0.45$. The corresponding acids were eluted at longer retention times, $k' > 0.45$. Attempts to optimize the separation of the various anhydrides by altering the ratio between hexane and tetrahydrofuran and the flow-rate were unsuccessful. Under all conditions, the retention times for the anhydrides were short ($k' = 0.10$–0.45), which was not useful for the quantitative analysis of a mixture of anhydride molecules. This method, however, is useful for the determination of the acid content and the total anhydride content in mixtures of acids and anhydrides.

3.3. Determination of anhydrides by GC

Mixtures of various anhydrides and acids were analysed by GC. As shown in Fig. 2, a mixture containing hexanoic acid, benzoic acid, hexanoic anhydride, mixed benzoic–hexanoic anhydride and benzoic anhydride was separated. Aromatic anhydrides were retained longer than the aliphatic anhydrides, while mixed anhydrides were eluted at intermediate retention times.

These HPLC and GC methods were used for the quantitative analysis of reaction mixtures aimed at the formation of mixed anhydrides from acids and acid chlorides. These reaction mixtures contained mixed and symmetrical anhydrides and the corresponding acids. As shown in Table 2, the results obtained by HPLC and GC methods were in good agreement. Both methods showed distinct peaks for the symmetrical and mixed anhydrides and the corresponding acids, thus permitting the direct quantitative analysis of the reaction mixture in a single run.

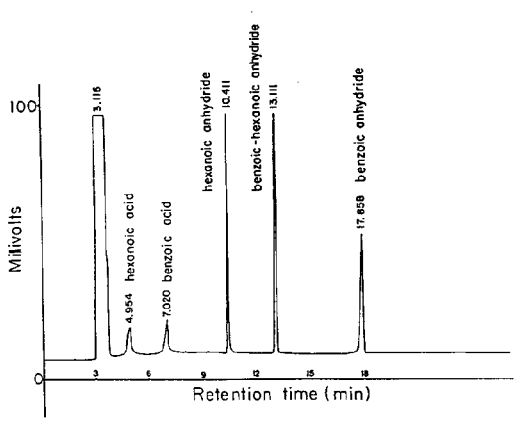

Fig. 2. Chromatogram of the symmetrical and mixed anhydrides of benzoic and lauric acid, obtained by GC using a methyl–5% phenylsilicone column with helium as gas carrier at 150°C and flame ionization detection.

Table 2
HPLC and GC analysis of mixed anhydrides from the reaction between acid and acid chlorides

Acid RCOOH (R)	Acid chloride R'COCl (R')	Total yield (%)	Mixed anhydride (%)	
			HPLC	GC
C_6H_5	CH_3	89	45	52
C_6H_5	CH_3CH_2	90	50	56
C_6H_5	$CH_3(CH_2)_4$	92	65	66
$CH_3(CH_2)_4$	C_6H_5	84	74	69
C_6H_5	$CH_3(CH_2)_6$	88	70	67
C_6H_5	$CH_3(CH_2)_{12}$	89	72	65
C_6H_5	$CH_3(CH_2)_{16}$	84	68	65
C_6H_5	4-$CH_3C_6H_5$	80	75	70
$CH_3(CH_2)_{10}$	C_6H_5	83	72	67
$CH_3(CH_2)_4$	$CH_3(CH_2)_{16}$	86	74	65
$CH_3(CH_2)_4$	$CH_3(CH_2)_{12}$	82	80	68

Analysis of the reaction mixture between the acid and acid chloride (1.1:1 molar ratio) and poly(4-vinylpyridine) (PVP) (2.5 equiv.) as acid acceptor at 0°C for 1 h. Results are for three independent experiments with an error of less than 5%.

Acknowledgements

The author thanks Mishael Haimove and Osnat Shaia for their help. This work was supported by grants from the Eliahu and Tatiana Leszczynski Research Foundation and the United States–Israel Binational Science Foundation, No. 91-0020/1.

References

[1] A.J. Domb, S. Amselem and M. Maniar, *Adv. Polym. Sci.*, 107 (1993) 93.
[2] A.J. Domb, presented at *ACS Meeting, Division of Organic Chemistry, Washington, DC, August 1992.*
[3] P.M. Hergenrother, in D. Wilson, H.D. Stenzenberger and P.M. Hergenrother (Editors), *Polyimides*, Chapman & Hall, New York, 1990.
[4] M.M. Koton, V.V. Kurdiavatse and V.M. Svetlichy, *Polyimides—Synthesis, Characterization and Applications*, Vol. 2, Plenum Press, New York, 1984.
[5] W. Heyde, *Fresenius' Z. Anal. Chem.*, 320 (1985) 667.
[6] K.K. Verma and P. Tyagi, *Anal. Chem.*, 56 (1984) 2157.
[7] J. Bartos, *Talanta*, 27 (1980) 583.
[8] E.P. Usova and G.S. Sirova, *Zh. Anal. Khim.*, 38 (1983) 946.
[9] R. Geyer and G.A. Saunders, *J. Liq. Chromatogr.*, 9 (1986) 2281.
[10] S.D. Patterson and R.E.A. Escott, *High Perform. Polym.*, 2 (1990) 197.

ELSEVIER

Journal of Chromatography A, 673 (1994) 37–43

JOURNAL OF CHROMATOGRAPHY A

High-performance liquid chromatographic determination of the enantiomers of carnitine and acetylcarnitine on a chiral stationary phase

Takahiro Hirota*, Kenjiro Minato, Kazuhiro Ishii, Noriyuki Nishimura, Tadashi Sato

Analytical Chemistry Research Laboratory, Tanabe Seiyaku Co., Ltd., 16-89, Kashima 3-chome, Yodogawa-ku, Osaka 532, Japan

(First received January 11th, 1994; revised manuscript received March 8th, 1994)

Abstract

A method was developed for determining the respective D-isomers in L-carnitine and acetyl-L-carnitine by high-performance liquid chromatography (HPLC). DL-Carnitine and acetyl-DL-carnitine were derivatized with 9-anthryldiazomethane to increase the interaction between the solutes and a chiral stationary phase and also the sensitivity; the simple derivatization was carried out under mild conditions of standing at 50°C for 20 min. The enantiomeric separations of the respective derivatives were achieved by HPLC on a commercially available chiral column (Chiralcel OD-R) with a mobile phase of 0.5 *M* sodium perchlorate solution–acetonitrile (3:2). It was confirmed that this method shows good specificity, reproducibility, linearity, accuracy and sensitivity (detection limit for acetyl-D-carnitine ≈0.01%).

1. Introduction

Both L-carnitine (L-C) and acetyl-L-carnitine (L-AC) are biological substances localized in various tissues such as the brain, heart, liver, kidney and muscle. L-C is essential for the transport and mitochondrial β-oxidation of long-chain fatty acids [1,2]. Another function of L-C is in the promotive excretion of accumulated short-chain fatty acids resulting from excess drug administration or metabolic disorder. Since 1960, DL-carnitine (DL-C) has been used as a drug for anorexia, dyspepsia, senile digestive hypergasia (because of its pharmacological effects of acceleration of digestive fluid secretion), enterokinesis and sugar and lipid metabolism. On the other hand, it is reported that D-C and L-C have different pharmacological activities and toxicity [3,4].

L-AC has stimulatory actions of learning behaviour from the viewpoint of ethopharmacology [5,6], so that it is expected to be useful as a cerebral metabolic enhancer [7,8]. On the other hand, the D-enantiomer does not show these effects [9,10].

It is very important to establish the enantiomeric determination and separation techniques for DL-C and DL-AC in order to ensure the quality of the drug and to investigate the phar-

* Corresponding author.

0021-9673/94/$07.00
SSDI 0021-9673(94)00246-6

macological effects and the pharmacokinetics of the enantiomers of DL-C and DL-AC in detail.

There has been only one report concerning the determination of the D-isomer contained in L-AC [11]. This method, however, is not a direct separation technique but an indirect assay by enzymatic reaction. The D-AC contained in L-AC is stereoselectively converted into D-C by treatment with acetylcholinesterase, and the D-C produced is determined by HPLC on a non-chiral column. That is, trace amounts of D-AC would not be able to be determined in the presence of carnitine initially as an impurity or decomposition product. Further, this method has some disadvantages regarding the cost, detection limit and reproducibility.

So far, no study has been reported on the HPLC separation of the enantiomers of carnitine or acylcarnitines. It is probable that the difficulties are due to their high polarity and low UV absorption.

We tried various chromatographic techniques to establish a practical method for the enantiomeric determination of carnitine and acetylcarnitine. As the result, it was found that the enantiomeric determination of these compounds could be achieved by HPLC on a commercially available chiral column (Chiralcel OD-R) [12–14], following derivatization with (9-anthryl-diazomethane (ADAM); ADAM has been widely used for the determination of variable fatty acids, etc. [15,16] and found to be able to react with acylcarnitines under mild conditions [17,18].

This paper reports the investigation of the various derivatization and HPLC conditions in order to establish the most suitable approach. We also describe the method validation and its application to optical purity testing for L-AC drug substances.

2. Experimental

2.1. Materials

DL-Carnitine was obtained from Nacalai Tesque (Kyoto, Japan), L-carnitine and acetyl-DL-carnitine from Sigma (St. Louis, MO, USA), acetyl-L-carnitine and crotonylbetain from Sigma Tau (Rome, Italy) and ADAM from Funakoshi Yakuhin (Tokyo, Japan). Acetonitrile of HPLC grade and other organic solvents of analytical-reagent grade were purchased from Katayama Kagaku (Osaka, Japan). Water was purified with a Millipore Ro-60 water system (Nihon Millipore, Tokyo, Japan) and mobile phases were passed through a membrane filter of 0.45-μm pore size (Fuji Photo Film, Tokyo, Japan) prior to use. All other reagents were of analytical-reagent grade from Katayama Kagaku.

2.2. Apparatus

The chromatographic system consisted of a Shimadzu (Kyoto, Japan) LC-9A pump, a Rheodyne Model 7125 injector with a 20-μl loop, a Shimadzu CTO-2A column oven, a Shimadzu SPD-6A variable-wavelength UV detector and a Shimadzu RF-535 fluorescence detector. The chromatograms were recorded on a Shimadzu Chromatopac C-R5A. A Shimadzu SPD-M6A photodiode-array detector was used to monitor the UV spectra of the peaks.

2.3. Derivatization procedure

To 0.5 ml of an aqueous solution of acetylcarnitine or carnitine (5 mg/ml) was added acetone to 100 ml. To 1 ml of this solution, 0.25 ml of a solution of ADAM in acetone (1 mg/ml) was added. The mixture was allowed to stand at 50°C for 20 min. After evaporating the solvent under a stream of nitrogen, 2 ml of dilute perchloric acid (1:1000) was added to the residue, and washed twice with 6 ml of diethyl ether to remove unchanged ADAM. To 1 ml of the aqueous phase was added 1 ml of acetonitrile, and 20 μl of the solution were injected into the HPLC system. The procedure was performed in light-resistant containers with protection from sunlight.

Fig. 1 shows the reaction of acetylcarnitine or carnitine with ADAM.

2.4. HPLC

The chromatographic separation was performed by using a Chiralcel OD-R column (250

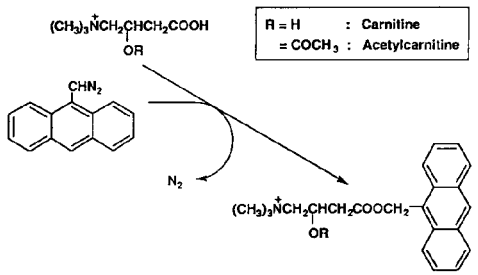

Fig. 1. Reaction of carnitine or acetylcarnitine with 9-anthryldiazomethane (ADAM).

mm × 4.6 mm I.D.) (Daicel Chemical Industries, Osaka, Japan). It was packed with silica-based cellulose tris(3,5-dimethylphenylcarbamate) as a chiral stationary phase (particle size 10 μm). The mobile phase was 0.5 *M* sodium perchlorate solution–acetonitrile (3:2) at a flow-rate of 0.8 ml/min. The column temperature was 25°C (ambient). The effluent was measured with a UV detector (254 nm) or fluorescence detector (excitation at 365 nm, emission at 412 nm); 254 nm was the UV absorption maximum of the solutes measured with a photodiode-array detector.

2.5. Calculation of D-form content

The content of the D-form in L-AC (or L-C) was calculated by the following equation:

$$\text{D-form content } (\%) = \frac{A_D}{A_D + A_L} \cdot 100$$

where A_D = peak area of D-AC (or D-C)–ADAM and A_L = peak area of L-AC (or L-C)–ADAM.

3. Results

3.1. Preparation of the ADAM derivatives

Effect of water content in the reaction mixture

Taking into account the solubility of acetylcarnitine or carnitine and the application to a biological sample, the derivatization was carried out in acetone containing a small amount of water. The effect of the water content on the yield of the ADAM derivatives was investigated. The peak areas of L-AC–ADAM and L-C–ADAM were observed to be constant and maximum over the range of water content in the reaction mixture from 0.16 to 8.0%. The high water content causes a long evaporation time. Therefore, the water content in the reaction mixture was fixed at 0.4%, which could dissolve L-AC or L-C.

Effect of ADAM concentration

The effect of the ADAM concentration on the reaction yield was investigated and the results are shown in Fig. 2. With both L-AC and L-C the peak areas were constant and maximum when the ADAM concentration of an additional acetone solution was more than about 0.5 mg/ml. From the results, the ADAM concentration was fixed at 1.0 mg/ml, that is, about a tenfold molar excess of the reagent.

Effects of reaction temperature and time

First the effect of the reaction temperature on the yield was investigated. The highest and constant peak area of L-AC–ADAM or L-C–ADAM was obtained over the range of the reaction temperature *ca.* 40–60°C. A high temperature leads to decomposition of ADAM and slight hydrolysis of L-AC. Next the effect of the reaction time at 50°C was examined. The results shown in Fig. 3 indicate that the derivatization reaction was completed in about 20 min at 50°C, and this condition was adopted.

Stability of ADAM derivatives

The stability of ADAM derivatives of L-AC and L-C was investigated. Fig. 4 shows the effect

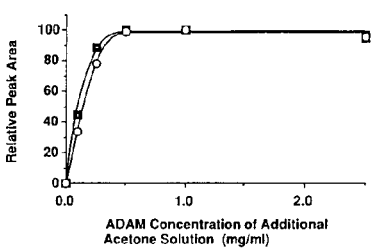

Fig. 2. Effect of ADAM concentration on the reaction yield of (○) carnitine and (□) acetylcarnitine.

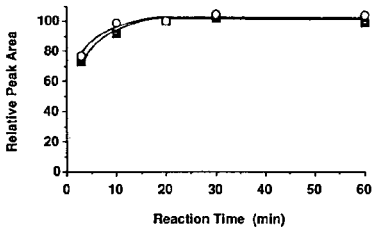

Fig. 3. Effect of reaction time on the reaction yield of (○) carnitine and (□) acetylcarnitine.

of acetonitrile addition and protection from light on the stability at room temperature. Evidently both the addition of acetonitrile and protection from light contributed to the stability of ADAM derivatives, and made them stable for 24 h at room temperature. Further, the theoretical plate numbers of the peaks increased following acetonitrile addition compared with water addition.

3.2. Conditions for HPLC

Mobile phase

In the following investigations, different aqueous solutions mixed with acetonitrile (3:2) were used for elution.

Effect of ionic species. The effect of ionic species on the solutes (D,L-AC–ADAM and D,L-C–ADAM) was investigated using perchlorate and phosphate. The retention times, theoretical plate numbers of the peaks and enantioselectivity increased with the use of perchlorate instead of phosphate.

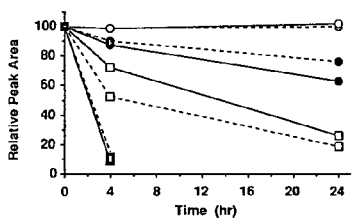

Fig. 4. Stability of carnitine–ADAM and acetylcarnitine–ADAM derivatives. ○ = Addition of acetonitrile, protection from light; □ = addition of acetonitrile, no protection from light; ● = no addition of acetonitrile, protection from light; ■ = no addition of acetonitrile, no protection from light. Dashed lines = carnitine; solid lines = acetylcarnitine.

Effect of ionic strength. The effect of ionic strength on the solutes was investigated using perchlorate over the concentration range 0.1–1.0 *M*. The retention times of the solutes increased slightly with increase in the ionic strength. However, little effect was observed on the other factors.

Effect of pH. The effect of pH on the solutes was investigated using 0.5 *M* perchlorate buffer over the pH range 2–6. The peaks were hardly affected by the pH of the buffer.

Effect of organic solvents. The difference in the effect on the solutes between acetonitrile (40%) and methanol (80%) was examined using 0.5 *M* sodium perchlorate solution. Methanol contributed to a better enantioselectivity, but resulted in decreases in the theoretical plate numbers and selectivity between carnitine and acetylcarnitine.

Column temperature

The effect of column temperature on the solutes was investigated over the range of 25°C (ambient)–50°C using 0.5 *M* sodium perchlorate solution–acetonitrile (3:2). As expected, the retention times of the solutes decreased with increase in column temperature. Further, it was found that a combination of a low column temperature and a high flow-rate gave a better enantioselectivity than that of a high column temperature and a low flow-rate.

Fig. 5 shows a typical chromatogram for the simultaneous chiral separation of carnitine and acetylcarnitine.

3.3. Method validation

Specificity

D-AC, L-C and crotonylbetain are possible impurities or decomposition products in L-AC as a drug. Fig. 6 shows the chromatograms of the following samples obtained by this method; (A) L-AC (spiked with 1% of D-AC), (B) L-C (spiked with 1% of D-C), (C) crotonylbetain and (D) the reagent blank. The results indicate that this method has good specificity for the optical

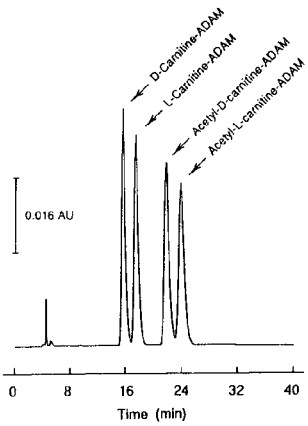

Fig. 5. Chiral separation of the enantiomers of carnitine and acetylcarnitine.

purity testing of L-AC, and permits the simultaneous determination of the enantiomers of carnitine and acetylcarnitine.

Reproducibility (precision)

The reproducibility was investigated from six determinations of the content of the D-form in a single batch of L-AC (Lot No. 3). The results are given in Table 1. The relative standard deviation (R.S.D.) was 0.84%; the good reproducibility of this method was confirmed.

Linearity and accuracy

The linearity and accuracy was investigated from determinations of the content of the D-form in L-AC standard (free from D-AC) spiked with D-AC over the range 0.2–10.0%. The relationship between the found values (y) and the theoretical values (x) was found to be a straight line that passed through the origin ($y = 0.970x - 0.053$) (correlation coefficient = 1.000); the good linearity and accuracy on this method were confirmed. In addition, similar results were obtained with respect to carnitine ($y = 0.974x - 0.059$) (correlation coefficient = 1.000).

Detection limit

The detection limit of D-AC with this method was investigated, comparing UV detection (254 nm) with fluorescence detection (excitation at 365 nm, emission at 412 nm). It was confirmed to

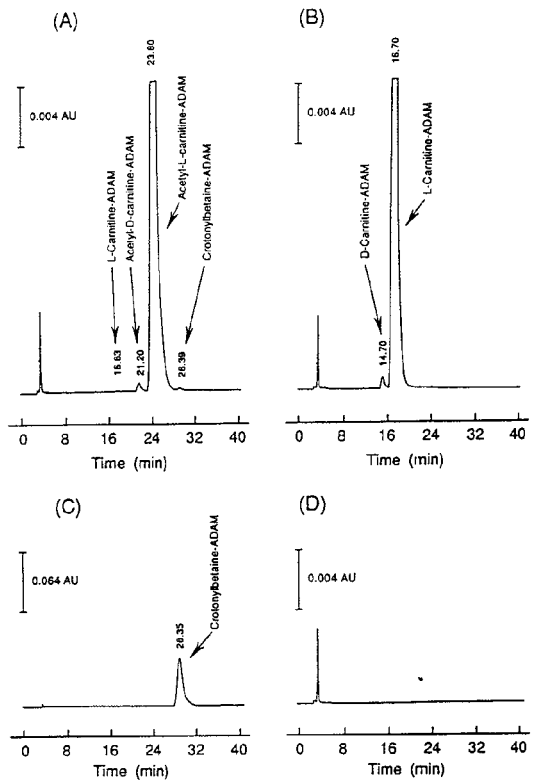

Fig. 6. Chromatograms of (A) acetyl-L-carnitine spiked with 1% of acetyl-D-carnitine, (B) L-carnitine spiked with 1% of D-carnitine, (C) crotonylbetain and (D) the reagent blank.

be almost same, in both instances, *ca.* 0.01% of D-AC in L-AC, *i.e.*, *ca.* 0.05 pmol of D-AC per injection (signal-to-noise ratio = 4).

Table 1
Reproducibility of assay of D-form in acetyl-L-carnitine (Lot No. 3)

Repetition	Assay value (%)
1	1.39
2	1.38
3	1.41
4	1.40
5	1.40
6	1.41
Mean	1.40
Standard deviation	0.0117
R.S.D. (%)	0.84

Table 2
Optical purity testing for acetyl-L-carnitine drug substance

Sample	Lot No.	D-Form content (%)
Acetyl-L-carnitine drug substances	1	3.82
	2	1.42
	3	1.40
	4	0.62
Standard sample	S1	N.D.[a]

[a] Not detected.

3.4. Application to optical purity testing

Optical purity testing for L-AC drug substances and standard samples was performed with this method. The results were given in Table 2.

Considerable differences in the content of the D-form were found between several batches of L-AC.

4. Discussion

Methods for the chromatographic separation of enantiomers may be roughly divided into indirect diastereomeric methods using a chiral derivatization reagent followed by separation on a non-chiral column, and direct methods using a chiral column or chiral mobile phase. Indirect methods have several disadvantages, *e.g.*, the cost and the steady supply of the chiral reagent, and the direct influence of the optical purity of the reagent on the analytical value.

For DL-AC and DL-C, which have weak absorption only in the low-wavelength region, direct methods using a chiral mobile phase may be inappropriate because of the background absorption of the chiral additive. Therefore, in order to develop a direct method using a chiral column for DL-AC or DL-C, various types of chiral stationary phases (CSPs) were tried under a variety of conditions; for example, the following CSPs were investigated in consideration of the chemical structure of DL-AC or DL-C (presence of β-oxycarboxyl group) and its peculiar solubility (high polarity): ligand-exchange types [Chiralpak MA (+), Chiralpak WH], crown ether type (Crownpak CR), metal complex type (Ceramospher), bonded protein type (Ultron ES-OVM) [19] and cellulose carbamate type (Chiralcel OD-R). However, all attempts at the direct separation of the enantiomers failed. The difficulties are probably due to their remarkable motility in elution and the weak interaction between DL-AC or DL-C and the CSPs.

Derivatization methods on the carboxyl site of DL-AC or DL-C were then investigated in order to increase the interaction between the solutes and the CSPs. DL-AC and DL-C methyl esters gave no effect on the enantioselectivities on these CSPs, but it was found that the ADAM derivatives achieved enantiomeric separations on a cellulose carbamate-type CSP (Chiralcel OD-R) using the reversed-phase mode. It is considered that the success depends greatly on $\pi-\pi$ interactions between the anthracene skeleton of ADAM and the CSP and the increase in hydrophobicity of the solutes. 1-Pyrenyldiazomethane (PDAM), which was developed as a reagent for the determination of carboxylic acids and is more stable than ADAM [20], was also investigated. The enantioselectivities of the PDAM derivatives on a Chiralcel OD-R column were so poor that the separation could not be achieved, probably because the bulky pyrenyl skeleton prevents effective access of the active sites for chiral recognition.

A Chiralcel OD-R column has great enantioselectivity for widely different compounds, and these results suggest that the use of ADAM makes possible a wider application to carboxylic acids, especially low-molecular-mass and highly polar compounds.

With the use of reversed-phase chromatography, the present method is probably applicable to the simultaneous determination of the enantiomers of acylcarnitines with an appropriate gradient. In addition, as the ADAM derivatization can be performed under mild and water-containing conditions and specific fluorescence detection can be used, this method can be expected to be applicable to the enantiomeric study of acylcarnitines in biological systems.

References

[1] J. Bremer, *J. Biol. Chem.*, 237 (1962) 3628.
[2] I.B. Fritz and K.T.N. Yue, *J. Lipid Res.*, 4 (1963) 279.
[3] W. Rotzsch, I. Lorenz and E. Strack, *Acta Biol. Med. Ger.*, 3 (1959) 28.
[4] D. Kuenze, R. Drechsler, R. Rotzsch and E. Strack, *Dtsch. Z. Verdau.-Stoffwechselkrank.*, 23 (1963) 137.
[5] F. Drago, M. Calvani, G. Continella, G. Pennisi, M.C. Alloro and U. Scapagnini, *Pharmacol. Biochem. Behav.*, 24 (1986) 1393.
[6] A. Blokland, W. Raaijmakers, F.J. van der Staay and J. Jolles, *Physiol. Behav.*, 47 (1990) 783.
[7] E. Bonavita, *Int. J. Clin. Pharmacol. Ther. Toxicol.*, 24 (1986) 511.
[8] G. Acierno, *Clin. Ter.*, 105 (1983) 135.
[9] V. Dolezal and S. Tucek, *J. Neurochem.*, 36 (1981) 1323.
[10] A. Imperato, M.T. Ramacci and L. Angelucci, *Neurosci. Lett.*, 107 (1989) 251.
[11] T. Yasuda, K. Nakashima, K. Kawata and T. Achi, *Iyakuhin Kenkyu*, 23 (1992) 149.
[12] K. Ikeda, T. Hamasaki, H. Kohno, T. Ogawa, T. Matsumoto and J. Sakai, *Chem. Lett.*, (1989) 1089.
[13] A. Ishikawa and T. Shibata, *J. Liq. Chromatogr.*, 16 (1993) 859.
[14] A. Ishikawa, *Chromatography*, 13 (1992) 190.
[15] N. Nimura and T. Kinoshita, *Anal. Lett.*, 13 (1980) 191.
[16] J.D. Baty, R.G. Willis and R. Tavendale, *Biomed. Mass Spectrom.*, 12 (1985) 565.
[17] T. Shinka, T. Mizuno and I. Matsumoto, *Kanazawa Ika Daigaku Zasshi*, 13 (1988) 238.
[18] T. Yoshida, A. Aetake, H. Yamaguchi, N. Nimura and T. Kinoshita, *J. Chromatogr.*, 445 (1988) 175.
[19] J. Iredale, A.F. Aubry and I. Wainer, *Chromatographia*, 31 (1991) 329.
[20] N. Nimura, T. Kinoshita, T. Yoshida, A. Uetake and C. Nakai, *Anal. Chem.*, 60 (1988) 2067.

ELSEVIER

Journal of Chromatography A, 673 (1994) 45–53

JOURNAL OF CHROMATOGRAPHY A

Chromatographic purification of immunoglobulin G from bovine milk whey

Premysl Konecny*, Rodney J. Brown, William H. Scouten

Biotechnology Center, Utah State University, Logan, UT 84322-4700, USA

(First received January 6th, 1994; revised manuscript received March 4th, 1994)

Abstract

We used thiophilic chromatography on T-gel, a resin of the structure agarose–O–$CH_2CH_2SO_2CH_2CH_2SCH_2CH_2OH$, to purify immunoglobulin G from "sweet" cheese whey. The purity of immunoglobulin G, as indicated by radial immunodiffusion, was 74% after a single chromatography on T-gel. Preparation of samples for adsorption onto thiophilic gels requires only the addition of salt (sodium/potassium sulfate) to the samples. Thus, this method may be suitable for large-scale whey IgG isolation.

1. Introduction

Thiophilic gel (T-gel) introduced by Porath and co-workers [1,2] has proved to be a useful tool for selective purification of immunoglobulins (including monoclonal antibodies) from various sources, mainly mammalian sera and ascites fluid [3–9]. One chromatography step was sufficient to obtain the desired purity, although T-gel can be used in tandem with other purification methods such as hydrophobic chromatography [1] or phase partitioning [10]. Thiophilic gel did not display a marked selectivity for human immunoglobulin G (IgG) subclasses [11]. Thiophilic affinity is not restricted to immunoglobulins, and T-gel could be employed also for purification of certain other proteins, such as α_1-macroglobulin [1], papain, trypsin [4] and sweet potato β-amylase [12].

The thiophilic interactions are salt promoted, but distinct from hydrophobic interactions that also require the presence of lyotropic (water-structure-forming) salts. The thiophilic adsorption of immunoglobulins and some other proteins is based on an interaction with a sulfone group in close proximity to a thioether group of the T-gel ligand. Other nucleophiles (X), such as nitrogen or oxygen, may take the place of sulfur in the general thiophilic ligand structure, matrix–O–CH_2CH_2–SO_2–CH_2CH_2–X–R, where R is usually an alkyl function. The postulated mechanism of thiophilic interactions involves either an electron-donor/acceptor or a proton-transfer process [4,13,14].

Adsorbents with sulfone–aromatic ligands and those with 3-(2-pyridyldithio)-2-hydroxypropyl ligand also have thiophilic properties and are useful for purifying immunoglobulins [15–17].

Among the lyotropic salts, sulfates provide the

* Corresponding author. On leave from Institute of Analytical Chemistry, Academy of Sciences of the Czech Republic, Veveri 97, 611 42 Brno, Czech Republic.

0021-9673/94/$07.00
SSDI 0021-9673(94)00225-X

best environment for thiophilic-type adsorption. Ammonium, sodium and potassium sulfates are used extensively. Bound proteins can be easily eluted by lowering the salt concentration. The yield is generally high and up to 85–90% immunoglobulins are recovered from T-gels at low-salt conditions. Thus, only the addition of salt is required prior to chromatography [1,2,4,5].

Immunoglobulins are minor whey protein components [18–20] but have a high potential economic value. For example, whey immunoglobulins have been suggested as a dietary supplement for newborn calves instead of colostrum or colostrum-derived immunoglobulin-rich preparations [21–23]. The treatment provides prophylactic and/or therapeutic benefits by enhancing the calves immune response. The concentration of immunoglobulins in "sweet" cheese whey is *ca.* 0.4–0.6 g/l, of which about 90% is IgG (mainly IgG1) [20,24]. The "sweet" whey is derived from manufacture of ripened cheeses (Swiss, Cheddar, Provolone, etc.) that are prevalent in cheese production.

So far, purification of IgG from cheese whey has been attempted using various methods, usually membrane filtration/ultrafiltration techniques and/or chromatography, although low-resolution salt ($(NH_4)_2SO_4$, $FeCl_3$) fractionation was also used [25,26]. Membrane separation according to molecular mass (ultrafiltration) does not give high resolution and results in a rather impure mixture of proteins, that is enriched in immunoglobulins [22,27]. Chromatographic methods employed for immunoglobulin purification from whey provide significantly better resolution but are usually not easily scaled-up.

Gel permeation chromatography yielded 92% pure IgG from sweet cheese whey [28] but would not be feasible in pilot and/or large-scale whey processing. On the other hand it can be used for analytical purposes [29,30], along with reversed-phase chromatography [31]. Ion-exchange chromatography is not frequently used to purify cheese whey immunoglobulins, despite a common use in the purification of immunoglobulins from sera [32], in the routine preparation of whey protein concentrates [33] and also in the isolation of other whey proteins (β-lactoglobulin, α-lactalbumin, lactoferrin) [34]. Anion-exchange chromatography is not suitable because immunoglobulins are not retained on the adsorbent [30,35], and it has only been employed to enrich whey protein preparations in immunoglobulins [27], or for analytical purposes [30]. Other chromatographic methods used include metal chelation chromatography [36,37], silica adsorption chromatography [38] and immunoaffinity chromatography with immobilized specific monoclonal antibodies [21]. Protein G used as an affinity ligand in combination with membrane microfiltration yields a 90% pure IgG [39]. A review of the previous research shows that preparation of a pure immunoglobulin requires the application of a selective purification method in order to permit economic scale-up.

We present the use of a thiophilic gel for one-step purification of IgG from "sweet" cheese whey. Thiophilic gel is less costly than protein G (A) type adsorbents, yet providing a high specificity for IgG. The procedure requires a very simple pretreatment of the whey, the addition of an appropriate salt, which might be subsequently removed by ultrafiltration of the IgG-depleted whey and possibly even reused. The resulting IgG is 74% pure after one-step thiophilic chromatography, compared to 81% purity for IgG prepared by protein G chromatography.

2. Experimental

2.1. Materials

Protein G-Sepharose 4FF was obtained from Pharmacia LKB (Alameda, CA, USA), 40% acrylamide–N,N′-methylenebisacrylamide (37.5:1, premixed solution); N,N,N′,N′-tetramethylethylenediamine and ammonium persulfate were purchased from Bio-Rad (Hercules, CA, USA), sodium sulfate and potassium sulfate were from Mallinckrodt (Paris, KY, USA), thiophilic gels (the same thiophilic ligands attached to cross-linked 4 and 6% beaded agarose, respectively), bovine γ-globulin, bovine IgG, α-lactalbumin, β-lactoglobulin, Coomassie Brilliant Blue R-250,

molecular mass standard kit SDS-7, glycine and all other chemicals (research-grade purity) were purchased from Sigma (St. Louis, MO, USA), Spectrapor dialysis membrane was from Spectrum Medical Industries (Los Angeles, CA, USA); SP-filter paper, grade 391 was purchased from Baxter (McGaw Park, IL, USA), 0.45-μm ultrafilters Acrodisc 13 were from Gelman (Ann Arbor, MI, USA), Electrophoresis duplicating paper EDP was purchased from Kodak (Rochester, NY, USA), Centrex filtration cartridges were from Schleicher & Schuell (Keene, NH, USA), radial immunodiffusion kit (bovine IgG, low) was purchased from ICN Biochemicals (Costa Mesa, CA, USA), "sweet" cheese whey was obtained from Gossner Foods (Logan, UT, USA).

Low-pressure chromatographic columns of 1.5 cm I.D. were obtained from Kontes (Vineland, NJ, USA), low-pressure modular chromatograph Econo System, MiniProtean II vertical gel electrophoresis and PowerPac 3000 power supply were purchased from Bio-Rad.

2.2. Methods

Salt effects on thiophilic adsorption of bovine IgG

Thiophilic gel was suction-dried and 0.5-g aliquots were equilibrated with 0.05 *M* sodium/potassium phosphate buffer, pH 7.5 containing various salts at 0.5 *M* concentration: potassium sulfate, sodium sulfate and ammonium sulfate. After 30 min equilibration, the buffer was removed by centrifugal filtration in Centrex cartridges and gel samples were incubated batchwise with 2 ml of IgG solutions (1 mg/ml) in appropriate 0.5 *M* sulfate buffers at 20°C for 30 min with gentle mixing. The protein solution was removed by filtration and the gels were washed with 2-ml aliquots of 0.5 *M* sulfate buffers until the absorbance of washings was less than 0.01 at 280 nm. Subsequently bound IgG was eluted with a low-salt elution buffer, 0.05 *M* sodium/potassium phosphate buffer, pH 7.5 and quantified spectrophotometrically at 280 nm.

The same procedure was used to determine the effect of salt concentration and temperature on binding efficiency of T-gel for bovine IgG. When the effect of temperature on adsorption was tested, the adsorption was performed at 20 and 40°C, respectively, while elution was carried out at 20°C.

Determination of capacity of adsorbents for IgG

Bovine γ-globulin or IgG (both commercial products, Sigma) (1 mg/ml) in 0.5 *M* sodium sulfate/0.05 *M* sodium/potassium phosphate buffer, pH 7.5 was applied to 2.3-ml gel beds in chromatographic columns (1.5 cm × 1.3 cm) at flow-rate 1.0 ml/min. The sample application proceeded until a 10% breakthrough was detected by UV monitor (280 nm) at the outlet of the column. (The 10% breakthrough is defined as 1/10 of the absorbance of the IgG solution applied. This parameter would be an important factor in process-scale purification). At this point the column was washed with the binding buffer (0.5 *M* sodium sulfate/0.05 *M* sodium/potassium phosphate, pH 7.5) and the bound IgG was eluted with 0.05 *M* sodium/potassium phosphate, pH 7.5 (elution buffer).

The dynamic capacity at 10% breakthrough was calculated from the volume of the IgG solution applied to the column (until 10% breakthrough reached) minus the volume of the IgG solution retained in the inlet/outlet tubings and in the void volume of the column. The dynamic capacity was compared with the amount of IgG eluted from the column after extensive washing (eluted capacity), which was determined spectrophotometrically at 280 nm.

Bovine γ-globulin (electrophoretic purity *ca.* 99%) was used instead of much more expensive IgG to determine the capacity as well as the effects of salts and temperature on thiophilic adsorption.

Pretreatment of whey prior to chromatography

Fresh whey (pH 6.2–6.6 in various batches) was cooled to 4–6°C and centrifuged at 10 000 *g* for 30 min. Residual milk fat floating on top of the liquid was removed and the resulting supernatant was collected and passed first through a SP-glass fiber filter and subsequently through

0.45-μm ultrafilter. The clarified whey was then ready for chromatography.

Sodium azide was added as a preservative to 0.02% final concentration. The clarified, sodium azide treated whey can be stored for over 30 days at 4°C without any signs of a bacterial growth. Presence of the preservative did not affect subsequent chromatography.

Chromatographic purification of IgG from cheese whey

Solid sodium sulfate was added to clarified cheese whey (see pretreatment) to a final concentration of 0.5 *M*. The pH of the resulting solution was not adjusted. The treated whey (85 ml) was then applied to a chromatographic column (1.5 cm × 1.3 cm) with the appropriate adsorbent equilibrated with 0.5 *M* sodium sulfate/0.05 *M* sodium/potassium phosphate buffer, pH 7.5 (binding buffer) at a flow-rate of 1.0 ml/min (linear flow-rate 34 cm/h). The protein elution was detected by UV monitor at 280 nm. The column was thoroughly washed with the binding buffer until absorbance reached baseline and then the IgG was eluted with a low-salt 0.05 *M* sodium/potassium phosphate buffer, pH 7.5, at the same flow-rate. The adsorption of whey IgG was performed at both 20 and 40°C (the column, sample solution and buffers were placed in a thermostated incubator).

In a similar fashion, IgG was purified from whey on protein G-Sepharose 4FF column equilibrated with 0.1 *M* sodium/potassium phosphate buffer, pH 6.9. The clarified whey (85 ml) was applied to the column at flow-rate 1.0 ml/min, the column was washed with the binding buffer, and the adsorbed material was eluted with 0.1 *M* glycine–HCl buffer, pH 2.8.

Eluates containing IgG were dialyzed against distilled water overnight, frozen and lyophilized.

Protein concentration assay

Total protein concentration of column effluents was determined spectrophotometrically at 280 nm using highly purified bovine IgG as a standard.

Sodium dodecyl sulfate–polyacrylamide gel electrophoresis (SDS-PAGE)

Chromatographically purified IgG fractions were analyzed for purity by vertical SDS-PAGE using 12% resolving gel and 4% stacking gel under denaturing conditions [40]. Protein staining was performed with 0.1% Coomassie Brilliant Blue R-250 solution in 10% acetic acid–40% methanol–50% water. Positive photographic images of the stained protein patterns were obtained using the Kodak EDP direct duplication method.

Radial immunodiffusion

Immunochemical analysis was carried out using radial immunodiffusion. The lyophilized IgG preparations were dissolved in 0.9% sodium chloride (*ca.* 1 mg/ml) and 5-μl aliquots were pipetted into wells of the radial immunodiffusion gel. Highly purified bovine IgG was used as a standard. The concentrations of IgG were compared with total protein concentration.

3. Results and discussion

3.1. Salt effects on thiophilic adsorption of IgG

Among the salts tested, sodium sulfate most efficiently promoted IgG adsorption on T-gel; 94% of the IgG was bound to the gel at 0.5 *M* salt concentration. The amount of IgG eluted with sodium sulfate was also higher (75%) than with potassium or ammonium sulfates (Fig. 1). IgG from T-gels was only partially eluted by three batchwise elutions (most IgG, 44–52%, was recovered in the first eluate). Since all the T-gel aliquots were treated identically, the amount of eluted IgG accurately represented the effects of different salts. These results indicated that sodium sulfate should be employed in subsequent experiments.

3.2. Effect of salt concentration on thiophilic adsorption of IgG

The 0.5 *M* salt concentration was used as described previously since it was reported to be

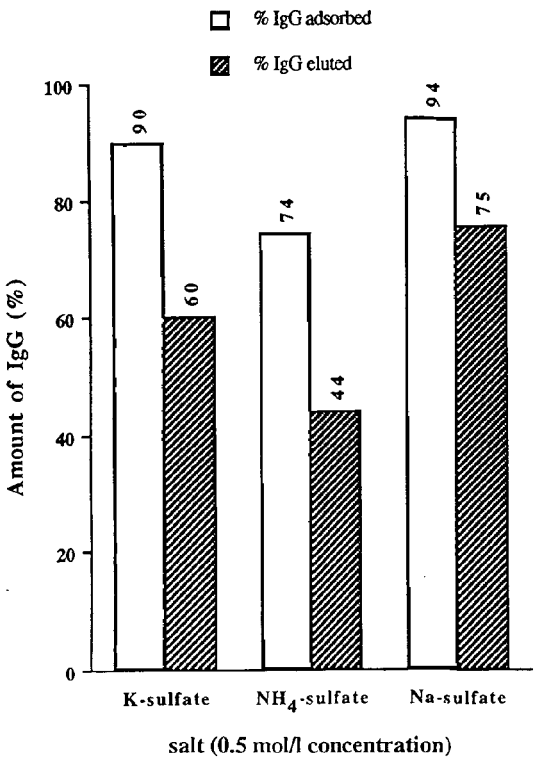

Fig. 1. Effect of salts on thiophilic adsorption of bovine IgG. Aliquots (0.5 g) of suction-dried T-gel (matrix: cross-linked 4% beaded agarose) were equilibrated with 0.5 *M* salt solutions in 0.05 *M* sodium/potassium phosphate buffer, pH 7.5, then treated with 2 ml of IgG solutions (1 mg/ml) for 30 min. The gels were washed with the appropriate salt/buffer, then adsorbed IgG was eluted with 0.05 *M* sodium/potassium phosphate buffer, pH 7.5. IgG concentration in both washings and elution fractions was quantified. The experiment was done in a batchwise mode. Values reported are the average of five determinations, the standard deviation being less than ± 4%.

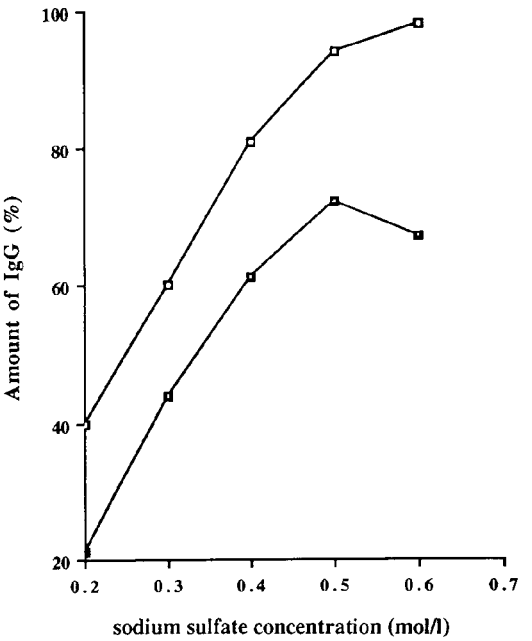

Fig. 2. Effect of salt concentration on thiophilic adsorption of bovine IgG. T-gel was equilibrated with sodium sulfate solutions of 0.2–0.6 *M* concentration and then treated as described (*Methods*, Fig. 1). The amount of IgG in washing and elution fractions was determined for various salt concentrations. Values reported are the average of five determinations, the standard deviation being less than ± 4%. □ = IgG adsorbed; ■ = IgG eluted.

optimal for potassium sulfate, the most frequently used salt in thiophilic chromatography [1,3,5]. We demonstrated that this was also the optimal concentration for sodium sulfate in thiophilic chromatography of bovine IgG (Fig. 2). The amount of bound IgG continued to increase above 0.5 *M* sodium sulfate concentration. However, the yield of eluted IgG was lower indicating that part of the protein adsorbed at the high salt concentration cannot be recovered using low-salt elution. That portion of the IgG could only be released by using 8 *M* guanidine–HCl during regeneration of the T-gel. Also, increasing ionic strength during adsorption was not desirable because the salt must be removed from IgG-free whey before subsequent processing.

The experimental procedure was basically the same as in the previous experiment and thus IgG was only partially eluted by three batchwise elutions. Nevertheless, total amount of IgG eluted as well as the amount of IgG in individual eluates showed that the yield of IgG was the highest at 0.5 *M* sodium sulfate.

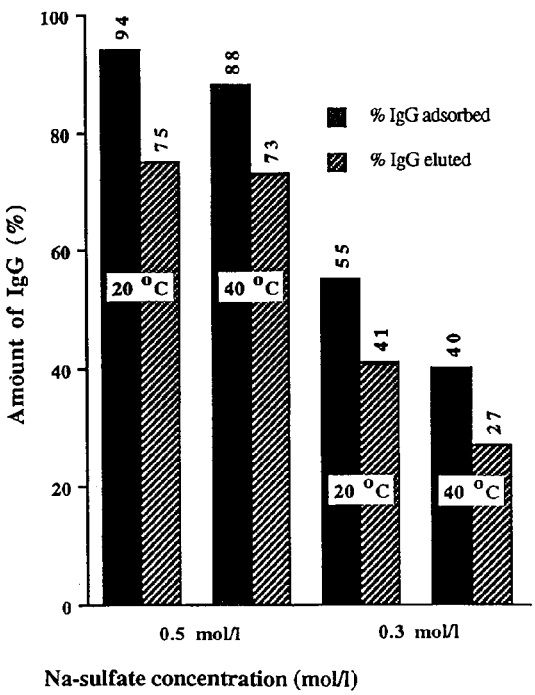

Fig. 3. Effect of temperature on thiophilic adsorption of bovine IgG. Adsorption of IgG to T-gel (0.5-g aliquots of suction-dried gel) equilibrated with sodium sulfate solutions of 0.3 and 0.5 *M* concentrations (in 0.05 *M* sodium/potassium phosphate buffer, pH 7.5) was performed at 20 and 40°C. Elution was done as described (*Methods*, Fig. 1) at 20°C and amounts of IgG in all fractions were quantified spectrophotometrically. Values reported are the average of five determinations, the standard deviation being less than ± 4%.

3.3. Effect of temperature on thiophilic adsorption of bovine IgG

The amount of IgG eluted from T-gel after adsorption (batchwise experiment) of the protein at 40°C was comparable to that carried out at 20°C (Fig. 3). Although slightly less IgG was bound at 40°C (88%) than at 20°C (94%), the amounts of eluted protein were essentially the same (73 *vs.* 75%). These results are consistent with similarities in adsorption isotherms of IgG adsorption on T-gel at 4 and 20°C [3].

However, at a salt concentration of 0.3 *M*, less IgG was adsorbed and eluted at 40 than at 20°C. This confirms the differences between thiophilic and hydrophobic chromatography. Unlike hydrophobic interactions, thiophilic interactions are not promoted at higher temperatures.

3.4. Capacity of adsorbents for bovine IgG

Under the conditions described above (see *Methods*), we determined the capacity of commercially available T-gels (with the same thiophilic ligand attached to cross-linked 4% beaded agarose and 6% beaded agarose, respectively) and protein G-Sepharose 4FF (Table 1). The capacity of the T-gel based on 6% beaded agarose was approximately the same at 20 and 40°C and was only about 20% lower than the capacity of protein G-Sepharose 4FF.

The capacities for bovine IgG determined in our experiments differed from capacities for

Table 1
Capacity of T-gels and protein G-Sepharose 4FF for bovine IgG

	Temperature (°C)	Dynamic capacity at 10% breakthrough (linear flow-rate 34 cm/h) (mg IgG/ml gel)	Eluted capacity (mg IgG/ml gel)
T-gel (cross-linked 4% beaded agarose)	20	12.1 ± 0.3	12.0 ± 0.4
T-gel (6% beaded agarose)	20	18.2 ± 0.3	19.0 ± 0.4
	40	17.3 ± 0.5	18.3 ± 0.5
Protein G-Sepharose 4FF	20	22.1 ± 0.4	19.0 ± 0.6

human IgG as reported by the manufacturer (cross-linked 4% beaded agarose T-gel: 1–3 mg/ml gel, 6% beaded agarose T-gel: 30–45 mg/ml gel). The capacities for bovine and human IgG are significantly different for the T-gel with cross-linked 4% agarose matrix, with bovine IgG giving higher yields. In contrast, the reported capacity for human IgG of the other T-gel, based on 6% agarose, is about twice that found for bovine IgG.

The observation that the eluted capacity of protein G-Sepharose 4FF was lower (*ca.* 15%) than the dynamic capacity at 10% breakthrough could be linked with leakage of a small portion of the bound IgG during the washing phase. That implies that the adsorption of IgG onto the adsorbent might not be strong enough under the typical washing conditions.

3.5. Chromatographic purification of IgG from cheese whey

IgG was purified from whey by chromatography on the two thiophilic gels described above. Adsorption was carried out at 20 and 40°C, while elution was performed at 20°C. In a typical T-gel chromatography (Fig. 4) the yield was 0.29–0.32 mg IgG/ml whey. The bulk flow-through fraction contained less than 0.08 mg IgG/ml. Protein G-Sepharose 4FF, which was chosen as a reference adsorbent for the IgG purification, yielded 0.38–0.42 mg IgG/ml whey. Radial immunodiffusion indicated that the flow-through fractions were essentially IgG-free. Fractions containing IgG were assayed for total protein concentration (A_{280} assay), and purity by radial immunodiffusion and SDS-PAGE under denaturing conditions (Fig. 5). The two quantitative assays show that the IgG prepared by thiophilic chromatography was 74% pure, while the IgG preparation from protein G-Sepharose 4FF was 81% pure. Thus, the purity of IgG prepared by T-gel chromatography was 91% of that prepared by protein G-chromatography. The electrophoretic pattern suggests a higher purity of the IgG purified by protein G chromatography than determined by radial immunodiffusion. The reason could be that part of the

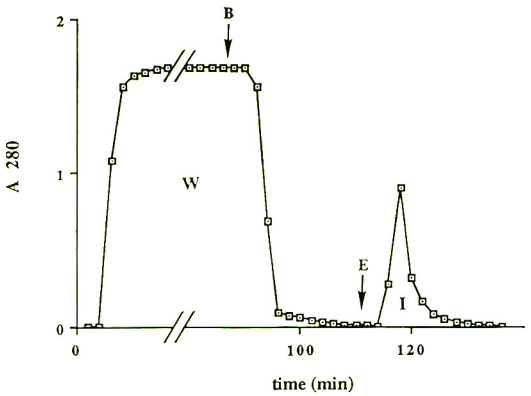

Fig. 4. Purification of IgG from whey by thiophilic chromatography. Clarified sweet whey (85 ml), with solid sodium sulfate added to a concentration of 0.5 *M*, was applied to a column (1.5 cm × 1.3 cm) of T-gel (matrix: 6% beaded agarose) equilibrated with 0.5 *M* sodium sulfate/0.05 *M* sodium/potassium phosphate, pH 7.5. After washing with the same buffer (B), adsorbed IgG was eluted with the elution buffer (E) of 0.05 *M* sodium/potassium phosphate, pH 7.5. The chromatography was performed at a flow-rate of 1.0 ml/min. Fractions from the chromatography (W = IgG-depleted whey, I = IgG fraction) were characterized by SDS-PAGE (see Fig. 5).

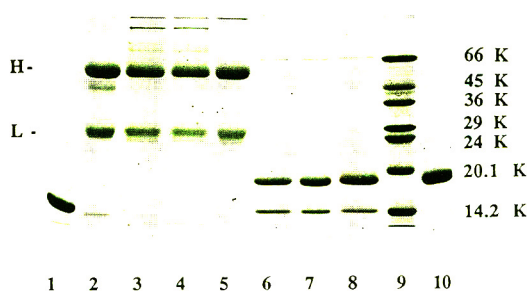

Fig. 5. SDS-PAGE (denaturing conditions) of fractions from chromatographic purifications of sweet whey on T-gel and protein G-Sepharose 4FF. SDS-PAGE was run on a 8 cm × 7 cm × 0.75 mm gel (stacking gel: 4% acrylamide, separating gel: 12% acrylamide), using the Laemmli buffer system [40] at constant voltage 200 V. Lanes: 1 = α-lactalbumin; 2 = bovine IgG (standard; H = heavy chain, L = light chain); 3 = bovine whey IgG from T-gel chromatography at 20°C (see Fig. 4, fraction I); 4 = bovine whey IgG from T-gel chromatography at 40°C; 5 = bovine whey IgG from protein G chromatography; 6 = IgG-depleted whey after T-gel chromatography (see Fig. 4, fraction W); 7 = IgG-depleted whey after protein G chromatography; 8 = whey; 9 = molecular mass standards (K = kilodalton); 10 = β-lactoglobulin.

protein lost its antigenic activity, possibly during the low-pH elution.

Whey was applied on T-gel without prior adjustment of pH, although thiophilic chromatography usually requires pH 7.5–8.0 to reach the highest yield, and possibly also to obtain the maximum purity of the product [3,6]. We did not adjust the pH (6.2–6.6) to avoid another procedure to the sample preparation, which might also negatively affect further processing of the IgG-free whey. If pH adjustment is feasible on a large scale, it might increase the adsorption and the yield of IgG.

4. Conclusions

The purification of IgG from whey requires a selective purification method. Affinity chromatography on IgG-binding adsorbents is one such method. Protein G-adsorbents would theoretically fit the concept of a highly specific adsorbent but they are rather vulnerable to harsh conditions (including higher temperatures) and may also leak small amounts of protein G which could be undesirable in both whey IgG preparations and for further processing of the IgG-depleted whey (*e.g.* production of whey protein concentrate). Also, low-pH elution may denature the purified immunoglobulin and is not viewed as a favorable process-scale purification feature. Unless a preparation of a highly specific antibody is required, the use of immunoaffinity chromatography is questionable.

At this point the thiophilic gel, which is stable, sturdier and less expensive than most of other commercially available affinity chromatography materials, seemed to be worth studying. The thiophilic gel proved to be useful for the isolation of IgG, giving IgG with a purity comparable to that obtained by protein G chromatography. The capacity of a randomly chosen commercially available thiophilic gel was found to be reasonable for bovine IgG. It is likely that other thiophilic gels might be more suited for this purpose, including other than "classical" T-gel [1,2], *e.g.* gels with sulfone–aromatic ligands [15] or 3-(2-pyridyldithio)-2-hydroxypropyl ligands [16].

The gel proved to be capable of binding bovine IgG efficiently at 40°C and should easily withstand even higher temperatures without a substantial decrease in binding capacity. The IgG purified in one step by T-gel chromatography from "sweet" whey was slightly less pure (74%) than that prepared by protein G chromatography (81%), also in one step. The purity of whey IgG from single T-gel chromatography was significantly higher than that prepared by metal chelation chromatography, which yielded a 53% pure product [36], but it was lower than the purity of whey IgG (90%) obtained from a combined use of ultrafiltration and protein G-adsorbent [39]. Higher purity of IgG could be achieved by rechromatography. Another option would be a combination of an ultrafiltration preseparation step and thiophilic chromatography which might also lead to a purer product. Sodium sulfate (at 0.5 *M* concentration) was found to be the most effective among the salts tested for IgG adsorption on T-gel. The use of less costly sodium sulfate instead of potassium sulfate would have an additional advantage in lower production expenses.

The ability to use T-gel at elevated temperatures would not require cooling the whey to room temperature. The preparation of whey prior to thiophilic chromatography is simple, only the addition of salt (preferably sodium sulfate) is needed. This would fit a large-scale purification process, although it might cause a need for additional post-column treatment of the IgG-free whey. Concentrating whey by ultrafiltration (which is routinely used in whey processing [20]) could reduce the amount of whey to as little as 10%, and thus reduce the amount of salt added. That would also reduce the throughput and the amount of chromatographic adsorbent required. Similarly, separation membrane techniques (ultrafiltration combined with reverse osmosis) could be used to desalt washings from the T-gel column.

5. Acknowledgements

This research was supported by grant No. 5-47989 from the Western Dairy Center and by the

Utah Agricultural Experiment Station, Utah State University, Logan, UT, USA. Approved as journal paper No. 4566.

References

[1] J. Porath, F. Maisano and M. Belew, *FEBS Lett.*, 185 (1985) 306.
[2] J. Porath, *US Pat.*, 4 696 980 (Sept. 29, 1987).
[3] T.W. Hutchens and J. Porath, *Anal. Biochem.*, 159 (1986) 217.
[4] T.W. Hutchens and J. Porath, *Biochemistry*, 26 (1987) 7199.
[5] M. Belew, N. Juntti, A. Larsson and J. Porath, *J. Immunol. Methods*, 102 (1987) 173.
[6] B. Nopper, F. Kohen and M. Wilchek, *Anal. Biochem.*, 180 (1989) 66.
[7] A. Lihme and P.M.H. Heegaard, *Anal. Biochem.*, 192 (1991) 64.
[8] A.K. Mallia, J.R. Nevens, R.I. Krohn and P.K. Smith, *FASEB J.*, 6 (1992) A 1450.
[9] R.I. Krohn, J.R. Nevens and A.K. Malia, *FASEB J.*, 6 (1992) A 1451.
[10] B. Sulk, G. Birkenmeier and G. Kopperschlager, *J. Immunol. Methods*, 149 (1992) 165.
[11] P. Bridonneau and F. Lederer, *J. Chromatogr.*, 616 (1993) 197.
[12] L. Franco-Fraguas and F. Batista-Viera, *J. Chromatogr.*, 604 (1992) 103.
[13] J. Porath and M. Belew, *Trends Biotechnol.*, 5 (1987) 225.
[14] T.W. Hutchens and J. Porath, *Clin. Chem.*, 33 (1987) 1502.
[15] K.L. Knudsen, M.B. Hansen, L.R. Henriksen, B.K. Andersen and A. Lihme, *Anal. Biochem.*, 201 (1992) 170.
[16] S. Oscarsson and J. Porath, *Anal. Biochem.*, 176 (1989) 330.
[17] S. Oscarsson, A. Medin and J. Porath, *J. Colloid Interf. Sci.*, 152 (1992) 114.
[18] R.McL. Whitney, in N.P. Wong (Editor), *Fundamentals of Dairy Chemistry*, Van Nostrand Reinhold, New York, 1988, Ch. 3, p. 81.
[19] P. Walstra and R. Jenness, *Dairy Chemistry and Physics*, Wiley, New York, 1984.
[20] K.R. Marshall, in P.F. Fox (Editor), *Developments in Dairy Cheistry*, Vol. 1, Applied Science Publ., London, 1982, Ch. 11, p. 339.
[21] M.M. Gani, K. May and P. Porter, *US Pat.*, 4 490 290 (Dec. 25, 1984).
[22] G.H. Stott and D.O. Lucas, *US Pat.*, 4 834 974 (May 30, 1989).
[23] G.H. Stott and D.O. Lucas, *US Pat.*, 4 816 252 (March 28, 1989).
[24] J.E. Butler, *J. Dairy Sci.*, 54 (1971) 1315.
[25] H.E. Swaisgood, in P.F. Fox (Editor), *Developments in Dairy Chemistry*, Vol. 1, Applied Science Publ., London, 1982, Ch. 1, p. 1.
[26] T. Kaneko, B.T. Wu and S. Nakai, *J. Food Sci.*, 50 (1985) 1531.
[27] R.C. Bottomley, *US Pat.*, 5 194 591 (March 16, 1993).
[28] S.A. Al-Mashikhi and S. Nakai, *J. Dairy Sci.*, 70 (1987) 2486.
[29] J.C. Monti, D. Fumeaux, V. Barrois-Larouze and P. Jolles, *Milchwissenschaft*, 39 (1984) 219.
[30] A.T. Andrews, M.D. Taylor and A.J. Owen, *J. Chromatogr.*, 348 (1985) 177.
[31] N. Parris and M.A. Bagginski, *J. Dairy Sci.*, 74 (1991) 58.
[32] C.J. van Oss, *Sep. Purif. Methods*, 11 (1982) 131.
[33] C.V. Morr, in P.F. Fox (Editor), *Developments in Dairy Chemistry*, Vol. 4, Elsevier Applied Science, London, 1989, Ch. 6, p. 245.
[34] E.D. Strange, E.L. Malin, D.L. Van Hekken and J.J. Basch, *J. Chromatogr.*, 624 (1992) 81.
[35] J.M. Girardet, D. Paquet and G. Linden, *Milchwissenschaft*, 44 (1989) 692.
[36] S.A. Al-Mashikhi, E. Li-Chan and S. Nakai, *J. Dairy Sci.*, 71 (1988) 1747.
[37] E. Li-Chan, L. Kwan and S. Nakai, *J. Dairy Sci.*, 73 (1990) 2075.
[38] A. Peyrouset and F. Spring, *US Pat.*, 4 436 658 (March 13, 1984).
[39] J.-P. Chen and C.-H. Wang, *J. Food Sci.*, 56 (1991) 701.
[40] U.K. Laemmli, *Nature*, 227 (1970) 680.

ELSEVIER

Journal of Chromatography A, 673 (1994) 55–64

JOURNAL OF CHROMATOGRAPHY A

Comparative study of various size-exclusion chromatographic columns for the clean-up of selected pesticides in soil samples

David Puig, Damià Barceló*

Environmental Chemistry Department, CID–CSIC, c/Jordi Girona 18–26, 08034 Barcelona, Spain

(First received November 8th, 1993; revised manuscript received February 25th, 1994)

Abstract

A comparative study was carried out using various types of size-exclusion chromatographic (SEC) columns (Bio-Beads SX-3, SX-8 and SX-12, Phenogel polystyrene and Zorbax PSM 60S, silica based) for the isolation of the pesticides monuron, linuron, monolinuron, isoproturon, propanil, fenitrothion, molinate, alachlor, bensulfuron, chloridazon, trifluoralin and atrazine from soil samples. Spiked soil samples (10 μg/g) were Soxhlet extracted and fractionated with SEC columns using different mobile phases. The SEC extracts were analysed either by liquid chromatography with diode-array detection or gas chromatography with nitrogen–phosphorus detection. Recoveries varying from 70 to 82% were found for all the analytes. With the low-resolution polystyrene columns better results were found using columns with a high size-exclusion range. The Phenogel column was more efficient than the Bio Beads columns for phenylurea herbicides. The method developed was applied to the determination of linuron and atrazine in a candidate reference material and was applied to investigate the decay of molinate in real soil samples at ng/g levels.

1. Introduction

Since the introduction of size-exclusion chromatography (SEC) for the isolation of organic contaminants from environmental matrices [1], its use has not been as popular as other clean-up methods such as solid-phase extraction or column chromatography. This is probably caused by the need for further equipment, such as a liquid chromatographic pump and a detector. In addition, SEC columns are not currently available as disposable cartridges, *e.g.*, Florisil and C_{18} type. SEC is a useful technique as it is not destructive, in contrast to other methods involving acid or base treatment, it can isolate a variety of compounds of different chemical types in the same fraction and it can remove a large number of interfering materials from the matrix. Moreover, SEC has been reported to give higher reproducibility than Florisil clean-up [2]. The main disadvantage is that the removal of interfering materials is not complete in many instances, especially when using low-resolution SEC columns, and so some of the samples need to be analysed twice in order to eliminate the matrix interferences completely.

In current environmental analyses, SEC is used as a clean-up procedure for organochlorine and organophosphorus pesticides, polychlorobiphenyls and herbicides, using different mobile phases in each instance, *e.g.*, cyclohexane [1,3], ethyl acetate–toluene [4,5], cyclohexane–dichloromethane [6–12] and cyclohexane–ethyl acetate [2,13–17].

* Corresponding author.

0021-9673/94/$07.00
SSDI 0021-9673(94)00194-E

The aim of this work was to compare the performances of different SEC columns for the isolation of a group of pesticides from soil matrices. This study was accomplished by comparing the low-resolution SEC polystyrene columns Bio-Beads SX-3, SX-8 and SX-12 with a high-resolution SEC polystyrene column. The final purpose was to select the best SEC column that can eliminate the matrix interferences from the pesticides. In addition, a silica-based SEC column was also tested. This column material had a silica structure deactivated with special reagents (*e.g.*, short hydrocarbon chains containing diol groups) to prevent strong hydrophobic interactions. The main advantage of these silica-based columns is that they can withstand high pressures, flow-rates and temperatures and are compatible with a wide variety of organic and aqueous solvents.

Application to the determination of atrazine and linuron in a soil candidate reference material from the BCR (Bureau Communitaire de Référence) of the Commission of the European Communities and to study the decay of molinate in real environmental soil samples from the Ebro Delta (Tarragona, Spain) is also reported.

2. Experimental

2.1. Materials

HPLC-grade water and analytical-reagent grade cyclohexane, dichloromethane, diethyl ether, methanol and acetonitrile were obtained from Merck (Darmstadt, Germany). Hexane and tetrahydrofuran of HPLC grade were obtained from Romil Chemicals (Shepshed, Leics., UK). Ethyl acetate for residue analysis was purchased from Scharlau (Barcelona, Spain). All the solvents were passed through a 0.45-μm filter from Scharlau. Atrazine, linuron and isoproturon were obtained from Riedel-de Haën (Seelze–Hannover, Germany). Molinate, alachlor, bensulfuron, chloridazon, monuron and monolinuron were purchased from Dr. S. Ehrenstorfer Promochem (Wessel, Germany) and propanil and trifluoralin from Polyscience (Niles, IL, USA). Fenitrothion was a gift from Sumitomo Chemical (Osaka, Japan).

2.2. Sample preparation

A method developed previously in our department was used for the extraction of the pesticides from soil samples [2]. Real soil samples were collected in the Ebro delta (Tarragona, Spain). After collection, the samples were freeze-dried, sieved through a 120-μm sieve and homogenized for 2 weeks with mechanical shaking in order to obtain a homogeneous soil material that could be used as a candidate reference material. Subsequently the samples were stored at −20°C prior to carrying out the experiments. A 10-g amount of sample at room temperature was wetted and spiked with 10 μg of each pesticide with homogenization. The wet soil spiked with the pesticides was kept for 2 days and then Soxhlet extracted from 12 h with methanol. The extract was concentrated in a rotary evaporator (30°C) to *ca.* 2–3 ml. The evaporation of the solvent was carefully finished with nitrogen, and the extracts were then dissolved in 300 μl of dichloromethane or methanol depending on whether the SEC clean-up was carried out with an organic or aqueous mobile phase, respectively.

2.3. SEC clean-up

Eluent delivery was provided by a Model 64 high-pressure pump (Knauer, Hamburg, Germany) and the detection was carried out with a Vari-chrom UV–Vis detector (Varian, Sunnyvale, CA, USA). Samples were injected via a 160-μl loop (Rheodyne, Cotati, CA, USA). The columns investigated were three low-resolution columns (450 mm × 10 mm I.D.) packed with Bio-Beads SX-3, SX-8 and SX-12 with size exclusion of M_r 2000, 1000 and 400, respectively (Bio-Rad Labs., Richmond, CA, USA); a 250 mm × 6.2 mm I.D. high-resolution silica-based Zorbax PSM-60S column with a molecular mass range from 100 to 10 000 (Rockland Technologies, through Chrompack, Middelburg, Netherlands) and a 300 mm × 7.8 mm I.D. high-

resolution SEC polystyrene column (Phenogel) with a size exclusion of M_r 800 (Phenomenex, Ramuko, Palos Verdes, CA, USA). The mobile phases consisted of mixtures of dichloromethane and cyclohexane for the polystyrene columns and additionally methanol–water (70:30) for the silica-based column. A flow-rate of 1 ml/min was used throughout.

2.4. Chromatographic analysis

Liquid chromatography with diode-array detection (LC–DAD)

An HP 1090A liquid chromatograph equipped with an automatic injector and a diode-array detector was used (Hewlett-Packard, Palo Alto, CA, USA). A 20-μl volume of sample was injected into a Zorbax C_8 reversed-phase analytical column (Rockland Technologies). Elution was carried out with water–methanol–acetonitrile (60:20:20) for 3 min followed by gradient elution to 100% acetonitrile in 30 minutes at a flow-rate of 1 ml/min.

Gas chromatography with nitrogen–phosphorus detection (GC–NPD)

A GC 5300 Mega Series gas chromatograph (Carlo Erba, Milan, Italy) equipped with a nitrogen–phosphorus detector was used. The column was a 15 m × 0.15 mm I.D. fused-silica capillary column coated with chemically bonded cyanopropylphenyl DB 225 (J & W Scientific, Folsom, CA, USA). Hydrogen was the carrier gas and helium the make-up gas at 60 and 110 kPa, respectively. The temperatures of the injector and detector were held at 270°C. The column was programmed from 60 to 90°C at 10°C/min and from 90 to 220°C at 6°C/min.

Quantification

Both LC–DAD and GC–NPD quantification was performed with external standard calibration methods, except for the validation analyses, which were carried out using deethylatrazine and monuron as internal standards for atrazine and linuron, respectively. Calibration graphs were constructed for all the compounds over the concentration range 0.01–20 mg/ml for LC and 0.005–10 mg/ml for GC. The repeatability and reproducibility varied from 5 to 9% and from 7 to 12% ($n = 6$), respectively.

3. Results and discussion

3.1. SEC fractionation

Low-resolution polystyrene columns: Bio-Beads SX

The retention times of the pesticides with different columns and experimental conditions are given in Table 1 and are in the expected range found for other similar pesticides using a Bio-Beads SX-3 column [8]. As expected, the exclusion size decreased from SX-3 to SX-12 columns together with the retention times of the analytes. The dispersion observed in the retention times of the analytes could be attributed more to the existence of additional adsorption and partition interactions than to differences in the exclusion size of the pesticides. The increase in the retention time dispersion for the high exclusion size columns would be explained by the fact that the percentage of the excluded pesticide decreased when the exclusion size increased. Hence low interaction occurs in the columns with low exclusion size and consequently better peak shapes for the pesticides are obtained (Fig. 1).

It can also be observed that the trend of the matrix soil interference retention times is different, and it increases when the exclusion size decreases. This may be related to the different packing densities of the stationary phases, with a lower swelling ratio for the low exclusion size polymers. Hence when columns with the same physical dimensions are used, a higher packing density will be observed with the low exclusion size columns. Thus, when the packing density increases, the retention times of the soil matrix interferences also increase.

Another relevant parameter in SEC in the eluent. In this work a comparison was made between the performance of dichloromethane–cyclohexane and that of the ethyl acetate–cyclohexane mixture used in previous work [2].

Table 1
Elution volumes (ml) of the pesticides using four different eluents with Bio-Beads columns

Pesticide	Elution volume (ml)				
	SX-3		SX-8		SX-12
	Cyclohexane–ethyl acetate (1:1)	Cyclohexane–dichloromethane (1:1)	Cyclohexane–dichloromethane (1:1)	Cyclohexane–dichloromethane (1:3)	Cyclohexane–dichloromethane (3:1)
Monuron	22–39	18–30	17.0–24.1	14.2–19.0	13.3–12.2
Linuron	22–30	19–29	15.3–23.0	13.3–19.1	13.1–16.4
Isoproturon	21–39	18–27	15.3–22.4	n.d.	12.3–15.2
Propanil	26–38	25–35	22.1–27.3	20.0–28.1	15.1–19.3
Monolinuron	n.d.	n.d.	16.0–22.1	13.4–17.4	13.1–17.0
Fenitrothion	n.d.	n.d.	15.0–21.0	14.2–20.0	12.3–16.3
Trifluoralin	18–29	16.6–21	12.2–16.4	12.0–15.4	12.0–14.4
Alachlor	n.d.	16–27	13.1–16.1	13.0–15.2	12.0–15.0
Atrazine	n.d.	16–25	13.0–16.3	12.3–15.3	12.0–15.4
Bensulfuron	n.d.	16.6–22	12.3–17.2	11.2–19.0	11.0–11.2
Molinate	n.d.	19–26	16.0–23.0	15.3–22.0	15.1–19.4
Chloridazon	n.d.	16–25	12.1–16.1	n.d.	11.1–11.3
S.M.I.	n.d.	7–25	9.1–17.0	8.1–19.0	10.3–19.0

Chromatographic conditions: see Experimental. S.M.I. = Soil matrix interferences; n.d. = not determined.

Dichloromethane gave the best results for phenylurea herbicides, molinate, fenitrothion and propanil. The viscosities of dichloromethane and ethyl acetate are very similar (0.41 *vs.* 0.44 cP), so this parameter does not play a relevant role in the SEC separation.

The differences in the separation using the two mixtures could be explained either by using Lewis acid–base arguments or by the presence of dipoles in the molecular structure which could interact with the polystyrene via dipole–dipole interactions [18,19]. Polystyrene can be considered as a weak Lewis base so, depending on the type of mobile phase used (acidic or basic nature) different retentions can be expected. For analytes with basic groups and without important molecular dipoles in their structure, such as atrazine, alachlor and fenitrothion, a basic type of mobile phase such as ethyl acetate is recommended. Analytes such as phenylurea herbicides and propanil showed worse peak shapes using ethyl acetate as the mobile phase. When using ethyl acetate, dipole–dipole interactions between these compounds and the stationary phase become very important, giving tailing peaks. This problem does not occur when using dichloromethane (acidic character), because acid–base interactions prevent such undesirable strong dipole–dipole interaction.

Because the aim of this work was to develop a screening method that could eliminate the soil matrix interferences and monitor all the pesticides under the optimum conditions, it was decided to use dichloromethane as the eluent, as in general it gave better results than ethyl acetate. The effect of the changes in the ratio of the mobile phase components was also studied. When the proportion of dichloromethane was increased, the retention time of the analytes decreased and it was found that dichloromethane–cyclohexane (1:1) afforded the best separation. As an example, the elution profiles and the collection time from an extract of a spiked sediment sample after being processed with the Bio-Beads SX-3 and SX-8 columns are shown in Fig. 1. The Bio-Beads SX-12 column was not studied because from the retention times of the analytes and the soil matrix interferences fraction it was concluded that a good separation could not be achieved.

High-resolution SEC columns

Table 2 gives the retention times obtained for the different analytes in one of these columns.

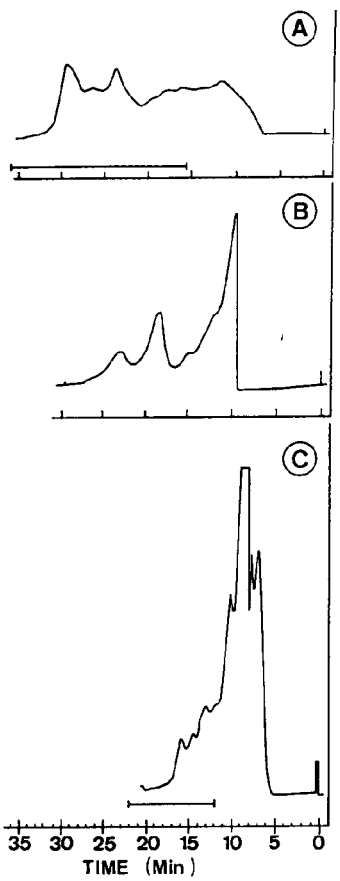

Fig. 1. SEC profiles of a soil sample spiked with all the studied pesticides (10 μg/g of each pesticide). (A) Bio-Beads SX-3; (B) Bio-Beads SX-8; (C) Phenogel high-resolution SEC. Eluent: dichloromethane–cyclohexane (1:1) (Bio-Beads columns) and dichloromethane–cyclohexane (1:3) (Phenogel high-resolution SEC). Flow-rate of eluent, 1 ml/min. Detection at 254 nm. For other chromatographic conditions, see Experimental. The sample collection intervals are indicated by the horizontal bars.

First, the conditions that were optimum for the low-resolution polystyrene columns were used, but most of the analytes co-eluted totally with the soil matrix interferences. The percentage of dichloromethane in the eluent was then reduced to 25% so the interactions of the analytes with the stationary phase increased. Even though some of the pesticides still co-eluted with the soil matrix interferences, phenylurea herbicides and propanil showed almost complete separation from the soil matrix interferences (see Fig. 1).

Table 2
Elution volumes (ml) of the pesticides using two different mobile phases with Phenogel column

Pesticide	Cyclohexane–dichloromethane (1:1)	Cyclohexane–dichloromethane (3:1)
Monuron	12.0	18.2–23.6
Linuron	8.6	13.6–15.6
Propanil	13.6	22.0–25.2
Monolinuron	11.4	18.2–23.2
Molinate	8.4	10.1–11.4
Alachlor	8.0	9.6–10.6
Atrazine	7.9	9.5–10.3
Trifluoralin	n.d.	9.4–10.2
Fenitrothion	8.4	10.0–12.8
Bensulfuron	n.d.	9.4–10.4
S.M.I.	n.d.	6.0–13.0
Blank	n.d.	9.4–10.2

Chromatographic conditions: see Experimental. S.M.I. = Soil matrix interferences; n.d. = not determined.

In Table 3, the retention times of the analytes in different mobile phases (organic and aqueous) are given. When an aqueous mobile phase was used, the samples were eluted with methanol–water (70:30). As can be seen from Table 3, the analytes were eluted in the same order as would be expected for a reversed-phase analytical column. These results were promising because in this instance the pesticides with a better separation with respect to the soil matrix interferences were less separated with the polystyrene columns (see Tables 1 and 3). The main drawback of this method is that a high percentage of water is needed. Hence in order to carry out the analytical determinations, there is the need to eliminate the water. In this operation losses of sample during the evaporation of the solvent are expected. This could be solved by connecting the SEC column on-line with an analytical LC column as reported [20], or by applying dichloromethane liquid–liquid extraction of the analytes

Table 3
Elution volumes (ml) of the pesticides using five different mobile phases from Zorbax HRSEC silica-based column

Pesticide	Methanol	Methanol–water (70:30)	Cyclohexane–dichloromethane		
			1:1 + 5% THF	1:1 + 3% THF	3:1 + 3% THF
Monuron	5.6	8.8	19.0	24.0	–[a]
Isoproturon	6	10.0	16.6	23.2	–[a]
Monolinuron	5.6	9.2	7.4	8.4	11.1
Propanil	5.8	9.8	9.2	10.6	17.0
Linuron	5.8	10.2	7.4	8.0	11.0
Alachlor	5.8	10.4	5.6	5.6	n.d.
Trifluoralin	5.8	19.0	5.6	5.6	n.d.
Atrazine	5.8	n.d.	n.d.	n.d.	n.d.
Molinate	5.7	11.6	5.8	5.9	n.d.
Fenitrothion	5.8	11.2	5.6	5.6	n.d.
Bensulfuron	5.8	5.0	5.6	5.6	n.d.
Chloridazon	5.8	10.1	5.4	5.6	n.d.
Blank sample	5.7	2.4	5.5	5.6	n.d.
S.M.I.	5.7	2.5	n.d.	5.6	5.5

Chromatographic conditions: see Experimental. S.M.I. = Soil matrix interferences; n.d. = not determined.
[a] Irreversible adsorption in the elution conditions.

from the SEC eluent. As specific on-line connection was not available in our laboratory, the latter option was performed and good results (recoveries up to 80%) for all the analytes were obtained.

It should be noted that the performance of the column is more like that of a reversed-phase column than an SEC column. When using 100% methanol most of the analytes were eluted in the solvent front (see Table 3). Hence in this instance the size exclusion contribution to the separation was minimal.

When an organic mobile phase was used, experiments were started using the same conditions as with the polystyrene columns. However, in this instance the performance of the system was more like that of an adsorption chromatographic column with large molecules (soil matrix interferences) being retained together with the pesticides. This can be attributed to a combined effect of adsorption of the diol groups of the bonded reagent and the active silanol groups left uncovered by incomplete silanization. We solved this problem by adding a small percentage of tetrahydrofuran to the mobile phase to compete for these active sites as suggested [21]. In this instance a good separation of the phenylurea herbicides and propanil was found but the other analytes were eluted with the solvent front. Similarly to the use of an aqueous mobile phase, the contribution of size exclusion to the separation process was minimal.

In spite of the good results obtained for the phenylurea herbicides and propanil, the method had the drawback that the retention time of the analytes was too dependent on the proportion of THF used (see Table 3). In this instance the possibility of making errors during the collection of the analytes is very high. Additionally, there was also a problem with optimizing the proportion of THF because it differed for the different phenylureas. For instance, 3% is optimum for monolinuron and linuron, but this was too low for monuron and isoproturon (see Table 3). Further work in this direction was therefore abandoned.

The aqueous and organic mobile phase profile of an extract of a spiked sample are shown in

Fig. 2. High band broadening for monuron and isoproturon using an organic mobile phase was observed.

3.2. Comparison between low- and high-resolution SEC columns: environmental applications

Fig. 3 shows the liquid chromatograms of the extracts obtained from pesticides added to Ebro Delta soil samples purified with the SEC columns Bio-Beads SX-3 and SX-8 and Phenogel. No significant differences were found between the Bio-Beads columns, but excellent results were achieved with the high-resolution SEC column, with a chromatogram exhibiting no interferences.

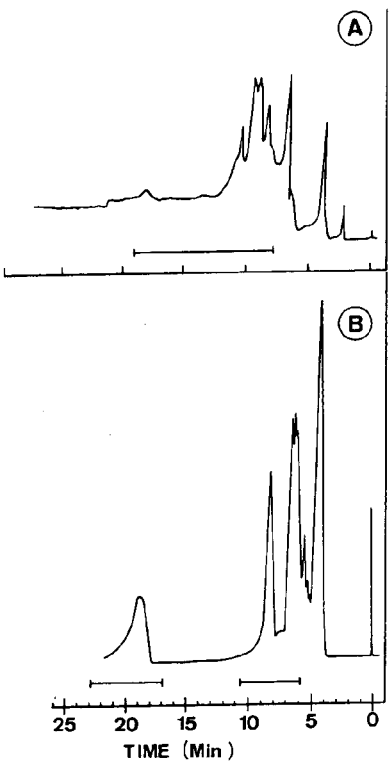

Fig. 2. SEC profiles of a soil sample spiked with all the studied pesticides (10 μg/g of each pesticide) eluted from the Zorbax silica-based column with (A) an aqueous eluent [methanol–water (70:30)] and (B) an organic eluent [dichloromethane–cyclohexane (1:1) + 5% THF]. Flow-rate of eluent, 1 ml/min. Detection at 254 nm. For other chromatographic conditions, see Experimental. The sample collection intervals are indicated by the horizontal bars.

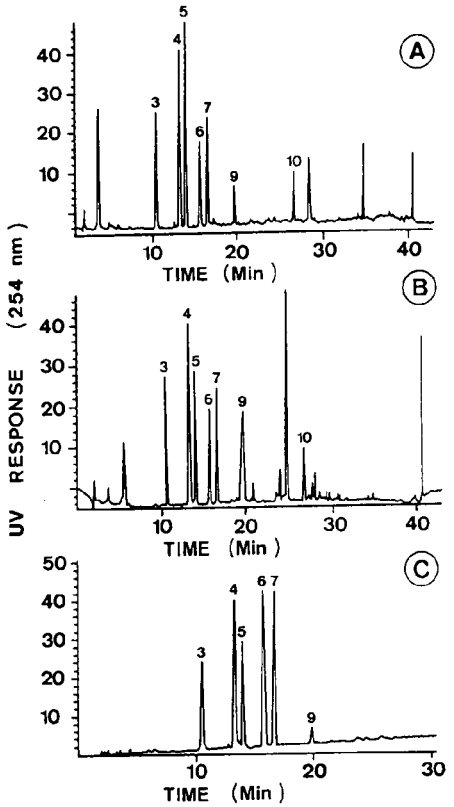

Fig. 3. Reversed-phase LC profiles of spiked samples (10 μg/g) after SEC clean-up with (A) Bio-Beads SX-3, (B) Bio-Beads SX-8 and (C) Phenogel polystyrene columns. Peaks: 3 = monuron; 4 = isoproturon; 5 = monolinuron; 6 = linuron; 7 = propanil; 8 = molinate; 9 = alachlor + fenitrothion; 10 = trifluoralin. For chromatographic conditions, see Experimental.

The results of GC–NPD of the extracts obtained from pesticides added to Ebro Delta soil samples purified with the SEC columns Bio-Beads SX-3 and SX-8 and Zorbax with an aqueous phase are shown in Fig. 4. For the less

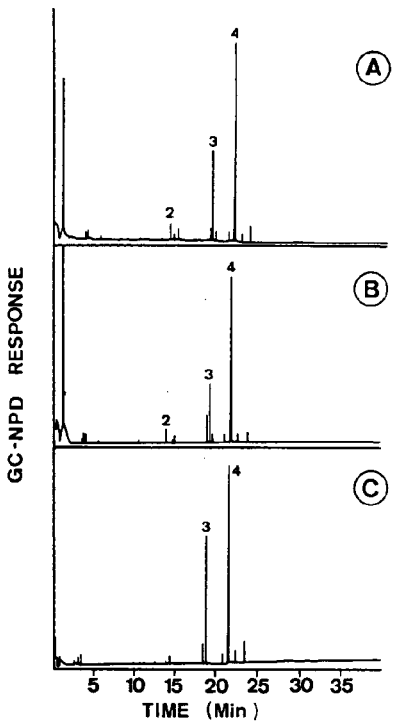

Fig. 4. GC–NPD profiles of a spiked sample (10 μg/g) after SEC clean-up with (A) Bio-Beads SX-3, (B) Bio-Beads SX-8 and (C) Zorbax silica-based columns using an aqueous mobile phase. Peaks: 2 = trifluoralin; 3 = alachlor; 4 = fenitrothion. For chromatographic conditions, see Experimental.

polar analytes good results with the Zorbax column were obtained. In general, the powerful clean-up effect of high-resolution SEC in combination with a selective analytical determination method such as GC–NPD should be emphasized.

The recoveries for the analytes after their addition to soil samples (10 μg/g) are given in Table 4. Recoveries of up to 70% for all the analytes were found. The slightly high standard deviation found with the Zorbax column can be attributed to the additional liquid–liquid extraction step, which was performed manually.

To conclude the comparative study between low- and high-resolution SEC columns, for the determination of phenylurea herbicides the use of high-resolution SEC columns (*e.g.*, Phenogel) offers the best solution. When it is required to determine volatile pesticide residues, *e.g.*, atrazine and fenitrothion, in a soil sample, the method of choice will be GC–NPD, as it offers the best sensitivity and selectivity. However, for pesticides such as isoproturon and linuron, a final determination by LC–DAD is recommended, otherwise, if it is still desired to use GC, derivatization will be required.

In order to evaluate the performance of the developed method, a candidate reference material containing atrazine and linuron was analysed. The real sediment, previously collected in the Ebro Delta area, has been treated as described

Table 4
Average recoveries from spiked soil samples (10 μg/g) ($n = 6$)

Method	Pesticide	SX-3		Phenogel		Zorbax	
		Recovery (%)	R.S.D. (%)	Recovery (%)	R.S.D. (%)	Recovery (%)	R.S.D. (%)
LC–DAD	Monuron	76	5	80	5	n.d.	
	Linuron	77	6	79	5	n.d.	
	Monolinuron	76	5	80	4	n.d.	
	Isoproturon	75	4	82	5	n.d.	
	Propanil	75	7	79	6	n.d.	
GC–NPD	Alachlor	77	4	n.d.		80	8
	Trifluoralin	77	5	n.d.		79	8
	Atrazine	69	4	n.d.		75	9

SEC eluents: dichloromethane–cyclohexane (1:1) (Bio-Beads SX-3), dichloromethane–cyclohexane (1:3) (Phenogel HRSEC) and methanol–water (70:30) (Zorbax HRSEC). Other chromatographic conditions: see Experimental.

under Experimental. The amounts of each pesticide were determined with the proposed method, using selected SEC columns, and also with another method based on clean-up with Florisil columns [2]. The values obtained for atrazine using Bio-Beads SX-3 and Phenogel were 106 ± 4 and 104 ± 4 ng/g, respectively (111 ± 10 ng/g with Florisil) and for linuron the values were 238 ± 6 and 239 ± 5 ng/g, respectively (250 ± 10 ng/g with Florisil).

The determination of the degradation profile of the pesticide molinate under real environmental conditions was carried out. This herbicide, usually applied in rice crop fields in the Ebro delta area, was found at low residue levels (below 0.1 μg/l) in earlier water analyses [22]. It was therefore decided to carry out study of its behaviour in real soil samples. Samples were collected in from rice crop fields in the Ebro Delta area with an interval of *ca.* 3 months between samples, the first sample being collected a few days after herbicide application. The analyses were carried out using the Bio-Beads SX-3 SEC column under the conditions given above.

It was found that under the Delta Ebro area conditions molinate had a half-life of *ca.* 20–25 days. This result is in agreement with others reported previously [23]. This value is lower than those for other pesticides, such as atrazine (28–30 days) and linuron (1–2 months) studied previously [24]. This may be due to the rapid oxidation of the molinate to sulphoxide by chemical and microbiological processes and also to its higher vapour pressure, which increases its volatility. Nevertheless, the sulphoxide metabolites have superior water solubility and slower degradation kinetics and are even more toxic than the parent compound [25].

4. Conclusions

A study of the use of different SEC columns as a clean-up method for analyses for pesticide residues in soil samples was undertaken.

With the Bio-Beads packings, better results were found when using columns with higher exclusion size range. Even though the efficiency of the peaks is increased by using a smaller pore diameter column, high co-elution with interferences was also observed. The benefit of the existence of weak adsorption phenomena was also confirmed. Therefore, a comparison between two different mobile phases (dichloromethane–cyclohexane and ethyl acetate–cyclohexane) was undertaken, and showed that dichloromethane–cyclohexane generally provided better results for all the compounds studied.

The excellent performance of the high-resolution SEC columns was demonstrated. The efficiency of the clean-up process was improved owing to the higher resolution and these columns are particularly appropriate for the isolation of propanil and phenylurea herbicides from soil matrix interferences. In general, high-resolution SEC is to be preferred over low-resolution SEC in order to eliminate the soil matrix interferences more effectively. Nevertheless, one of the major drawbacks is still the cost of such high-resolution SEC columns. In general, high-resolution SEC columns cost three times more than the low-solution SEC columns, which can be a serious problem for the implementation of high-resolution SEC columns in routine environmental analyses for pesticides in soil samples.

The difficulty of carrying out a clean-up process with the silica-based columns without a high degree of adsorption, owing to their wide exclusion range, was demonstrated. Further studies to obtain silica packings with narrow exclusion ranges would be desirable.

In a comparison of GC–NPD and LC–DAD, fewer interferences were found in GC–NPD owing to the superior detector selectivity, but LC–DAD offered the possibility of monitoring a larger number of compounds, their sensitivity being sufficient at the level required in soil analyses.

The method developed in this work was validated by determining linuron and atrazine herbicides in a reference candidate material of the BCR and was applied to the determination of the decay of molinate in real soil samples.

Acknowledgements

We acknowledge the support of the Commission of the European Communities (Project No. CIPA-CT92-3005) and of PLANICYT (AMB94-0950-CE). Mario Serà of the Departament d'Agricultura Ramaderia i Pesca (Generalitat de Catalunya) is thanked for providing soil samples. Hewlett-Packard (Mr. R. Soniassy) is acknowledged for the loan of an LC-DAD 1090A.

References

[1] D.L. Stalling, R.C. Tindle and J.L. Johnson, *J. Assoc. Off. Anal. Chem.*, 55 (1972) 32.
[2] G. Durand, R. Forteza and D. Barceló, *Chromatographia*, 28 (1989) 597.
[3] K.R. Griffitt and J.C. Craun, *J. Assoc. Off. Anal. Chem.*, 57 (1974) 168.
[4] L.D. Johnson, R.H. Waltz, J.P. Ussary and F.E. Kaiser, *J. Assoc. Off. Anal. Chem.*, 59 (1976) 174.
[5] L.G.M.Th. Tuinstra, W.A. Traag and H.J. Keukens, *J. Chromatogr.*, 279 (1983) 533.
[6] J.A. Ault, C.M. Schofield, L.D. Johnsson and R.H. Waltz, *J. Agric. Food Chem.*, 27 (1979) 825.
[7] G. Fuchsbichler, *Landwirtsch. Forsch.*, 35 (1982) 90.
[8] H. Steinwandter, *Fresenius' Z. Anal. Chem.*, 313 (1982) 536.
[9] J.M. Czuczwa and A. Aford-Stevens, *J. Assoc. Off. Anal. Chem.*, 72 (1989) 752.
[10] A. Venant, S. Borrel, J. Mallet and E. Van Neste, *Analusis*, 17 (1989) 64.
[11] R.C. Hale, E. Bush, K. Gallagher, J.L. Gundersen and R.F. Mothershead, *J. Chromatogr.*, 539 (1991) 149.
[12] J.F. Lawrence, *Int. J. Environ. Anal. Chem.*, 29 (1987) 289.
[13] A.H. Roos, A.J. Van Munsteren, F.M. Nab and L.G.M. Th. Tuinstra, *Anal. Chim. Acta*, 196 (1987) 95.
[14] W. Specht and M. Tillkes, *Fresenius' Z. Anal. Chem.*, 322 (1985) 443.
[15] J.A. Van Rhijn and L.G.M.Th. Tuinstra, *J. Chromatogr.*, 552 (1991) 517.
[16] S. Williams (Editor), *Official Methods of Analysis of the Association of Official Analytical Chemists*, AOAC, Washington, DC, 14th ed., 1984, Sections 29037–29043.
[17] IUPAC, Commission of Pesticide Chemistry, *Pure Appl. Chem.*, 58 (1986) 1035.
[18] M.K.L. Bicking, *Anal. Chem.*, 56 (1984) 2671.
[19] M.K.L. Bicking and S.J. Serwon, *J. Liq. Chromatogr.*, 10 (1987) 1369.
[20] R.E. Majors and T.V. Alfredson, in J.F. Lawrence (Editor), *Trace Analysis*, Vol. 2, Academic Press, London, 1982, p. 111.
[21] A.M. Guillespie, *J. Liq. Chromatogr.*, 9 (1986) 2111.
[22] G. Durand, V. Buovot and D. Barceló, *J. Chromatogr.*, 607 (1992) 319.
[23] R.D. Wauchope, T.M. Buttler, A.G. Hornsby, P.W.M. Augustijn-Beckers and J.P. Burt, *Rev. Environ. Contam. Toxicol.*, 123 (1992) 1.
[24] G. Durand and D. Barceló, *Toxicol. Environ. Chem.*, 36 (1992) 225.
[25] P.S. Rosen, J.D. Magee and J.E. Casida (Editors), *Sulfur in Pesticide Action and Metabolism* (*ACS Symposium Series*, No. 158), American Chemical Society, Washington, DC, 1981.

ELSEVIER

Journal of Chromatography A, 673 (1994) 65–76

JOURNAL OF CHROMATOGRAPHY A

Size-exclusion chromatographic and viscometric study of polymer solutions containing nicotine or silicic acid

Iolanda Porcar, Rosa García, Agustín Campos, Vicente Soria*

Departament de Química Física, Universitat de València, E-46100 Burjassot, València, Spain

(First received December 6th, 1993; revised manuscript received March 11th, 1994)

Abstract

Preferential interactions of polymers with low-molecular-mass compounds were investigated regarding mainly the preferential solvation parameter and the intrinsic viscosity of ternary polymer solutions. Well characterized poly(vinylpyrrolidone) and poly(4-vinylpyridine) as macromolecular components in the presence of pure water or buffered solutions of nicotine or silicic acid served to formulate several ternary systems. Measurements included size-exclusion chromatography (SEC) and viscometry (off-line) at the appropriate concentration ranges, in order to obtain a linear response of the SEC detector and to describe the concentration dependence of the reduced viscosity by means of the Huggins equation for dilute polymer solutions. The former technique allows the so-called vacant peak to be attained, closely related to the preferential solvation parameter, which was directly monitored by means of a refractive index detector. Numerical evaluation of the preferential solvation parameter and intrinsic viscosity was used to account for overall interactions between linear vinyl polymers and nicotine and silicic acid as precursors of toxic agents.

1. Introduction

Polymers dissolved in a binary mixture of two low-molecular-mass molecules can often exhibit preferential solvation phenomena. In other words, the concentration of the solution in the close vicinity of the macromolecules is different from that in the bulk solution. Theoretical and experimental aspects of preferential solvation have been reported in the past mainly concerning synthetic polymers in binary organic and inorganic mixtures [1–4]. The first concerns to both Flory–Huggins and Flory–Prigogine–Patterson theories of polymer solutions, where complex expressions dealing with this phenomena have been reported [5,6]. From an experimental viewpoint over the past two decades, there has been increasing interest in incorporating new techniques and in developing the corresponding theoretical background. The pioneering experimental techniques available include equilibrium dialysis in conjunction with differential refractometry and light scattering, which are now employed fairly widely [7–9]. Others developed more recently include ultracentrifugation [10], differential densitometry and NMR, infrared and fluorescence spectroscopy [11–14]. Despite the important progress in experiment and theory, gaps in our knowledge still exist

* Corresponding author.

* Presented at the *22nd Annual Meeting of the Spanish Chromatography Group, Barcelona, October 20–22, 1993.*

0021-9673/94/$07.00
SSDI 0021-9673(94)00254-7

regarding multi-component polymer solutions [15–18].

In 1976, Berek *et al.* [19] reported a method based on the so-called "vacant peak" for polymer–mixed solvent systems, which was monitored by high-performance size-exclusion chromatography (HPSEC), assuming proportionality between the amount of polymer injected and the area of this singular peak. Since then, this assumption has made amenable the direct determination, rapidly and accurately, of the preferential solvation parameter, λ, by means of the SEC technique. Full details of the operational procedure and theoretical basis of this method have been given elsewhere [20–22]. Liquid chromatography has become one of the most widely used techniques for the evaluation of λ using size-exclusion and reversed-phase separation mechanisms [23,24].

We present in this paper a study of preferential solvation for poly(vinylpyrrolidone) (PVP) and poly(4-vinylpyridine) (P4VPy) in binary aqueous solutions of a toxic agent such as nicotine (NIC) or silicic acid (SA). PVP was selected because of its biocompatible character, so that it is suitable for use in injections and other parenteral applications. Moreover, the polymer is supplied in various molecular mass grades, including specially purified grades for pharmacological applications [25–27]. Nicotine is a highly toxic alkaloid which was first isolated in 1828 from tobacco, being present in amounts of 0.5–8.0% by mass. It exists as a tertiary amine with one chiral carbon located at the 2′-position of the N-methylpyrrolidine ring. Nicotine and other related metabolites can be found in the urine and hair of smokers and most non-smokers [28,29]. Moreover, the salt form has been used as a natural insecticide [30], and the free base as an anthelmintic agent in medicine [31] and as an experimental drug in the treatment of Parkinson's and Alzeimer's diseases [32,33]. Numerous gas chromatographic (GC) and liquid chromatographic (LC) [29,34,35] methods for assaying nicotine have been reported. The last low-molecular-mass component involved in this work is the (macro) silicic acid, $Si(OH)_4$, which was selected because of the toxicological character of silica dust [36]. Silica dissolves in water to form monosilicic acid. It has been found that the toxic effects of silica are due to the capacity of silicic acid to act as a hydrogen donor in the formation of hydrogen-bonded complexes with active groups such as phospholipids or secondary amide groups of proteins [37–39].

We formulated the following ternary polymer systems: water–nicotine–PVP and water or buffer solution–PVP–silicic acid, the two first components being considered as a binary solvent and the third as the solute. In choosing these compounds for study we were guided by the desire to correlate macroscopic physico-chemical properties of the polymer, represented by the preferential solvation parameter and the intrinsic viscosity, with the protective effects of some polymers on the toxicity exhibited by some low-molecular-mass substances, of which nicotine or silicic acid were selected in this work owing to their organic and inorganic nature, respectively.

2. Experimental

2.1. Chemicals and reagents

HPLC-grade water was produced by a Milli-Q water-purification system (Millipore, Bedford, MA, USA), consisting of prefilter, charcoal, ion-exchange and Organex cartridges. Buffer solutions were prepared using different reagents such as $NaHCO_3$, NaOH, $NaCH_3COO \cdot 3H_2O$ and CH_3COOH and Milli-Q-purified water. All reagents were of analytical-reagent grade from Merck (Darmstadt, Germany). Dextran samples obtained from Pharmacia (Uppsala, Sweden) of nominal molar masses 10, 17.7, 40, 66.9, 83.3, 170 and 500 kg mol^{-1} were used as standards for SEC column calibration. Poly(vinylpyrrolidone) of two molecular mass grades, 10 and 40 kg mol^{-1}, were obtained from Fluka (Darmstadt, Germany). Nicotine (NIC) and silicic acid (SA) were of puriss reagent grade from Merck. All reagents were used as obtained from the supplier. A poly(4-vinylpyridine) (P4VPy) sample was obtained by ultrafiltration of a commercial

sample of nominal molecular mass 40 kg mol^{-1}, supplied by Polysciencies (Washington, PA, USA). Ultrafiltration was carried out with a Millipore 142-mm diameter HI-FLUX UF cell.

2.2. Chromatographic measurements

A Waters Model ALC/GPC 202 liquid chromatograph equipped with an M-45 solvent-delivery system, a U6K universal injector and an R-410 refractive index detector was used. All chromatograms were recorded on a Spectra-Physics Model 4290 computing integrator, which was set at an attenuation of 4 or 8 for experiments involving SA or NIC, respectively. A Spherogel TSK PW 4000 column with 500 Å nominal pore size was used. The interstitial packing volume and total pore volume were 5.15 and 10.40 ml, as measured with high-molecular-mass dextran and ^2H_2O, respectively. The mobile phase flow-rate was adjusted to 1.0 ± 0.02 ml and thermostated at 25.0 ± 0.1°C in all experiments.

Two sets of experiments were performed. In those involving PVP as solute, the mobile phases were dilute solutions of NIC in pure water; in those involving SA as solute, the following mobile phases were prepared: solution of PVP-10 in a $NaHCO_3$–NaOH buffer (pH 10.0), solution of PVP-40 in the same buffer, PVP-10 in pure water, PVP-40 in pure water and P4VPy in NaOAc–CH_3COOH buffer (pH 4.0). The mobile phase compositions and the solute concentrations (PVP or SA) will be indicated in the next section.

The column was equilibrated overnight before injection of the analyte solution, which was always prepared using the corresponding mobile phase as solvent. Eluents and solutions injected were degassed and filtered, in all instances, through regenerated cellulose 0.45-μm pore diameter filters from Micro Filtration Systems (Dublin, CA, USA). The calibration graph for TSK PW 4000, using dextrans as standards, was obtained by extrapolation to zero concentration of peak elution volumes obtained for at least three injected concentrations.

2.3. Viscosities

Viscosity measurements were performed with an AVS 440 automatic Ubbelohde-type capillary viscometer from Schott Geräte (Hofheim, Germany). The instrument was equipped with a Model CT 1450 thermostated bath and with a Model T80.20 piston burette, moved by a microprocessor-controlled stepping motor for sample autodilution. For each solution, a 15-ml sample was loaded into the viscometer and placed in the thermostated bath. Measurements were initiated after an equilibration time of *ca.* 5–10 min and were continued until several elution time readings agreed to within 0.5%. All the viscosity measurements were performed at 25.0 ± 0.1°C. The viscosity η follows from $\eta = A\rho t - B\rho/t$, ρ being the solution density, t the elution time and A and B calibration constants. Elution times were determined as the average of several readings and the values obtained for the calibration constants were $A = 4.943 \cdot 10^{-5}$ cm^2 s^{-2} and $B = 1.783 \cdot 10^{-2}$ cm^2.

3. Results and discussion

Table 1 lists the polymer–toxic agent systems studied. Sample codes in the first column with N and S refer to those containing nicotine and silicic acid, respectively The probes (second column) were PVP for N-systems and SA for S-systems. Note that in the first set of systems, the toxic agent (NIC) exists as a component of the solvent, whereas the polymer probes act as the solute. In contrast, in the second set of systems PVP exists as a component of the binary solvent whereas the SA probe acts as the solute. The reason for using the systems in this particular form was the low solubility of SA in pure water [39], whereas its solubility increases when binary aqueous solutions, as shown in Table 1, are used instead of pure water.

As outlined in the Introduction, we explored the polymer–toxic agent interactions by means of SEC and viscometric (off-line) techniques. The proposed analysis is based on the evaluation of the preferential solvation parameter, λ, and of

Table 1
Polymer–toxic agent systems studied in different aqueous media, with the range of concentrations covered by each component, expressed as % (w/v), for λ determination in parentheses

Code	Probe	Binary eluent
N1	PVP-10 (0.1–0.8)	Water + nicotine (0.20–0.45)
N2	PVP-40 (0.4–1.7)	Water + nicotine (0.20–0.45)
S1	SA (0.016–0.035)	Water + PVP-10 (0.25–0.40)
S2	SA (0.010–0.030)	Water + PVP-10 (0.20–0.40)
S3	SA (0.015–0.045)	Buffer (pH 10) + PVP-10 (0.20–0.45)
S4	SA (0.015–0.045)	Buffer (pH 10) + PVP-40 (0.20–0.45)
S5	SA (0.005–0.035)	Buffer (pH 4) + P4VPy (0.10)

the reduced viscosity (η_{sp}/c). Next, we outline briefly the theoretical background for ternary polymer systems, dealing with the above parameters. Thus, for convenience, we begin by reproducing some of the previously derived equations because they are required for the discussion.

(a) When a solvent (1) is preferentially adsorbed by a polymer in a ternary system S(1)–S(2)–polymer(3), λ can be defined as the change in the volume fraction of component 1 with respect to the polymer concentration at infinite dilution. Thus, the expression for λ would be [20]

$$\lambda = \frac{\Delta\nu_1^0}{c_3} \cdot \frac{A_2}{A_1(+,-)} \tag{1}$$

c_3 being the concentration of the component designated the probe in Table 1 and $\Delta\nu_1^0$ refers to the difference in the volume fraction of the solute between the solution and the mixture (binary eluent), being related to the peak area obtained in the calibration (*i.e.*, NIC) A_1. Subsequent injection of a ternary system will give a vacant NIC peak area, A_2. Thus, the preferential interaction parameter, λ, can be calculated from the experimentally observed parameters through Eq. 1.

(b) The viscosity of binary polymer solutions at low concentrations can be expressed as

$$\eta(c) = \eta_s(1 + [\eta]c + k_H[\eta]^2c^2 + \cdots) \tag{2}$$

where η_s is the solvent viscosity, $[\eta]$ the intrinsic viscosity of the polymer and k_H the Huggins coefficient.

Rearrangement of Eq. 2 yields

$$\frac{\eta_{sp}}{c} = [\eta] + bc \tag{3}$$

where $b = k_H[\eta]^2$ and

$$\frac{\eta(c) - \eta_s}{\eta_s c} = \frac{\eta_{sp}}{c} \tag{4}$$

The same functionality can be assumed for ternary systems, here PVP in a binary mixture composed of pure water or buffered solution in the presence of NIC or SA. In this way, the viscosity of a ternary solution at low concentrations can be similarly expressed as

$$\left(\frac{\eta_{sp}}{c}\right)_m = [\eta]_m + b_m c_m \tag{5}$$

where the subscript m denotes the polymer–toxic agent mixture. A plot of Eq. 5 will yield $[\eta]_m$ and b_m from the intercept and the slope, respectively. In the light of this equation, two features can be examined: the dimension of the PVP coils, as evidenced by $[\eta]_m$, and the polymer–toxic agent interaction, as evidence by b_m.

3.1. Calibration of RID response

Before injecting a ternary solution formed by the probe in a binary solvent, as listed in Table 1, an NIC solution of known concentration in a given solvent mixture was injected. The difference in the volume fraction of NIC between the above solution and the mixture, $\Delta\nu_1^0$, was related

to the area of the NIC peak, A_1. Subsequent injection of a ternary system will give a vacant NIC peak area, A_2. The application of Eq. 1 with the above parameters as input data allows us to obtain the λ values for both the N- and S-systems listed in Table 1.

Fig. 1 displays the detector response on injection of diverse aqueous NIC solutions, with [NIC] ranging from 0.06 to 0.34% (w/v). The baseline corresponds to a 0.20% aqueous solution of NIC. A derivative-shaped signal was observed on injection of NIC solutions at concentrations other than 0.20%. Hence, when the values of [NIC] are greater than 0.20%, the direction of this signal first shows an increase, denoted by (+). In contrast, when the contrary occurs, the signal obtained then decreases (−) in the relative transmittance. Fig. 2 depicts the plot of the deviation of [NIC] with respect to the reference binary eluent, [NIC] = 0.20% as indicated above, against the area of the deflection peaks shown in Fig. 1. A good linear correlation was found for both the positive N(+) and negative N(−) directions of signal deflection for

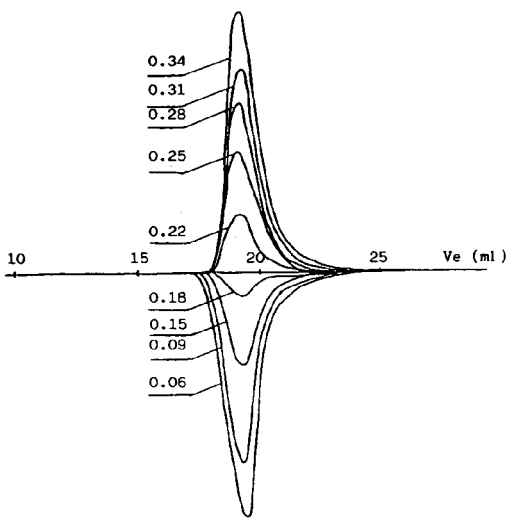

Fig. 1. Positive (●) and negative (○) signal deflections from refractive index detector on injection of 500 μl of nicotine solutions. Baseline corresponds to a mobile phase composition of 0.20% aqueous solution of nicotine and the detector attenuation is fixed at 8.

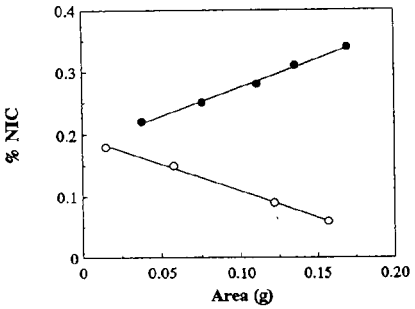

Fig. 2. Calibration graph for the deflection peaks obtained from different nicotine solutions. Symbols [○ = N(−); ● = N(+)] refers to experimental data and lines to a linear regression fit. Mobile phase composition corresponds to a 0.20% aqueous solution of nicotine.

nicotine-containing eluents. The same procedure was applied to calibrate the silicic acid-containing systems. The linear regression equations and their correlation coefficients are given in Table 2 for all the systems studied; $A(+,-)$ denotes the area of the deflection peak in both directions.

3.2. Evaluation of λ

We next proceeded to obtain the elution profile of diverse ternary polymer systems constituted by a probe in a binary eluent as specified in Table 1. When size exclusion is the main factor governing the separation mechanism in LC, the first peaks correspond to macromolecular species whereas the last peak or "vacant peak" denotes preferential interaction of the polymer, PVP or P4VPy, with one of the remaining components. As an example, Fig. 3 shows the elution profile of PVP-10 (0.30%) in an eluent formed by a dilute aqueous solution of NIC (0.20%). The amount of NIC preferentially solvated by PVP can be evaluated from the area of the last peak in conjunction with the calibration $A(-)$ equation from Table 2 for the nicotine-containing systems, and Eq. 1 for λ determination. Fig. 4 shows λ values as a function of both PVP and NIC concentrations. From Fig. 4a, there was no clear dependence of λ for PVP-10 on the above parameters because a gross scatter of data has been found. Fig. 4b shows the same plot for

Table 2
Calibration equations of the detector response on injection of diverse binary mixtures at different compositions

Mobile phase[a]	Code	Calibration equation[b]	Correlation coefficient
Water + NIC (0.20)	N1, N2	$A(+) = 0.1823 + 0.9242$ [NIC]	0.9977
	N1, N2	$A(-) = 0.1954 - 0.8594$ [NIC]	0.9986
Water + PVP-10 (0.20)	S1	$A(-) = 0.2025 - 0.2327$ [PVP-10]	0.9979
Water + PVP-40 (0.25)	S2	$A(-) = 0.2456 - 0.4637$ [PVP-40]	0.9978
Buffer (pH 10) + PVP-10 (0.20)	S3	$A(+) = 0.2237 + 0.4334$ [PVP-10]	0.9872
	S3	$A(-) = 0.2094 - 0.6273$ [PVP-10]	0.9950
Buffer (pH 10) + PVP-40 (0.20)	S4	$A(+) = 9.8847 + 0.2621$ [NaOH]	0.9761
	S4	$A(-) = 9.9021 - 0.1235$ [NaOH]	0.9993
	S4	$A(-) = 25.378 - 61.337$ [$NaHCO_3$]	0.9912
	S4	$A(+) = 0.1949 + 0.0013$ [PVP-40]	0.9996
	S4	$A(-) = 0.1900 - 0.0019$ [PVP-40]	0.9996
Buffer (pH 4) + P4VPy (0.10)	S5	$A(-) = 0.1003 - 0.3097$ [P4VPy]	0.9970

[a] Values in parentheses are concentrations of the second component (%).
[b] $A(+/-)$ refers to the area of the signal deflection when the direction shows an increase or a decrease in the relative transmittance.

PVP-40, the scatter of points being more pronounced and the λ values lower than those for the preceding systems. It is clear that the values of λ are strongly dependent on the PVP molar mass, being more pronounced as the latter decreases. In contrast with most polymer–mixed solvent systems, where the value of the preferential interaction parameter changes from positive to negative or *vice versa*, going through a maximum (or minimum) depending on the cosolvent or co-non-solvent behaviour of the binary solvent mixture [15–18], for the N-systems studied here the condition $\lambda = 0$ was not reached, at least in the range of NIC concentrations assayed.

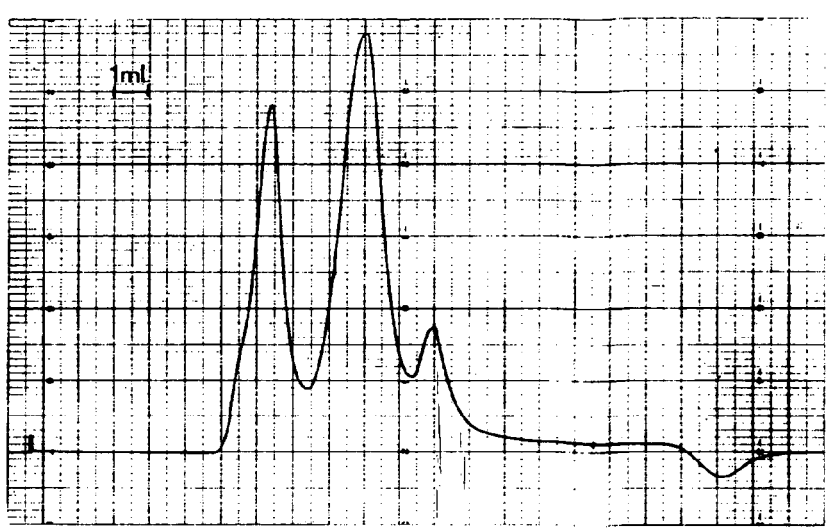

Fig. 3. Elution profile of poly(vinylpyrrolidone) (M_r 10^4) at 0.30% in a 0.20% solution of nicotine as eluent. The last signal corresponds to vacant peak.

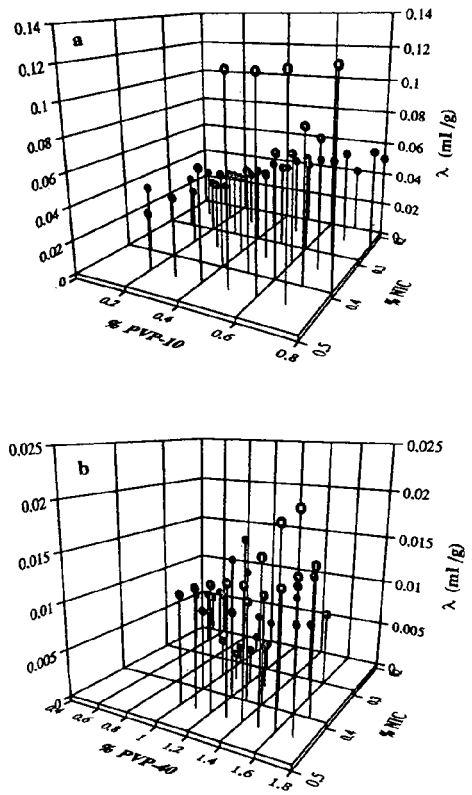

Fig. 4. Dependence of the experimental preferential interaction parameter λ (from Eq. 1) on nicotine and poly(vinylpyrrolidone) concentrations. PVP molar mass: (a) 10^4 and (b) $4 \cdot 10^4$ g/mol.

Moreover, a positive value of the preferential solvation parameter at low NIC concentrations means that these are more nicotine molecules in the vicinity of PVP because of the high affinity of nicotine for this polymer. The affinity of PVP for diverse co-solute molecules has been explained in depth by Molyneaux and Vekavakayanondha [40], but from our experimental measurements nothing can be inferred about these specific interactions.

Fig. 5a and b illustrate plots of the dependence of λ on SA and PVP concentrations in aqueous buffer (pH 10.0) media, corresponding to systems S3 and S4 in Tables 1 and 2, respectively. The same methodology as detailed above for N-systems was used for the evaluation of λ. From Fig. 5a, it can be seen that the λ values become higher at lower contents of both SA and PVP-10 components. A sudden increase in λ close to [PVP-10] = 0.25% and [SA] < 0.03% is observed, being positive in all instances. The positive values of λ at low SA concentrations mean that there are more SA molecules in the vicinity of PVP-10 as a consequence of the high affinity between both components under the adopted conditions. The same arguments can be used to explain the evolution of λ values for S-systems containing PVP-40, showed in Fig. 5b. However, in the latter system the λ values increase smoothly as both SA and PVP-40 concentrations decrease, being 50% lower than those obtained for the system in Fig. 5a.

In order to explore the effect of the aqueous media on λ, we applied two systems referred to as S1 and S2 in Tables 1 and 2, with the same polymer–toxic agent pairs dissolved in pure water instead of the above buffered solution. All details of the compositions and the calculation of the $A(+,-)$ parameter, necessary to apply Eq. 1, are also included in Tables 1 and 2. Fig. 6 depicts λ values as a function of both SA and PVP concentrations; the lines connecting points were drawn for the sake of visualization. Thus, for systems S1 and S2, positive λ values were always obtained, increasing as the SA and NIC concentrations decreased. The same trend was observed for systems S3 and S4 (see Fig. 5). An interesting observation from Fig. 6 is that λ increases as the PVP molar mass increases, in contrast with that observed in Fig. 5, where the opposite trend was found. The reason for this behaviour is not understood. In addition, from comparison of the λ values plotted in Figs. 5 and 6, it is clear that the data from the former are, in all instances, higher than those in the latter. For example, choosing as a representative value from each figure the top value for λ, we can see that 0.08 and 0.1 correspond to systems S1 and S2 where pure water is the bulk solvent, whereas for systems S3 and S4 where the bulk solvent is buffer (pH 10.0) solution, λ values of 0.6 and 0.3, greater than the preceding ones, were obtained. In the light of these results, it can be inferred that the change in the bulk water

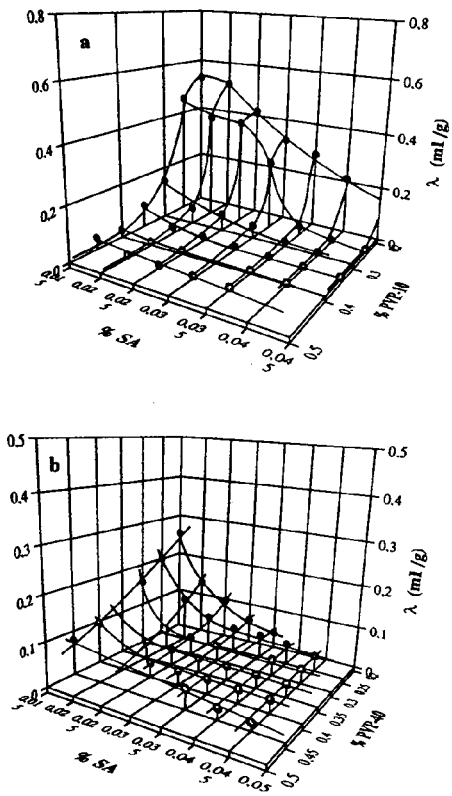

Fig. 5. Dependence of the experimental preferential interaction parameter λ (from Eq. 1) on silicic acid and poly(vinylpyrrolidone) concentrations. The bulk solvent is a buffer solution of pH 10.0.

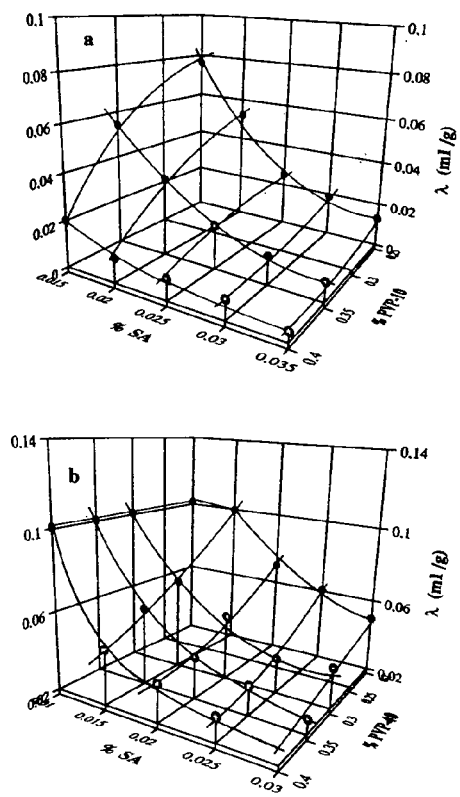

Fig. 6. Dependence of the experimental preferential interaction parameter λ (from Eq. 1) on silicic acid and poly(vinylpyrrolidone) concentrations. The bulk solvent is pure water.

structure on addition of electrolytes, as for systems S3 and S4, plays an important role in facilitating the diffusion of SA molecules in the vicinity of the polymer coil.

Lastly, we conducted exploratory experiments on a polymer containing pyridine rings instead of pyrrole in order to discuss the effect of the functional group on λ. A 0.10% solution of P4VPy in buffer (pH 4.0) as eluent and SA solutions as solute were used in SEC experiments. This system is denoted S5 and the concentration range covered by the SA is given in Table 1. The $A(-)$ values necessary to apply Eq. 1 were also obtained from a linear regression fit and the corresponding equation is reported in Table 2. The λ values obtained for this system are depicted in Fig. 7, where a unique mobile phase composition was applied. This plot reveals that λ follows a similar trend to that observed for the already discussed S-systems. As the molar masses of PVP-40 and P4VPy are the same, it seems reasonable to compare the λ values obtained for the systems where both polymers are involved. This comparison can easily be done by inspection of Figs. 5b, 6b and 7b, and it is concluded that the dependence of λ on P4VPy and SA concentrations follows qualitative and quantitatively the same trend as in S-systems.

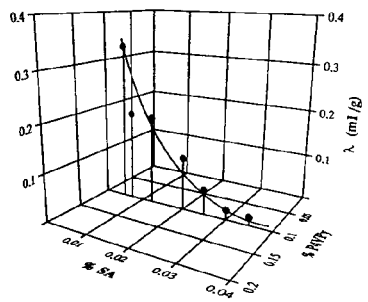

Fig. 7. Dependence of the experimental preferential interaction parameter λ (from Eq. 1) on silicic acid concentration, using a 0.1% solution of poly(4-vinylpyridine) in buffer of pH 4.0 as eluent.

3.3. Viscosity from ternary solutions

Results from binary and ternary solutions were compared to determine if the interaction between the polymer and the toxic molecules produces some additional effects. Two features were analysed: the dimension of the polymer coil, as evidenced by $[\eta]_m$, and the polymer–toxic agent interaction, quantified by the parameter b_m from Eq. 5.

The intrinsic viscosities and Huggins coefficients for binary systems, such as PVP-10, PVP-40 and P4VPy in pure water, buffer (pH 10.0) and buffer (pH 4.0), were determined from the dilute binary solution data, not reported here for simplicity. Plotting these data according to Eq. 3 produced $[\eta]$ and b from the intercept and slope, respectively. Table 3 gives these data along with the correlation coefficient, yielding fair linear fits, as expected.

The ternary solution viscosities were plotted according to Eq. 5. The intercepts $[\eta]_m$, the slopes b_m and the correlation coefficients are also given in Table 3. The nicotine-containing systems exhibit a concentration dependence of the reduced viscosity with two zones clearly delimited by a crossover concentration, $c_m^* = 0.15 \cdot 10^{-3}$ g ml^{-1}. At $c_m < c_m^*$, the reduced viscosity shows a reasonable linear behaviour, indicating that Eq. 5 is an adequate representation of the viscosity; however, at $c_m > c_m^*$, both $[\eta]_m$ and b_m are not dependent on concentration, at least in the concentration range measured. In Table 3 the data obtained for the intercept and slope of Eq. 5 for the PVP-10 + NIC and PVP-40 + NIC systems in pure water are also given. Comparison of the intercept values for binary PVP-10 + pure water and ternary PVP-10 + NIC + pure water systems at $c_m < c_m^*$, indicates that there is a

Table 3
Viscosity data at 25°C for pure polymer (Eq. 3) and for polymer–toxic agent mixtures (Eq. 5) in different aqueous media

Solute	Solvent	Intercept (ml g^{-1})	Slope	Correlation coefficient
PVP-10	Pure water	7.90	0.019	0.987
PVP-40	Pure water	21.6	0.136	0.997
PVP-10	Buffer (pH 10.0)	5.71	0.146	0.998
PVP-40	Buffer (pH 10.0)	18.7	0.351	0.998
P4VPy	Buffer (pH 4.0)	149.8	2.184	0.985
PVP-10 + NIC	Pure water	6.21	−0.058	–
		11.0	−4.210	–
PVP-40 + NIC	Pure water	12.7	−0.056	–
		15.8	−1.479	–
PVP-10 + SA	Pure water	5.54	0.309	0.996
PVP-10 + SA	Buffer (pH 10.0)	4.04	0.674	0.987
PVP-40 + SA	Pure water	16.6	1.290	0.996
PVP-40 + SA	Buffer (pH 10.0)	16.5	0.756	0.996
P4VPy + SA	Buffer (pH 4.0)	154.1	0.371	0.992

considerable increase ranging from 7.902 to 11.019 ml g^{-1}, which denotes an expansion of the PVP-10 random coil itself or an increase in the hydrodynamic size as a consequence of the preferential binding of the NIC molecules to the polymer. In contrast, at $c_m > c_m^*$ the intrinsic viscosity decreases from 7.902 to 6.207 ml g^{-1}, which means a coil contraction, probably due to the NIC + pure water being a poor solvent for PVP-10 compared with pure water. This argument can also be used to explain the viscosity of PVP-40 + NIC + pure water. From the comparison of the intercept values for ternary and binary systems, we obtain 15.8 ml g^{-1} at $c_m < c_m^*$ and 12.7 ml g^{-1} when $c_m > c_m^*$, both values being lower than the 21.6 ml g^{-1} corresponding to the PVP-40 + pure water binary system.

Analysis of the S-containing systems indicates that the intercepts for ternary solutions are always lower than those corresponding to binary solutions, independent of the bulk solvent composition. This shows that the polymer coil contracts, owing to the presence of SA in the system. In the light of these results, nothing can be inferred about the possible PVP–SA association. However, as claimed by other workers [36–39], similar macromolecular compounds can associate with SA molecules via hydrogen bonding. When P4VPy is incorporated instead of PVP in a ternary system, an increase from 149.8 (binary) to 154.1 (ternary) is detected. The increment in $[\eta]_m$ supports, on the one hand, the idea of a coil expansion and, on the other, a considerable increase in the hydrodynamic size, probably because SA has a proton-donating ability strong enough to form a hydrogen bond with the nitrogen of the pyridine ring placed on the polymer.

The second feature analysed was the solute–solvent interactions by comparison of the slopes obtained for binary (see Eq. 3) and ternary systems (see Eq. 5), with the data summarized in Table 3. Considering the N-containing systems, the slope values obtained for the ternary systems are, in all instances, lower than those for the corresponding binary systems. This behaviour could be attributed to the hydrophobic nature of the NIC molecules preferentially solvated in the vicinity of the PVP coil rather than a true association between PVP and NIC (macro)molecules. In contrast with the above behaviour, the values of the slopes for S-containing systems are larger for ternary than for binary systems. A possible argument to justify this trend could be the weak hydrophobicity displayed by the SA bound to PVP. In this context, and as pointed out by other workers [37–39], the capability of SA to bind PVP is supported by the proton-donating ability of SA to create hydrogen-bonded links with carbonyl groups from pyrrole rings of PVP.

Fig. 8 shows an example of the reduced viscosity for S-containing systems in a buffer (pH 10.0) as a function of the solute concentration. For binary systems, the polymer samples PVP-10 [(a), open symbols] and PVP-40 [(b), open symbols] must be considered as solutes. For ternary systems, the solute consists of a binary mixture of PVP + SA [(a) and (b), closed symbols]. The good linear correlation fits in all experiments depicted in Fig. 8 support the idea

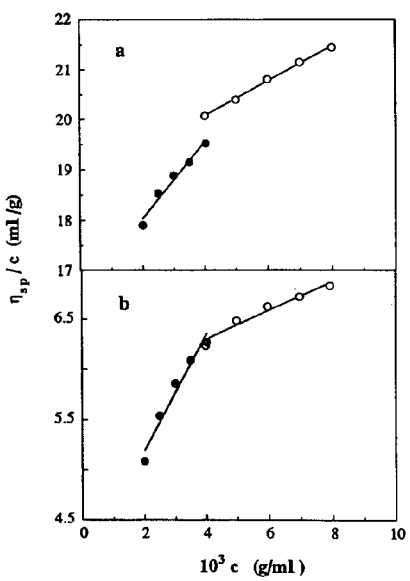

Fig. 8. Concentration dependence of the reduced viscosity for binary (open symbols) and ternary (closed symbols) silicic acid-containing systems in a buffer solution of pH 10.0. (a) ○ = PVP-40, ● = PVP-40 + SA; (b) ○ = PVP-10, ● = PVP-10 + SA.

that Eqs. 3 and 5 are adequate representations of the viscosity data over the concentration range studied. The same is true of the remaining S-systems, not plotted here for simplicity. The last system in Table 3 concerns a sample of P4VPy dissolved in a buffer solution (pH 4.0) for a binary system, and P4VPy + SA in the same buffer for a ternary system. The slope values for the two systems were 2.184 and 0.371, respectively. Note that this trend is contrary to the above-mentioned conclusion drawn for PVP + SA systems. However, in the present instance the experiments were carried out at pH 4.0 and taking into account that the pK_a of the silicic acid is 9.8, hence it will be in a fully protonated form. Moreover, it can be assumed that the pyridine ring of P4VPy will adopt a partially protonated form, at the same pH. Consequently, the existence of ionic repulsion between the two species could explain the above decrease in the slope value for both systems. The apparent affinity between the P4VPy and SA, supported by the λ values and corroborated by the intercept value derived from viscosity measurements, is clearly in disagreement with the above arguments. Regarding this unsolved question, additional experiments using other techniques must be done. We think, however, that our explanations open up a new approach to the study of polymer–toxic agent affinity.

4. Conclusions

The techniques used here, SEC and capillary viscometry, have been valuable in the study of preferential binding to polymers in dilute aqueous solutions of toxic agents. From the analysis of the vacant peaks obtained from SEC experiments for PVP and P4VPy samples in the presence of NIC or SA, as low-molecular-mass toxic agents, accurate information regarding the preferential solvation parameter, λ, has been obtained in addition to its concentration dependence on both polymer and toxic agent.

For PVP + NIC + pure water ternary systems, no correlation of λ with polymer molar mass and/or concentration of NIC was found. In contrast, for PVP + SA + pure water (or buffer pH 10.0), a clear dependence of λ on the above parameters was established, as can be seen in Figs. 5 and 6. The results obtained for λ reveal that the ability of NIC to solvate PVP is much less than that for SA, probably owing to the hydrophobic character of the former compound. In addition, a short series of experiments under the same experimental conditions but using P4VPy instead of PVP was carried out in order to analyse the effect of the pyridine ring on the preferential interaction. For this system, the effects on λ remain unaltered, ranging over the same order as for PVP-containing systems. Complementary information about the preferential interaction concerning polymers and a toxic agent was obtained from capillary viscosity measurements. Over the concentration range assayed, the experimental data on the reduced viscosity show a linear dependence on total concentration, allowing us to accommodate experimental data in conventional equations dealing with the viscosity of uncharged dilute polymer solutions (see Eqs. 3 and 5). Two main features were explored regarding the above equations, the intrinsic viscosity and the solute–solvent interaction. The conclusions obtained from the viscosity experiments support the behaviour of λ; however, some contradiction arguments derived from the interpretation of the viscosity data for P4VPy + SA system demand additional experiments to understand in depth the nature of these interactions. A complete description of the specific interactions is complicated and beyond the scope of this paper.

Acknowledgements

Financial support from the DGICYT (project No. PB91-0808) is gratefully acknowledged. A grant from the Ministerio de Educación y Ciencia (Spain) to I.P. is deeply appreciated.

References

[1] A. Dondos and H. Benoit, *Makromol. Chem.*, 133 (1970) 119.

[2] J.M.G. Cowie and I. McEwen, *Macromolecules*, 7 (1974) 291.
[3] M. Apostolopoulos, M. Morcellet and C. Lucheux, *Makromol. Chem.*, 183 (1982) 1293.
[4] M. Apostolopoulos, M. Morcellet and C. Lucheux, *Makromol. Chem.*, 184 (1983) 2519.
[5] P.J. Flory, *Principles of Polymer Chemistry*, Cornell University Press, Ithaca, New York, 1953.
[6] A. Horta, *Macromolecules*, 12 (1979) 785.
[7] C. Strazielle and H. Benoit, *J. Chim. Phys.*, 58 (1961) 675.
[8] S.N. Timasheff, *Acc. Chem. Res.*, 3 (1970) 62.
[9] Y. Shindo and K. Kimura, *J. Chem. Soc., Faraday Trans. 1*, 80 (1984) 2199.
[10] R.C. Patel and T.M. Aminabhavi, *J. Macromol. Sci. Rev. Macromol. Chem. Phys.*, C22 (1982) 203.
[11] S. Bronstein, S. Bywater and J.M.G. Cowie, *Trans. Faraday Soc.*, 9 (1969) 2480.
[12] L. Moldovan and G. Weill, *Eur. Polym. J.*, 7 (1971) 1023.
[13] C. Lety-Sistel, B. Chaufer, B. Sebille and C. Quivoron, *Eur. Polym. J.*, 11 (1975) 689.
[14] B. Chaufer, B. Sebille and C. Quivoron, *Eur. Polym. J.*, 11 (1975) 695.
[15] C.M. Gomez, V. Soria and A. Campos, *Colloid Polym. Sci.*, 270 (1992) 197.
[16] C.M. Gomez, R. García, V. Soria and A. Campos, *Colloid Polym. Sci.*, 271 (1993) 30.
[17] C.M. Gomez, R. García, V. Soria and A. Campos, *Colloid Polym. Sci.*, 271 (1993) 372.
[18] C.M. Gomez, R. García, V. Soria and A. Campos, *Colloid Polym. Sci.*, 271 (1993) 646.
[19] D. Berek, T. Bleha and Z. Pevna, *J. Polym. Sci., Polym. Lett. Ed.*, 14 (1976) 323.
[20] A. Campos, L. Borque and J.E. Figueruelo, *J. Chromatogr.*, 140 (1977) 219.
[21] A. Campos and J.E. Figueruelo, *Polymer*, 18 (1977) 1296.
[22] V. Soria, A. Campos and J.E. Figueruelo, *An. Quim.*, 74 (1978) 1026.
[23] M. Okubo, I. Azume and Y. Yamamoto, *Colloid Polym. Sci.*, 268 (1990) 598.
[24] W.E. Rudzinski and T.M. Aminabhavi, *J. Macromol. Sci. Chem.*, A19 (1983) 1247.
[25] *Polyvinylpirrolidone (PVP): Kollidon Luviskol*, BASF, Ludwigshafen, 1979.
[26] *Kollidon Grades: Polyvinylpirrolidone for the Pharmaceutical Industry*, BASF, Ludwigshafen, 1982.
[27] P. Molineux, *Br. Polym. J.*, 18 (1986) 32.
[28] J. Elenhorn and D.O. Barcelaux, *Medical Toxicology*, Elsevier, Amsterdam, 1988, p. 912.
[29] P. Kintz, *J. Chromatogr.*, 580 (1992) 347.
[30] N.E. McIndoo, R.C. Roark and R.L. Bushey, *A Bibliography of Nicotine. Part II. The Insecticidal Uses of Nicotine and Tobacco (Publication E-392)*, Vol. 2, Section 1, US Department of Agriculture, Bureau of Entomology, Washington, DC, 1936.
[31] J. Wilbert, *Tobacco and Shamanism in South America*, Yale University Press, New Haven, CT, 1987, Ch. 4.
[32] J.A. Baron, *Neurology*, 36 (1986) 1490.
[33] B. Sahakian, G. Jones, R. Levy, J. Gray and D. Warburton, *Br. J. Psychiatry*, 154 (1989) 797.
[34] T.H. Perfetti and J.K. Swadesh, *J. Chromatogr.*, 543 (1991) 129.
[35] M.R. Moeller, *J. Chromatogr.*, 580 (1992) 125.
[36] P. Ferruti and M.A. Marchisio, *Med. Lav.*, 57 (1966) 481.
[37] P.F. Holt and E.T. Nasrallah, *J. Chem. Soc. B*, (1968) 233.
[38] P.F. Holt, H. Lindsay and E.G. Beek, *Br. J. Pharmacol.*, 38 (1970) 192.
[39] T. Nash, A.C. Allison and J.S. Harrington, *Nature*, 210 (1966) 259.
[40] P. Molyneux and S. Vekavakayanondha, *J. Chem. Soc., Faraday Trans. 1*, 82 (1986) 291.

ELSEVIER

Journal of Chromatography A, 673 (1994) 77–84

JOURNAL OF CHROMATOGRAPHY A

Rapid and sensitive determination of nitrite in foods and biological materials by flow injection or high-performance liquid chromatography with chemiluminescence detection

Nrisinha P. Sen*, Philander A. Baddoo, Stephen W. Seaman

Food Research Division, Food Directorate, Health Protection Branch, Health Canada, Ottawa, K1A 0L2, Canada

(First received January 18th, 1994; revised manuscript received March 16th, 1994)

Abstract

A method is described for the determination of nitrite that is based on reduction of nitrite with potassium iodide followed by chemiluminescence detection of the liberated NO using a thermal energy analyzer. The method worked well both in the flow injection mode and upon interfacing with a reversed-phase high-performance liquid chromatography system. Limited data available indicated a good agreement between results obtained by the chemiluminescence method and those obtained by using a well established colorimetric procedure when they were applied for the determination of nitrite in a number of cured meats, human saliva, and baby foods. The chemiluminescence method is, however, much superior to the colorimetric one in its speed, versatility, as well as sensitivity (200 times more), and requires only a minimum of sample preparation. The detection limit of the new method is about 0.1 ng $NaNO_2$ per injection or 5 μg/kg in cured meats and other substrates analyzed.

1. Introduction

There is extensive interest in the determination of nitrite in both foods and biological materials. This is mainly because of three reasons. First, it is highly toxic to man, especially to infants, causing methemoglobinemia and possibly death [1–3]. Secondly, nitrite can lead to the formation of various carcinogenic N-nitroso compounds after reaction with secondary amines and amides which are abundant in foods [4,5]. Thirdly, nitrite is widely used as a preservative in cured meat products and certain kinds of fish that suggests the need for accurate control and monitoring of nitrite levels in such products throughout various stages of processing and storage [2,6]. Nitrite also occurs naturally, mostly at low ppm (μg/g) levels, in water, certain vegetables, storage-abused leafy vegetables (levels can exceed 100 ppm), and many processed foods (*e.g.* cereals and dairy products) [2,7].

Besides ingested nitrite through foods, salivary nitrite, produced due to microbial reduction of nitrate in the oral cavity, constitutes one of the major sources of man's exposure to this chemical [2,8]. There is conclusive evidence to suggest that both ingested and salivary nitrite can react *in vivo* with various amines and amides in the food to form N-nitroso compounds [2,4,9]. Such a reaction can occur in the acidic environment of the human stomach or other parts of the body. This has prompted many to investigate the effects of various nitrate-rich diets on salivary

* Corresponding author.

0021-9673/94/$07.00
SSDI 0021-9673(94)00270-J

nitrite levels and, ultimately, on *in vivo* N-nitrosation [2,4,10].

Numerous methods have been reported for the determination of nitrite in foods and biological materials [11,12]. These include the classical colorimetric methods based on Griess reaction [11,13], polarographic methods [14], gas chromatographic methods following derivatization [15], high-performance liquid chromatography (HPLC) using different detectors [16–21], and chemiluminescence detection following reduction of nitrite to NO using suitable reductants [22–26]. Although these methods are reliable and adequate for the purposes developed, some of them are lengthy and time consuming, some lack specificity or sensitivity, and some have not been tested adequately to determine their applicability to a wide variety of substrates. It was felt that there is a need for a highly sensitive and specific method for the determination of nitrite in foods and biological materials that is fast and requires only a minimum of sample preparation. In this paper, we wish to report such a method that is based on chemiluminescence detection of nitrite after reduction with iodide ion. It requires only a few minutes to 1.5 h to complete an analysis depending on the nature of the sample being analyzed. The determination can be carried out either in the flow injection mode or HPLC mode using a reversed-phase and ion-pair chromatography system.

2. Experimental

2.1. Apparatus

A schematic diagram of the whole detection system used is shown in Fig. 1. It can be roughly divided into three parts: (a) HPLC assembly, (b) post-column reactor for reduction of nitrite to NO, and (c) chemiluminescence detection of NO using a thermal energy analyzer (TEA).

(a) HPLC unit

The unit (Fig. 1) consisted of a solvent delivery system (pump Model 110B, Beckman, San Ramon, CA, USA) and an Altex Rheodyne injector (Model 7125, sample loop 50 μl or 100 μl). The HPLC separation was carried out using a 250 mm × 4.6 mm I.D. stainless-steel column packed with C_{18} packing (5 μm) (Techsil, Cheshire, UK) and a mobile phase consisting of 0.05 *M* KH_2PO_4 (pH 6) and 5 m*M* tetrabutylammonium hydrogen sulfate. The mobile phase flow-rate was either 1 or 2 ml/min. In the flow injection mode, the HPLC column was omitted from the system.

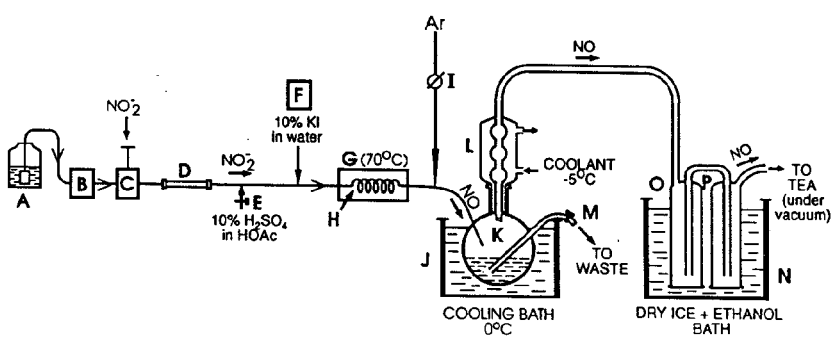

Fig. 1. Schematic diagram of the detection system. (A) Mobile phase; (B) mobile phase delivery system (pump); (C) injector; (D) HPLC column; (E) PTFE stopcock [27]; (F) peristaltic pump; (G) temperature-controlled hot water bath; (H) coiled tubing (reactor); (I) precision gas flow controller; (J) cooling bath (ice + water); (K) collection flask (500 ml); (L) condenser; (M) glass stopcock; (N) cooling bath (dry ice + ethanol); (O) and (P), cold traps. The trap O should be connected exactly as shown so that the moisture collects on the outside wall of the trap. Modified from that described by Havery [27].

(b) Post-column reactor

The reactor used was essentially the same reported previously by Havery [27] for the determination of N-nitroso compounds. The main differences were that, in this study, a temperature-controlled hot water bath (instead of a heating mantle) was used to heat the coiled PTFE tubing (300 cm × 0.16 cm O.D., and 0.08 cm I.D.), and a peristaltic pump was used to introduce the 10% KI solution (flow-rate *ca.* 0.5 ml/min). Also, a condenser was added between the two cooling baths (Fig. 1) for a more efficient removal of moisture that otherwise resulted in frozen lines in traps O or P. It should be emphasized that all tubings and connections that come in contact with NO must be made of PTFE or glass. Further details regarding design and assembly of the reactor can be obtained from the above reference.

As will be discussed later, two other variations of nitrite reduction conditions were investigated. These were: (i) glacial acetic acid alone (instead of 10% H_2SO_4 in HOAc) and no KI solution in flask F, and (ii) 10% ascorbic acid solution in flask F (instead of KI solution) and glacial acetic acid (without H_2SO_4). It should be noted that there was no need to pump in the acid (HOAc or mixture of H_2SO_4/HOAc). It was slowly drawn in by the TEA vacuum which was maintained between 1–1.2 mmHg. Other conditions were as follows: acid flow-rate, *ca.* 2 ml/min; ascorbic acid solution flow-rate, *ca.* 0.5 ml/min; and Ar carrier gas flow-rate, 30–60 ml/min (optimum flow determined by trial and error).

After a few runs, when the flask K became *ca.* 60% full, the TEA vacuum was switched to the vent position which blocked the tubing going into the TEA (thus disconnecting the system from the vacuum). Immediately following this the stopcock E was closed and that at M was opened. Within a few minutes the carrier gas (Ar) pushed out the liquid in flask K into a waste reservoir which should be kept inside a fume-hood. After emptying the flask the above manipulations were carried out in the reverse order and analyses were resumed after a few minutes of equilibration. Care should be taken to watch for a frozen line in the system that is usually indicated by a sudden drop in TEA vacuum or by a build-up of pressure inside flask K thus resulting in a reverse flow of KI solution into the flask containing the H_2SO_4/HOAc mixture.

(c) Chemiluminescence detection

The NO produced by reduction of nitrite and purged out by the carrier gas was detected using a TEA detector (Model 502, Thermedics Detection, Chelmsford, MA, USA). Basically, it is a chemiluminescence detector originally developed for specific determination of N-nitroso compounds [28,29]. The liberated NO is allowed to react with ozone to form electronically excited molecules of NO_2^* which then decays back to ground state with the emission of light in the near infra red region (600–3000 nm). The emitted light is allowed to pass through a filter (600–800 nm), the signal amplified, and detected using a 1-mV recorder. The TEA has been shown to be highly sensitive and specific to NO, and to give a linear response over a wide range of concentration. Since moisture interferes with the detection, the series of condenser and cold traps serve to remove it as much as possible.

2.2. Reagents

All reagents used were of analytical or high purity grade. Tetrabutylammonium hydrogen sulfate was purchased from Sigma, St Louis, MO, USA. All reagents were used without further purification. Water used for preparing reagents and mobile phase was distilled in an all glass apparatus. Sodium nitrite standard solutions were prepared fresh daily.

2.3. Samples

The cured meats and the baby food samples were purchased locally from retail outlets. Each sample was mixed well either by homogenizing in a blender (for the meats) or stirring with a spatula (for the baby foods) before taking an aliquot for analysis. The human saliva and the urine samples were made slightly alkaline (*ca.* pH 10), immediately after collection, by the addition of 2% NaOH solution, and then stored

at 4°C until analysis. This was done to prevent bacterial reduction of nitrate to nitrite, and to stabilize nitrite during storage.

2.4. Determination of nitrite

Before beginning analysis, the TEA and the post-column reactor were set up as described by Havery [27] with modifications as mentioned above. A series of duplicate injections (50 or 100 μl) of appropriate dilute nitrite standards (0.01 to 10 μg $NaNO_2$/ml) were made allowing approximately a 10-min gap between injections (the nitrite peak eluted within 6 min). The TEA attenuation was set between 16 and 1024 depending on the amount of $NaNO_2$ injected. A 4-min interval between injections was adequate in the flow injection mode for nitrite eluted within 1 min.

2.5. Standard curve for nitrite

Two sets of standard curves for sodium nitrite, one in the range of 0.5 to 100 ng per injection and the other between 0.1 to 1 μg per injection were constructed to determine the linearity of response over this entire range. Each standard was analyzed in duplicate, and an average of the peak heights were used to construct the curves. This was, however, not carried out regularly (done only once a month). For routine analysis the concentration of nitrite in a sample extract was calculated from its relative response to that of an appropriate standard giving a comparable (within ± 50%) response.

2.6. Analysis of cured meats and baby foods

A 10-g aliquot of a well homogenized sample was extracted with water, and the extract processed and filtered as described previously [30]. A 50–100 μl aliquot of the final filtrate was analyzed as above after appropriate dilutions (2 to 10-fold) with the HPLC mobile phase.

2.7. Analysis of urine and saliva

No sample preparation or clean-up was necessary for the analysis of these samples. They were analyzed as above after 10 to 100 fold dilutions with the HPLC mobile phase.

2.8. Colorimetric determination of nitrite

A method based on Griess colorimetric procedure [30] was used for the spectrophotometric determination of nitrite in cured meats and the baby food samples. It was also used for the analysis of human saliva samples, but because of the smaller size and lesser amounts of suspended solids in these samples, the method was operated on a micro scale. This involved mixing 2 ml sample with 1 ml of 2% NaOH solution, addition of 0.5 ml of 0.42 *M* $ZnSO_4$ solution (to precipitate proteins), heating the mixture for 15 min in a 50–60°C water bath, making up volume to 5 ml with water, centrifuging and pipetting out a 2-ml aliquot of clear supernatant, and finally determining the level of nitrite by the Griess colorimetric procedure as described previously [30]. The detection limit of the colorimetric method was about 1 ppm (μg/g) in each of the above substrates. Although no urine samples were analyzed by this method, this can be done, if desired, using the method for cured meats and baby foods [30].

3. Results and discussion

The chemiluminescence method described in this paper is based on an earlier procedure reported by Cox [22], but it differs significantly both in the design of the apparatus and in its operating conditions from those previously reported [22]. Cox used an apparatus in which nitrite was reduced to NO, by heating a 20-ml aliquot of nitrite standard or sample with various reducing agents, on a batch operation basis. After each analysis, the apparatus had to be dismantled, cleaned, and reassembled before resuming the next analysis. In our method a post-column reactor developed by Havery [27] for the determination of N-nitroso compounds was used. This allowed rapid successive determination of nitrite until the flask K became *ca.* 60% full. At that point, the flask could be emptied and analyses resumed, without dis-

mantling the apparatus, as described under Experimental. Furthermore, this technique has the added advantage that it can be used either in the flow injection or HPLC mode thus making the method versatile. The former mode is more suitable for the analysis of relatively dirtier samples which otherwise might reduce the life of an expensive HPLC column. In the HPLC mode, the retention time of the nitrite peak can be used as an additional parameter for its identification which makes the technique more specific. The same thing can be said about another chemiluminescence method [23] reported recently that is also operated on a batch operation basis, but uses a gas sampling valve that allows replicate analyses of the same sample in a single run.

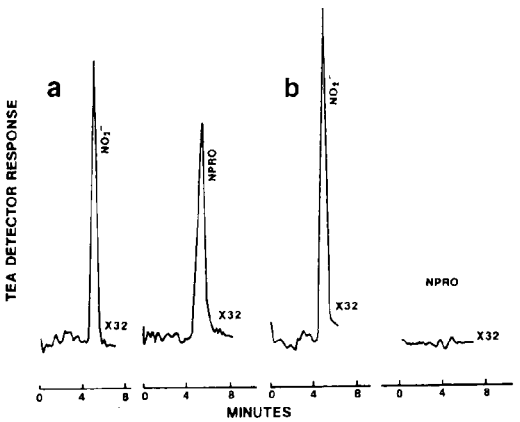

Fig. 2. HPLC chemiluminescence determination of nitrite. (a) With KI flowing into the reactor (2 ng $NaNO_2$ and 17.5 ng N-nitrosoproline (NPRO), respectively); (b) without KI and only glacial acetic acid flowing into the reactor (2 ng $NaNO_2$ and 17.5 ng NPRO, respectively). Mobile phase flow-rate, 1 ml/min.

4. Selectivity, sensitivity, and reproducibility

Since the method is based on the detection of NO, any compound producing NO under the post-column reactor conditions will give a false-positive response for nitrite. Previous research [25,27] has shown that most N-nitroso compounds and organic nitrites (*e.g.*, butyl nitrite) do give a positive response in such a system. Therefore, an attempt was made to minimize interferences from these compounds by varying the reagents in the reactor. It was observed that if the KI solution and the sulfuric acid–acetic acid mixture were replaced, respectively, with 10% ascorbic acid solution (in flask, F) and glacial acetic acid, the response from N-nitroso compounds became negligible. Omitting the ascorbic solution in flask F with only glacial acetic acid flowing into the reactor also gave no or negligible (*ca.* 1–5%) response for N-nitroso compounds (Fig. 2). In the absence of any reductant under the latter conditions, acid dismutation reactions, yielding NO from HNO_2, are responsible for the positive response from nitrite [23,24]. Since foods and biological materials contain only extremely low concentrations of N-nitroso compounds, their presence would not interfere with the determination of nitrite in these substrates provided the above modified conditions are used. Organic nitrites, however, may still give a positive response. It is highly unlikely, however, that these compounds would be present in foods in high enough concentrations to interfere with the determination of nitrite. Nitrate (as the Na salt) even at a relatively large amount (50 to 100 ng/injection) did not produce a detectable response.

In view of the above, most analyses were carried out without any KI solution flowing into

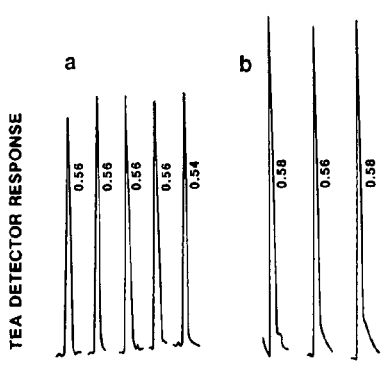

Fig. 3. Reproducibility of nitrite determination by flow injection chemiluminescence technique. (a) 5 replicate injections of 10 ng $NaNO_2$ each (attenuation, 256); (b) 3 replicate analyses of a cured turkey breast extract containing 26 ppm $NaNO_2$ (attenuation, 128). The peak elution times are printed beside each peak.

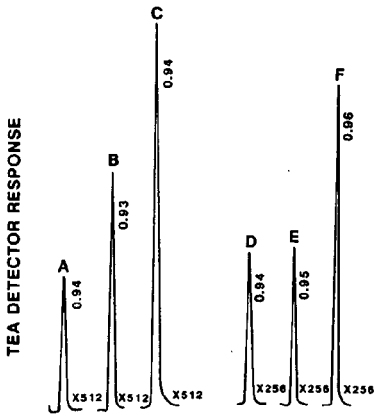

Fig. 4. Recovery studies using flow injection chemiluminescence determination. (A) 0.1 ml out of 400 ml final dilution of a pepperoni sample found to contain 11 ppm $NaNO_2$; (B) 0.1 ml of $NaNO_2$ spiking solution (spiking level, 20 ppm $NaNO_2$); (C) 0.1 ml out of 400 ml final dilution of the above pepperoni spiked with 20 ppm $NaNO_2$ (calculated recovery, 97.8%); (D) 0.1 ml of a human saliva sample after a 100-fold dilution; (E) 0.1 ml of $NaNO_2$ spiking solution (spiking level, 5 ppm $NaNO_2$); (F) 0.1 ml of above saliva after spiking with 5 ppm $NaNO_2$ and a 100-fold dilution (calculated recovery, 105%).

the reactor because this minimized the possibility of interference from N-nitroso compounds. The method worked highly satisfactorily both in the flow injection and HPLC modes, and was found to be highly sensitive and reproducible. The minimum detection limit ($>3\times$ noise level) seemed to be about 0.1 ng per injection. The response was linear over a wide range (1 to 1000 ng) of $NaNO_2$ injected. Replicate injections (n = 4 or 5) of both standards and sample extracts gave highly reproducible responses (Fig. 3), and these ranged between 0.2 to 4% for replicate injections of 50 ng (attenuation, 256) and 1 ng $NaNO_2$ (attenuation, 64; not shown in Fig. 3), respectively. Although distilled water was adequate as a mobile phase in the flow injection mode, for ease of operation, the HPLC mobile phase containing the ion-pair reagent was used throughout. In the HPLC mode, the nitrite ion usually eluted after 3 or 6 min depending on the mobile phase flow-rates (Figs. 2 and 5). With a more active (brand new) HPLC column, the retention time of nitrite was found to be slightly longer (not shown).

Table 1
Comparison of nitrite levels in some selected samples as determined by two different methods

Sample	Levels (ppm) of nitrite (as $NaNO_2$) detected	
	Chemiluminescence technique	Colorimetric method
Cured meats		
All beef wieners	17.1	18.3
All beef salami	33.5	30.7
Pepperoni	8.2	7.8
Human saliva		
Person A	3.7	3.1
Person B	8.2	6.5
Person C	3.8	4.4
Person D	13.1	10.6
Baby foods		
Junior mixed vegetables	0.11	Negative[a]
Beginner green beans	0.10	Negative
Beginner carrots	0.09	Negative
Strained vegetables and ham	0.15	Negative

[a] Detection limit, *ca.* 1 ppm.

5. Applications

The method was used to determine its suitability for the determination of nitrite in a few selected samples of foods and human biological materials. The average recoveries of sodium nitrite added to cured meats (spiking level, 10 ppm), human saliva (spiking level, 5 ppm), and human urine (spiking level, 0.02 ppm) were found to be 108% ($n = 3$), 105% ($n = 2$), and 92% ($n = 6$), respectively. A few representative chromatograms from these recovery studies are shown in Fig. 4. For comparison purposes, a few samples of cured meats, human saliva, and baby foods were reanalyzed by the above mentioned colorimetric procedure which is a well established method and has been shown to give highly reliable and accurate results in a number of laboratories [30,31–33]. The two sets of results compared well with each other except that the colorimetric method was not sensitive enough to detect the extremely low levels of nitrite in the baby foods, and hence gave negative results for these samples (Table 1). The overall detection limit of the chemiluminescence method was estimated to be about 5 ppb (μg/kg) which is 200 times lower than that of the colorimetric method. Moreover, the new method is much faster and requires very little sample preparation, especially in the flow injection mode. If needed, an analysis can be completed within 5 to 90 min depending on the sample analyzed.

Thus far, the majority of the experiments mentioned above were carried out using the flow injection mode. But, in a few cases, the sample extracts or the diluted samples (*e.g.*, saliva) were reanalyzed using the HPLC mode. Here again, the two sets of results agreed fairly well with each other (Fig. 5). Experiments along these lines should occasionally be carried out to double check the results obtained by flow injection analysis. This is particularly advisable for samples containing extremely low levels of nitrite or where the results appear to be abnormal. However, for samples containing high levels (> 10 ppm) of nitrite there is no need to use the HPLC column. The data obtained by using the flow injection technique should be reliable because the likelihood of interferences from N-nitroso compounds and organic nitrites at such high levels of nitrite is very remote. Also, for rapid monitoring purposes, where only an idea about the maximum possible level of nitrite present is required, the flow injection technique should be the method of choice.

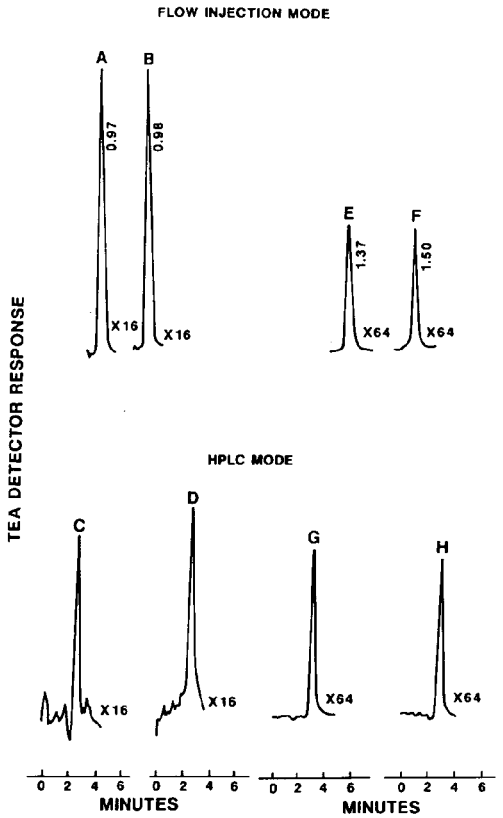

Fig. 5. Comparison of flow injection with HPLC chemiluminescence determination of nitrite. (A) 0.1 ml out of 400 ml final dilution of a baby food (carrot); (B) 0.5 ng $NaNO_2$ standard. Both A and B analyzed by the flow injection technique (sample was found to contain 0.17 ppm $NaNO_2$). (C) The same baby food extract and (D) the same standard analyzed by the HPLC technique (sample in this case was found to contain 0.18 ppm $NaNO_2$). (E) A human saliva sample and (F) 1.25 ng $NaNO_2$ standard both analyzed by the flow injection technique (sample was found to contain 1.3 ppm $NaNO_2$). (G) The same saliva sample and (H) the same standard as above both analyzed by the HPLC technique (sample in this case was found to contain 1.4 ppm $NaNO_2$).

In summary, we have developed a sensitive and rapid technique that is useful for both low and high level determination of nitrite in foods and biological materials. The technique should be particularly useful to the meat industry where critical control and monitoring of nitrite levels at various stages of manufacturing and storage of cured meat products are extremely important. Although TEA is a fairly expensive equipment, other commercially available chemiluminescence detectors, which are cheaper than a TEA, could be employed to carry out such analyses. It is hoped that other workers will find the technique useful.

References

[1] *Nitrates, Nitrites and N-Nitroso Compounds, Environmental Health Criteria 5*, World Health Organization, Geneva, 1978.

[2] National Academy of Sciences/National Research Council, *The Health Effects of Nitrate, Nitrite, and N-Nitroso Compounds*, National Academy Press, Washington, DC, 1981, Ch. 9.

[3] M.C. Archer, in J.N. Hathcock (Editor), *Nutrition Toxicology*, Vol.1, Academic Science, New York, 1982, p. 327.

[4] S.S. Mirvish, *Toxicol. Appl. Pharmacol.*, 31 (1975) 325.

[5] T.A. Smith, *Food Chem.*, 6 (1980) 169.

[6] J. Meester, in B. Kroll and B.J. Tinbergen (Editors), *Proceedings International Symposium on Nitrite in Meat Products*, Pudoc, Wageningen, 1974, p. 265.

[7] W.E.J. Phillips, *J. Agric. Food Chem.*, 16 (1968) 88.

[8] S.R. Tannenbaum, A.J. Sinskey, M. Weissman and W. Bishop, *J. Natl. Cancer Inst.*, 53 (1974) 79.

[9] R. Preussmann and G. Eisenbrand, in C.E. Searle (Editor), *Chemical Carcinogens, Vol. 2, ACS Monograph 182*, American Chemical Society, Washington, DC, 2nd ed., 1984, p. 829.

[10] I.K. O'Neill, R.C. von Borstel, C.T. Miller, J. Long and H. Bartsch (Editors), *N-nitroso Compounds: Occurrence, Biological Effects and Relevance to Human Cancer, IARC Sci. Publ. No. 57*, International Agency for Research on Cancer, Lyon, 1984.

[11] C.D. Usher and G.M. Telling, *J. Sci. Food Agric.*, 26 (1975) 1793.

[12] Ministry of Agriculture, Fisheries and Food, *Nitrate, Nitrite and N-Nitroso Compounds in Food, Food Surveillance Paper No. 20*, Her Majesty's Stationery Office, London, 1987.

[13] R.N. Fiddler and J.B. Fox, Jr., *J. Assoc. Off. Anal. Chem.*, 61 (1978) 1063.

[14] W. Holak and J.J. Specchio, *Anal. Chem.*, 64 (1992) 1313.

[15] T. Mitsuhashi, *J. Chromatogr.*, 629 (1993) 339.

[16] M. Lookabaugh and I.S. Krull, *J. Chromatogr.*, 452 (1988) 295.

[17] P. Pastore, I. Lavagnini, A. Boaretto and F. Magno, *J. Chromatogr.*, 475 (1989) 331.

[18] K. Ito, Y. Ariyoshi, F. Tanabiki and H. Sunahara, *Anal. Chem.*, 63 (1991) 273.

[19] K.K. Verma and A. Verma, *Anal. Lett.*, 25 (1992) 2083.

[20] M.I. Santillana, E. Ruiz, M.T. Nieto and M. De Alba, *J. Liq. Chromatogr.*, 16 (1993) 1561.

[21] J.Y. Zhou, P. Prognon, C. Dauphin and M. Hamon, *Chromatographia*, 36 (1993) 57.

[22] R.D. Cox, *Anal. Chem.*, 52 (1980) 332.

[23] R.C. Doerr, J.B. Fox, Jr., L. Lakritz and W. Fiddler, *Anal. Chem.*, 53 (1981) 381.

[24] A.R. Thornton, J. Pfab and R.C. Massey, *Analyst*, 114 (1989) 747.

[25] C.L. Walters, P.N. Gillat, R.C. Palmer and P.L.R. Smith, *Food Addit. Contam.*, 4 (1987) 133.

[26] T. Aoki, *Biomed. Chromatogr.*, 4 (1990) 128.

[27] D.C. Havery, *J. Anal. Toxicol.*, 14 (1990) 181.

[28] D.H. Fine, D. Lieb and F. Rufeh, *J. Chromatogr.*, 107 (1975) 351.

[29] D.H. Fine, D. Lieb and D.P. Rounbehler, *Anal. Chem.*, 47 (1975) 1188.

[30] N.P. Sen and B. Donaldson, *J. Assoc. Off. Anal. Chem.*, 61 (1978) 1389.

[31] R.L. Saul, S.H. Kabir, Z. Cohen, W.R. Bruce and M.C. Archer, *Cancer Res.*, 41 (1981) 2280.

[32] H. Ohshima, S. Calmels, B. Pignatelli, P. Vincent and H. Bartsch, in H. Bartsch, I.K. O'Neill and R. Schutte-Hermann (Editors), *Relevance of N-Nitroso Compounds to Human Cancer: Exposure and Mechanisms, IARC Sci. Publ. No. 84*, International Agency for Research on Cancer, Lyon, 1987, p. 384.

[33] N.P. Sen, Y.C. Lee and M. McPherson, *J. Assoc. Off. Anal. Chem.*, 62 (1979) 1186.

ELSEVIER

Journal of Chromatography A, 673 (1994) 85–92

JOURNAL OF CHROMATOGRAPHY A

Determination of infinite dilution activity coefficients and second virial coefficients using gas–liquid chromatography I. The dilute mixtures of water and unsaturated chlorinated hydrocarbons and of water and benzene

B. Khalfaoui*, D.M.T. Newsham

Department of Chemical Engineering, UMIST, Sackville Street, Manchester M60 1QD, UK

(First received December 20th, 1993; revised manuscript received March 15th, 1994)

Abstract

Specific-retention volume data from gas–liquid chromatographic measurements can be used to obtain infinite dilution activity coefficients and second cross virial coefficients for the solute–carrier gas mixtures.

The gas–liquid chromatographic measurements have been carried out for benzene and three unsaturated chlorinated hydrocarbon + water mixtures in the temperature range 285.15–323.15 K, with water as stationary phase and nitrogen as carrier gas. A gas–liquid chromatographic apparatus was used for measurements on water rich mixtures, and organic rich mixtures were studied using an isopiestic technique. The chromatographic specific retention volume data and the results from the isopiestic technique may be used to estimate group interaction parameters for the UNIFAC correlation to predict activity coefficients.

1. Introduction

The aliphatic and aromatic chlorinated hydrocarbons have many and various applications. These include use in the manufacture of products such as resin and pharmaceuticals, they also serve as aerosols solvents and as reaction media. The mutual solubilities of water and unsaturated chlorinated hydrocarbons and aromatic chlorinated hydrocarbons are very small and special techniques are required for the determination of vapour–liquid equilibria of mixtures in their miscible regions. In a previous paper [1] we reported measurements of the infinite dilution activity coefficients for mixtures of water with benzene, chlorobenzene, trichloroethene, *trans*-1,2-dichloroethene and 1,1-dichloroethene in the temperature range 285.15–323.15 K. In this paper we report the results of the continuation of ref. 1. In particular the results reported are the estimates of the second cross virial coefficients for the solute/nitrogen mixtures. Also Henry's constants for solute–water mixtures have been derived, as well as the excess partial molar enthalpies for water at infinite dilution in the solutes for the temperature range studied. The experimental infinite dilution activity coefficients for solute–water mixtures previously reported [1], have been used to obtain updated effective UNIFAC group interaction parameters for the ACH–water, ACCl–water (where A defines the aromatic ring), C=C–water and Cl(C=C)–water

* Corresponding author.

0021-9673/94/$07.00
SSDI 0021-9673(94)00263-9

interactions. The new parameters have been used to predict activity coefficients at infinite dilution for several chlorinated hydrocarbon–water mixtures and these have been compared with experimental values where possible.

2. Theory of gas–liquid chromatographic (GLC) technique

The technique allows the determination of activity coefficients γ_1 of a non-electrolyte solute (component 1) at very low concentrations (10^{-3} to 10^{-6} mole fraction) in a solvent (component 2). The technique is feasible to ternary systems in which component 3 is a carrier gas that is relatively insoluble in the solvent. Usually the solvent is either an involatile non-electrolyte or water. Many treatments of GLC retention theory have been reported in the literature [2–5]. These differ in the procedure used for extrapolating measured retention data to zero carrier gas pressure. The relationship between the net retention volume V_N and the carrier gas flow-rate at column outlet F_C and retention times t_R and t_M for an absorbed solute vapour and a non-absorbed maker gas, respectively, is given in Eq. 1. The factor J_3^2 allows for the pressure-drop across the chromatographic column and is defined by Eq. 2, in which p_i and p_o are the column inlet and outlet pressures, respectively

$$V_N = J_3^2 F_C (t_R - t_M) \quad (1)$$

$$J_3^2 = \frac{3}{2} \cdot \left(\frac{(p_i/p_o)^2 - 1}{(p_i/p_o)^3 - 1} \right) \quad (2)$$

Eq. 3 due to Cruickshank *et al.* [5] shows the relationship between V_N and p_o for real gases at moderate carrier gas pressures and allows for the non-ideality of the solute vapour, the solute–carrier gas molecular interactions and the pressure dependence of the partition coefficient.

$$\ln V_N = \ln (k^0 V_2) + \beta p_o J_3^4 + \xi (p_o J_3^4)^2 \quad (3)$$

where

$$J_3^4 = \frac{3}{4} \cdot \left(\frac{(p_i/p_o)^4 - 1}{(p_i/p_o)^3 - 1} \right) \quad (4)$$

and V_2 is the volume of solvent on the chromatographic support material. The three coefficients k^0, β and ξ in Eq. 3, are defined as follows

$$\ln k^0 = \ln \frac{RT}{\gamma_1^\infty v_2^0 p_1^0} - \frac{B_{11} - v_1^0}{RT} \cdot p_1^0 \quad (5)$$

$$\beta = (2B_{13} - \bar{v}_{12}^\infty)/RT \quad (6)$$

$$\xi = (3C_{133} - 4B_{13}B_{33})/2(RT)^2 \quad (7)$$

Here, k^0 is the zero pressure partition coefficient which is related to γ_1^∞ through Eq. 5. B_{11} is the solute second virial coefficient, p_1^0 the vapour pressure of pure solute, v_1^0 is the molar volume of pure solute and v_2^0 is the molar volume of pure solvent. B_{33} is the second virial coefficient of carrier gas and $\bar{v}_{12}^\infty$ is the partial molar volume of the solute infinitely dilute in the solvent (where $\bar{v}_{12}^\infty$ is not available then v_1^0 is used instead as an approximation). B_{13} and C_{133} are, respectively, the second and third cross virial coefficients between the solute and carrier gas. Pemberton and Mash [6] stated that if the carrier gas pressure $p_o < 2$ MPa and the carrier gas is not appreciably soluble in the solvent at the column temperature, and also if $(p_i - p_o) < 200$ kPa and $|B_{13}| < 180$ cm^3 mol^{-1}, then for solute samples of <2 μmol admitted to packed columns of 4 mm internal diameter, Eq. 3 can be reduced to Eq. 8.

$$\ln V_N = \ln (k^0 V_2) + \beta p_o J_3^4 \quad (8)$$

The selection of nitrogen as carrier gas for the mixtures investigated in this work permits the use of Eq. 8. Thus a plot of $\ln (V_N/V_2)$ *versus* $p_o J_3^4$ should give a straight line from which γ_1^∞ and B_{13} can be found.

3. Experimental

The measurements for water-rich mixtures were carried out using a GLC apparatus, and for organic-rich mixtures an isopiestic technique was used. Both of these techniques have been described in detail previously [1,6–8]. Only a brief

description is given here for the gas–liquid chromatograph.

3.1. The gas–liquid chromatograph

A schematic diagram of the apparatus was shown previously [7]. A typical chromatogram is shown in Fig. 1, from which the retention time is obtained. The sharp peak of the methane marker gas is followed by a broader solute peak. To obtain an accurate measurement of $(t_R - t_M)$, the solute retention time corrected for gas hold-up, it is necessary to measure the times t_n and t_n' at a displacement height h_n on the leading and trailing edges of the solute peak, respectively. Then $(t_R - t_M)$ can be found, by extrapolation of $(t_n + t_n')/2$ to maximum solute peak height.

The chromatographic columns were made from 1.2 m lengths of soft annealed 7 mm copper tubing. They were packed with diatomaceous earth (Diatomite S, 60-72 BSS mesh) supplied by JJ's Chromatography. They were prepared in a similar manner to those used previously [1,7].

3.2. Materials

The water used was doubly-distilled tap water. Benzene and trichloroethene was supplied by Fisons and chlorobenzene, 1,1-dichloroethene and *trans*-1,2-dichloroethene by BDH. All of these had purities in excess of 99%.

4. Group interaction parameters

In this paper we also report the results of an analysis of the new measurements in terms of one of the modifications of the UNIFAC group contribution model, the effective UNIFAC model. The detailed form of the UNIFAC equation of Fredenslund *et al.* [9], has been previously reported [7]. However, the effective UNIFAC method reported here has been developed by Nagata and Koyabu [10]. The combinatorial term of the effective UNIFAC equation is the same as in the UNIFAC and is given by Eq. 9

$$\ln \gamma_i^c = \left(\ln\left(\frac{\phi_i}{x_i}\right) + 1 - \frac{\phi_i}{x_i}\right) - \frac{1}{2} \cdot Zq_i\left(\ln\left(\frac{\phi_i}{\theta_i}\right) + 1 - \frac{\phi_i}{\theta_i}\right) \quad (9)$$

where γ_i^c is the combinatorial activity coefficient, q_i is the pure component surface area parameter, x_i is the mole fraction of component i, θ_i is the

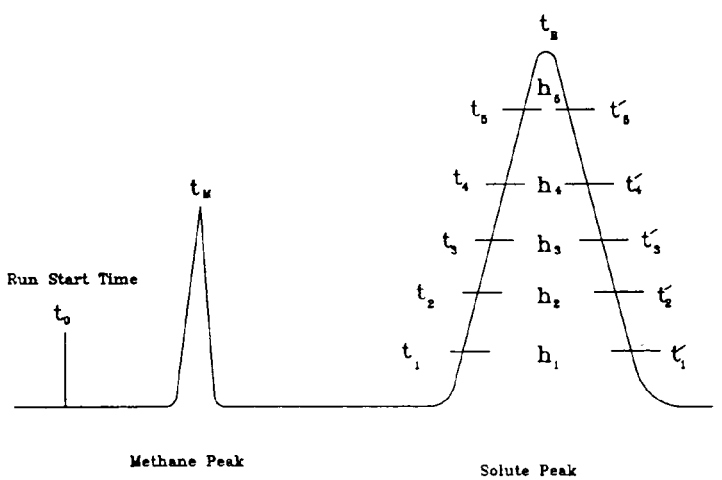

Fig. 1. A typical GLC chromatogram.

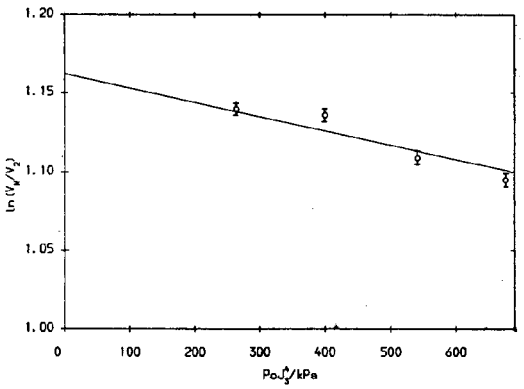

Fig. 2. A plot of ln (V_N/V_2) against $p_o J_3^4$ for trichloroethene + water system at 293.15 K.

area fraction and ϕ_i is the segment fraction which is similar to the volume fraction. The coordination number Z is taken as 10 [9]. But the main modification has been made in the residual activity coefficients, by adding a term that is a function of the area fraction.

Thus

$$\ln \gamma_i = \ln \gamma_i^c + \sum_k v_k^i (\ln \Gamma_k - \ln \Gamma_k^i) - \left(\ln\left(\frac{\theta_i}{x_i}\right) + 1 - \frac{\theta_i}{x_i}\right) \quad (10)$$

and

$$\ln \Gamma_k = 1 - \ln\left(\sum_m X_m \psi_{mk}\right) - \sum_m \left(\frac{X_m \psi_{km}}{\sum_n X_{nn} \psi_{nm}}\right) \quad (11)$$

where Γ_k is the group residual activity coefficient, Γ_k^i is the residual activity coefficient of group k in a reference liquid containing only molecules of type i and X_m is the mole fraction of group m. The group interaction parameters are given by

$$\psi_{mn} = \frac{Q_m}{Q_n} \exp\left[-\left(\frac{a_{mn}}{T}\right)\right] \quad (12)$$

where Q is the group surface area parameter, a_{mn} is the group interaction parameter and T is the temperature (K).

Table 1
Second cross virial coefficients (B_{13}) for benzene or chlorinated hydrocarbon (1)–nitrogen (3) mixtures and group assignments for benzene and chlorinated hydrocarbons

Solvent	T (K)	B_{13} (cm^3 mol^{-1})	Group assignment
Benzene	293.15	−118.95	6ACH
	303.15	14.15	
	313.15	76.96	
	323.15	113.81	
Chlorobenzene	293.15	202.56	5ACH · 1ACCl
	303.15	175.38	
	313.15	142.07	
	323.15	−15.67	
Trichloroethene	293.15	−66.23	3Cl(C=C) · 1CH=C
	303.15	−24.83	
	313.15	−10.15	
	323.15	102.60	
trans-1,2-Dichloroethene	293.15	−27.64	2Cl(C=C) · 1CH=CH
	303.15	152.55	
	313.15	169.30	
	323.15	177.51	
1,1-Dichloroethene	285.15	–	2Cl(C=C) · 1CH$_2$=C
	293.15	–	

5. Results and discussion

Specific retention volumes were measured for column inlet pressures in the range 200–700 kPa at four different temperatures (293.15, 303.15, 313.15 and 323.15 K) for each solute studied. Typical results for trichloroethene + water system are shown in Fig. 2, where ln (V_N/V_2) is plotted against $p_o J_3^4$. Each point on the plot represents the average value of up to seven measurements. The slope of the plot allows estimation of the second cross virial coefficient of the solute and carrier gas, and the derived values are given in Table 1. Unfortunately, because of a serious lack of literature data, the comparison with the values of B_{13} cannot be made. The pure component properties required for calculating these quantities were taken from different sources (vapour pressures [11,12]; molar volumes [13,14] and virial coefficients [15]). For the systems studied Henry's law can be applied, and the derived constants from the activity coefficients ($k_i = \gamma_i^\infty p_i^0$) are given in Table 2 where some values quoted by Kavanaugh and Rhodes-Trussell [16] are also included. As can be seen the agreement is good. The estimation of the absolute accuracy of the experimental results is difficult. But an examination of the likely experimental errors leads to the following estimates: B_{13}, ±10%; γ_1^∞, ±1%; γ_2^∞, ±2%. Since the excess partial molar enthalpy of solution at infinite dilution is related to infinite dilution activity coefficient as follows

$$\mathrm{d}\ln\gamma_i^\infty/\mathrm{d}(1/T) = (\bar{H}_i^\infty - H_i^0)/R = \Delta\bar{H}_i^\infty/R \quad (13)$$

where $\bar{H}_i^\infty$ is the partial molar enthalpy of component i in the solution at infinite dilution and H_i^0 is the pure component molar enthalpy. One would expect an almost linear relationship

Table 2
Henry's law constants (k_i) for benzene or chlorinated hydrocarbon (1)–water (2) mixtures

	T (K)	$k_1 \cdot 10^{-4}$ (Pa)	$k_2 \cdot 10^{-4}$ (Pa)	$k_1 \cdot 10^{-4}$ (Pa)
Benzene	293.15	2512.65	57.25	2330.92
	303.15	4013.57	–	3737.70
	308.15	–	95.65	
	313.15	6065.12	–	5879.09
	323.15	8914.52	166.50	8987.11
Chlorobenzene	293.15	1549.90	76.90	
	303.15	2156.07	–	
	308.15	–	136.68	
	313.15	2619.42	–	
	323.15	2809.97	247.84	
Trichloroethene	293.15	4312.96	93.52	5452.08
	303.15	7640.23	–	8532.08
	308.15	–	199.09	
	313.15	11532.00	–	12982.62
	323.15	17072.58	347.74	19230.20
trans-1,2-Dichloroethene	285.15	–	53.90	
	293.15	4418.50	50.25	
	303.15	7770.78	–	
	308.15	–	104.05	
	313.15	11572.75	–	
	323.15	16514.26	–	
1,1-Dichloroethene	285.15	–	124.72	
	293.15	–	107.80	

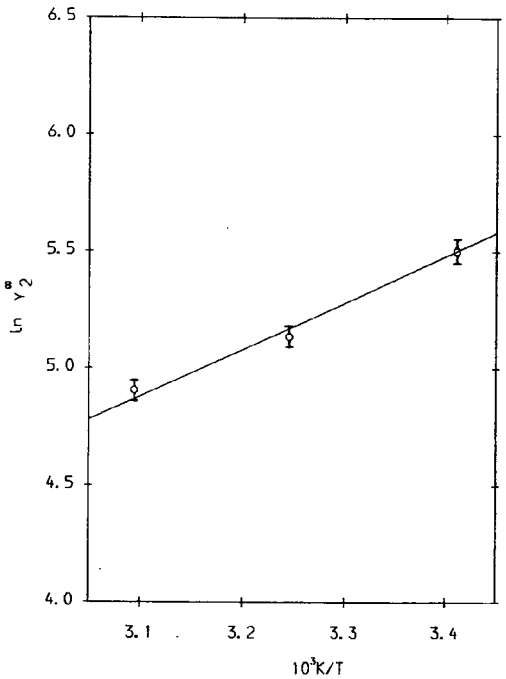

Fig. 3. Infinite dilution activity coefficients as a function of temperature for the benzene (1)–water (2) system.

between $\ln \gamma_2^\infty$ and $1/T$. This is indeed the case for γ_2^∞, as can be seen from Fig. 3, where $\ln \gamma_2^\infty$ has been plotted against $1/T$ for benzene–water mixtures. Similar linearity has been obtained for the remaining systems. The derived values of $\Delta \bar{H}_2^\infty$ are given in Table 3. Group assignments for the five organic solvents investigated whose mixtures with water are given in Table 1. It can be seen that all these solvents contain two types of groups and their mixtures with water, therefore, constitute ternary mixtures of groups, except benzene which is composed by only one group. Water is considered as a single group. The group interaction parameters were estimated by minimization of the following objective function:

$$F = \sum_i \sum_j (\ln \gamma_i^\infty(\text{experimental}) - \ln \gamma_i^\infty(\text{UNIFAC}))_j^2 \quad (14)$$

The summations are taken over all binary data sets j and components i. The minimization was done by using a sequential search procedure first

Table 3
Excess partial molar enthalpies for water at infinite dilution in benzene or chlorinated hydrocarbon for the temperature range 285.15–323.15 K

	$\Delta \bar{H}_2^\infty$ (kJ mol^{-1})
Benzene	15.48
Chlorobenzene	12.81
Trichloroethene	09.15
trans-1,2-Dichloroethene	19.30
1,1-Dichloroethene	57.58

Table 4
Effective UNIFAC group interaction parameters for benzene and unsaturated chlorinated hydrocarbon–water mixtures

	H_2O	ACH	ACCl	C=C	Cl(C=C)
H_2O	0.0	324.7 (327.8)	436.7 (525.5)	946.0 (1156.0)	205.9
ACH	1006.0 (1193.0)	0.0			
ACCl	1565.0 (1471.0)		0.0		
C=C	1489.0 (5008.0)			0.0	
Cl(C=C)	1148.0				0.0

The group parameters a_{mn} are in K, m is the row and n is the column of the matrix. The values in parentheses are those of Nagata and Koyabu [10].

Table 5
Comparison of experimental (Expt.) and calculated infinite dilution activity coefficients using the new and updated parameters for benzene and chlorinated hydrocarbon (1)–water (2) mixtures

Chlorinated hydrocarbon	Source	T (K)	$\gamma_1^\infty \times 10^{-4}$		γ_2^∞	
			Expt.	I	Expt.	I
Benzene	VLE	293	0.251	0.253(0.277)	245.0	246.8(472.7)
Chlorobenzene	VLE	293	1.296	1.133(1.890)	329.0	301.4(608.9)
1,2-Dichlorobenzene	LLE	293	6.089	7.340(14.24)	–	449.8(758.2)
1,3-Dichlorobenzene	LLE	293	7.350	7.340(14.24)	–	449.8(758.2)
1,4-Dichlorobenzene	LLE	293	11.656	7.340(14.24)	–	449.8(758.2)
1,2,3-Trichlorobenzene	LLE	298	31.872	34.542(87.987)	–	556.0(823.2)
1,2,4-Trichlorobenzene	LLE	298	1.007	34.542(87.987)	–	556.0(823.2)
1,2,3,4-Tetrachlorobenzene	LLE	298	277.40	173.113(584.357)	–	742.0(944.6)
1,2,3,5-Tetrachlorobenzene	LLE	298	341.43	173.113(584.357)	–	742.0(944.6)
1,2,4,5-Tetrachlorobenzene	LLE	298	2011.1	173.113(584.357)	–	742.0(944.6)
Pentachlorobenzene	LLE	298	2472.4	814.795(3645.35)	–	1010.9(1059.5)
Hexachlorobenzene	LLE	298	316200.0	3629.32(21520.7)	–	1452.4(1169.7)
1,1-Dichloroethene	LLE	293	1.076	0.0438(–)	461.0[a]	248.6(–)
cis-1,2-Dichloroethene	LLE	298	0.154	1.576(–)	35.0	351.8(–)
trans-1,2-Dichloroethene	VLE	293	0.122	1.576(–)	215.0	381.0(–)
Trichloroethene	VLE	293	0.545	0.089(–)	400.0	227.0(–)
1,1,2,2-Tetrachloroethene	LLE	298	6.136	0.141(–)	35.6	182.2(–)

The experimental values were determined either from vapour–liquid equilibria (VLE) or liquid–liquid equilibria (LLE); I = effective UNIFAC, values of γ_i^∞ in parentheses are calculated from the parameters of Nagata and Koyabu [10].
[a] From VLE.

developed by Nelder and Mead [17] and later used by Fredenslund *et al.* [18]. The new and updated parameters are given in Table 4, where they are compared with the values given by Nagata and Koyabu [10]. The derived parameters were obtained from the experimental results at 293.15 K. It can be seen from Table 4, that the only major change in the parameters occurs for C=C–water interaction. The new and updated parameters and also the parameters of Nagata and Koyabu have been used to predict the infinite dilution activity coefficients for several solvents and these are shown in Table 5. The calculated values have been compared with the experimental values of γ_i^∞ reported in ref. 1 and with the activity coefficients for the remaining solvent–water mixtures which were estimated from the liquid–liquid mutual solubilities. Table 6 gives a comparison of errors for the effective UNIFAC model for the original and updated parameters. It can be seen that the updated parameters give a significant improvement in the predictions for this particular set of chlorinated hydrocarbon–water mixtures. It can be concluded that GLC is a very useful technique for the estimation of the second cross virial coefficients and UNIFAC group interaction param-

Table 6
Comparison of errors in calculated activity coefficients for the original and the new and updated parameters

Error range (%), effective UNIFAC	Data points in error range (%)	
	Original parameters	Updated parameters
0–20	7.0	29.0 (50.0)
20–50	21.4	25.0 (29.0)
50–100	43.0	29.0 (14.0)
100–200	21.6	0.0 (0.0)
200$^+$	7.0	17.0 (7.0)

The quoted errors are $[\gamma_i^\infty(\text{expt.}) - \gamma_i^\infty(\text{calc})]/\gamma_i^\infty(\text{expt.})$. Values in parentheses refer to the same set of data as for the original parameters.

eters. However, the results obtained from GLC are subject to some systematic measurement errors, in flow, pressure and retention time. Furthermore, it is well known that the UNIFAC equations give poor predictions in the very dilute region. Consequently, these interaction parameters are probably not as accurate as those obtained from reduction of vapour–liquid equilibria data only.

References

[1] R.M. Cooling, B. Khalfaoui and D.M.T. Newsham, *Fluid Phase Equilibria*, 81 (1992) 217.
[2] A. Kwantes and G.W.A. Rijnders, *Gas Chromatography*, Butterworths, London, 1958.
[3] D.H. Everett and C.T.H. Skoddart, *Trans. Faraday. Soc.*, 57 (1961) 746.
[4] D.H. Everett, *Trans. Faraday. Soc.*, 61 (1965) 1637.
[5] A.J.B. Cruickshank, M.L. Windsor and C.L. Young, *Proc. R. Soc. London*, A, 295 (1966) 259.
[6] R.C. Pemberton and C.J. Mash, *National Physical Laboratory Report Chemistry*, Teddington, UK, 1974, p. 33.
[7] R.S. Barr and D.M.T. Newsham, *Fluid Phase Equilibria*, 35 (1987) 189; 35 (1987) 207.
[8] S.D. Christian, H.E. Affsprung, J.R. Johnson and J.R. Worley, *J. Chem. Educ.*, 40 (1963) 419.
[9] A. Fredenslund, R.L. Jones and J.M. Prausnitz, *AIChE J.*, 21 (1975) 1086.
[10] I. Nagata and J. Koyabu, *Thermochim. Acta*, 48 (1981) 187.
[11] T. Boublik, V. Fried and E. Hala, *Vapour Pressures of Pure Substances*, Elsevier, Amsterdam, 1973.
[12] S. Ohe, *Computer Aided Data Book of Vapour Pressure*, Data Book Publ. Co., Tokyo, 1976.
[13] R.R. Dreisbach, *Am. Chem. Soc. Adv. Chem. Ser.*, 15 (1955) 536.
[14] J. Timmermans, *Physico-Chemical Constants of Pure Organic Compounds*, Vol. II, Elsevier, Amsterdam, 1965.
[15] J.H. Dymond and E.B. Smith, *Virial Coefficients of Pure Gases and Mixtures*, Clarendon Press, Oxford, 1980.
[16] M.C. Kavanaugh and R. Rhodes-Trussell, *Aqua Sci. Tech. Rev.*, 6 (1980) 0118.
[17] J.A. Nelder and R. Mead, *Comput. J.*, 7 (1965) 308.
[18] A. Fredenslund, J. Gmehling and P. Rasmoussen, *Vapour-Liquid Equilibria Using UNIFAC*, Elsevier, Amsterdam, 1977.

ELSEVIER

Journal of Chromatography A, 673 (1994) 93–99

JOURNAL OF CHROMATOGRAPHY A

Silicone gum of OV-225 type for open-tubular gas chromatography

I. Hägglund[a], L.G. Blomberg[*,a], K. Janák[☆,a], S.G. Claude[b], R. Tabacchi[b]

[a]*Department of Analytical Chemistry, Arrhenius Laboratory, Stockholm University, S-106 91 Stockholm, Sweden*
[b]*Institute de Chimie de l'Université de Neuchâtel, Avenue de Bellevaux 51, CH-2000 Neuchâtel, Switzerland*

(Received January 31st, 1994)

Abstract

A silanol-terminated silicone having 25% cyanopropyl, 50% methyl and 25% phenyl substitution was prepared and a method for its immobilization in open-tubular columns was developed. This stationary phase showed good thermal stability at temperatures up to 300°C, and it was immobilized to 80% by means of thermal treatment. Its selectivity was excellent for the separation of azaarenes.

1. Introduction

Silicones are by far the most widely applied type of stationary phases for gas chromatography (GC). The properties of silicone stationary phases can be varied by the use of different types of substituent groups on the silicone backbone. Polysiloxanes containing at least two different selectively acting substituent groups constitute an important class of medium-polarity stationary phases. These phases provide a relatively broad range of selectivities that could be useful for the separation of samples containing different classes of organic compounds. In recent years, a relatively large number of phases belonging to this group have been developed, such as methoxyphenylpolysiloxanes [1], cyanophenylpolysiloxanes [2], nitrophenyl- and nitromethoxyphenylpolysiloxanes [3] and a cyanobiphenylpolysiloxane [4].

In the development of new stationary phases for open-tubular GC, it may be advantageous to consider the extensive experience concerning stationary phase selectivity that was obtained during the packed column era [5–7]. The silicone OV-225, which contains 25% cyanopropyl, 50% methyl and 25% phenyl substitution, was one of the more useful moderately polar stationary phases at that time. The application of this phase to open-tubular columns has, however, been less successful. In the original version OV-225 is an oil, and physically stable films cannot be created in open-tubular columns with this polymer. In order to provide possibilities for immobilization in open-tubular columns, two more recent versions of OV-225 have been made commercially available by Ohio Valley Specialty Chemical (Marietta, OH, USA). These were a vinyl-terminated version intended for immobilization by means of radical initiators and a silanol-terminated version intended for thermal immobiliza-

* Corresponding author.
☆ On leave from the Institute of Analytical Chemistry, Czech Academy of Sciences, 611 42 Brno, Czech Republic.

0021-9673/94/$07.00
SSDI 0021-9673(94)00247-7

tion. The viscosity of these polymers was low, however.

The silanol-terminated polymer OV-225-OH (Ohio Valley) was applied to open-tubular glass columns by Blum *et al.* [8]. A trifunctional cross-linking reagent, cyanopropyltriethoxysilane, was added to the coating solution in order to facilitate immobilization, and thermal stability up to 390°C was claimed. The degree of immobilization was not given. The vinylated OV-225 has been immobilized in fused-silica [9] and glass columns [10] by means of dicumyl peroxide-initiated cross-linking. The maximum operation temperature of the columns was 250°C.

The aim of this work was to develop an immobilizable, thermally stable version of the classical polymer OV-225. Two polymers, having the same gross composition but with different arrangements of the substituent groups, were synthesized. The chromatographic properties of the polymers were demonstrated. One of the polymers showed good thermal stability and immobilizability.

2. Experimental

Three types of silanol-terminated silicones of the OV-225 type have been evaluated for use as stationary phases. Two of these were synthesized in our laboratories; polymer 1 was composed of cyanopropyl–methyl and phenyl–methyl units, and in polymer 2 the basic unit consisted of one bis(cyanopropyl), one diphenyl and two dimethyl groups. The third polymer was the commercially available OV-225-OH. Polymer 1 was synthesized by cohydrolysis of dimethoxydiphenyldimethyldisiloxane and dimethoxymethylcyanopropylsilane in appropriate amounts followed by polymerization at 100°C using tetramethylammonium hydroxide (TMAH) as catalyst. Polymer 2 was synthesized by cohydrolysis of dimethoxydiphenyltetramethyltrisiloxane and bis(cyanopropyl)dimethoxysilane in appropriate amounts. Polymerization was performed as for polymer 1.

Fused-silica capillary tubing of I.D. 0.25 μm (Chrompack, Middelburg, Netherlands) was used as the column material in lengths of 10 m. Before coating, some capillaries were treated with HCl and dehydrated as described previously [11]. A few capillaries were deactivated by heat treatment at 280°C with a silicone oil of the same composition as polymer 1.

For coating, the stationary phase was dissolved in dichloromethane in appropriate concentrations and a trifunctional cross-linking reagent, cyanopropyltrimethoxysilane, was added to the coating solution. All columns were coated by the static method at room temperature. After coating, the columns were closed and heated at 60°C for 1 h as recommended by Blum [12] when using tetramethoxydimethyldisiloxane as a cross-linking reagent.

2.1. Column evaluation and stationary phase immobilization

The GC columns were evaluated on a Carlo Erba HRGC 5300 Mega system connected to a laboratory data system (ELDS; Chromatography Data Systems, Kungshög, Sweden). A polarity mixture was injected at 100°C, and a test mixture containing *n*-alkanes and biphenyl was injected at a column temperature of 125°C. Hydrogen at a rate of 50 cm/s was used as the mobile phase, and the injector splitting ratio was 1:100. The injector temperature was 280°C and the detector temperature was 300°C. For column bleeding tests at temperatures above 300°C, the detector temperature was set to the maximum column temperature.

A first test was performed after heating at a rate of 1°C/min to 100°C and maintaining this temperature for 1 h. The second test was performed after heating to 280°C at a rate of 0.5°C/min, and maintaining this temperature for 10 h. A third test was performed after rinsing of the column with 5 ml of dichloromethane. Column bleeding was evaluated in temperature-programmed runs at 5°C/min.

3. Results and discussion

The commercial phase OV-225-OH is a low-viscosity silicone oil. Polymer 1 was a gum, but polymer 2 could not be polymerized to a true

gum when TMAH was used as a catalyst. In order to obtain the highest possible molecular mass, equilibration with TMAH was interrupted when the viscosity of the polymer was at a maximum. A highly viscous oil was obtained.

Silanol-terminated polymers were used in this work. It has been established that, for phenyl-containing silicones, silanol termination results in better thermal stability than trimethylsiloxy termination [13–15]. Further, end-capping of a polysiloxane by means of a chlorosilane involves the formation of HCl, which can attack the cyano groups.

3.1. Stationary phase immobilization

Immobilization of polymer 1 was first attempted by heating without a cross-linker. No immobilization was achieved after such a treatment. With the addition of a cross-linker, the stationary phases could be immobilized, but only when coated on HCl-treated surfaces. Immobilization therefore could not be achieved when using untreated fused silica (H_2 flushed), deactivated fused silica or fused silica that had been HCl treated and deactivated. Clearly, surface silanol groups are necessary for the immobilization. The importance of condensation between terminal OH groups on the stationary phase and surface silanols for the immobilization has been emphasised by Blum and co-workers [16,17].

The highest degree of immobilization was achieved with 2% of the cross-linking reagent (Table 1). Polymer 2 was immobilized to a much lower extent than polymer 1 (Table 1). It seems that the combination of bis(cyanopropyl) and diphenyl groups makes immobilization more difficult. Immobilization of the commercial OV-225-OH was not successful (Table 1).

The addition of trimethoxycyanopropylsilane to the stationary phase alters the surface tension. Deactivated fused silica was therefore not wetted when 1% or more of this cross-linker has been added to the phase, and the wettability of HCl-treated fused silica was lost when 4% of cross-linker was added to the stationary phase.

The mechanisms active in the immobilization of polymers of OV-225-OH composition are different from those active in the immobilization of the silanol-terminated phenyl-containing silicones investigated previously, Sila 1 [11], OV-61-OH and Sila 3 [18] and OV-17-OH [19]. These polymers have high thermal stabilities, and immobilization could be attempted at 370°C. At this temperature, phenyl groups in silanol-terminated polysiloxanes are cleaved off and branched structures are formed [13,20]. It was concluded that such a cleavage of phenyl groups contributed strongly to the relatively high degree of immobilization that was achieved with these polymers [11,18,19]. Neither HCl treatment of the supporting fused silica nor the addition of a trifunctional cross-linker was found necessary for the immobilization of these polymers. As a consequence of the destabilizing effect of the cyanopropyl groups, polymers of the OV-225 type could not be heated to the high temperatures applied for phenylsilicones. Immobilization was therefore attempted by the addition of a reagent that promoted cross-linking and surface bonding.

Table 1
Influence of percentage of cross-linker and type of polymer on immobilization

Polymer	Cross-linker (%)	Polymer immobilization (%)
Polymer 1	0.5	30
	1	61
	2	79
	3	66
	4	–[a]
Polymer 2	2	5
OV-225-OH	2	0

[a] The stationary phase does not wet the support.

3.2. Column adsorptive activity

Columns where polymer 2 had been coated on untreated fused silica showed relatively good deactivation (Fig. 1A). Coating Polymers 1 and 2 on HCl-treated capillaries resulted in acidic columns; nicotine was not eluted (Fig. 1B). Conditioning at 280°C resulted in an improved elution of nicotine (Fig. 1C).

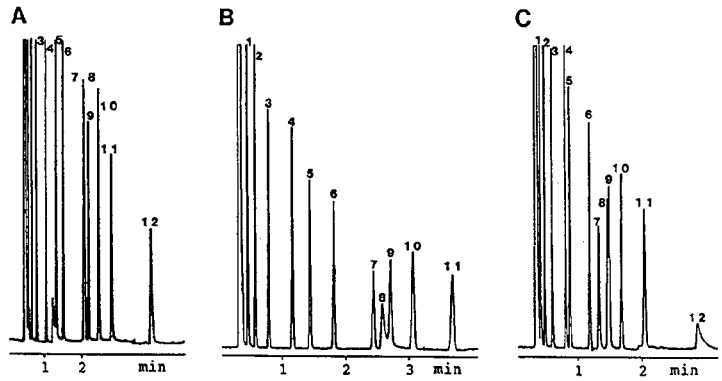

Fig. 1. Gas chromatograms (flame ionization detection) of a polarity mixture on capillary columns of dimensions 10 m × 0.25 mm I.D. Columns: (A) untreated fused silica coated with polymer 2 and 2% of cross-linker; (B) HCl-treated fused silica coated with polymer 1 and 2% of cross-linker; (C) same column as in (B), but after thermal treatment for 10 h at 280°C. Film thickness: (A and B) 0.15 μm; (C) 0.13 μm. Conditions: split injection; isothermal at 100°C. In (A) and (B) the columns were tested after conditioning for 1 h at 100°C. Peaks: 1 = *n*-undecane; 2 = *n*-dodecane; 3 = *n*-tridecane; 4 = *n*-tetradecane; 5 = aniline; 6 = *n*-pentadecane; 7 = phenol; 8 = decanol; 9 = 2,6-dimethylphenol; 10 = 2,6-dimethylaniline; 11 = 2-methylnaphthalene; 12 = nicotine. Sample amount, *ca.* 1 ng of each substance.

3.3. Column polarity and thermal stability

The commercial OV-225-OH showed a lower polarity than polymers 1 and 2 (Table 2). Further, the film thickness and the polarity of columns coated with OV-225-OH decreased drastically on conditioning. Also, the commercially available OV-225 gives a lower Kováts retention index for biphenyl than the polymers that were synthesized for this work. A value of

Table 2
Properties of open-tubular columns (10 m × 0.25 mm I.D.) coated with silicones of the OV-225 type with an original film thickness of 0.15 μm

Column No.	Stationary phase	Cross-linker (%)	Column treatment[a]	*k'* (100°C)		HETP (100°C)		Kováts index		
				2-Me-naphthalene	C_{15}	2-Me-naphthalene	C_{15}	2-Me-naphthalene (100°C)	Decanol (100°C)	Biphenyl (125°C)
1	OV-225-OH	2	A	11.6	5.8	1.71	0.59	1614	1560	1737
			B	7.2	3.0	0.56	0.91	–	1533	1706
2	Polymer 1	2	A	10.1	4.5	0.27	0.43	1639	1573	1773
			B	8.6	3.9	0.30	0.41	1637	1568	1769
			C	6.7	3.1	0.30	0.40	1634	1567	1767
3	Polymer 1	3	A	10.3	4.6	0.30	0.40	1639	1572	1773
			B	7.9	3.6	0.30	0.39	1634	1563	1765
			C	5.1	2.4	0.30	0.36	1629	1564	1761
4	Polymer 2	2	A	9.6	4.0	0.30	0.49	1655	1588	1792
			B	8.5	3.7	0.25	0.32	1646	1580	1782

[a] A = Conditioned at 100°C; B = programmed at 0.5°C/min to 280°C, isothermal for 10 h; C = after extraction with methylene chloride.

1748 at 120°C has been reported for OV-225 [2], whereas polymer 1, without crosslinker, gave 1756 at that temperature. Further, the polymer containing diphenyl and bis(cyanopropyl) units (polymer 2) showed a higher polarity than the cyanopropyl–methyl, methyl–phenyl polymer (polymer 1). The retention index for biphenyl at 125°C on polymer 1 (2% of cross-linker) was thus 1773 and on polymer 2 (2% of cross-linker) it was 1792. On the other hand, silicones of the OV-17 type showed a higher polarity when composed of methyl–phenyl units than when composed of diphenyl and dimethyl units [19]. It therefore seems that biscyanopropyl units result in higher polarities than cyanopropyl–methyl units for the polymer gross composition investigated in this work.

Columns coated with polymer 1 showed higher thermal stabilities than columns coated with polymer 2 (Table 3). The capacity factor of biphenyl on polymer 1 was thus 88% of the original after conditioning for 10 h at 280°C, whereas 56% remained after such a treatment of columns coated with Polymer 2. Polymer 1 was, however, fairly stable up to 300°C (Table 3). After conditioning of polymer 2-coated columns at 300°C for 10 h, the capacity factor of biphenyl was only 25% of its original value. In general, diphenyl substituents increase the thermal stability of a silicone [19,21], and polymer 2 was expected to show the highest thermal stability. The relatively low thermal stability of polymer 2 could be explained by two factors: it had a relatively low molecular mass and it could not be immobilized.

3.4. Separation of azaarenes

The separation of a test mixture of azaarenes has been extensively investigated [1–4,18,22,23]. Complete separation of the mixture was obtained on polymer 1 under isothermal conditions with a column of dimensions 10 m × 0.25 mm I.D. (Fig. 2). Peaks 3 and 4 in Fig. 2 are the most difficult to separate in the test mixture; they have been separated on 20 m × 0.31 mm I.D. columns coated with highly polar phases having 75 or 88% cyano substitution [22,23]. However, separation was achieved also on a trimethoxyphenyl- [1], a cyanophenyl- [2] and a nitromethoxyphenyl-substituted polysiloxane [3]. The separations were here obtained on narrower columns of 0.20 mm I.D. The length of the trimethoxyphenyl- and nitromethoxyphenylsilicone-coated columns were 10.5 or 10 m, the number of theoretical plates, N, on these columns being 41 000–44 000; the separation on the cyanophenylsilicone-coated column was achieved on a 20-m capillary with $N = 82\,000$. The separation in Fig. 2 was obtained on a

Table 3
Column properties after conditioning

Thermal treatment	Polymer 1			Polymer 2		
	k' (biphenyl)	Phase content (%)	Kováts index (biphenyl) (125°C)	k' (biphenyl)	Phase content (%)	Kováts index (biphenyl) (125°C)
Short conditioning	6.1	100	1773	5.6	100	1790
280°C, 10 h	5.3	88	1769	3.1	56	1774
After extraction	4.1	67	1767	–	–	–
300°C, 10 h	3.4	56	1763	1.4	25	1733
320°C, 10 h	2.8	46	1757			
340°C, 10 h	2.3	38	1746			
360°C, 10 h	1.3	21	1723			
380°C, 10 h	1.0	16	1702			

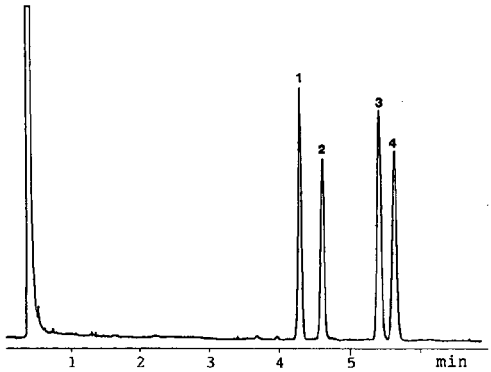

Fig. 2. Gas chromatogram (flame ionization detection) of azaarenes. Column as in Fig. 1B. Conditions: split injection; isothermal at 160°C. Peaks: 1 = 7,8-benzoquinoline; 2 = acridine; 3 = phenanthridine; 4 = 5,6-benzoquinoline.

column having larger I.D. and the plate count was accordingly lower, $N \approx 33\,000$ plates. In spite of this, the separation was better than previously published, illustrating the excellent selectivity that can be achieved with polymer 1. Further, the time of analysis was *ca.* 22 min in refs. 2 and 3 and 17 min in ref. 1, whereas in this work (Fig. 2) the time of analysis was below 6 min.

The polarities of the trimethoxyphenyl- and nitromethoxyphenyl-substituted polymers, as expressed by the Kováts retention index of biphenyl [1,3], were in the same range as for polymer 1, whereas the polarity of the cyanophenyl-substituted polysiloxane was lower [2]. The thermal stabilities of the trimethoxyphenyl- and the cyanophenyl-substituted silicones and polymer 1 were in the same range, 280–300°C. The nitromethoxyphenyl phase was stable only up to 230°C.

In conclusion, polymer 1 showed acceptable thermal stability up to 300°C. After addition of a cross-linking reagent, the phase could be immobilized to 80% by means of thermal treatment. Excellent separation of azaarenes was demonstrated. Although several new stationary phases, intended for the same purpose in GC as OV-225, have been reported, the classical OV-225 type of phase still provides an attractive alternative.

Acknowledgements

This work was supported by the Swedish Natural Science Research Council.

References

[1] M.A. Pulsipher, R.S. Johnson, K.E. Markides, J.S. Bradshaw and M.L. Lee, *J. Chromatogr. Sci.*, 24 (1986) 383.
[2] Z. Juvancz, M.A. Pulsipher, B.J. Tarbet, M.M. Schirmer, R.S. Johnson, K.E. Markides, J.S. Bradshaw and M.L. Lee, *J. Microcol. Sep.*, 1 (1989) 142.
[3] Z. Juvancz, M.A. Pulsipher, M.M. Schirmer, R.S. Johnson, K.E. Markides, J.S. Bradshaw and M.L. Lee, *J. Microcol. Sep.*, 1 (1989) 309.
[4] A. Malik, I. Ostrovsky, S.R. Sumpter, S.L. Reese, S. Morgan, B.E. Rossiter, J.S. Bradshaw and M.L. Lee, *J. Microcol. Sep.*, 4 (1992) 529.
[5] G.E. Baiulescu and V.A. Ilie, *Stationary Phases in Gas Chromatography*, Pergamon Press, Oxford, 1975.
[6] J.K. Haken, *J. Chromatogr.*, 300 (1984) 1.
[7] H. Rotzsche, *Stationary Phases in Gas Chromatography* (*Journal of Chromatography Library*, Vol. 48), Elsevier, Amsterdam, 1991.
[8] W. Blum, W.J. Richter and G. Eglinton, *J. High Resolut. Chromatogr. Chromatogr. Commun.*, 11 (1988) 148.
[9] K. Markides, L. Blomberg, J. Buijten and T. Wännman, *J. Chromatogr.*, 254 (1983) 53.
[10] W. Blum, *J. High Resolut. Chromatogr. Chromatogr. Commun.*, 9 (1986) 120.
[11] A. Bemgård, L. Blomberg, M. Lymann, S. Claude and R. Tabacchi, *J. High Resolut. Chromatogr. Chromatogr. Commun.*, 10 (1987) 302.
[12] W. Blum, *J. High Resolut. Chromatogr. Chromatogr. Commun.*, 9 (1986) 350.
[13] N. Grassie, I.G. Macfarlane and K.F. Francey, *Eur. Polym. J.*, 15 (1979) 415.
[14] N. Grassie and K.F. Francey, *Polym. Degrad. Stab.*, 2 (1980) 53.
[15] N. Grassie, K.F. Francey and I.G. Macfarlane, *Polym. Degrad. Stab.*, 2 (1980) 67.
[16] W. Blum and L. Damasceno, *J. High Resolut. Chromatogr. Chromatogr. Commun.*, 10 (1987) 472.
[17] W. Blum, K. Grolimund, P.E. Jordi and P. Ramstein, *J. High Resolut. Chromatogr. Chromatogr. Commun.*, 11 (1988) 441.

[18] A. Bemgård, L. Blomberg, M. Lymann, S. Claude and R. Tabacchi, *J. High Resolut. Chromatogr. Chromatogr. Commun.*, 11 (1988) 881.
[19] I. Hägglund, L. Blomberg, A. Bemgård, K. Janák, S.G. Claude, M. Lymann and R. Tabacchi, *J. Chromatogr. Sci.* 29 (1991) 396.
[20] T. Welsch and U. Teichmann, *J. High Resolut. Chromatogr.*, 14 (1991) 153.
[21] Q. Wu, M. Hetem, C.A. Cramers and J.A. Rijks, *J. High Resolut. Chromatogr.*, 13 (1990) 811.
[22] I. Ignatiadis, J.M. Schmitter and G. Guiochon, *J. Chromatogr.*, 246 (1982) 23.
[23] M.L. Lee, J.C. Kuei, N.W. Adams, B.J. Tarbet, M. Nishioka, B.A. Jones and J.S. Bradshaw, *J. Chromatogr.*, 302 (1984) 303.

ELSEVIER

Journal of Chromatography A, 673 (1994) 101–105

JOURNAL OF CHROMATOGRAPHY A

One-step conversion of fatty acids into their 2-alkenyl-4,4-dimethyloxazoline derivatives directly from total lipids

J.L. Garrido*, I. Medina

Instituto de Investigaciones Marinas (CSIC), Av. Eduardo Cabello 6, E-36208 Vigo, Spain

(First received December 29th, 1993; revised manuscript received March 7th, 1994)

Abstract

2-Alkenyl-4,4-dimethyloxazoline derivatives of fatty acids were obtained by direct reaction of 2-amino-2-methylpropanol with oils or total lipid extracts. The yields were similar to those obtained by the formation of oxazoline derivatives from fatty acid methyl esters after transesterification of the starting lipids. The procedure is especially useful in the analysis by gas chromatography–mass spectrometry of samples rich in lipids containing α-unsaturated ethers (alkenylglycerols), as it avoids the formation of the corresponding dimethylacetals that can complicate the chromatograms and the mass spectra of the fatty acid oxazoline derivatives.

1. Introduction

The location of the positions of the double bonds in the alkyl chain of fatty acids has been accomplished by gas chromatography–mass spectrometry (GC–MS) following two different strategies, both involving chemical modification prior to the analysis: derivatization at the double bonds ("on-site" modification) to give compounds with distinctive fragmentation patterns or, more commonly, derivatization of the terminal carboxilic acid group ("remote-site" modification) with reagents that enhance charge stabilization to minimize double bond migration. Various functional group modifiers have been successfully employed in the structure elucidation of complex mixtures of fatty acids, mainly N-acylpyrrolidine [1,2], picolinyl esters [3,4] and dimethyloxazoline [5–11].

4,4-Dimethyloxazoline derivatives of fatty acids have been found to show several advantages over other fragmentation-directing derivatives: they are readily prepared and purified, markedly stable towards most reagents and capable of hydrolytic decomposition on heating in acidic media to regenerate the starting material [5,6]. They show good chromatographic properties with volatilities comparable to those of simple esters, and have been successfully resolved by means of capillary columns of medium and low polarity. However, perhaps the most important advantage in the use of these derivatives is that they produce clear mass spectra, with abundant diagnostic peaks and regular fragmentation patterns [5–12].

2-Alkenyl-4,4-dimethyloxazoline (DMOX) derivatives are usually prepared, after saponification of the starting lipids, by heating the free acids with 2-amino-2-methylpropanol (AMP) or by reaction with dicyclohexylcarbodiimide followed by treatment with $SOCl_2$ [5–10]. Recently, Fay and Richli [12] described a procedure

* Corresponding author.

0021-9673/94/$07.00
SSDI 0021-9673(94)00236-3

that, by means of prolonged heating with AMP at high temperature, allows the preparation of DMOX derivatives starting from the fatty acid methyl esters (routinely used for the analysis of lipids by GC) obtained from total lipid by acid-catalysed transmethylation. The DMOX derivatives so obtained are easily purified from the reaction mixture by extraction into dichloromethane.

However, when samples containing aliphatic aldehydes or alkenylglycerol-derived lipids are subjected to acidic methanolysis, dimethylacetals (compounds derived from aldehydes, either initially free or released from alkenylglycerides) are formed [13]. These products are subsequently extracted into the DMOX fraction in the purification step, contaminating the chromatograms and complicating the mass spectra.

In this paper, we describe a procedure for the direct conversion of fatty acids (either free or esterified) in oils or total lipid extracts into their DMOX derivatives. The procedure is rapid and simple as it eliminates the saponification and/or transesterification steps, and thus avoids the formation of the interfering dimethylacetals.

2. Experimental

2.1. Materials

2-Amino-2-methylpropanol (for synthesis) (AMP), acetyl chloride (for analysis), toluene (analytical-reagent grade) and methanol (HPLC grade) were purchased from Merck (Darmstadt, Germany). Cod liver oil (CLO) was purchased from a local pharmacy. Mussels (*Mytillus edulis galloprivincialis*) were collected from the Ria of Arosa coast (Pontevedra, Spain) and the lipids were extracted by the method of Bligh and Dyer as described by Christie [14]. The total lipid amount was determined gravimetrically as described by Herbes and Allen [15].

2.2. Gas chromatography

A Perkin–Elmer Model 8700 gas chromatograph equipped with a flame ionization detector, a programmed-temperature vaporization injection system and an SP-2330 fused-silica capillary column (30 m × 0.25 mm I.D., 0.2 μm phase thickness) was used. Nitrogen was the carrier gas at a head pressure of 10 p.s.i. (1 p.s.i. = 6894.76 Pa). The oven temperature was raised from 150 to 210°C at 1°C/min and held at the final temperature for 10 min. The injector was operated in the solvent elimination mode, receiving the sample cold, eliminating the solvent at low temperature (45°C, splitting ratio 1:140), and then being programmed to 300°C at 15°C/s. The detector temperature was 265°C. The same conditions were used for fatty acid methyl esters and for DMOX derivatives.

2.3. Gas chromatography–mass spectrometry

A Hewlett-Packard Model 5890 gas chromatograph equipped with a split–splitless injection system in combination with a Hewlett-Packard Model 5971 mass-selective detector was used. The column was the same as for GC analysis. Helium was used as the carrier gas at a column head pressure of 5 p.s.i. The oven temperature was kept at 80°C for 2 min, then raised at 40°C/min to 150°C and then at 1°C/min to a final temperature of 210°C. The mass spectrometer was operated in the electron impact ionization mode (70 eV). The transfer line and ion source temperatures were both 280°C.

2.4. Derivatization

Lipid samples (CLO or mussel total lipid extract) were dissolved in hexane. Each sample was subjected to three different derivatization procedures, as follows.

Methylation

A 4-mg amount of total lipids was subjected to acidic transmethylation according to Lepage and Roy [16], and the resulting methyl esters were dissolved in 1 ml of toluene.

Methylation and oxazolination

Samples (4 mg) were subjected to the two-step derivatization procedure of Fay and Richli [12].

Direct oxazolination

Oil or total lipid extracts (4 mg) were dried under nitrogen at ambient temperature in PTFE-lined screw-capped tubes. To each tube, 500 μl of AMP (prewarmed at 40°C) were added and the tubes were throughly flushed with nitrogen, capped and heated in a heating block at 180°C for 18 h. The reaction mixtures were cooled and dissolved in 5 ml of CH_2Cl_2, then washed twice with 2 ml of distilled water. The organic layers were dried over anhydrous Na_2SO_4, filtered and evaporated with nitrogen and the residue was dissolved in 100 μl of hexane. This hexane solution was injected directly into the gas chromatograph.

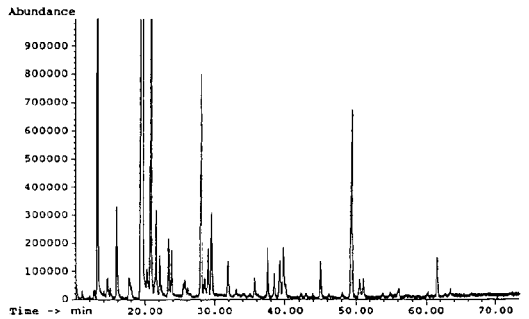

Fig. 1. Total ion current chromatogram of DMOX derivatives of fatty acids from mussel lipid extract on a fused-silica capillary column coated with a polar phenyl methyl silicone phase (SP-2330). For detailed analytical conditions, see Experimental.

3. Results and discussion

Most of the derivatives employed for the analysis of fatty acids by GC–MS show low volatilities, so high temperatures are needed to elute them within reasonable periods of time. This has limited their analysis to the use of low- and medium-polarity columns, operated at temperatures high enough to elute the components but low enough to avoid excessive column bleeding [17].

Taking advantage of the good chromatographic properties of oxazoline derivatives, the elution temperatures of which are around 10°C higher than those for their corresponding methyl esters [5,12], we applied a very polar column (SP-2330) to their analysis by GC–MS. Fig. 1 shows the total ion current chromatogram of mussel fatty acids as their DMOX derivatives (prepared by means of the acid-catalysed transmethylation and subsequent oxazolination procedure of Fay and Richli [12]), obtained with a temperature programme with a maximum temperature of 210°C, far below the recommended maximum column temperature (275°C). Good separation was achieved in a short analysis time, permitting good mass spectra to be obtained, even from certain minor peaks, for complicated fatty acid mixtures such as those coming from marine invertebrate lipids [18]. No column bleeding was observed under these conditions.

However, certain peaks in the chromatogram presented uncommon mass spectra which, below the molecular ion of the corresponding DMOX derivative, show odd-mass fragmentions. The suspected presence of co-eluting dimethylacetals that are frequent in marine samples subjected to acid transmethylation [13] and that show intense odd-mass peaks at M − 1 and M − 31 mass units, was confirmed when the chromatographic trace at *m/z* 75 (base peak in the dimethylacetal spectrum [13]) was extracted from the total ion current data. Fig. 2 shows the result of monitoring the same sample at two selected ions: *m/z* 113 (a typical fragment characteristic of DMOX derivatives [5]) and 75. As can be seen, peaks due to dimethylacetals co-eluted with those of certain DMOX derivatives.

To overcome this problem, several alternatives could be applied: the use of a base-catalysed transmethylation procedure that does not affect the vinyl ether linkage in alkenylglycerides, the purification of DMOX from dimethylacetals by thin-layer or column adsorption chromatography [19] or the improvement of the GC separation. All these approaches show different disadvantages such as an increased procedural time or, with basic methylation, the lack of esterification of free fatty acids [19]. From an operative point of view, the most convenient action seems to be to avoid the formation of these dimethylacetals. This alternative is possible if the oxazoline derivatization is carried out directly, without a prior transmethylation or saponification step. In

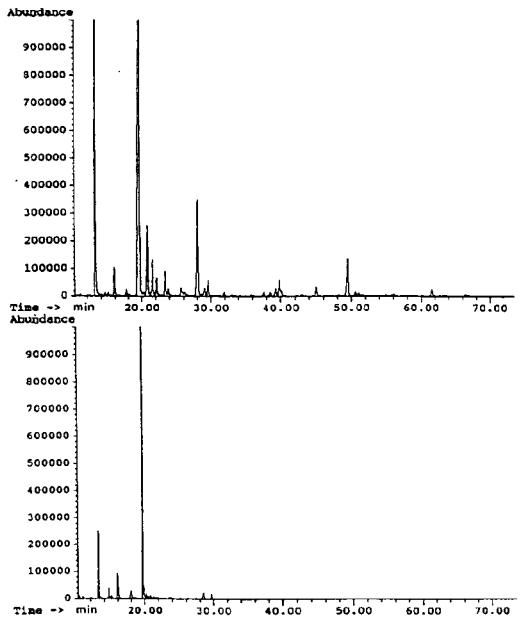

Fig. 2. Selected ion chromatograms at m/z 113 (top) and 75 (bottom) of DMOX derivatives of fatty acids from mussel lipid extract prepared by the two-step procedure (methylation plus DMOX formation).

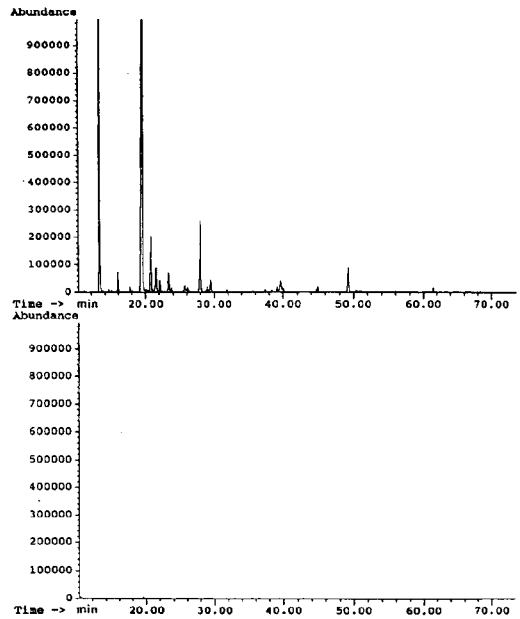

Fig. 3. Selected ion chromatograms at m/z 113 (top) and 75 (bottom) of DMOX derivatives of fatty acids from mussel lipid extract prepared by the direct procedure.

this way, the methodology proposed is rapid and direct, and reduces the time, cost and glassware needed for the analysis.

When an equivalent mussel total lipid extract was derivatized using the direct procedure described in this paper, and the corresponding chromatogram was monitored at m/z 75, no dimethylacetals could be detected (Fig. 3). On the other hand, it must be noted that the intensity of the peaks monitored at m/z 113 was approximately the same as in Fig. 2. This suggests that no significant losses occur when using the direct method compared with the methylation–oxazolination procedure.

To assess the yields of the direct oxazolination procedure, CLO was selected as the test sample as it contains fatty acids representative of different chain lengths and degrees of unsaturation and essentially lacks ether–lipids.

Equivalent CLO samples were subjected to acid-catalysed transmethylation, to acid-catalysed transmethylation plus DMOX derivative

Table 1
Peak area percentages of cod liver oil fatty acid derivatives

Fatty acid	Methyl ester	DMOX[a]	
		A	B
14:0	4.87	5.37	5.67
16:0	11.57	13.74	13.58
16:1ω7	10.00	11.99	11.93
18:0	2.78	3.06	2.93
18:1ω9	18.83	22.01	22.18
18:1ω7	5.12	6.24	6.42
18:2ω6	1.34	1.68	1.52
20:1ω9	15.10	16.39	16.58
18:4ω3	1.75	0.33	0.32
20:4ω6	0.46	0.25	0.27
22:1ω9	8.54	8.73	8.86
20:5ω3	9.40	5.50	5.57
22:5ω3	1.89	0.86	0.80
22:6ω3	9.07	3.83	3.38

[a] Peak-area distributions correspond to the following fatty acid derivatives: (A) DMOX obtained from oxazoline formation over methyl esters and (B) DMOX obtained from oxazoline formation directly from the oil.

formation or to direct oxazolination, and subsequently analysed by GC with flame ionization detection. The results are summarized in Table 1. As noted previously for picolinyl derivatives [17], when the peak-area distribution of the oxazoline derivatives was compared with that of the methyl esters, it was observed that polyunsaturated and late-eluting fatty acids were discriminated against to some extent. However, there is no sensible difference in the peak-area distribution of the DMOX derivatives obtained either from fatty acid methyl esters or directly from the oil.

4. References

[1] N.J. Jensen and M.L. Gross, *Lipids*, 21 (1986) 657.
[2] W.W. Christie, E.Y. Brechany, S.B. Johnson and R.T. Holman, *Lipids*, 21 (1986) 657.
[3] D.J. Harvey, *Biomed. Mass Spectrom.*, 9 (1982) 33.
[4] W.W. Christie, E.Y. Brechany, F.D. Gunstone, M.S.F. Lie Ken Jie and R.T. Holman, *Lipids*, 22 (1987) 664.
[5] J.Y. Zhang, Q.T. Yu, B.N. Liu and Z.H. Huang, *Biomed. Mass Spectrom.*, 15 (1988) 33.
[6] Q.T. Yu, B.N. Liu, J.Y. Zhang and Z.H. Huang, *Lipids*, 23 (1988) 804.
[7] J.Y. Zhang, H.Y. Wang, Q.T. Yu, X.J. Yu, B.N. Liu and Z.H. Huang, *J. Am. Oil Chem. Soc.*, 66 (1989) 242.
[8] J.Y. Zhang, X.J. Yu, H.Y. Wang, B.N. Liu, Q.T. Yu and Z.H. Huang, *J. Am. Oil Chem. Soc.*, 66 (1989) 256.
[9] Q.T. Yu, B.N. Liu, J.Y. Zhang and Z.H. Huang, *Lipids*, 24 (1989) 79.
[10] D.L. Luthria and H. Sprecher, *Lipids*, 28 (1993) 561.
[11] T. Rezanka, I.V. Zlatkin, I. Viden, O.I. Slabova and D.I. Nikitin, *J. Chromatogr.*, 558 (1991) 215.
[12] L. Fay and U. Richli, *J. Chromatogr.*, 541 (1991) 89.
[13] I. Medina, S. Aubourg and R. Pérez Martín, *J. Agric. Food Chem.*, 41 (1993) 2395.
[14] W.W. Christie, *Lipid Analysis*, Pergamon Press, Oxford, 1982.
[15] S.E. Herbes and C.P. Allen, *Can. J. Fish Aquat Sci.*, 40 (1983) 1316.
[16] G. Lepage and C. Roy, *J. Lipid Res.*, 27 (1986) 114.
[17] I. Wretensjö, L. Svensson and W.W. Christie, *J. Chromatogr.*, 521 (1990) 89.
[18] J.L. Garrido and I. Medina, *Lipids*, submitted for publication.
[19] W.W. Christie, *Gas Chromatography and Lipids*, Oily Press, Ayr, 1989.

ELSEVIER

Journal of Chromatography A, 673 (1994) 107–111

JOURNAL OF CHROMATOGRAPHY A

Gas chromatographic separation of amino acid enantiomers and their recognition mechanism on a 2,6-di-O-butyl-3-O-trifluoroacetylated-γ-cyclodextrin capillary column

Hong Wan*, Xin Zhou, Qingyu Ou

Lanzhou Institute of Chemical Physics, Chinese Academy of Sciences, Lanzhou 73000, China

(First received November 23rd, 1993; revised manuscript received February 22nd, 1994)

Abstract

Some amino acids and 2- and 3-hydroxybutyric acid derivatives were resolved on a chiral capillary column coated with 2,6-di-O-butyl-3-O-trifluoroacetylated-γ-cyclodextrin, and their thermodynamic data were obtained from this stationary phase. Obvious differences in $\Delta(\Delta H^\circ)$ and $\Delta(\Delta S^\circ)$ were observed among these amino acids. The enthalpy–entropy compensation and structural effects were analysed with consideration of chiral recognition. The results suggested that the induced conformation fit between enantiomers and cyclodextrin derivatives could be important in chiral recognition. The enantiomers with large negative $\Delta(\Delta H^\circ)$ and $\Delta(\Delta S^\circ)$ values could form inclusion complexes and the separation of enantiomers with small negative $\Delta(\Delta H^\circ)$ and $\Delta(\Delta S^\circ)$ values could be due to other types of interactions.

1. Introduction

During the past 5 years, differently modified cyclodextrins have been synthesized and found successful applications in gas chromatography [1–5]. A large number of enantiomers have been resolved on such modified cyclodextrins. Although modification of cyclodextrin has showed that substitution of the hydroxyl groups at positions 2, 3 and 6 has a great influence on enantioselectivity towards enantiomers, the mechanisms of interaction between enantiomers and cyclodextrin derivatives are still unclear. In some instances the experimental results are quite confusing, e.g., the 6-O-acyl derivative [3] and 2,6-di-O-pentyl-3-O-methyl-β-CD [6] display almost no enantioselectivity.

In order to gain a better understanding of the separation mechanisms, more attention has recently been paid to the thermodynamic data of enantiomer separations on cyclodextrin derivatives [7–10]. Venema *et al.* [7] investigated enantiomeric separations of some alkanes and alkanoic acid esters substituted at the C-2 position on alkylated β-CD and concluded that the stereochemistry and hydrophobic interactions were the major factors affecting the enantioselectivity for substituted cyclodextrins. Berthod *et al.* [8] recently suggested that there may be two mechanisms contributing to the separation obtained on a trifluoroacetylated phase, the formation of inclusion complexes and some form of external association. Smith and Simpson [9]

* Corresponding author.

0021-9673/94/$07.00
SSDI 0021-9673(94)00198-I

separated some alcohols and proposed that all these compounds interact by similar mechanisms. De Vries *et al.* [10] compared thermodynamic data for styrene oxide on four types of cyclodextrin derivatives and showed that both the size and the polarity of the CD have a great influence on the enantioselectivity. Several types of interactions have been suggested for chiral separations on cyclodextrin derivatives, including hydrophobic interactions, dipole–dipole interactions, geometry factors and the formation of inclusion complexes.

This work covers the enantiomeric separation of some amino acids, and 2- and 3-hydroxybutyric acid on 2,6-di-O-butyl-3-O-trifluoroacetylated-γ-cyclodextrin. Thermodynamic data measured on this stationary phase are given, and the possible separation mechanisms are discussed.

2. Experimental

2.1. Synthesis of 2,6-di-O-butyl-3-O-trifluoroacetylated-γ-CD (DB-TFA-γ-CD)

First, 1 g of γ-CD was converted into 2,6-di-O-butyl-γ-CD (DB-γ-CD) according to Li *et al.* [11]. The reaction mixture was extracted with $CHCl_3$. The organic layer was washed with water until neutral, then dried with Na_2SO_4, the solvent was carefully evaporated and drying was attempted at 60°C for 2 h under vacuum. The DB-γ-CD obtained was dissolved in tetrahydrofuran and a threefold molar excess of trifluoroacetic acid anhydride was added and refluxed for 4 h. After the extractive and drying work-up procedure, the raw product was purified by silica gel chromatography and finally a viscous oil of DB-TFA-γ-CD was obtained that was identified as described previously [12].

2.2. Preparation of chiral glass capillary column

The pretreatment and coating of glass capillary columns were as described previously [12]. Typically, a 25 m × 0.25 mm I.D. capillary column gives a column efficiency of 3740 plates/m.

2.3. Instrumentation

All chromatographic measurements were performed on a Model 1001 gas chromatograph (Shanghai Analytical Instrumentation Factory) equipped with a flame ionization detector. An HP-3390A integrator was used to record retention times and to calculate capacity factors (k') and separation factors (α). High-purity nitrogen was used as the carrier gas at a velocity of *ca.* 25 cm/s with a splitting ratio of 1:60–1:100.

2.4. Analytes and derivatization procedures

Most of the amino acids used were BDH products. 3-Aminobutyric acid, 2-hydroxybutyric acid and glutamic acid were obtained from Shanghai Chemical.

About 5 mg of each analyte were mixed with 0.5 mL of methanolic hydrochloric acid solution [acetyl chloride–methanol (1:10, v/v)] in a capped glass vial. The mixture was reacted at 80°C for 0.5 h, then the solvents was evaporated with a flow of nitrogen. The residue was dissolved in 0.2 ml of dry acetonitrile and 0.2 ml of trifluoroacetic acid anhydride was added. After the mixture had been kept at room temperature for 0.5 h, the excess reagents were removed. The final residue was dissolved in 0.4 ml of dichloromethane and was ready for chromatographic analysis.

3. Results and discussion

3.1. Enantiomeric separation of amino acids and 2- and 3-hydroxybutryic acid

Amino acids have been well separated on both Chirasil-Val [13] and 2,6-di-O-pentyl-3-O-butyryl-γ-cyclodextrin stationary phase [14]. 2,6-Di-O-pentyl-3-O-butyryl-γ-cyclodextrin seems to have displayed better enantioselectivity for almost all amino acids. Unfortunately, the recognition mechanism and effect of substitution of CD are not well understood. In our experiments,

most of the amino acids were resolved on DB-TFA-CD with high enantioselectivity. The D-configuration was first eluted for all resolved amino acids. However, a few amino acids, such as arginine, lysine, tryptophan and proline, were not resolved on this phase. Probably the entry of these amino acids into the cavity of CD was hindered by the relatively large groups linked at the C-3 position, thus reducing the enantioselectivity. We observed that 2- and 3-aminobutyric acid gave longer retention times than the corresponding 2- and 3-hydroxybutryic acid. This increased retention could be due to hydrogen bond formation between the amino acid and DB-TFA-γ-CD. A good separation was also observed for 2- and 3-hydroxybutyric acid, although the hydrogen bond could not be formed after derivatization. In this case, it is suggested that the dipole–dipole interactions might mainly contribute to the separation.

3.2. Thermodynamic parameters for enantiomeric resolution

In general, the absolute free energy $\Delta G^\circ = -RT \ln K$, where R is the gas constant, T is the absolute temperature and K is the thermodynamic stability constant of the association. To a first approximation, K may be considered as the partition coefficient between the mobile and the stationary phases, so it can be expressed as $\ln k' = -\Delta H^\circ/RT + \Delta S^\circ/R + \ln \beta$, where $K = k'/\beta$, k' is the capacity factor and β is the phase ratio. For each enantiomer pair, its ΔH° and $\Delta S^\circ + R \ln \beta$ values can be obtained by plotting $\ln k'$ *versus* $1/T$. In this experiment, k' was measured at intervals of 10°C in the temperature range $T_c \pm 20$°C (see Table 1) and all straight lines were obtained with good regression ($r > 0.994$). The slope is $-\Delta H^\circ$ and the intercept is $\Delta S^\circ + R \ln \beta$. The isoenantioselective temperature T_{iso} was calculated by the equation $T_{iso} = \Delta(\Delta H^\circ)/\Delta(\Delta S^\circ)$ [15]. Table 1 gives both separation and thermodynamic data for amino acids and 2- and 3-hydroxybutyric acid measured on DB-TFA-γ-CD. Table 1 shows obvious differences in $\Delta(\Delta H^\circ)$ and $\Delta(\Delta S^\circ)$ among the resolved amino acids. These $\Delta(\Delta H^\circ)$ and $\Delta(\Delta S^\circ)$ values are of approximately the same magnitude as those reported by Berthod *et al.* [8] and De Vries *et al.* [10]. From these data, it seems that the enantiomers investigated may fall into two groups. Group I includes $\Delta(\Delta S^\circ)$ values <1.15 cal/mol·K and group II has $\Delta(\Delta S^\circ)$ values ≥1.15 cal/

Table 1
Thermodynamic parameters of some enantiomers calculated from GC measurements on DB-TFA-γ-CD

Racemate	T_c (°C)	k'_1	α	$-\Delta H^\circ_1$ kcal/mol	$-\Delta H^\circ_2$ kcal/mol	$-\Delta(\Delta H^\circ)$ kcal/mol	$-\Delta(\Delta S^\circ)$ cal/(mol·K)	T_{iso} (°C)
Group I								
Serine	100	12.23	1.057	17.15	17.18	0.03	0.038	500
Cysteine	130	5.41	1.029	16.20	16.25	0.05	0.080	350
Threonine	80	19.69	1.052	17.75	17.94	0.19	0.44	150
β-Phenylalanine	130	19.12	1.038	15.78	16.04	0.26	0.57	180
Glutamic acid	130	13.11	1.066	16.21	16.64	0.43	0.94	190
Group II								
Methionine	130	12.31	1.084	15.96	16.49	0.53	1.15	150
Valine	100	6.87	1.221	14.29	15.56	1.27	3.01	150
3-Aminobutyric acid	100	12.35	1.248	16.37	17.75	1.38	3.26	150
Leucine	110	3.00	1.174	15.01	16.48	1.47	3.51	180
Aspartic acid	130	6.85	1.240	16.35	17.94	1.59	3.52	180
Alanine	90	7.286	1.400	14.97	16.56	1.59	3.71	150
2-Hydroxybutyric acid	80	4.230	1.373	14.10	15.81	1.71	4.21	130
2-Aminobutyric acid	100	5.327	1.587	14.51	17.45	2.94	6.96	150
3-Hydroxybutyric acid	100	1.505	1.449	12.12	15.43	3.14	7.68	130

mol·K. However, neither relationships nor differences were observed with regard to the isoenantioselective temperature in groups I and II. Serine and cysteine, with small $\Delta(\Delta H°)$ and $\Delta(\Delta S°)$ values, had much higher T_{iso} than other enantiomers. The decrease in the $\Delta(\Delta H°)$ values reflects the affinity of the cyclodextrin derivative for the enantiomers. The large negative entropy $\Delta(\Delta S°)$ may imply the loss of degree of freedom for enantiomers included in the cavity of the cyclodextrin derivative. The decrease in entropy from serine to 2-hydroxybutryic acid in Table 1 indicates that enantiomers are more ordered in the cavity of the cyclodextrin derivative than they are in the mobile phase in their inclusion complexes. Therefore, it is reasonable to suggest that the enantiomers with large negative $\Delta(\Delta S°)$ values in group II could form inclusion complexes during separation.

3.3. Enthalpy–entropy compensation and induced conformation fit

For enantiomers belonging to groups I and II, the differences in the chiral recognition mechanism were further investigated using enthalpy–entropy compensation. According to refs. 8 and 16, similar physico-chemical behaviour or interaction can be shown for a family of compounds at a compensation temperature T_Φ if enthalpy–entropy compensation occurs. $\Delta H°$ and ln k' are related by $\ln k'_T = -\Delta H°/R\ (T_\Phi - 1/\Phi) + \ln \beta$. Hence a straight line should be obtained on plotting ln k' *versus* $-\Delta H°$ for the enantiomers which have enthalpy–entropy compensation. The enthalpy–entropy compensation plots for both the first- and second-eluting peaks of these enantiomers are shown in Fig. 1. It can be seen from these plots that relatively good linearity was observed in group I. In contrast, a large dispersion was found for group II. This shows that enantiomers in group I follow enthalpy–entropy compensation and possibly interact by a mechanism that is completely different from that for enantiomers in group II. In group I, the amino acids at the C-3 position link with hydroxy, carboxy, thiol and phenyl groups, whereas in group II, the C-3 position of amino acids is, in general, occupied by alkane groups. Therefore, it is possible that hydrophobic interaction between the alkane group and the non-polar cavity of γ-CD resulted in the enantiomers approaching the γ-CD cavity closer by induced conformational fit and consequently the inclusion complex could be formed more easily. Whether or not the inclusion complex or other interaction occurred during separation, the conformational fit may play an important role in separation. That is why some amino acids display good enantioselectivity and some others may not on the same phase. Further investigation of the retention of amino acids on other cyclodextrin derivatives is in progress.

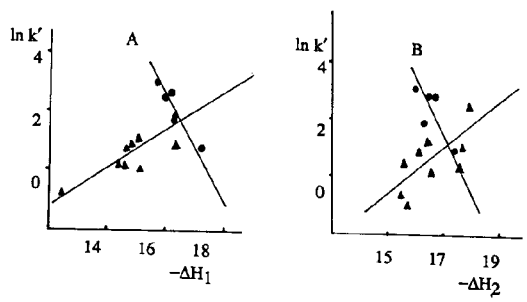

Fig. 1. Enthalpy–entropy compensation plots for (A) the first-eluted peaks and (B) the last-eluted peaks on DB-TFA-γ-CD at 130°C. ○ = Group I; ▲ = group II.

4. Conclusions

2,6-Di-O-butyl-3-O-trifluoroacetylated-γ-cyclodextrin displays variable enantioselectivity for amino acids having different functions at the C-3 position. The obvious thermodynamic data differences suggest that there may be more than one recognition mechanism on derivatized cyclodextrin stationary phases for amino acids in GC. Of these, the induced conformational fit between enantiomers and the cyclodextrin derivative could be the chief factor affecting enantioselectivity.

Acknowledgements

The financial support of this work by the National Natural Science Foundation of China is gratefully acknowledged. We thank Professor Lars Blomberg of the Department of Analytical Chemistry, Stockholm University, for his kind help in revising this paper and for useful suggestions.

References

[1] W.A. König, S. Lutz and G. Wenz, *Angew. Chem., Int. Ed. Engl.*, 27 (1988) 979.
[2] H.-P. Nowotny, D. Schmalzing, D. Wistuba and V. Schurig, *J. High Resolut. Chromatogr.*, 12 (1989) 383.
[3] W.A. König, D. Icheln, T. Runge, I. Pforr and A. Krebs, *J. High Resolut. Chromatogr.*, 13 (1990) 702.
[4] D.W. Armstrong, W. Li, C-D. Chang and J. Pitha, *Anal. Chem.*, 62 (1990) 914.
[5] W. Keim, A. Köhnes, W. Meltzow and H. Römer, *J. High Resolut. Chromatogr.*, 14 (1991) 507.
[6] C. Bicchi, G. Artuffo, A. D'Amato, V. Manzin, A. Galli and M. Galli, *J. High Resolut. Chromatogr.*, 15 (1992) 710.
[7] A. Venema, H. Henderiks and R.v. Geest, *J. High Resolut. Chromatogr.*, 14 (1991) 676.
[8] A. Berthod, W. Li and D.W. Armstrong, *Anal. Chem.*, 64 (1992) 873.
[9] I.D. Smith and C.F. Simpson, *J. High Resolut. Chromatogr.*, 15 (1992) 800.
[10] N.K. de Vries, B. Coussens, R.J. Meier and G. Heemels, *J. High Resolut. Chromatogr.*, 15 (1992) 499.
[11] W. Li, H.L. Li and D.W. Armstrong, *J. Chromatogr.*, 509 (1990) 303.
[12] H. Wan, Y. Wang, Q. Ou and W. Yu, *J. Chromatogr.*, 644 (1993) 202.
[13] H. Frank, G.J. Nicholson and E. Bayer, *J. Chromatogr. Sci.*, 15 (1977) 174.
[14] W.A. König, R. Krebber and P. Mischnick, *J. High Resolut. Chromatogr.*, 12 (1989) 732.
[15] B. Koppenhoefer and E. Bayer, *Chromatographia*, 19 (1984) 123.
[16] W. Melander, D.E. Campbell and C. Horváth, *J. Chromatogr.*, 158 (1978) 215.

ELSEVIER

Journal of Chromatography A, 673 (1994) 113–124

JOURNAL OF CHROMATOGRAPHY A

Determination of the hydrophobicity parameter R_{Mw} by reversed-phase thin-layer chromatography

Karl Dross[a], Christoph Sonntag[a], Raimund Mannhold*[,b]

[a]*Department of Brain Research, Heinrich-Heine-Universität, Universitätsstrasse 1, 40225 Düsseldorf, Germany*
[b]*Department of Laser-Medicine, Molecular Drug Research Group, Heinrich-Heine-Universität, Universitätsstrasse 1, 40225 Düsseldorf, Germany*

(First received January 14th, 1994; revised manuscript received March 3rd, 1994)

Abstract

Experimental conditions were established that permit the determination of chromatographic lipophilicity parameters on the basis of thermodynamically true R_M values. The superiority of methanol as compared with other modifiers (*e.g.*, acetonitrile) is substantiated; physico-chemical reasons are discussed. Solvent pH influences only the silanophilic effect; hence, with highly ionized structures, determination at neutral pH is to be preferred. Extrapolation to modifier-free conditions (R_{Mw} value) is essential to diminish the contribution of polar interactions. Advantages and disadvantages of non-linear extrapolation procedures are compared with linear regression. Correctly estimated R_{Mw} values coincide numerically not only with log k_w values, as theoretically expected, but also with partitioning data from the octanol–water system.

1. Introduction

The prime role of lipophilicity among quantitative structure–activity relationship (QSAR) parameters is undisputed. The classical approach to quantifying lipophilicity, by octanol–water partitioning, is being supplanted by chromatographic procedures, in particular high-performance liquid chromatography on reversed-phase RP-18 phases (RP-HPLC). Using methanol as a modifier, water-extrapolated log k values (log k_w) derived in this system show an excellent correlation with octanol–water partition coefficients, as summarized by Braumann in a valuable review [1]. As thin-layer chromatographic (TLC) procedures and HPLC exhibit the same dependence on the stationary and mobile phases, this correlation should also apply to TLC.

R_M values, obtained by RP-TLC, have a long tradition as lipophilicity parameters (see, *e.g.*, ref. 2), but they are often viewed as "quick and dirty" parameters. In a previous paper [3], we showed that this view is due to incorrect measurement of R_M. First, it is essential to determine R'_F values with the aid of front markers, which are the only means of calculating thermodynamically true R_M values. Because R_M values depend significantly on modifier content, Biagi *et al.* [4] preferred R_{Mw} values, *i.e.*, R_M extrapolated to 100% water, as lipophilicity parameters in QSAR studies. The theoretical and experimental correctness of such an extrapolation were demonstrated by Soczewinski and Wachtmeister [5]. However, a linear dependence of R_M

* Corresponding author.

0021-9673/94/$07.00
SSDI 0021-9673(94)00222-U

holds only at low modifier content φ; at high φ, the R_M values deviate from linearity [4,6].

Despite pronounced differences in experimental procedures, the basic partitioning conditions are similar in RP-TLC and RP-HPLC. The stationary phase, *i.e.*, silica gel etherified with octadecanol, is identical with that used on RP-TLC plates. Hence the partitioning process is governed by identical physico-chemical parameters when the same solvent is used [1,7]. Correspondingly, also in RP-HPLC it is common to apply water-extrapolated values (log k_w) as lipophilicity parameters. Also for RP-HPLC it has been shown by several workers [8–11] that in case of high modifier contents the log k' values can deviate from linearity and linear extrapolations therefore lead to erroneous log k_w.

In this work, we investigated the questions of linearity and extrapolation to R_{Mw} on the basis of thermodynamically true R_M values. In addition, a comparison of such R_{Mw} data with other lipophilicity data is given; experimental lipophilicity parameters such as log P_{Oct} and log k_w and also calculation parameters such as Σf [12] are included Finally, we report on the influence of acetonitrile as modifier and of the solvent pH on R_{Mw}.

2. Experimental

Precoated TLC plates (RP-18 F_{254S}, 20 × 10 cm) purchased from Merck (Darmstadt, Germany) were used. Compared with differently coated silica gel plates [4,6], these plates have the considerable advantage of high stability, permitting their use for large ranges of varying modifier/buffer contents; they are also similar to the material used in RP-HPLC. As solvent we used methanol–buffer mixtures with methanol contents between 20 and 100% (v/v) or acetonitrile–buffer mixtures with modifier contents between 40 and 75% (v/v) in 5% increments. Tris buffer [pH 7.4 (ionic strength 0.1 mol/l)] was used, prepared with water obtained from a Milli-Q Plus water system (Millipore, Bedford, MA, USA). In some instances, commercially available buffer (pH 12) from Riedel-de Haën (Seelze, Germany) was used. TLC was performed in twin-trough chambers (Camag, Muttenz, Switzerland), which were placed in an incubator adjusted to 30°C.

Detailed experimental conditions for the determination and calculation of thermodynamically true R'_F and R_M values have already been published [3]. For determining the thermodynamically true position of the front, KI was used. A 0.5-μl volume of an ethanolic solution of the test compounds was applied to the plates with the aid of a Nanomat II (Camag). Positioning of the starting points (Z_0) and the positions after the runs (Z_X) were exactly evaluated with the aid of a CD 50 densitomer (Desaga, Heidelberg, Germany). The R'_F value of a test compound X is calculated according to

$$R'_{FX} = 0.99(Z_X - Z_0)/(Z_{KI} - Z_0) \quad (1)$$

$Z_X - Z_0$ and $Z_{KI} - Z_0$ characterize the migration distances of the test compound X and of the front marker KI; the correction factor 0.99 corresponds to the front gradient [3,7,13].

From the R'_F values, the thermodynamically true R_M values were calculated according to the well known procedure of Bate-Smith and Westall [14]:

$$R_{MX} = \log(1/R'_{FX} - 1) \quad (2)$$

2.1. Test compounds

The compounds tested are listed in Table 1. Compounds **19–21** were kindly provided by Professor Weber, Department of Pharmaceutical Chemistry, University of Düsseldorf. The remaining compounds were obtained from Aldrich (Milwaukee, WI, USA).

2.2. Statistics

All statistical procedures were run with Graph Pad InPlot, version 4.04 (Graph Pad Software, San Diego, CA, USA). Deviations are given as 95% confidence intervals.

Table 1
R_{Mw} values, obtained by linear regression or according to Eq. 10, as compared with log k_w, log P_{Oct} [27] and Σf values, calculated according to ref. 12

No.	Compound	$R_{Mw} \pm 95\%$ c.i.[a]		Log k_w	Log P_{Oct}	$\Sigma f_{rev.}$
		Linear	Non-linear (Eq. 10)			
1	Benzoic acid	1.649 ± 0.018	1.661 ± 0.136	1.92	1.87	1.84
2	2-Methylbenzoic acid	1.967 ± 0.029	1.974 ± 0.267		2.18	2.14
3	3-Methylbenzoic acid	2.208 ± 0.020	2.218 ± 0.100		2.37	2.36
4	4-Methylbenzoic acid	2.218 ± 0.043	2.270 ± 0.115	2.48	2.27	2.36
5	3,4-Dimethylbenzoic acid	2.668 ± 0.058	2.701 ± 0.300			2.87
6	3-Methoxybenzoic acid	1.804 ± 0.024	1.801 ± 0.169		2.02	1.91
7	4-Methoxybenzoic acid	1.954 ± 0.037	2.002 ± 0.126		1.96	1.91
8	3-Fluorobenzoic acid	1.763 ± 0.030	1.853 ± 0.400		2.15	2.08
9	4-Fluorobenzoic acid	1.797 ± 0.028	1.798 ± 0.191		2.07	2.08
10	3-Chlorobenzoic acid	2.106 ± 0.032	2.096 ± 0.111		2.68	2.57
11	4-Chlorobenzoic acid	2.190 ± 0.027	2.179 ± 0.099	2.70	2.65	2.57
12	3-Bromobenzoic acid	2.265 ± 0.031	2.260 ± 0.150		2.87	2.77
13	4-Bromobenzoic acid	2.368 ± 0.032	2.383 ± 0.145		2.86	2.77
14	3-Iodobenzoic acid	2.536 ± 0.059	2.529 ± 0.185		3.13	3.08
15	4-Iodobenzoic acid	2.628 ± 0.054	2.603 ± 0.154		3.02	3.08
16	4-Butylbenzoic acid	3.940 ± 0.155	4.002 ± 0.594			3.91
17	4-Pentylbenzoic acid	4.429 ± 0.131	4.430 ± 0.332			4.43
18	4-Heptylbenzoic acid	5.440 ± 0.103	5.410 ± 0.380			5.47
19	2-Hydroxybenzoic acid	1.165 ± 0.044	1.169 ± 0.626		2.21	2.16
20	4-Hydroxybenzoic acid	1.068 ± 0.022	1.033 ± 0.910	1.20	1.57	1.50
21	2,4-Dihydroxybenzoic acid	0.872 ± 0.056	0.737 ± 1.275		1.44	1.60
22	1-Naphthalenecarboxylic acid	3.047 ± 0.063	3.016 ± 0.215		3.10	3.12
23	3-Methylphenylacetic acid	2.049 ± 0.029	2.039 ± 0.120		1.86	2.00
24	3-Fluorophenylacetic acid	1.644 ± 0.055	1.624 ± 0.192		1.65	1.72
25	4-Fluorophenylacetic acid	1.649 ± 0.047	1.628 ± 0.161		1.55	1.72
26	4-Chlorophenylacetic acid	2.166 ± 0.036	2.146 ± 0.175		2.12	2.21
27	4-Bromophenylacetic acid	2.306 ± 0.017	2.302 ± 0.087		2.31	2.41
28	3-Phenylpropionic acid	2.095 ± 0.027	2.106 ± 0.133		1.84	2.00
29	4-Phenylbutyric acid	2.527 ± 0.018	2.524 ± 0.083		2.42	2.52
30	Benzophenone	3.361 ± 0.082	3.385 ± 0.239	3.15	3.38	3.05
31	2,6-Dimethylbenzophenone	4.038 ± 0.104	4.029 ± 0.189			3.65
32	2,2′-Dimethylbenzophenone	4.121 ± 0.155	4.116 ± 0.416			3.87
33	2,6,2′,6′-Tetramethylbenzophenone	4.463 ± 0.132	4.418 ± 0.179			4.69
34	2,6,2′,6′-Tetraethylbenzophenone	6.131 ± 0.097	6.169 ± 0.408			6.54
35	4-Bromoacetophenone	2.938 ± 0.052	2.950 ± 0.195		2.43	2.58
36	2-Hydroxybenzamide	1.380 ± 0.013	1.385 ± 0.123	1.24	1.28	1.09
37	4-Hydroxybenzamide	0.460 ± 0.027	0.470 ± 0.166		0.33	0.43
38	Phenol	1.278 ± 0.056	1.250 ± 0.556	1.30	1.46	1.55
39	4-Chlorophenol	2.031 ± 0.026	2.039 ± 0.163	2.24	2.35	2.28
40	4-Bromophenol	2.223 ± 0.023	2.209 ± 0.138		2.43	2.48
41	1-Naphthol	2.572 ± 0.035	2.592 ± 0.133	1.71	2.65	2.84
42	2-Naphthol	2.577 ± 0.041	2.609 ± 0.124	2.15	2.70	2.84
43	4-Methylbenzyl alcohol	1.916 ± 0.026	1.952 ± 0.113		1.59	1.71
44	4-Chlorobenzyl alcohol	2.120 ± 0.012	2.124 ± 0.074		1.96	1.92
45	Imidazole	−0.130 ± 0.022	0.033 ± 1.020		−0.08	0.16
46	2-Methylimidazole	0.014 ± 0.009	0.088 ± 0.638			0.68
47	2-Ethylimidazole	0.155 ± 0.016	0.262 ± 1.116			1.20
48	2-Propylimidazole	0.309 ± 0.009	0.335 ± 0.117			1.72
49	1-Butylimidazole	0.614 ± 0.014	0.602 ± 0.262			2.02
50	2-Phenylimidazole	1.170 ± 0.041	1.094 ± 1.129		1.87	2.08
51	Benzimidazole	0.821 ± 0.032	0.866 ± 0.365		1.20	1.45
52	2-Methylbenzimidazole	0.917 ± 0.018	0.960 ± 0.592		1.43	1.96
53	5,6-Dimethylbenzimidazole	1.685 ± 0.074	1.726 ± 0.515		2.35	2.48

(Continued on p. 116)

Table 1 (*Continued*)

No.	Compound	$R_{Mw} \pm 95\%$ c.i.[a]		Log k_w	Log P_{Oct}	$\Sigma f_{rev.}$
		Linear	Non-linear (Eq. 10)			
54	4-Nitroaniline	1.415 ± 0.032	1.421 ± 0.171	1.46	1.39	0.76
55	4-Chloroaniline	1.692 ± 0.040	1.695 ± 0.227	1.80	1.83	1.73
56	4-Bromoaniline	1.989 ± 0.031	2.014 ± 0.186	2.01	2.05	1.93
57	2,5-Di-*tert.*-butylaniline	4.383 ± 0.043	4.388 ± 0.188			5.15
58	2-Naphthylamine	2.201 ± 0.043	2.207 ± 0.178		2.28	2.29
59	4-Bromo-1-naphthylamine	3.341 ± 0.033	3.358 ± 0.267			3.22
60	2-Aminobiphenyl	2.988 ± 0.027	2.977 ± 0.112		2.84	2.92
61	2-Aminofluorene	3.421 ± 0.045	3.381 ± 0.387			3.02
62	2-Amino-7-bromofluorene	4.110 ± 0.070	4.134 ± 0.497			3.95
63	2-Amino-1,3-dibromofluorene	4.867 ± 0.026	4.888 ± 0.240			4.88
64	1-Aminoanthracene	3.562 ± 0.037	3.563 ± 0.255			3.58
65	3-Aminofluoranthene	4.588 ± 0.079	4.581 ± 0.444			4.01
66	1-Aminopyrene	4.661 ± 0.089	4.666 ± 0.294 .			4.01
67	Acridine	3.400 ± 0.060	3.386 ± 0.399	2.87	3.40	3.31
68	4-Nitrotoluene	2.605 ± 0.022	2.607 ± 0.115	2.40	2.42	2.38
69	4-Chloronitrobenzene	2.701 ± 0.025	2.734 ± 0.049	2.35	2.41	2.59
70	4-Bromonitrobenzene	2.760 ± 0.037	2.757 ± 0.160		2.55	2.79
71	1-Nitronaphthalene	3.248 ± 0.016	3.260 ± 0.094		3.19	3.15
72	Pentamethylbenzene	4.352 ± 0.182	4.369 ± 0.583	4.70	4.56	4.70
73	Biphenyl	3.920 ± 0.084	3.937 ± 0.342	4.09	4.08	4.02
74	Bibenzyl	4.676 ± 0.072	4.682 ± 0.349	4.92	4.79	4.84
75	Naphthalene	3.168 ± 0.053	3.171 ± 0.179	3.31	3.35	3.39
76	2-Methylnaphthalene	3.747 ± 0.083	3.751 ± 0.253		3.86	3.91
77	2,6-Dimethylnaphthalene	4.290 ± 0.090	4.331 ± 0.196		4.31	4.43
78	1-Phenylnaphthalene	4.529 ± 0.036	4.542 ± 0.105			5.31
79	2,6-Di-*tert.*-butylnaphthalene	6.416 ± 0.137	6.319 ± 0.776			7.55
80	Anthracene	4.228 ± 0.039	4.243 ± 0.151	4.58	4.45	4.68
81	2-Methylanthracene	4.623 ± 0.069	4.632 ± 0.154		5.07	5.20
82	2-Ethylanthracene	5.085 ± 0.092	5.075 ± 0.202			5.72
83	2-Chloroanthracene	4.750 ± 0.170	4.725 ± 0.417			5.41
84	9-Bromoanthracene	4.959 ± 0.163	5.023 ± 0.501			5.61
85	9-Phenylanthracene	5.158 ± 0.037	5.174 ± 0.135			6.60
86	9,10-Diphenylanthracene	6.938 ± 0.197	6.963 ± 0.540			8.52
87	2-Methylphenanthrene	5.158 ± 0.023	5.205 ± 0.332		4.86	5.20
88	1,3,5-Trichlorobenzene	4.047 ± 0.035	4.064 ± 0.221	4.26	4.02	4.29
89	1,2,4,5-Tetrachlorobenzene	4.524 ± 0.103	4.635 ± 0.638	4.65	4.52	5.02
90	Pentachlorobenzene	4.896 ± 0.079	4.901 ± 0.205	5.25	5.03	5.75
91	Hexachlorobenzene	5.360 ± 0.131	5.375 ± 0.354	5.46	5.37	6.48
92	1,4-Dibromobenzene	3.877 ± 0.065	3.873 ± 0.285		3.64	3.97

[a] c.i. = Confidence interval.

3. Results and discussion

3.1. Determination of R_{Mw} values by linear extrapolation

To test the linearity between R_M and methanol content φ, in general 16 data points were available for each test compound. For compounds with $R_{Mw} > 3$, R_M values cannot be calculated with sufficient accuracy at low φ, owing to inaccurate measurement of migration distances around 0.01 mm. For only 4 out of 92 investigated compounds, the R_M values decline linearly up to φ values of 0.85 (Fig. 1A); these four compounds (tri-, tetra-, penta- and hexachlorobenzene, **88–91**) are extremely non-polar. Kamlet *et al.* [15] specified their α and β values, which quantify the proton-accepting and proton-

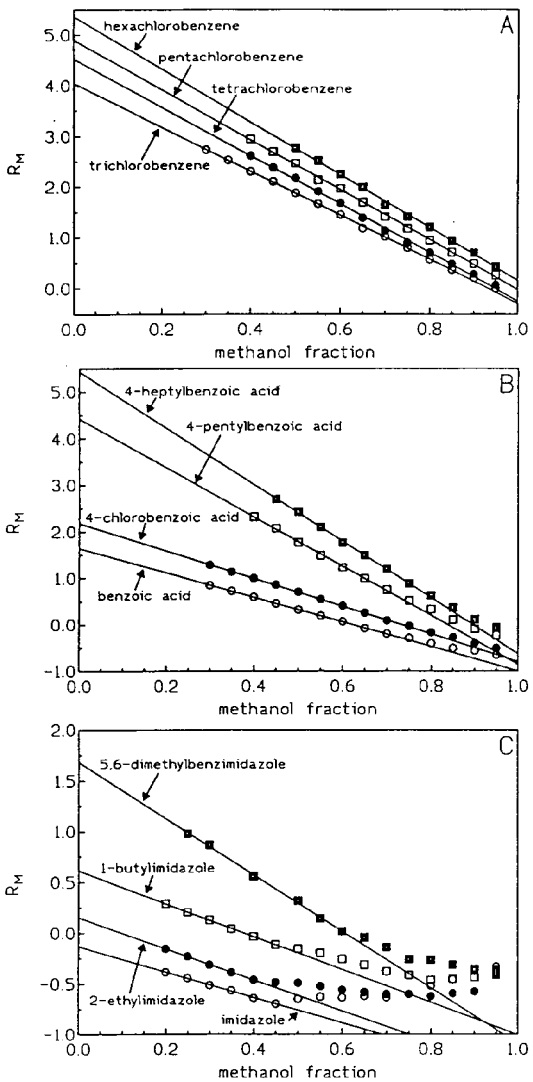

Fig. 1. Dependence of R_M values on the methanol fraction (φ). (A) Non-polar compounds; (B) acids; (C) bases.

donating behaviour, as zero. For all other test compounds, deviations from linearity are found at methanol contents of 45–75% (Fig. 1B and C), presumably owing to the so-called silanophilic effect, which has been described by Nahum and Horvath [10] for RP-HPLC. This effect is based on polar interactions between free silanol moieties of the RP material and polar moieties of the test molecules. In the RP material the silanol groups are only partially etherified with octadecanol for stereochemical reasons; for the Merck plates used in this investigation, the amount of etherification is given as 22% [16]. In solvents with a high buffer content, silanol groups are quantitatively protected by water molecules and the chromatographic process is based almost exclusively on partitioning (reversed-phase behaviour). With increasing modifier content the possibility of polar interactions of the silanol groups increases (normal-phase behaviour).

One way to reduce the silanophilic effect and achieve an improved determination of R_M would be to use Merck RP-18 HPTLC plates, which are coated with a silica gel material with higher etherification with octadecyl groups. However, these plates can only be moistened by solvents containing less than 40% of water. This makes extrapolation to modifier-free conditions less accurate. Similar experience has been reported by Butte *et al.* [17].

The linear part of the relationship between R_M and methanol content was determined by the aid of a computer program [18]. Because the silanophilic effect always initiates an increase in the measured R_M values, the necessary procedure was unequivocally defined. Correspondingly calculated R_{Mw} values are summarized in Table 1.

3.2. Determination of R_{Mw} by non-linear regression

Schoenmakers and co-workers [19,20] described the correlation between log k' and φ with a Scatchard–Hildebrand extended solubility parameter model [21,22] by means of the following equation:

$$\log k' = \log k_w + A\varphi^2 - S\varphi \quad (3)$$

The application of this approach to the determination of R_{Mw} necessitates, for an accurate calculation, the availability of a large number of data points, particularly at low modifier contents; mainly for technical reasons these data were not always available. Log k_w values calcu-

lated according to Eq. 3 have been correlated with log P_{Oct} data by Braumann [1] and El Tayar *et al.* [23]. From these correlations, it is concluded that in the case of lipophilic compounds the above approach yields overestimated parameters.

The shape of the plots of R_M *versus* φ resembles a decreasing exponential in the first part followed by an increasing one. We therefore attempted to describe this pattern empirically by the following equation:

$$R_M = \log(Ae^{-B\varphi} + Ce^{D\varphi}) \quad (4)$$

The decreasing exponential in Eq. 4 expresses the contribution of hydrophobic interactions between the test compound, the stationary hydrophobic phase and the aqueous mobile phase to R_M, while the increasing exponential corresponds to the contribution of polar adsorption. Parameters A, B, C and D were calculated by non-linear regression. If the parameters A, B, C and D are given, R_{Mw} is calculated by setting $\varphi = 0$:

$$R_{Mw} = \log(A + C) \quad (5)$$

Table 2 summarizes some R_{Mw} values, calculated according to this approach for six test compounds representing the chemical classes included in this study. These results agree well with those obtained by linear extrapolation. However, in some instances the iteration program calculated negative values for D, which means that the program fits the plot of R_{Mw} *versus* φ to two decreasing exponentials. This is obviously misleading, as the adsorptive, polar contribution to R_M increases with increasing modifier content. Hence Eq. 4 is not generally applicable.

Nahum and Horváth [10] developed an equation that separates two contributions to log k' depending on the buffer content of the eluent. Owing to the above-mentioned free silanol groups, they assumed the simultaneous existence of both reversed-phase (solvophobicity) and normal-phase (silanophilicity) behaviour. Solvophobic behaviour is expressed as follows:

$$k_1 = Ae^{B\psi} \quad (6)$$

where ψ defines the water content. In normal-phase chromatography with polar adsorbents such as silica gel, the interdependence between the retention factor and the composition of a binary solvent is expressed as follows [24,25]:

$$k_2 = 1/(C + D\psi) \quad (7)$$

The entire retention factor k' is then the sum of k_1 and k_2:

$$k' = Ae^{B\psi} + 1/(C + D\psi) \quad (8)$$

or, in logarithmic form,

$$\log k' = \log[Ae^{B\psi} + 1/(C + D\psi)] \quad (9)$$

As already outlined above, this calculation can also be applied to the determination of R_{Mw}.

Table 2
Comparison of some R_{Mw} values, obtained by non-linear regression (Eq. 4), with linearly extrapolated data

No.	Compound	$R_{Mw} \pm 95\%$ c.i.[a]		Δ
		Nonlinear regression by Eq. 4	Linear regression	
1	Benzoic acid	1.682 ± 0.061	1.649 ± 0.018	0.033
26	Benzophenone	3.457 ± 0.121	3.361 ± 0.082	0.096
40	Imidazole	−0.075 ± 0.173	−0.130 ± 0.022	0.055
50	4-Chloroaniline	1.691 ± 0.054	1.692 ± 0.040	−0.001
72	Anthracene	4.197 ± 0.065	4.228 ± 0.039	−0.031
82	Pentachlorobenzene	4.896 ± 0.148	4.896 ± 0.079	0.000

[a] c.i. = Confidence interval.

Calculation of the paramcters A, B, C and D and setting $\psi = 1$ (modifier free) then gives

$$R_{Mw} = \log[Ae^B + 1/(C + D)] \quad (10)$$

Correspondingly calculated R_{Mw} data are summarized in column 2 in Table 1. Linear extrapolation and non-linear regression according to Horváth (Eq. 10) results in almost identical R_{Mw} values ranging between −0.13 and 6.98, as shown by the regression equation

$$R_{Mw,Hor} = 0.997(\pm 0.005)R_{Mw,lin} + 0.016(\pm 0.017) \quad (11)$$

$n = 92$; $s = 0.039$; $r = 0.9997$; $F = 144\,000$

The mean difference between the two calculation procedures is 0.01 ± 0.04; only in three cases it is greater than 0.1.

Although non-linear regression according to Nahum and Horváth [10] is the better approach for the determination of R_{Mw}, our results demonstrate that the far more convenient linear extrapolation yields almost identical results, if carefully applied. In addition, confidence intervals are significantly smaller in the latter instance, as expected from the calculation procedure.

3.3. Influence of solvent pH on R_M

Concerning the influence of solvent pH on the R_M values of strong bases, we have already reported [3] that the silanophilic effect, but not the lipophilic distribution, depends on solvent pH. For a validation of this hypothesis, we selected some imidazole derivatives exhibiting pK values around 7 [26]. R_{Mw} values were measured at pH 7.4 (50% dissociation) and 12 (no protonation). As shown in Table 3, the measured data are well correlated, with the greatest deviation being 0.067. This is shown by the regression equation

$$R_{Mw,pH7.4} = 0.969(\pm 0.042)R_{Mw,pH12} + 0.010(\pm 0.036) \quad (12)$$

$n = 9$; $s = 0.031$; $r = 0.9988$; $F = 2973$

The influence of solvent pH is shown in detail in Fig. 2. At higher pH, polar interactions are

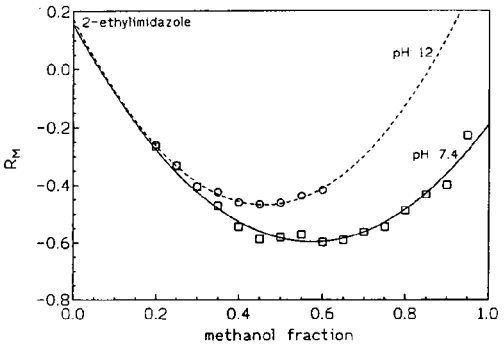

Fig. 2. Influence of pH on R_M values. Curves were calculated according to Horváth (see also Eq. 10).

Table 3
R_{Mw} values of imidazoles

No.	Compound	R_{Mw} (pH 7)	n	R_{Mw} (pH 12)	n	Δ
45	Imidazole	−0.130	6	−0.130	4	0.000
46	2-Methylimidazole	0.014	5	0.037	3	−0.023
47	2-Ethylimidazole	0.155	5	0.173	3	−0.018
48	2-Propylimidazole	0.309	7	0.253	4	0.056
49	1-Butylimidazole	0.614	6	0.611	5	0.003
50	2-Phenylimidazole	1.170	4	1.188	3	−0.018
51	Benzimidazole	0.821	9	0.803	8	0.018
52	2-Methylbenzimidazole	0.917	5	0.949	4	−0.032
53	5,6-Dimethylbenzimidazole	1.685	6	1.752	5	−0.067

Data measured at pH 7.4 are compared with values derived at pH 12.0 and their differences (Δ) are given. n = Number of data points included for linear extrapolation.

strengthened. Accordingly, the curve shape is linear between 20 and 40% methanol at pH 7.4, but only up to 30% methanol at pH 12. Hence, uncertainties in the extrapolation to R_{Mw} arise, which underlie the deviations in Eq. 12. At low methanol contents, where R_M depends solely on the lipophilic distribution, the data coincide almost exactly.

3.4. Influence of the modifier on R_M

The pronounced influence of the modifier on the quality of chromatographic data has been comprehensively described by Braumann [1]. The distribution of the test compounds into the octadecyl phase of the RP-18 phase depends significantly on physico-chemical properties of the modifier such as dipole moment or proton-donating properties. In this respect, the properties of acetonitrile are distinctly different from those of water, whereas methanol is very similar. Accordingly, methanol has to be viewed as the modifier of choice for the chromatographic determination of lipophilicity. These considerations are impressively substantiated by our present investigations. R_{Mw} values determined with acetonitrile as modifier (Table 4) are significantly lower than the data measured in the methanol system:

$$R_{Mw,ACN} = 0.679(\pm 0.070)R_{Mw,MeOH} + 0.232(\pm 0.217) \quad (13)$$

$$n = 22;\ s = 0.179;\ r = 0.9766;\ F = 412$$

The mean difference is 0.69 ± 0.41. Also in comparison with log P_{Oct} the acetonitrile-related data show a significant negative deviation with a mean value of 0.87 ± 0.30. Correspondingly, the correlations of the chromatographic data with log P_{Oct} are less significant in the case of the

Table 4
R_{Mw} values of some selected test compounds measured in the acetonitrile system, and the differences from the values obtained in the methanol system

No.	Compound	$R_{Mw,ACN} \pm 95\%$ c.i.[a]	$\Delta R_{Mw,MeOH}$
1	Benzoic acid	1.360 ± 0.112	0.289
2	2-Methylbenzoic acid	1.548 ± 0.065	0.419
4	4-Methylbenzoic acid	1.561 ± 0.049	0.657
5	3,4-Dimethylbenzoic acid	1.756 ± 0.050	0.912
6	3-Methoxybenzoic acid	1.476 ± 0.098	0.328
7	4-Methoxybenzoic acid	1.441 ± 0.109	0.513
8	3-Fluorobenzoic acid	1.530 ± 0.092	0.233
9	4-Fluorobenzoic acid	1.507 ± 0.095	0.290
10	3-Chlorobenzoic acid	1.696 ± 0.071	0.410
11	4-Chlorobenzoic acid	1.711 ± 0.059	0.479
12	3-Bromobenzoic acid	1.779 ± 0.054	0.486
13	4-Bromobenzoic acid	1.773 ± 0.056	0.595
14	3-Iodobenzoic acid	1.867 ± 0.072	0.669
15	4-Iodobenzoic acid	3.998 ± 0.072	0.748
30	Benzophenone	2.757 ± 0.097	0.604
31	2,6-Dimethylbenzophenone	3.239 ± 0.286	0.799
32	2,2′-Dimethylbenzophenone	3.277 ± 0.356	0.844
33	2,6,2′,6′-Tetramethylbenzophenone	3.582 ± 0.226	0.881
34	2,6,2′,6′-Tetraethylbenzophenone	3.998 ± 0.060	2.133
72	Pentamethylbenzene	3.119 ± 0.092	1.233
73	Biphenyl	2.843 ± 0.115	1.077
75	Naphthalene	2.489 ± 0.074	0.679

[a] c.i. = Confidence interval.

acetonitrile system (Eq. 14) as compared with the methanol system (Eq. 15):

$$R_{Mw,ACN} = 0.677(\pm 0.126) \log P_{Oct} + 0.028(\pm 0.360) \quad (14)$$

$n = 17$; $s = 0.180$; $r = 0.9476$; $F = 132$

3.5. Comparison of R_{Mw} with log P_{Oct}

For 65 of 92 test compounds (see Table 1), log P_{Oct} values have been published [27]. For the latter a measuring accuracy of 0.3 log units is generally accepted [28]; 52 pairs are located within this range.

Correlations between log P_{Oct} and R_{Mw} data, obtained either by linear extrapolation (Eq. 15) or by non-linear regression (Eq. 16), yield the following results:

$$R_{Mw,lin} = 1.008(\pm 0.064) \log P_{Oct} - 0.151(\pm 0.183) \quad (15)$$

$n = 65$; $s = 0.294$; $r = 0.9699$; $F = 1000$

$$R_{Mw,Hor} = 1.009(\pm 0.066) \log P_{Oct} - 0.147(\pm 0.190) \quad (16)$$

$n = 65$; $s = 0.304$; $r = 0.9679$; $F = 935$

The average R_{Mw} values are 0.13 ± 0.29 lower than the corresponding log P_{Oct} values. In five cases (three benzoic acids and two imidazoles), the values were more than two standard deviations lower. The R_{Mw} values of all acids exhibit lower values than log P_{Oct} with a mean difference of 0.24 ± 0.31. Omission of these acids results in correlation equations with regression coefficients approximating 1 and with intercepts only marginally differing from zero:

$$R_{Mw,lin} = 1.000(\pm 0.062) \log P_{Oct} - 0.059(\pm 0.197) \quad (17)$$

$n = 40$; $s = 0.260$; $r = 0.9827$; $F = 1070$

$$R_{Mw,Hor} = 0.998(\pm 0.063) \log P_{Oct} - 0.036(\pm 0.202) \quad (18)$$

$n = 40$; $s = 0.267$; $r = 0.9818$; $F = 1013$

Not surprisingly, the mean differences for this set of 40 compounds are as low as 0.06 ± 0.26, ranging within the measurement accuracy of 0.3 units, as accepted for log P.

On closer inspection (see also Fig. 3), the halogenated and hydroxylated benzoic acids are seen to be underestimated in comparison with log P_{Oct}. An extraordinarily strong deviation is found for salicylic acid (**19**) and some substituted imidazoles (**50–53**). It remains to be clarified whether the chromatographic or the partitioning approach supplies more precise data. Nevertheless, it is striking that all these compounds are polar. Octanol–water distribution coefficients of ionizable compounds depend strictly on the compound pK values and the pH of the buffer phase. Hence an exact determination of log P necessitates precise measurements of both log D and pK. Mannhold *et al.* [29] demonstrated the profound influence of questionable pK values on transforming log D into log P. On the other hand, chromatography-based lipophilicity determinations are independent of pK/pH, are only influenced by one parameter and therefore represent from our point of view the more accurate data.

A number of workers [1,17,30–34] have concluded that R_{Mw} or log k_w values better correlate

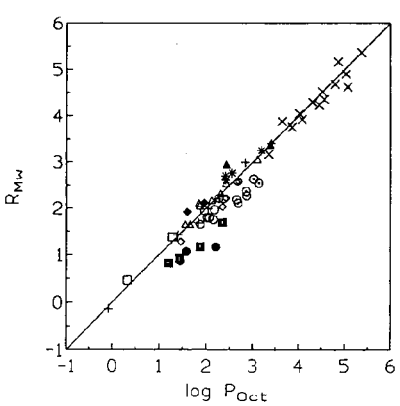

Fig. 3. Correlation of R_{Mw} with log P_{Oct} values. × = Non-polar compounds (**72–92**); ● = hydroxybenzoic acids (**19–21**); ⊙ = halogenated benzoic acids (**8–15**); ○ = remaining benzoic acids (**1–7**, **16–18**); △ = phenones (**30**, **35**); □ = benzamides (**36**, **37**); ◇ = phenols (**38–42**); ■ = substituted imidazoles (**50–53**); + = amines (**45**, **54–56**, **58**, **60**, **67**); * = nitro compounds (**68–71**).

with log P_{Oct} than R_M or log k' values measured at one given modifier content. Regression equations with respect to the varying modifier contents have been calculated according to

$$R_{M,\varphi} = a \log P_{Oct} + b \quad (19)$$

Fig. 4 shows the slopes a and the intercepts b for the individual regression equations as a function of the modifier content φ. In the range 20–45% methanol content, R_M determinations were not possible for some test compounds owing to their high lipophilicity. Correspondingly, the number of test compounds (n) included differs for the various methanol–buffer mixtures.

Our investigations substantiate the findings of

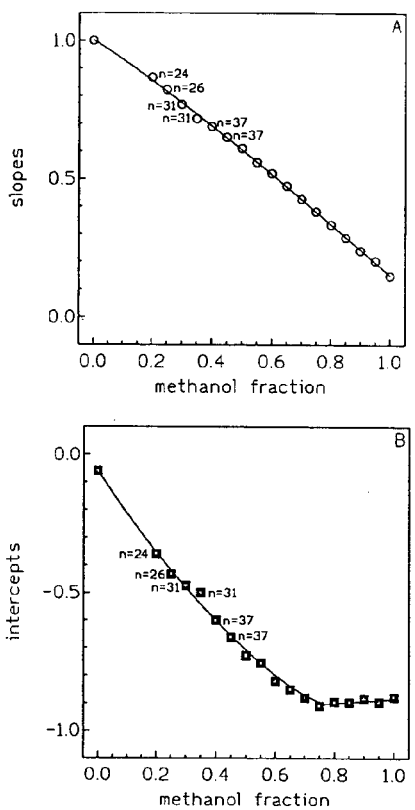

Fig. 4. (A) Slopes and (B) intercepts of the function $R_M = A \log P_{Oct} + B$, calculated for various methanol fractions φ. For $\varphi > 0.45$ up to 1.0 the number of included compounds is 65 (for further explanations, see text).

the above-mentioned workers that correlations between R_M and log P_{Oct} are optimum when using the extrapolated data (see Eqs. 15–18). With increasing methanol content the correlation coefficient decreases from 0.97 to 0.80. This decreasing interrelation is due to additional polar effects, which significantly emerge with increasing modifier content.

Fig. 4 clearly demonstrates that with decreasing modifier content the slope of Eq. 19 approximates to 1 and the intercept approximates to zero. Correspondingly, R_{Mw} and log P_{Oct} can be considered as interchangeable lipophilicity parameters. These results coincide completely with the investigations of Braumann [1] and several other workers [17,31,33] concerned with RP-HPLC. The conclusion of Braumann that log k_w has to be accepted as an *a priori* parameter for lipophilicity is identically applicable to R_{Mw} from our investigations.

3.6. Comparison between R_{Mw} and log k_w

According to our introductory remarks and the considerations detailed above, R_{Mw} and log k_w should be correlated, provided they have been measured under comparable conditions. For 25 of the test compounds studied here, log k_w values were available from the literature [1,31,34–39]. Their correlation with our R_{Mw} data gives the following equation:

$$R_{Mw} = 0.905(\pm 0.091) \log k_w + 0.246(\pm 0.298) \quad (20)$$

$$n = 25;\ s = 0.296;\ r = 0.9737;\ F = 421$$

The most discrepant compounds are 1-naphthol (**41**) and acridine (**67**), the R_{Mw} data for which are almost identical with log P_{Oct}. Omitting these two yields

$$R_{Mw} = 0.931(\pm 0.069) \log k_w + 0.111(\pm 0.229) \quad (21)$$

$$n = 23;\ s = 0.219;\ r = 0.9869;\ F = 787$$

Also in this correlation a certain trend to somewhat lower R_M as compared with log k_w emerges; nevertheless, the theoretically expected

coincidence between these parameters seems to be proved.

Correspondingly, we view RP-TLC as a feasible alternative to lipophilicity determination by HPLC. One of the major advantages of RP-TLC is its rapidity. As described in detail (see Experimental), 30 compounds can be tested simultaneously. This number can even be increased by the double use of at least some starting positions. One has only to guarantee that the compounds sharing a starting position should differ in lipophilicity by at least one unit. Lipophilicity can easily be determined ahead of time by calculating the Σf values.

3.7. Comparison between R_{Mw} and Σf

We compared our R_{Mw} data with calculated lipophilicity values using the Σf system of Rekker [11,40–42]. The correlation between R_{Mw} and the calculated data is given by

$$R_{Mw,lin} = 0.914(\pm 0.057)\Sigma f_{rev.} + 0.013(\pm 0.204) \quad (22)$$

$$n = 92;\ s = 0.444;\ r = 0.9585;\ F = 1017$$

The high interrelation, also found in this comparison, again substantiates the general applicability of R_{Mw} as a reliable lipophilicity parameter.

References

[1] T. Braumann, *J. Chromatogr.*, 373 (1986) 191.
[2] E. Tomlinson, *J. Chromatogr.*, 113 (1975) 1.
[3] K. Dross, Ch. Sonntag and R. Mannhold, *J. Chromatogr.*, 639 (1993) 287.
[4] G.L. Biagi, A.M. Barbaro, M.F. Gamba and M.C. Guerra, *J. Chromatogr.* 41 (1969) 371.
[5] E. Soczewinski and C.A. Wachtmeister, *J. Chromatogr.*, 7 (1962) 311.
[6] G.L. Biagi, M.C. Guerra and A.M. Barbaro, *J. Med. Chem.*, 13 (1970) 944.
[7] F. Geiss, *Fundamentals of Thin Layer Chromatography*, Hüthig, Basle, 1987.
[8] N.El Tayar, H. van de Waterbeemd and B. Testa, *J. Chromatogr.* 320 (1985) 293.
[9] N. Tanaka and E.R. Thornton, *J. Am. Chem. Soc.*, 99 (1977) 7300.
[10] A. Nahum and Cs. Horváth, *J. Chromatogr.*, 203 (1981) 53.
[11] K.E. Bij, Cs. Horváth, W.R. Melander and A. Nahum, *J. Chromatogr.*, 203 (1981) 65.
[12] R.F. Rekker and R. Mannhold, *Calculation of Drug Lipophilicity*, VCH, Weinheim, 1992.
[13] S.L. Bolotov, *Kontakte (Darmstadt)*, 2 (1990) 36.
[14] E.C. Bate-Smith and R.G. Westall, *Biochim. Biophys. Acta*, 4 (1950) 427.
[15] M.J. Kamlet, R.M. Doherty, M.H. Abraham, Y. Marcus and R.W. Taft, *J. Phys. Chem.*, 92 (1988) 5244.
[16] Merck, Darmstadt, personal communication.
[17] W. Butte, C. Fooken, R. Kluusmann and D. Schüller, *J. Chromatogr.*, 214 (1981) 59.
[18] S. Lehmkühler, *Statistik-Programm "Finke MediStat", Version 2.2*, 1991.
[19] P.J. Schoenmakers, H.A.H. Billiet, R. Tijssen and L. de Galan, *J. Chromatogr.*, 149 (1978) 519.
[20] R. Tijssen, H.A.H. Billiet and P.J. Schoemakers, *J., Chromatogr.*, 122 (1976) 185.
[21] J.H. Hildebrand and R.L. Scott, *The Solubility of Non-Electrolytes*, Dover, New York, 1964.
[22] J.H. Hildebrand, J.M. Prausnitz and R.L. Scott, *Regular and Related Solutions*, Van Nostrand-Reinhold, New York, 1970.
[23] N. El Tayar, H. van de Waterbeemd and B. Testa, *J. Chromatogr.*, 320 (1985) 305.
[24] C.F. Simpson, *Practical High-Performance Liquid Chromatography*, Heyden, London, 1976, pp. 81–96.
[25] J. Narkiewicz, M. Jaroniec, M. Borowka and A. Patrykiejew, *J. Chromatogr.*, 157 (1978) 1.
[26] H.J. Roth, K. Eger and R. Troschütz, *Pharmazeutische Chemie II—Arzneistoffanalyse*, Georg Thieme, Stuttgart, 1985.
[27] C. Hansch and A. Leo, *Substituent Constants for Correlation Analysis in Chemistry and Biology*, Wiley-Interscience, New York, 1979.
[28] J.C. Dearden and G.M. Bresnen, *Quant. Struct.–Act. Relat.*, 7 (1988) 133.
[29] R. Mannhold, K.P. Dross and R.F. Rekker, *Quant. Struct.–Act. Relat.*, 9 (1990) 21.
[30] N.El Tayar, H. van de Waterbeemd and B. Testa, *Quant. Struct.–Act. Relat.*, 4 (1985) 69.
[31] W.E. Hammers, G.J. Meurs and C.L. de Ligny, *J. Chromatogr.*, 247 (1982) 1.
[32] J.E. Haky and A.M. Young, *J. Liq. Chromatogr.* 7 (1984) 675.
[33] T. Braumann, H.-G. Genieser, C. Lüllmann and B. Jastorff, *Chromatographia*, 24 (1987) 777.
[34] M. Harnisch, H.J. Möckel and G. Schulz, *J. Chromatogr.*, 282 (1983) 315.
[35] D.J. Minick, D.A. Brent and J. Frenz, *J. Chromatogr.*, 461 (1989) 177.
[36] T. Braumann, G. Weber and L.H. Grimme, *J. Chromatogr.*, 261 (1983) 329.
[37] H.A. Cooper and R.J. Hurtubise, *J. Chromatogr.*, 360 (1986) 313.

[38] T.L. Hafkenscheid and E. Tomlinson, *J. Chromatogr.*, 218 (1981) 409.
[39] R.W. Ross and C.A. Lau-Cam, *J. Chromatogr.*, 370 (1986) 403.
[40] R.F. Rekker, *The Hydrophobic Fragmental Constant*, Elsevier, Amsterdam, 1977.
[41] G.G. Nys and R.F. Rekker, *Eur. J. Med. Chem.*, 9 (1974) 361.
[42] R.F. Rekker and H.M. de Kort, *Eur. J. Med. Chem.*, 14 (1979) 479.

ELSEVIER

Journal of Chromatography A, 673 (1994) 125–132

JOURNAL OF CHROMATOGRAPHY A

Field-amplified sample stacking in micellar electrokinetic chromatography for on-column sample concentration of neutral molecules

Zaiyou Liu*, Patrick Sam, Sarath R. Sirimanne, P.C. McClure, James Grainger, Donald G. Patterson, Jr.

US Centers for Disease Control and Prevention (CDC), National Center for Environmental Health, Division of Environmental Health Laboratory Sciences, Toxicology Branch, 4770 Buford Highway NE, Atlanta, GA 30341, USA

(First received December 7th, 1993; revised manuscript received February 21st, 1994)

Abstract

On-column concentration of neutral molecules was achieved for the first time in micellar electrokinetic chromatography by means of field-amplified sample stacking. The stacking process was accomplished by dissolving the neutral analytes in a low-concentration micellar solution that was still above the critical micelle concentration. The lower total ionic strength in the sample buffer compared to the electrophoresis buffer allowed the negatively charged micelles to migrate rapidly into the boundary between the sample and the running buffer where they slow down. This field-amplified sample stacking was achieved by using normal or reversed electrode polarity and produced a 75–85-fold increase in sensitivity for 1,2,4,7- and 1,2,4,8-tetrachlorodibenzo-*p*-dioxins. The peak area counts obtained from the sample stacking process were proportional to the sample volume injected, and the stacking efficiency was dependent on the micellar concentration. The best stacking efficiency was obtained when the micelle concentration was slightly higher than the critical micelle concentration. When the injection volume was relatively small, the normal-polarity stacking procedure produced a higher stacking efficiency. However, when the injection volume was large, reversed polarity produced a higher stacking efficiency because the non-uniform distribution of the electrical field strength had been eliminated.

1. Introduction

In micellar electrokinetic capillary chromatography (MEKC), a micellar pseudo stationary phase, such as sodium dodecyl sulfate (SDS) and an aqueous buffer as the mobile phase are used to separate both charged and neutral molecules. An untreated fused-silica capillary surface is negatively charged, so that the bulk electroosmotic flow is toward the negative electrode, whereas the micelles, formed from an anionic surfactant, migrate in the opposite direction, toward the positive electrode. However, when standard MEKC conditions are used with anionic micelles, the dominant electroosmotic flow still drives the negatively charged micelles toward the negative end of the capillary.

Species having the same charge as that of the micelle do not interact with the micelle, while those having the opposite charge strongly interact with the micelle. The separation of charged

* Corresponding author.

0021-9673/94/$07.00
SSDI 0021-9673(94)00211-Q

species depends on the species' difference in electrophoretic mobility. On the other hand, the formation of micelles provides a unique chromatographic process for the separation of neutral molecules, whereby solute liquid–liquid differential partitioning between the micellar pseudo stationary phase and the electroosmotically pumped aqueous phase takes place [1]. Several published articles have described applications of MEKC for the separation of neutral molecules [2–4] and of charged species [5,6]. MEKC has become a popular microcolumn separation technique because of its high separation efficiency. Isotopically substituted compounds [7] and chiral molecules [8] have been separated by MEKC when organic modifiers were added to the mobile phase.

The high resolution of MEKC requires a small sample-injection volume. Small sample volumes, however, make the detection of low-concentration samples difficult. For example, in the case of UV-absorbance detection, typical concentration limits of detection (LODs) are of the order of 10^{-6} M [9], which is inadequate for the analysis of low-concentration constituents in biological samples, such as dioxins in human serum.

Sample stacking of charged species with discontinuous buffer systems has been used extensively in many areas of electrophoresis [9–11] to enhance the sensitivity of the measurements. When a sample is dissolved in a buffer with lower electrical conductivity than that of the electrophoresis running buffer, concentration or solute stacking occurs when the sample is injected electrokinetically. Because the electrical field strength in the sample medium is higher than that in the running buffer, the electrophoretic velocity is accelerated and the ions migrate rapidly to the boundary between the lower and higher conductivity zone. At this boundary the electrophoretic velocity of the ions is reduced, and the ions stack into a narrow zone.

Field-amplified sample injection is another way of achieving on-column concentration of charged species in capillary electrophoresis. In this procedure, a small plug of water is introduced at the inlet end of the capillary prior to electrokinetic sample injection. When a high voltage is applied across the capillary, a higher electric field strength is established across the water plug. Because the electroosmotic velocity of the bulk solution is slower than the electrophoretic velocity of the sample ions under the enhanced field strength, both positive and negative ions can be concentrated by switching the electrode polarity at the proper time [12]. Field-amplified sample injection can also be achieved by directly injecting low-conductivity sample buffers without using the water plug [13]. Researchers have shown that with this technique concentration-detection sensitivity can be increased several hundred fold [13].

In capillary electrophoresis, charged species have been shown to stack when extremely large injection volumes are used and when the sample buffer is pumped electroosmotically from the capillary while the stacking is in progress [14]. Although sample stacking can be effective for both positively and negatively charged species at high electroosmotic velocity or by polarity switching, neutral molecules are not affected by these techniques. In this report, we present a simple technique for on-column sample concentration of neutral molecules by using field-amplified sample stacking in MEKC media.

The dominant electroosmotic velocity of the buffer solution and the dragging force of the micelles in MEKC provide an excellent opportunity for stacking neutral molecules. To do so, we took a sample plug containing neutral molecules in a lower-conductivity micellar solution with the same surfactant as in the running buffer and introduced this plug hydrodynamically into the capillary filled with running buffer. Under high voltages, a higher electrical-field strength was established across the sample plug because of its higher resistivity. Stacking occurred when neutral molecules which were partitioned into the negatively charged micelles migrated rapidly into the boundary between the sample and the running buffer and slowed down. Using reversed electrode polarity during the sample stacking process, we were able to eliminate the non-uniform distribution of the electrical field by backing the sample buffer out of the capillary.

2. Experimental

An electrophoresis system similar to that described by Jorgenson and Lukacs [15] was constructed in our laboratory. The high-voltage power supply (0–60 kV) was from Glassman High Voltage (Whitehouse Station, NJ, USA). The high-voltage power supply can be configured to output either positive or negative voltages. Two power supplies configured with opposite polarity were used when reversed-electrode-polarity sample stacking was performed. Each end of the electrophoretic capillary was placed in a small glass reservoir containing the appropriate buffer and a platinum electrode connected to the power supply. The two reservoirs must be level for normal running conditions. A CV^4 UV detector from Isco (Lincoln, NB, USA) was operated at 230 nm, and the UV absorbance was recorded by a Shimadzu C-R3A integrator (Kyoto, Japan). The current running through the capillary was monitored on a chart recorder. An on-column optical detection cell was created by removing the polyimide coating from a short segment of the fused-silica capillary (10 cm from one end). The system, except for the detector and the integrator, was enclosed in a Plexiglass box with an interlock switch to protect analysts from high voltages. Timing and switching of the applied high voltage were accomplished by using a timer and a high-voltage relay, which was enclosed in a lead-impregnated plastic box to protect the operator.

Fused-silica capillary columns (50 μm I.D. × 360 μm O.D.) were purchased from Polymicro Technologies (Phoenix, AZ, USA) and used without surface modification. The total length of the capillary was 75 cm with an effective length of 65 cm. Ultrapure SDS was from Life Technologies (Gaithersburg, MD, USA). The 1,2,4,7- and 1,2,4,8-tetrachlorodibenzo-*p*-dioxins (TCDDs) used to characterize the stacking process were synthesized in our laboratory [16]. The polycyclic aromatic hydrocarbons (PAHs) were obtained from Aldrich (Milwaukee, WI, USA). All running and sample buffers were prepared with distilled water and filtered through a 0.45-μm disk filter (Alltech, Deerfield, IL, USA).

Sample injections were performed in one of two ways. When a very short injection band was desired (as in the case of a normal MEKC run without field-amplified sample stacking), the sample vial was placed 25 cm above the level of the buffer reservoir. The inlet end of the capillary was then inserted into the sample vial for a predetermined amount of time. An injection band length of approximately 0.2 cm was obtained with a 10-s injection. A 5-s injection resulted in an injection volume of approximately 2 nl. If a longer injection band was needed, a pressure of 10 p.s.i. (1 p.s.i. = 6894.76 Pa) was applied in the sample reservoir. With this method, we produced a rapid injection of various sample volumes onto the capillary by varying the injection time.

Sample stacking under reversed electroosmotic flow was monitored by measuring the electrical current through the capillary. Before the sample was introduced, the current through the capillary filled with the running buffer was measured. After the sample was introduced, the current decreased because of the lower electrical conductivity of the sample buffer. As the sample buffer was pumped out of the capillary by the reversed electroosmotic flow, the current increased gradually until it reached the initial measured value. At this point, the electrode polarity was set back to the normal configuration for the MEKC separation.

3. Results and discussion

Fig. 1 is a schematic diagram showing the field-amplified sample-stacking process under normal and reversed electrode polarity. Fig. 1A shows the stacking process being carried out with the same electrode polarity as in the separation process. The injected sample plug contains neutral molecules and a lower concentration of SDS than the running-buffer SDS concentration. In the sample buffer, no electrolytes were added, so the electrical conductivity was much lower than that in the running buffer region. The neutral molecules incorporated into the negatively charged micelles experienced a much higher

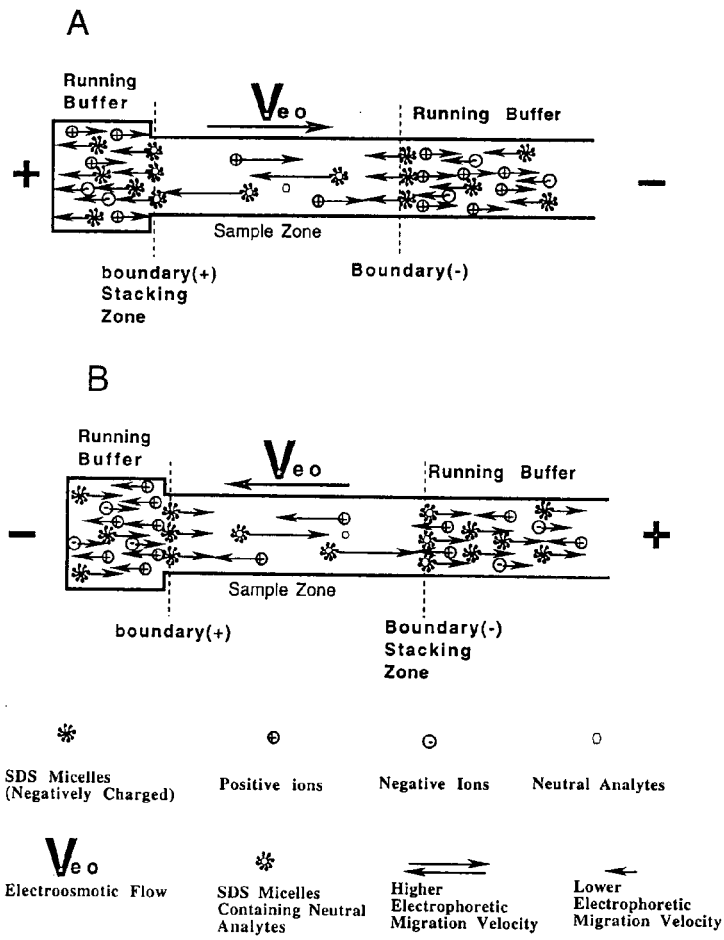

Fig. 1. Schematic diagrams showing the field-amplified sample-stacking process under normal (A) and reversed (B) electrode polarity.

electrical field strength and migrated rapidly toward the positive electrode. Their migration velocity was reduced when they encountered the boundary region where the electrical field strength was low. Therefore, the neutral molecules in the sample and running buffer boundary region were stacked toward the positive end of the electrical field across the sample zone. Since the bulk electroosmotic velocity (V_{eo}) was higher than the micelles electrophoretic migration velocity, the stacked sample zone migrated toward the negative electrode.

When a large volume of sample was introduced, the sample buffer had to be eliminated during stacking because a non-uniform distribution of the electrical field strength caused by the presence of the sample plug would deteriorate the chromatographic resolution. As depicted in Fig. 1B, neutral molecules in the sample can be stacked and buffer can be backed out of the capillary simultaneously by reversing the electrode polarity. This reversed polarity provides a possible procedure for introducing extremely large sample volumes into the capillary. In this

configuration, the neutral molecules incorporated within the negatively charged micelles are stacked toward the positive electrode while the direction of the bulk electroosmotic flow (V_{eo}) is reversed. The reversed electroosmotic flow causes the sample buffer to be pumped out the inlet end of the capillary while the stacking process is in progress. The stacking will be most efficient (higher number of theoretical plates) for neutral analytes with high partition coefficients into the micelles. On the other hand, neutral analytes with very low partition coefficients will be pumped out of the capillary under reversed electrode polarity.

The difference in migration velocity of micelles within the sample and the running buffer is the key to achieving the stacking effect in MEKC. As shown in Fig. 2, no stacking occurs when the sample buffer and the running buffer are the same. Chromatograms A and B in Fig. 2 were obtained by injecting 108 nl of the sample into a 65 cm × 50 μm I.D. capillary. The sample shown in Fig. 2A was prepared by using the running buffer as the sample solvent. Because the electrical conductivity of the sample buffer was identical to that of the running buffer, there was no field enhancement, and sample stacking did not occur. The injected sample plug was not compressed, and it eluted as a square-shaped peak because of the extended length of the injection plug (5.5 cm). Under these conditions, reversed electrode polarity backed out the sample plug without stacking of the analytes. In contrast, when the sample was prepared in a lower-concentration SDS solution, the initial sample band was compressed by both normal- and reversed-polarity sample-stacking processes. The injection volume shown in Fig. 2B is the same as that in Fig. 2A. In Fig. 2B, however, the sample was prepared in a 9 m*M* SDS solution, and the resulting sample zone was compressed by a factor of approximately 4.

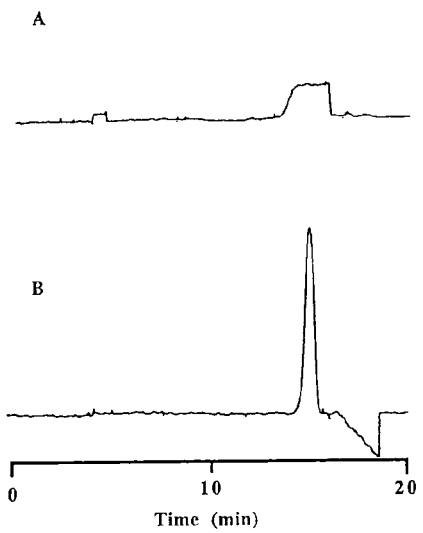

Fig. 2. Chromatograms obtained by using different sample buffers. (A) The running buffer consisted of 20 m*M* sodium phosphate, 40 m*M* SDS, and had a pH of 8.5; the sample buffer was the same as the running buffer. (B) Reversed-electrode-polarity sample stacking was performed using the running buffer shown in (A); the sample buffer was 9 m*M* SDS. The injection volume was 108 nl, applied voltage was 25 kV for both (A) and (B). Solutes were 1,2,4,7- and 1,2,4,8-TCDDs in both cases.

The three chromatograms in Fig. 3 show MEKC results following a normal injection and following field-amplified sample stacking under normal and reversed electrode polarity. Sample stacking allows a sample of relatively large volume to be injected without a significant effect on the chromatographic resolution. The UV response of the analyte was increased with either normal (Fig. 3B) or reversed (Fig. 3C) electrode polarity field-amplified stacking than with the non-stacking signal in Fig. 3A. As shown by the peak widths in Fig. 3B and C, at an injection volume of 32 nl, field-amplified sample stacking with the normal electrode polarity produced a higher stacking efficiency than reversed electrode polarity. This increased efficiency is due to the insignificant disturbance in the distribution of the electrical field strength across the capillary caused by the presence of a short sample plug (1.6 cm). The lower stacking efficiency for the reversed electrode polarity procedure (Fig. 3C) is not due to the sample buffer backing out from the injection end of the capillary but rather to the reversal of the electroosmotic flow during the stacking and the separation processes. The current laboratory-built system requires more than 1

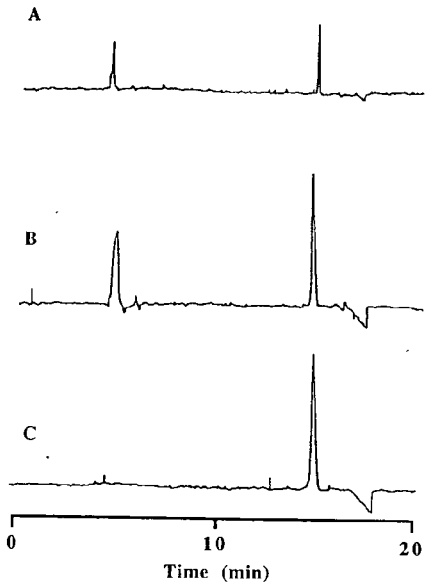

Fig. 3. Comparison chromatograms obtained with and without field-amplified sample stacking. Running buffer as in Fig. 2. The sample buffer was 9 m*M* SDS in all cases. Separation was carried out at 25 kV. (A) Gravity injection of 2 nl. (B) Pressure injection of 32 nl with normal-electrode-polarity sample stacking. (C) Pressure injection of 32 nl with reversed electrode polarity during sample stacking. Solutes were 1,2,4,7- and 1,2,4,8-TCDDs in all cases.

min to reverse the electrode polarity which allows additional time for peak diffusion and mixing effects to occur.

Fig. 3B and C show one advantage of using reversed electrode polarity during sample stacking to back out the sample buffer. The positive response at 4 min in Fig. 3B (which was due to the presence of the sample buffer) was not seen in Fig. 3C. The negative response in the chromatograms (Figs. 2B and 3B and C) after the analyte peak was caused by the excessive accumulation of SDS, which in turn was due to charge balance requirements.

We evaluated the stacking efficiency by measuring the theoretical plates at various injection volumes under both normal and reversed electrode polarity (Fig. 4). The highest stacking efficiency was obtained for a 2-nl injection volume. The stacking efficiency decreases with

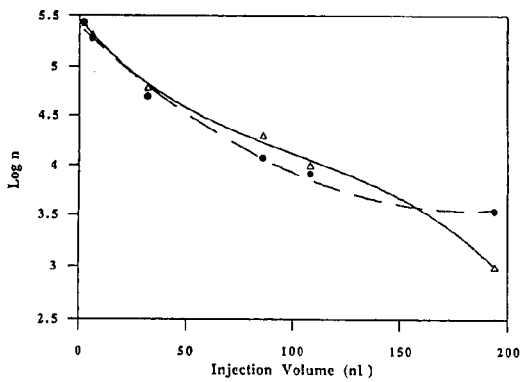

Fig. 4. Relationship between stacking efficiency and sample injection volume at different electrode polarities. Conditions as in Fig. 3B and C. The solid line is for normal electrode polarity, and the dashed line is for reversed electrode polarity. n = Number of theoretical plates.

increasing injection volumes (Fig. 4). At injection volumes smaller than 160 nl (8.2 cm injection band length) but greater than approximately 80 nl, normal electrode polarity gave a higher stacking efficiency even though the presence of the sample buffer, which is approximately 11 to 5.5% of the total length of the capillary, caused a non-uniform distribution of the electrical field. However, the extra peak-broadening effect caused by the reversal of the electrode polarity during the reversed electroosmotic flow had a greater negative effect on the resolution for injection volumes greater than 80 nl but less than 160 nl. When the injection volume was less than about 80 nl, the observed difference in stacking efficiency was marginal. However, when the injection volume was greater than 160 nl, the non-uniform electrical field distribution due to the longer injected band length caused the reversed-electrode-polarity method to give a higher stacking efficiency (Fig. 4). The actual value of the injection volume at which these two effects are equal needs to be experimentally determined for a particular chromatographic system. Depending on the injection volume, one can select whichever of the two modes for sample stacking that provides higher stacking efficiency.

We studied the effect of the micelles con-

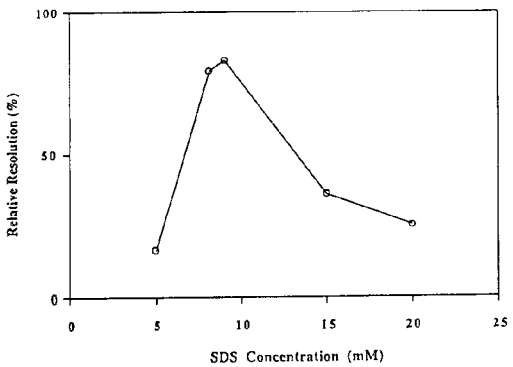

Fig. 5. Effect of SDS concentration on stacking efficiency. Conditions as in Fig. 3C. Injection volume was 32 nl. Resolution was normalized to the resolution obtained at 2 nl injection without stacking.

centration on the stacking efficiency over a range of SDS concentrations, and the results are summarized in Fig. 5. The first data point at a SDS concentration of 5 m*M* is below the critical micelle concentration; field-amplified sample stacking does not occur at this level. As expected, the best sample-stacking efficiency was obtained when the SDS concentration was at, or slightly higher than, its critical micelle concentration (8.1 m*M*). The electrical conductivity of the sample buffer increased with the increase of the SDS concentration. The stacking efficiency was proportional to the field-enhancement factor, which has been defined as the ratio of the electrical field strength of the running buffer to that of the sample buffer in capillary electrophoresis [17]. As shown in Fig. 5, this proportionality seemed true for MEKC measurements when field-amplified sample stacking was used, since the electrophoretic velocity of the micelles was proportional to the electrical field strength, which is in turn proportional to the stacking efficiency.

We also conducted a calibration experiment to determine the peak area counts over a range of injection volumes from 2 to 194 nl (Table 1). The peak area was proportional to the sample volume injected for both polarity configurations in the stacking process. We obtained regression coefficients of 0.9897 for normal electrode polarity and 0.9961 for reversed electrode polarity. The sensitivity for 1,2,4,7- and 1,2,4,8-TCDDs

Table 1
Calibration of peak area counts against injection volume for 1,2,4,7- and 1,2,4,8-TCDDs

Injection volume (nl)	Band length (cm)	Peak area (counts)	
		Normal	Reversed
2	0.10	3 266	3 266
6	0.31	8 063	8 250
32	1.63	36 550	46 298
86	4.38	82 125	126 690
108	5.50	140 740	152 310
194	10.0	271 220	243 490
r		0.9897	0.9961
S_a		9771	5564
S_b		99.6	56.7
Maximum sensitivity enhancement factor		75	85

Conditions: the running buffer consisted of 20 m*M* sodium phosphate and 40 m*M* SDS at pH 8.5; sample buffer consisted of 9.0 m*M* SDS; capillary was 65 cm × 50 μm I.D. untreated fused silica; 25 kV was used for both stacking and separation processes. S_a and S_b are the standard error of the regression on the intercept and the slope, respectively.

under the conditions outlined in Table 1 was increased by a factor of 75 to 85 for the two stacking processes.

Fig. 6 shows the separation of a mixture of 16 PAHs using cyclodextrin-modified MEKC. A normal 2-nl injection of the low-concentration PAH standard solution shown in Fig. 6A produced very small peaks for only three of the PAHs. A 54-nl injection of the same low-concentration standard using normal-electrode-polarity sample stacking conditions produced a significant sensitivity enhancement while maintaining high chromatographic resolution (Fig. 6B).

In conclusion, during MEKC neutral molecules can be effectively concentrated on-column by field-amplified sample stacking. The stacking process can be performed in either normal or reversed electrode polarities depending on the injection volume. For a small injection volume (smaller than 160 nl) with an SDS concentration of 9 m*M* in the sample buffer, the use of normal electrode polarity during the sample-stacking process gives better stacking efficiency. For volumes of greater than 160 nl at the same SDS concentration, however, the use of reversed electrode polarity during the sample-stacking process provides a higher stacking efficiency. Because reversed polarity allows large sample volumes to be injected, the concentration detection limits for neutral molecules can be significantly improved.

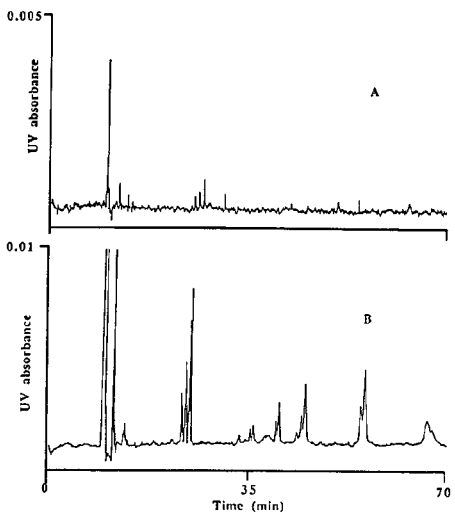

Fig. 6. MEKC chromatograms of a PAH mixture with and without field-amplified sample stacking: (A) 2-nl injection (0.005 absorbance range setting); (B) 54-nl injection (0.01 absorbance range setting) with normal electrode-polarity sample stacking. Conditions: The running buffer consisted of 100 m*M* sodium borate, 100 m*M* SDS, 5 *M* urea and 10 m*M* γ-cyclodextrin, and had a pH of 9.0. The sample buffer consisted of 9 m*M* SDS. The applied voltage was 27 kV.

4. References

[1] S. Terabe, K. Otsuka, K Ichikawa, A. Tsuchiya and T. Ando, *Anal. Chem.*, 56 (1984) 111.
[2] T. Imasaka, K. Nishitani and N. Ishibashi, *Anal. Chim. Acta*, 256 (1992) 2.
[3] S. Terabe, Y. Miyashita, O. Shibata, E.R. Barnhart, L.R. Alexander, D.G. Patterson, Jr., B.L. Karger, K. Hosoya and N. Tanaka, *J. Chromatogr.*, 516 (1990) 23.
[4] J. Cai and Z. El Rassi, *J. Chromatogr.*, 608 (1992) 31.
[5] J. Liu, J.F. Banks and M. Novotny, *J. Microcol. Sep.*, 1 (1989) 136.
[6] K.H. Row, W.H. Griest and M.P. Maskarinec, *J. Chromatogr.*, 409 (1987) 193.
[7] M.M. Bushey and J.W. Jorgenson, *J. Microcol. Sep.*, 1 (1989) 125.
[8] H. Nishi, T. Fukuyama and S. Terabe, *J. Chromatogr.*, 553 (1991) 503.
[9] M. Albin, P.D. Grossman and S.E. Moring, *Anal. Chem.*, 65 (1993) 489A.
[10] R.-L. Chien and D.S. Burgi, *Anal. Chem.*, 64 (1992) 489A.
[11] R. Aebersold and H.D. Morrison, *J. Chromatogr.*, 516 (1990) 79.
[12] R.-L. Chien and D.S. Burgi, *J. Chromatogr.*, 559 (1991) 141.
[13] R.-L. Chien and D.S. Burgi, *J. Chromatogr.*, 559 (1991) 152.
[14] R.-L Chien and D.S. Burgi, *Anal. Chem.*, 64 (1992) 1046.
[15] J.W. Jorgenson and K. Lukacs, *Anal. Chem.*, 53 (1981) 1928.
[16] L.T. Gelbaum, D.G. Patterson, Jr., D.F. Groce and D. Ashley, *Chemosphere*, 17 (1988) 551.
[17] D.S. Burgi and R.-L. Chien, *Anal. Chem.*, 63 (1991) 2042.

ELSEVIER

Journal of Chromatography A, 673 (1994) 133–141

JOURNAL OF CHROMATOGRAPHY A

Short Communication

Imprinted dispersion polymers: a new class of easily accessible affinity stationary phases

Börje Sellergren*

Department of Analytical Chemistry, University of Lund, P.O. Box 124, S-221 00 Lund, Sweden

(First received January 24th, 1994)

Abstract

Non-stabilizing dispersion polymerization in combination with molecular imprinting was used to prepare agglomerates of globular micron-sized particles exhibiting molecular recognition properties. These could be prepared either *in situ* in a chromatographic column or separately followed by wet or dry packing of the material. This allowed a rapid chromatographic evaluation of the molecular recognition properties of the materials. Depending on the monomer concentration and the solvency of the dispersion medium the particle dispersity, the degree of particle agglomeration and the average particle size varied. The choice of dispersion medium was mainly dictated by the template solubility and the nature of the interactions between the functionalized monomers (methacrylic acid) and the template used for producing the molecular recognition sites. Addition of water to the dispersion medium allowed imprinting of the poorly soluble template pentamidine (PAM), a drug used for the treatment of AIDS-related disorders. The PAM-imprinted materials prepared *in situ* in the chromatographic column strongly retained the drug in the chromatographic evaluation compared to the retention of PAM on a reference material prepared using benzamidine as template (separation factor $\alpha' = 6.8$). Meanwhile weakly or moderately basic templates from the group nucleotide bases (tri-O-acetyladenosine), herbicides (atrazine) and chiral amino acid derivatives (L-phenylalanine anilide) required low temperature and exclusion of water during imprinting in order to produce the recognition effect.

1. Introduction

In the medical and environmental fields the analysis or isolation of target molecules in complex mixtures is often achieved by the use of biological macromolecules. Immunoassays [1] and affinity chromatography [2] are techniques based on the high selectivity and affinity of antibodies and enzymes towards their antigens and substrates. The biomolecules of these systems often suffer from poor stability and a complicated preparation scheme. Imprinted polymers capable of molecular recognition but without these shortcomings constitute an interesting alternative. These materials are prepared by molecular imprinting [3–10] whereby functional monomers, preorganized around a template molecule, are copolymerized in homogeneous solution with a cross-linking monomer leading to the formation of a highly cross-linked

*Present address: Department of Inorganic and Analytical Chemistry, Johannes Gutenberg University Mainz, Joh.-Joachim-Becherweg 24, D-55099 Mainz, Germany.

0021-9673/94/$07.00
SSDI 0021-9673(94)00310-6

network polymer. After washing out the template the materials can be used as affinity stationary phases in the chromatographic mode. Strong, highly selective binding has been observed for enantiomers of basic compounds [4–8], for nucleotide bases [9] and for commercial drugs [7,10].

The imprinted polymers are usually obtained as blocks that need to be ground and sieved before use. This results in irregular particles, poor chromatographic performance and a loss of unsized material. Following a general procedure developed by Svec and Fréchet [11] describing *in situ* prepared continuous rods of macroporous polymer as HPLC separation medium, Matsui *et al.* [12] showed a way to circumvent these difficulties by preparing columns of flow through continuous rods of imprinted polymers. Independently of their work we have developed a dispersion polymerization procedure for *in situ* preparation of imprinted affinity phases in aqueous or polar media [13,14] (dispersion polymerization is defined as a modified precipitation polymerization where the monomer but not the polymer is soluble in the dispersion medium and where well defined polymer particles are formed. Addition of a stabilizer results in the formation of spherical particles of a low dispersity) [15,16]. The resulting materials consist of agglomerates of micron-sized globular particles (Fig. 1) with a microporous (Fig. 1a, b) or mesoporous (Fig. 1c, d) morphology. In analogy with the acrylamide-based materials developed by Hjertén [17] our materials can be prepared *in situ* in a chromatographic column or dispersed separately for column packing by conventional techniques. The resulting columns are stable, they have a low flow resistance and are able to selectively retain the complementary substrate.

2. Experimental

2.1. Chemicals

Phenylalanine (D and L) anilide (PA) were synthesized as described elsewhere [4] whereas tri-O-acetylcytidine (TAC) and the template tri-O-acetyladenosine (TAA) were purchased from Sigma. Pentamidine (PAM) as the isethionate salt was a generous gift from Rhone Poulenc Pharma (Helsingborg, Sweden), the reference benzamidine (BAM) was purchased from Aldrich as the hydrochloride and atrazine (ATR) was purchased from Janssen Chimica. The monomers ethyleneglycoldimethacrylate (EDMA) and methacrylic acid (MAA) (Fig. 2) and the initiator azo-bisisobutyronitrile (AIBN) were all purchased from Aldrich and purified following standard procedures [8]. PAM isethionate was converted to the free base by basifying an aqueous solution (K_2CO_3) of the drug and collecting the hereby formed precipitate. Purification was done by redissolving the precipitate in EtOH, filtration of the EtOH solution and finally evaporation giving PAM as a white solid. BAM–HCl was converted to its free base by extraction into ethyl acetate.

2.2. Polymer preparation

The polymers were prepared using the monomer compositions and solvents indicated in Table 1. As a typical example the preparation of **P5**–PAM (Fig. 2) is described: PAM (0.125 mmol) in the free base form was dissolved in isopropanol (2.8 ml) and EDMA (12 mmol). Addition of MAA (0.5 mmol) caused formation of a precipitate which went back into solution by the addition of water (1.3 ml). Initiator (AIBN, 12 mg) in isopropanol (0.5 ml) was added and the solution purged with nitrogen and heated to 40°C for homogenization. The solution was then transferred under nitrogen to glass tubes (150 mm × 5 mm O.D. × 3 mm I.D.), the tubes sealed and left in an oven at 60°C for 24 h. The remaining polymers were prepared by photoinitiation [8] at 5°C using a Beamboost photolytic reaction chamber except for **P4** where a Hg medium pressure lamp was used.

2.3. Chromatographic evaluation

The tubes containing polymer were cut to a length of 140 mm and equipped with Valco column end fittings containing Vespel ferrules. Alternatively the material could be dispersed in

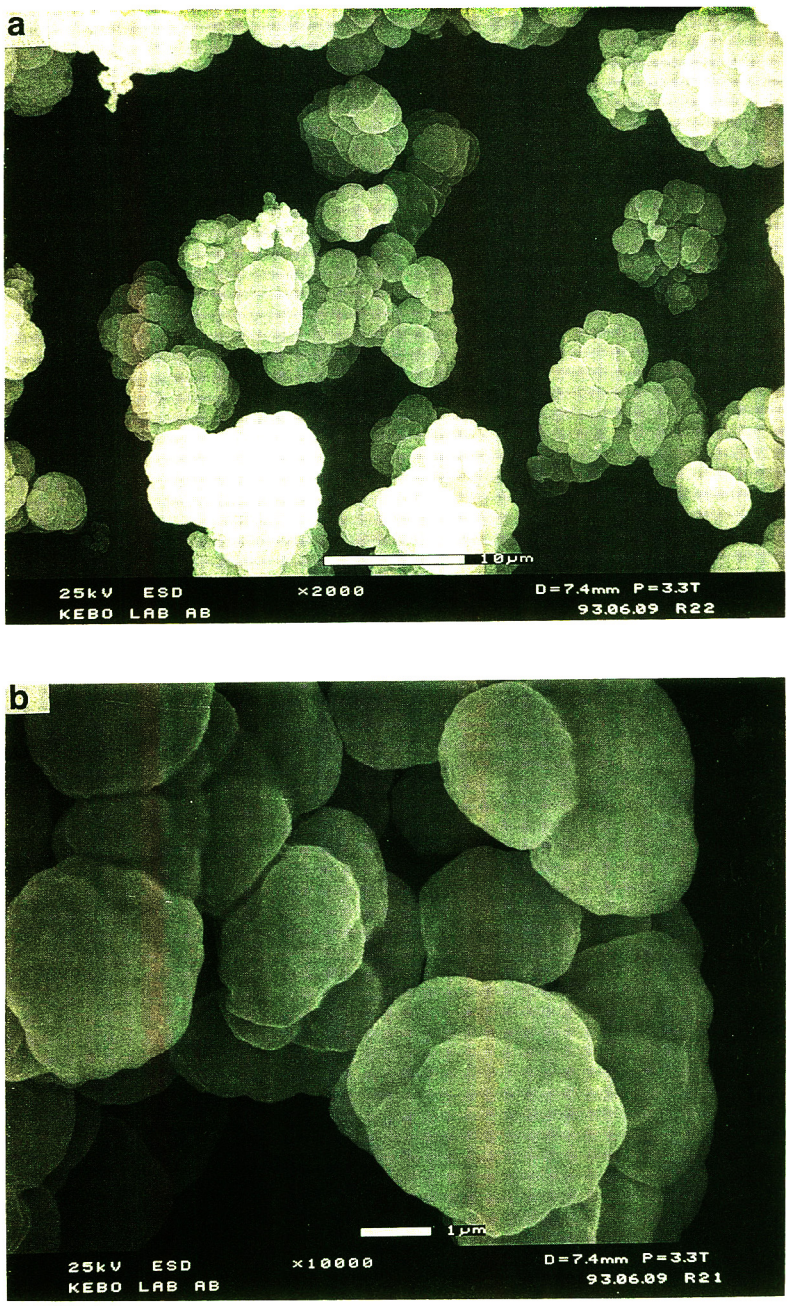
a
10μm
25kV ESD
KEBO LAB AB
×2000
D=7.4mm P=3.3T
93.06.09 R22
b
1μm
25kV ESD
KEBO LAB AB
×10000
D=7.4mm P=3.3T
93.06.09 R21

Fig. 4.

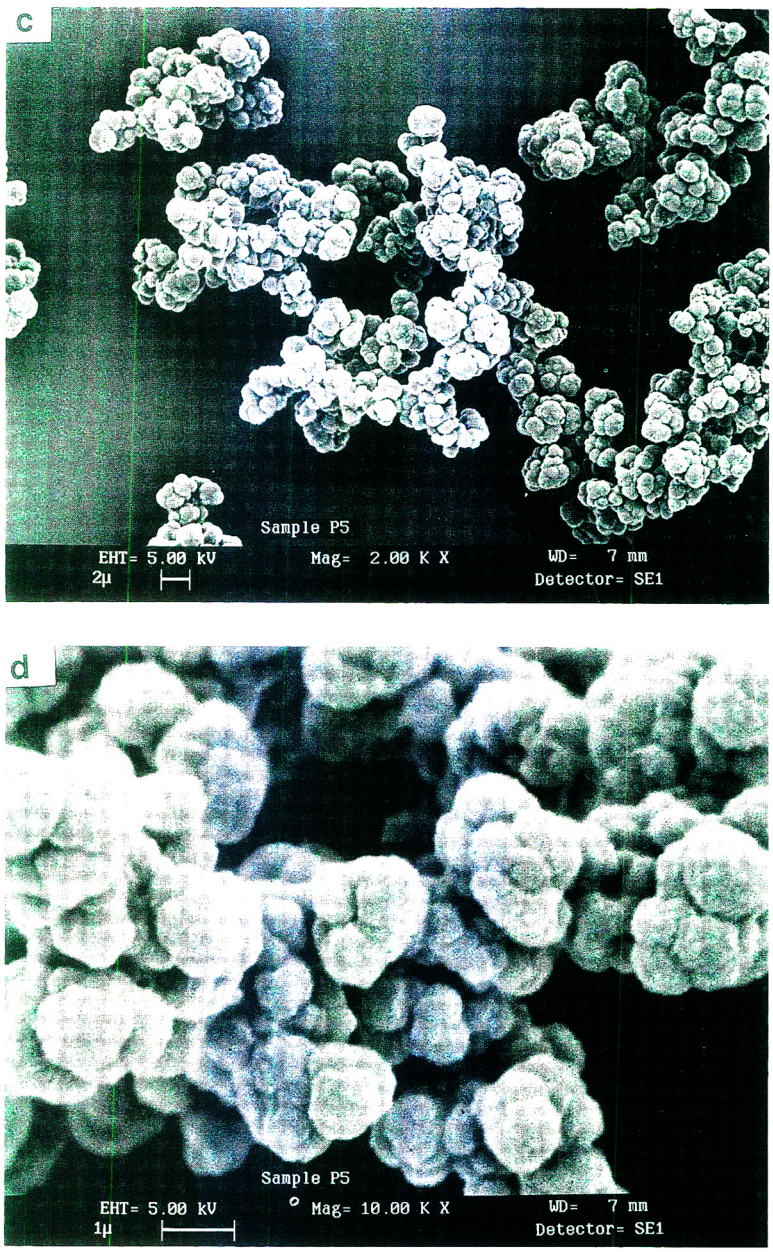

Fig. 1. Scanning electron micrographs of **P5**—PAM (a, b) and **P3**–LPA (c, d). Magnification: (a) 2000 × (Electroscan ESEM); (b 10 000 × (Electroscan ESEM); (c) 2000 × (Leica Stereoscan 420); (d) 10 000 × (Leica Stereoscan 420).

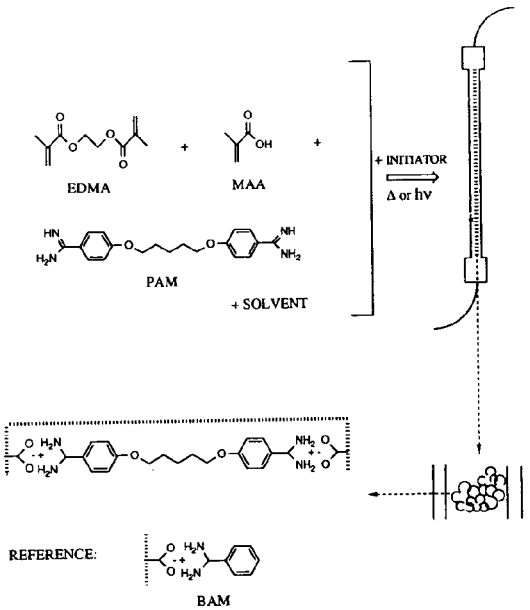

Fig. 2. *In situ* polymer preparation.

ethanol by sonication followed by a traditional column slurry packing. **P1** however was ground and sieved prior to packing. The columns were connected to a simple HPLC equipment and at least 10 ml of EtOH or MeCN–potassium phosphate buffer 0.05 *M*, pH 2 (7:3, v/v) (only for **P5**) was passed at flow-rates giving a back pressure of less than 1500 p.s.i. (1 p.s.i. = 6894.76 Pa). In the initial eluate extracted template was detected by TLC analysis. Due to some compression of the column bed the inlet end fitting was removed and the tube cut to a length of 100 mm. After reconnecting the column MeCN–potassium phosphate buffer 0.05 *M*, pH 5 (7:3, v/v) [in **P4**: MeCN–water (95:5, v/v)] was passed at a flow-rate of 0.3 ml/min until a stable baseline was attained. Substrate or reference (2 nmol in 20 μl eluent) was injected and the elution profile monitored by UV absorption at 270 nm (254 nm for D,L-PA).

3. Results and discussion

The procedure applied for the preparation of a material capable of recognizing PAM, a DNA-binding drug used in the treatment of AIDS-related disorders [18], is outlined in Fig. 2 (see Experimental section and Table 1 for details). Template, monomers (EDMA and MAA) and solvents are simply mixed and homogenized at elevated temperature. After addition of initiator (AIBN) the solution is transferred to a glass column and the polymerization carried out at elevated temperature. The column can then be directly connected to the HPLC equipment and rapidly evaluated. The retention of PAM and the reference BAM on a PAM (**P5**–PAM) and a BAM (**P5**–BAM) column were compared in an organic–aqueous mobile phase. While at pH 2 both compounds eluted essentially with the void volume, *at pH 5 PAM was 7 times more retained on the PAM- than on the BAM- column* (Fig. 3 and Table 2). BAM on the other hand showed a weaker pH dependence and was equally retained on both columns. The PAM column thus exhibits a pronounced selectivity for PAM whereas the BAM column did not appear to recognize BAM. This can be explained considering the number of potential interaction sites that the templates contain towards MAA. While PAM should be present as a bis-methacrylate ion pair (Fig. 2) BAM can only form a 1:1 complex with MAA prior to polymerization. In the complementary polymer PAM will thus be able to bind to the sites by two strong ion-pair interactions, each worth approximately the same in energy as the one ion-pair interaction that is possible between BAM and its complementary site [19]. The difference between the respective binding constants can in such cases amount to several orders of magnitude.

The fact that polymers imprinted with other basic templates, chosen from the group of nucleotide bases (TAA), herbicides (ATR) and chiral compounds (L-PA), also showed molecular recognition properties (Table 2) indicates that the technique may have broad applicability. However, the chiral separation factors (α) of the L-PA imprinted polymers are lower than those previously observed. This is related to the use of low monomer concentrations (compare α of **P1** and **P2**) and strongly hydrogen bonding solvents in the imprinting step [8]. According to our previous investigation [8], of the influence of

Table 1
Polymer preparation and characterization

Polymer[a]	Solvent[b]	EDMA (%)[c]	Monomer (%)[c]	Swelling (ml/ml)[d]	Particle size (μm)[e]	Bulk density (g/ml)[f]	Surface area (m^2/g)[g]	Pore diameter (Å)[g]	Pore volume (ml/g)[g]
P1–L-PA	1	80	40	1.25	<<1 sc	0.19	132	169	0.46
P2–L-PA	1	80	20	1.20	0.5–2	0.21	18	148	0.044
P3–L-PA	2	80	20	1.20	1–2	0.32	36	100	0.050
P3–ATR	2	80	20	1.20	1–2	0.28	43	92	0.078
P3–BL	2	80	20	1.20	1–2	0.28	19	114	0.041
P4–TAA	1	80	20	1.13	0.5–1	0.34	22	317	0.104
P4–BL	1	80	20		0.5–1		18	170	0.060
P5–PAM	3	96	33	1.00	2–4	0.51	210 (150)	22[h]	0.039 (0.066)
P5–BAM	3	96	33	1.05	2–4	0.49	181 (125)	25[h]	0.045 (0.055)
P6–L-PA	1	80	14	1.25	0.5–2	0.13	18	144	0.053
P7–BL	4	80	20	n.d.	<1 sc	n.d.	n.d.	n.d.	n.d.
P8–BL	1	100	20	n.d.	0.5–1	n.d.	n.d.	n.d.	n.d.

See Experimental section for details on the polymer preparation. n.d. = Not determined.

[a] Polymers that are different only in the template used during polymerization have been indicated with the same number. The templates are indicated after the polymer number (absence of template is indicated as BL = blank).

[b] 1 = Cyclohexanol–dodecanol (4:1, v/v); 2 = cyclohexanol; 3 = isopropanol–water (5:2, v/v); 4 = acetonitrile.

[c] EDMA (%) = Mol percent EDMA present in the monomer mixture with MAA beeing the other monomer. Monomer (%) = volume of monomers/(volume of monomers + volume of solvent).

[d] (Volume swollen polymer)/(volume dry polymer) in MeCN determined as described elsewhere [8].

[e] Approximate range in particle size and degree of agglomeration as judged from scanning electron micrographs (Fig. 1). sc = Strongly coagulated particles where the material had to be crushed before use.

[f] Determined as described elsewhere [8].

[g] Results from nitrogen adsorption using a Micromeritics ASAP 2000 covering pores between 17 and 3000 Å. The samples were degassed at 150°C and an 80-point pressure table was used with a 10-s equilibration time. The surface area was determined from a BET plot, the average pore diameter and the cumulative pore volume using the BJH model on the adsorption isotherm and the micropore surface area and pore volume (values in parentheses) from a *t*-plot using Harkins–Jura average thickness [8].

[h] Pore diameter calculated from the BET plot.

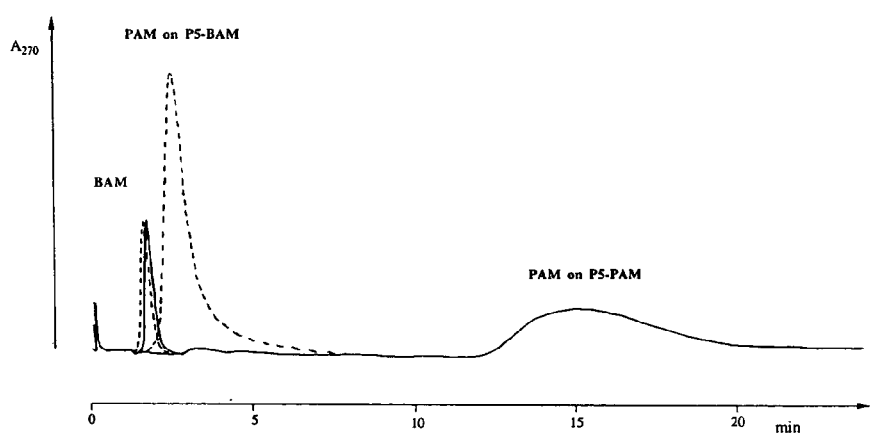

Fig. 3. Elution profiles of PAM and BAM (2 nmol) injected separately on a PAM-imprinted (**P5**–PAM) (solid line) and a BAM-imprinted (**P5**-BAM) (broken line) dispersion polymer prepared *in situ* in a chromatographic column. Mobile phase: MeCN–potassium phosphate buffer, 0.05 *M*, pH 5 (7:3, v/v). Flow-rate: 0.3 ml/min. For other details see Table 2.

Table 2
Chromatographic evaluation of imprinted dispersion polymers

Polymer[a]	Substrate[b]	Reference[b]	Retention[c] k'_{sub}	Separation factor[d] $\alpha(=k'_{sub}/k'_{ref})$
P1–L-PA	LPA	DPA	1.938	2.21
P2–L-PA	LPA	DPA	3.182	1.17
P3–L-PA	LPA	DPA	1.727	1.36
P3–ATR	ATR	DDC	1.243	2.64 (1.3)
P3–BL	ATR	DDC	0.888	2.00
P4–TAA	TAA	TAC	3.000	4.40 (4.2)
P4–BL	TAA	TAC	0.500	1.05
P5–PAM	PAM	BAM	16.0	54 (6.8)
P5–BAM	PAM	BAM	2.294	7.91

[a] The glass columns (150 mm × 5 mm O.D. × 3 mm I.D.) containing polymer were connected to a simple HPLC equipment and at least 10 ml of EtOH or MeCN–potassium phosphate buffer 0.05 *M*, pH 2 (7:3, v/v) (only for **P5**) was passed at 5 ml/min. The flow-rates and back pressures were: **P1**–L-PA: packing: 5 ml/min, < 1000 p.s.i.; **P2**–L-PA: packing: 5 ml/min, < 1000 p.s.i., run in MeCN: 1 ml/min, 250 p.s.i.; **P3**–L-PA: run in MeCN–water–HOAc (94:5:1, v/v/v): 9 ml/min, < 1000 p.s.i.; **P4**–TAA and **P4**–BL: run in MeCN–water (95:5, v/v): 0.1 ml/min, 360 and 630 p.s.i., respectively; **P5**–PAM and **P5**–BAM: packing: 4 ml/min, 643 and 571 p.s.i., respectively. MeCN–potassium phosphate buffer 0.05 *M*, pH 5 (7:3, v/v) [in **P4**: MeCN–water (95:5, v/v)] was then passed at a flow-rate of 0.3 ml/min until a stable baseline was attained.

[b] Substrate (sub) or reference (ref) [TAC = tri-O-acetylcytidine (HCl salt), DDC = dideoxycytidine] (2 nmol in 20 μl eluent) was injected and the elution profile monitored by UV absorption at 270 nm (254 nm for D,L-PA).

[c] Capacity factor (retention) defined as: $k'_{sub} = (t_{R,sub} - t_0)/t_0$; t_0 was determined from the elution time of MeCN–water (7:3, v/v).

[d] Separation factor defined as: $\alpha = k'_{sub}/k'_{ref}$. The values in parentheses represent a corrected separation factor: $\alpha' = (\alpha$ on templated polymer$)/(\alpha$ on reference polymer).

polymer morphology on the ability of L-PA imprinted polymers to resolve enantiomers, high selectivity is promoted by the use of solvents with a low hydrogen bond capacity, by preparing the polymers at low temperature and by increasing the MAA concentration. Such conditions promote the formation of template assemblies. Nevertheless the column efficiency of **P3**–L-PA was superior to that of the columns packed with crushed polymer particles. Thus the numbers of theoretical plates (N) of D- and L-PA obtained were 2000 and 1640/m, respectively. These numbers are about two times higher than the maximum plate number previously observed [8]. As seen in Fig. 3 however, **P5** exhibited a poorer column efficiency possibly related to the column packing procedure. In this context it should be noted that the flow resistance of the columns was small allowing a maximum flow-rate of 5 ml/min to be passed at a back pressure of less than 1000 p.s.i. (see Table 2 for further details).

The polymer particle size, degree of agglomeration and morphology varied with the solvent and monomer concentration used during polymerization (Table 1). Thus a low total monomer concentration (20%, v/v) and polar solvents favoured the formation of agglomerates (10 μm or less) of globular micron-sized particles (Fig. 1) with an estimated particle size range varying between 0.5 and 1 μm in **P4** and between 2 and 4 μm in **P5**. However, at a total monomer concentration of 40% (v/v) (**P1**–L-PA) the polymer was obtained as a continuous block that could not be dispersed in any solvent. Grinding the block resulted in irregular agglomerates of particles of about 0.1 μm and a poor chromatographic performance of the packed column (N_{sub} = 110/m). Likewise the use of MeCN as solvent produced only an ill-defined precipitate impossible to disperse.

In traditional dispersion polymerisations linear polymers are formed and the main role of the solvent is to function as a dispersion medium controlling particle size and dispersity [15,16]. However, in the formation of network polymers

the solvent has an additional role in controlling the morphology of the formed particles or agglomerates. This is reflected in properties such as particle swelling, surface area and porosity. The solvent had a marked influence on the particle morphology in the micro- and mesoporous domains (see Table 1). Polymers prepared using cyclohexanol and dodecanol as solvents (**P2–P4**) can thus be classified as mesoporous with a low surface area and pore volume but with a certain swellability [8]. This differs from the morphology of the polymers prepared using isopropanol–water as solvent (**P5**) which were essentially non-swellable materials with a larger surface area and more than half of the pore volume (total pore volume: 0.1 ml/g) in the microporous domain (<20 Å). An interesting feature is the difference in morphology between templated and reference material. The reason why the bifunctional template PAM gives rise to a material (**P5**–PAM) with a larger surface area (210 m^2/g) than a material (**P5**–BAM) (181 m^2/g) prepared using the monofunctional template BAM is not clear. These observations are in agreement with those made by Dunkin *et al.* [20] in the imprinting of other types of bifunctional templates. It may then be argued that this difference in morphology is the sole origin of the observed selectivity. Thus **P5**–PAM with the higher surface area may contain a larger number of accessible carboxylic acid groups resulting in a stronger retention of PAM. The strongest point against this argument is that the α values were calculated with reference to the retention of BAM. The latter was similar on **P5**–PAM and **P5**–BAM and increased from $k' = 0$ at pH 2 to $k' = 2.9$ at pH 7. Moreover in the enantioselective molecular recognition of L-PA (**P1–P3**–L-PA) the origin of the selectivity is undoubtedly related to substrate binding to imprinted sites [4–8].

In situ preparation of a particulate material with tailor-made affinity for a target substance is thus possible. The use of an aqueous environment during imprinting extends hereby the repertoire of small molecule imprinting to include also templates of low organic phase solubility. The molecular recognition of PAM, a goal in the design of PAM-selective receptors for sensor applications [21], is presently being explored in the development of selective sample enrichment systems for direct drug analysis [22].

Acknowledgements

The author is grateful to the Bank of Sweden Tercentenary Foundation and to the Swedish Natural Science Research Council for financial support. The PAM sample received from Rhone Poulenc Pharma (Helsingborg, Sweden) is gratefully acknowledged. The SEMs were kindly run by Bill Lif (KEBO, Sweden) and Tim Sparrow (Leica, UK).

References

[1] M. Vanderlaan, L.H. Stanker, B.E. Watkins and D.W. Roberts (Editors), *Immunoassays for Trace Chemical Analysis; Monitoring Toxic Chemicals in Humans, Food, and the Environment*, American Chemical Society, Washington, DC, 1991.
[2] P.D.G. Dean, W.S. Johnson and F.A. Middle (Editors), *Affinity Chromatography —A Practical Approach*, IRL Press, Washington, DC, 1985.
[3] G. Wulff, in W.T. Ford (Editor), *Polymeric Reagents and Catalysts* (*ACS Symposium Series*, No. 308), American Chemical Society, Washington, DC, 1986, pp. 186–230.
[4] B. Sellergren, M. Lepistö and K. Mosbach, *J. Am. Chem. Soc.*, 110 (1988) 5853.
[5] M. Lepistö and B. Sellergren, *J. Org. Chem.*, 54 (1989) 6010.
[6] B. Sellergren, *Chirality*, 1 (1989) 63.
[7] L. Fischer, R. Müller, B. Ekberg, L.I. Andersson and K. Mosbach, *J. Am. Chem. Soc.*, 113 (1991) 9358–9360.
[8] B. Sellergren and K.J. Shea, *J. Chromatogr.*, 635 (1993) 31–49.
[9] K.J. Shea, D.A. Spivak and B. Sellergren, *J. Am. Chem. Soc.*, 115 (1993) 3368–3369.
[10] G. Vlatakis, L.I. Andersson, R. Müller and K. Mosbach, *Nature*, 361 (1993) 645–647.
[11] F. Svec and J.M.J. Fréchet, *Anal. Chem.*, 64 (1992) 820–822.
[12] J. Matsui, T. Kato, T. Takeuchi, M. Suzuki, K. Yokoyama, E. Tamiya and I. Karube, *Anal. Chem.*, 65 (1993) 2223–2224.
[13] Poster presented at the *13th International Symposium on HPLC of Peptides, Proteins and Polynucleotides, San Fransisco, CA, November 30–December 3, 1993.*
[14] Patent pending.

[15] M.A. Winnik, R. Lukas, W.F. Chen, P. Furlong and M.D. Croucher, *Makromol. Chem., Macromol. Symp.*, 10/11 (1987) 483–501.
[16] S. Shen, E.D. Sudol and M.S. El-Aasser, *J. Polym. Sci: Part A: Polym. Chem.*, 31 (1993) 1393–1402.
[17] S. Hjertén, *J. Chromatogr.*, 646 (1993) 121–128.
[18] R.R. Tidwell, S.K. Jones, J.D. Geratz, K.A. Ohemeng, M. Cory and J.E. Hall, *J. Med. Chem.*, 33 (1990) 1252–1257.
[19] E. Fan, S.A. Van Arman, S. Kincaid and A.D. Hamilton, *J. Am. Chem. Soc.*, 115 (1993) 369–370.
[20] I.R. Dunkin, J. Lenfeld and D.C. Sherrington, *Polymer*, 34 (1993) 77–84.
[21] T.W. Bell and V.J. Santora, *J. Am. Chem. Soc.*, 114 (1992) 8300–8302.
[22] B. Sellergren, *Anal. Chem.*, in press.

ELSEVIER

Journal of Chromatography A, 673 (1994) 142–146

JOURNAL OF CHROMATOGRAPHY A

Short Communication

High-speed counter-current chromatographic separation of biflavanoids from *Garcinia kola* seeds☆

Govind J. Kapadia*, Babajide Oguntimein, Yogendra N. Shukla

Department of Medicinal Chemistry, College of Pharmacy and Pharmacal Sciences, Howard University, Washington, DC 20059, USA

(First received November 10th, 1993; revised manuscript received March 8th, 1994)

Abstract

Garcinia kola Heckel (Guttiferae) known in commerce as "bitter kola" is used extensively in Nigeria and Ghana for the treatment of coughs, mouth infection, liver disorders and antidote for arrow poisons. In our studies extracts of seed displayed appreciable activity against several selected microorganisms. To identify the antimicrobial compounds and study other biological effects of *G. kola* and its constituents, we have separated the constituents of the ethyl acetate extract of defatted seeds by high-speed counter-current chromatography. Using this technique with the solvent system *n*-hexane–ethyl acetate–methanol–water (1:4:2.5:2.5, upper phase as the stationary phase and the lower phase as the mobile phase), the ethyl acetate extract provided seven products. Four of these have been characterized as 3–8 linked biflavanoids, kolaflavanone, GB-1, GB-1a and GB-2 by spectral data.

1. Introduction

Garcinia kola Heckel (Guttiferae) commercially known as "bitter kola" is used extensively in the West African traditional medicine for the treatment of various diseases. It is served in Nigerian homes to guests as adjunct to the true kola nuts. The plant is used for the treatment of liver disorders, coughs, mouth infections and also as aphrodisiac, antidiarrheal and antidysentric [1]. Earlier phytochemical work on the various parts of this plant has resulted in the isolation of some flavanoids [1], triterpenoids, biflavanoids [2,3] and polyisoprenyl benzophenone [4].

Kolaviron, a fraction of defatted methanolic extract containing biflavanones of *G. kola* is reported to antagonize lethal poisoning in mice with phalloidin [5]. This fraction and its two compounds, GB-1 and GB-2, have also been shown to have antihepatotoxicity activity in mice in rendering them protection against carbon tetrachloride, galactosamine, α-amanitin and phalloidin [6]. The pharmacological and biological activities of biflavanones have been reviewed in 1986 [7]. Thereafter, kolaviron fraction has been shown to have antidiabetic activity in rabbits and aldose reductase activity in rats [8].

In our work the extracts of the seeds showed appreciable antimicrobial activity against *Bacillus subtilis*, *Mycobacterium intracellulare*, *Staphylococcus aureus* and *Cryptococcus neoformans*

* Corresponding author.

☆ This work was presented at the *34th Annual Meeting of the American Society of Pharmacognosy, San Diego, CA, July 18–22, 1993.*

0021-9673/94/$07.00
SSDI 0021-9673(94)00249-9

[9]. To identify the antimicrobial compounds and study other biological effects of *G. kola* and its constituents, we have separated the constituents of the ethyl acetate extract of defatted seeds by high-speed counter-current chromatography (HSCCC). HSCCC is proving to be a very mild but powerful technique which is useful on both the analytical and preparative scale. Using this method, most of the separations are completed within several hours and because no solid support is used in the column, loaded samples are totally recovered without loss or inactivation caused by solid supports [10].

In the work herein reported, as shown in Fig. 1, seven compounds were separated and were designated as GKE-1, -2, -3, -4, -5, -6 and -7. GKE-1, -2 and -3 remain to be identified. GKE-4, -5, -6 and -7 were identified as the biflavanoids GB-2, kolaflavanone, GB-1 and GB-1a (Fig. 2), respectively, by the interpretation of their spectral data [^{1}H and ^{13}C NMR, electron impact (EI) MS and fast atom bombardment (FAB) MS]. This is the first report of the separation of these biflavanoids by HSCCC.

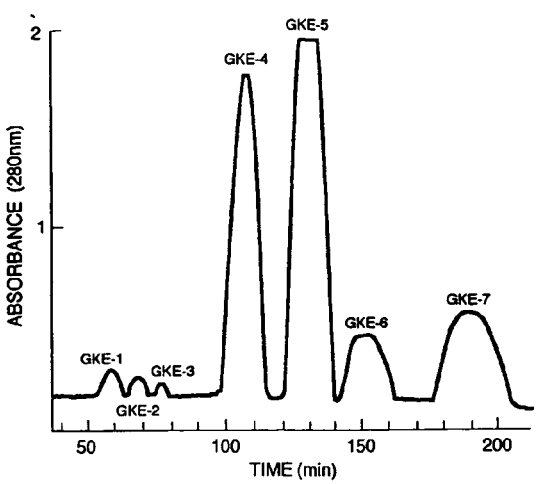

Fig. 1. Chromatogram of the ethyl acetate fraction of defatted *G. kola* seed extract using the upper phase of *n*-hexane–EtOAc–MeOH–water (1:4:2.5:2.5) mixture as the stationary and the lower phase as the mobile phase. GKE-1, GKE-2 and GKE-3 are unidentified compounds, GKE-4 is identified as the biflavanoid GB-2, GKE-5 as kolaflavanone, GKE-6 as GB-1 and GKE-7 as GB-1a.

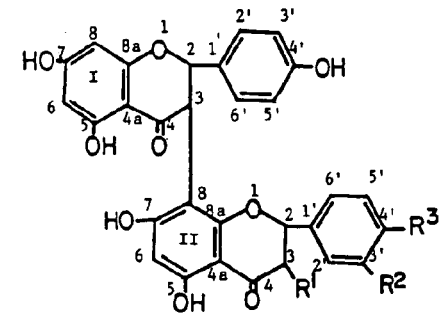

	R1	R2	R3
GB-1	OH	H	OH
GB-2	OH	OH	OH
GB-1a	H	H	OH
Kolaflavanone	OH	OH	OMe

Fig. 2. Biflavanoids separated by HSCCC from the ethyl acetate extract of defatted seeds of *G. kola*.

2. Experimental

2.1. General experimental procedures

IR spectra were determined in KBr on a Perkin-Elmer 2811B spectrometer. UV spectra were measured in MeOH on a Perkin-Elmer Lambda 3B UV–Vis spectrophotometer. ^{1}H and ^{13}C NMR spectra were taken in [$^2H_6$]dimethyl sulfoxide with tetramethylsilane as an internal standard on a Varian XL-300 spectrometer (^{1}H at 300 MHz and 75 MHz for ^{13}C). EI-MS spectra were measured at 70 eV on a Finnigan MAT-95. FAB-MS spectra were recorded on a VG7070E-HF spectrometer using Xe gas at 8 kV and *m*-nitrobenzyl alcohol as matrix. HSCCC was performed on high-speed counter chromatograph CCC-2000 with multilayer coil planet centrifuge (Pharma-Tech Research, Baltimore, MD, USA). Total capacity of the column was 260 ml, I.D. 1.6 mm. Revolution was 1400 rpm with a flow-

rate of 1 ml/min. Compounds were detected by a Shimadzu SPD-6A UV detector (Columbia, MD, USA) at 280 nm and each run consisted of 100 mg of the ethyl acetate extract from which the biflavanoids were separated and characterized.

2.2. Plant material

The seeds of *G. kola* were bought from a local market at Ife, Nigeria, and were identified by Mr. S.A. Adesakin, Department of Pharmacognosy, Olafemi Awolowo University. Voucher specimens were deposited in the herbarium of the Faculty of Pharmacy, Obafemi Awolowo University, Nigeria.

2.3. Extraction and isolation

Dried and powdered seeds (1.067 kg) were defatted with light petroleum (b.p. 35–60°C). The extract was divided into light petroleum-soluble (6.65 g) and 95% methanol-soluble (6.95 g) fractions. The defatted seeds were extracted with CH_2Cl_2 (35 g), followed by extraction with 95% EtOH. The EtOH extract was concentrated under reduced pressure to 100 ml and 100 ml water were added. The aqueous mixture was extracted with ethyl acetate (3 × 100 ml) which was evaporated to dryness to yield the ethyl acetate-soluble fraction (22.82 g). This fraction was extracted with *n*-BuOH to provide, on removing the solvent, 9.63 g *n*-BuOH fraction. Although biflavanoids were detected in the CH_2Cl_2 and ethyl acetate fractions, in the present study only the ethyl acetate extract was fractionated by HSCCC.

2.4. HSCCC of ethyl acetate fraction

The solvent used for HSCCC comprised of *n*-hexane–EtOAc–MeOH–water (1:4:2.5:2.5). The lower phase was used as the mobile phase. For chromatography, the ethyl acetate fraction was dissolved in the mobile phase (1 ml). As shown in Fig. 1 seven peaks were observed. On pooling the solutions under each of the seven peaks and evaporation of the solvents, the products obtained were: GKE-1 (14 mg), GKE-2 (8 mg), GKE-3 (6 mg), GKE-4 (11 mg), GKE-5 (42 mg), GKE- 6 (5 mg) and GKE-7 (7 mg).

2.5. GKE-4 (GB-2)

t_R 108 min; IR: 3340, 1634, 1515, 1280, 1179, 1090, 837 cm^{-1}; FAB-MS: *m/z* 575 $[M+H]^+$, 573 $[M-H]$, $C_{30}H_{22}O_{12}$; EI-MS: M^+ absent, 556, 430, 296, 270, 126, 123, 107; ^1H NMR:(300 MHz) Part I δ 5.41 (1H, d, J = 12 Hz, H-2), 4.39 (1H, d, J = 12 Hz, H-3), 5.82 (1H, d, J = 2 Hz, H-6), 5.76 (1H, d, J = 2 Hz, H-8), 7.03 (2H, d, J = 8 Hz, H-2′, 6′), 6.54 (2H, d, J = 8 Hz, H-3′,5′) 12.0 (1H, s, chelated OH), Part II δ 4.73 (1H, d, J = 12 Hz, H-2), 3.93 (1H, d, J = 11 Hz, H-3), 5.84 (1H, s, H-6), 6.80 (1H, d, J = 2 Hz, H-2′), 6.84 (1H, d, J = 8 Hz, H-5′), 6.70 (1H, d, J = 8 Hz, H-6′), 11.5 (1H, s, chelated OH); ^{13}C NMR; Part I δ 79.6 (C-2), 45.2 (C-3), 194.5 (C-4), 105.7 (C-4a), 160.2 (C-5), 97.5 (C-6), 160.7 (C-7), 96.6 (C-8), 162.7 (C-8a), 125.9 (C-1′), 126.9 (C-2′,6′), 115.8 (C-3′,5′), 155.7 (C-4′), Part II δ 80.8 (C-2), 70.0 (C-3), 195.5 (C-4), 106.0 (C-4a), 161.7 (C-5), 97.8 (C-6), 164.6 (C-7), 101.2 (C-8), 164.4 (C-8a), 126.1 (C-1′), 118.4(C- 2′,5′), 142.8 (C-3′), 143.6(C-4′), 124.4 (C-6′).

2.6. GKE-5 (Kolaflavanone)

t_R 130 min; IR: 3360, 1640, 1520, 1280, 1170, 1091, 840 cm^{-1}; UV: 292, 329 nm; FAB-MS: *m/z* 589 $[M+H]^+$, 587 $[M-H]$, $C_{31}H_{24}O_{12}$; EI-MS: M^+ absent, 570, 444, 296, 270, 137, 126, 107; ^1H NMR: Part I δ 5.50 (1H, d, J = 12 Hz, H-2), 4.49 (1H, d, J = 12 Hz, H-3), 5.82 (1H, d, J = 2 Hz, H-6), 5.76 (1H, d, J = 2 Hz, H-8), 7.03 (2H, d, J = 8 Hz, H-2′,6′), 6.65 (2H, d, J = 8 Hz, H-3′,5′), 11.90 (1H, s, chelated OH), Part II δ 4.90 (1H, d, J = 12 Hz, H-2), 4.04 (1H, d, J = 12 Hz, H-3), 5.84 (1H, s, H-6), 6.81 (1H, d, J = 2 Hz, H-2′), 6.83 (1H, d, J = 8 Hz, H-5′), 6.71 (1H, d, J = 8 Hz, H-6′), 11.5 (1H, s, chelated OH), 3.73 (3H, s, OMe); ^{13}C NMR: Part I δ 82.7 (C-2), 47.3 (C-3), 197.4 (C-4),

105.5 (C-4a), 166.4 (C-5), 101.3 (C-6), 164.6 (C-7), 101.8 (C-8), 163.7 (C-8a, 129.8 (C-1'), 128.8 (C-2',6'), 114.8 (C-3',5'), 157.7 (C-4'), Part II δ 82.7 (C-2), 70.1 (C-3), 196.5 (C-4), 106.0 (C-4a), 163.1 (C-5), 97.8 (C-6), 162.7 (C-7), 105.7 (C-8), 162.4 (C-8a), 126.7 (C-1'), 111.8 (C-2'), 140.5 (C-3'), 146.2 (C-4'), 114.8 (C-5'), 128.8 (C-6'), 55.6 (OMe).

2.7. GKE-6 (GB-1)

t_R 152 min; IR: 3360, 1638, 1520, 1270, 1170, 1091, 838 cm^{-1}; UV: 293, 328 nm; FAB-MS: m/z 559 $[M+H]^+$, 557 $[M-H]$, $C_{30}H_{22}O_{11}$; EI-MS: M^+ absent, 540, 414, 296, 270, 126, 107; ^1H NMR: Part I δ 5.38 (1H, d, J = 12 Hz, H-2), 4.38 (1H, d, J = 12 Hz, H-3), 5.76 (1H, d, J = 2 Hz, H-6), 5.72 (1H, d, J = 2 Hz, H-8), 7.02(2H, d, J = 8 Hz, H-2',6'), 6.54 (2H, d, J = 8 Hz, H-3',5'), 12.1 (1H, s, chelated OH), Part II δ 4.86 (1H, d, J = 12 Hz, H-2), 3.98 (1H, d, J = 12 Hz, H-3), 5.80 (1H, s, H-6), 7.0 (2H, d, J = 8 Hz, H-2',6'), 6.68 (2H, d, J = 12 Hz, H-3',5'), 11.7 (1H s, chelated OH); ^{13}C NMR: Part I δ 80.0 (C-2), 47.3 (C-3), 196.4 (C-4), 104.0 (C-4a), 164.5 (C-5), 97.5 (C-6), 163.0 (C-7), 98.5 (C-8), 165.0 (C-8a), 128.0 (C-1'), 126.5 (C-2',6'), 116.0 (C- 3',5'), 158.0 (C-4'), Part II δ 80.0 (C-2), 70.2 (C-3), 196.8 (C-4), 105.5 (C-4a), 164.0 (C-5), 97.8 (C-6), 164.0 (C-7), 102.0 (C-8), 165.5 (C-8a), 128.0 (C-1'), 128.5 (C-2',6'), 115.1 (C-3',5'), 158.0 (C-4').

2.8. GKE-7 (GB-1a)

t_R 189 min; IR: 3350, 1640, 1520, 1168, 1092, 838 cm^{-1}; FAB-MS: m/z 543 $[M+H]^+$, 541 $[M-H]$, $C_{30}H_{22}O_{10}$; ^1H NMR: Part I δ 5.42 (1H, d, J = 12 Hz, H-2), 5.18 (1H, d, J = 12 Hz,H-3), 5.82 (1H, d, J = 2 Hz, H-6), 5.71 (1H, d, J = 2 Hz, H-8), 7.03 (2H, d, J = 8 Hz, H-2',6'), 6.65 (2H, d, J = 8 Hz, H-3',5'), 12.5 (1H, s, chelated OH), Part II δ 5.29 (1H,d, J = 12 Hz, H-2), 2.56 (2H, m, H-3), 5.76 (1H, s, H-6), 7.20 (2H, d, J = 8 Hz, C-2',6'), 6.70 (2H, d, J = 8 Hz, C-3',5'), 11.50 (1H, s, chelated OH); ^{13}C NMR: Part I δ 78.3 (C-2), 47.4 (C-3), 195.9 (C-4), 105.7 (C-4a), 162.2 (C-5), 97.5 (C-6), 162.7 (C-7), 96.6 (C-8), 164.8 (C-8a), 128.0 (C-1'), 126.6 (C-2',6'), 115.8 (C-3',5'), 157.5 (C-4'), Part II δ 81.3 (C-2), 47.4 (C-3), 196.7 (C-4), 106.0 (C-4a), 163.1 (C-5), 97.8 (C-6), 164.7 (C-7), 105.7 (C-8), 164.9 (C-8a), 128.0 (C-1'), 128.9 (C-2',6'), 115.1 (C-3',5'), 157.5 (C-4').

3. Results and discussion

Seeds of *G. kola* were extracted in sequence with light petroleum, CH_2Cl_2 and 95% ethanol. The ethanol extract was fractionated into ethyl acetate and *n*-BuOH fractions. Biflavanoids detected in CH_2Cl_2 and ethyl acetate fractions were separated in the present study from the ethyl acetate fraction. As shown in Fig. 1, seven products were isolated (GKE-1–GKE-7) from this fraction. The products GKE-1, -2 and -3 consisted of unidentified compounds. Four biflavanoids present, in GKE-4, -5, -6 and -7, were characterized by spectral analyses as GB-2, kolaflavanone, GB-1 and GB-1a, respectively. Of the four biflavanoids and the other three unidentified products, kolaflavanone was found in the ethyl acetate fraction to be present in the highest amount. Earlier biflavanoid separation of *G. kola* has been reported using droplet countercurrent chromatography and $CHCl_3$–MeOH–water as the solvent system (the more polar layer as the mobile phase [5]. However, separation of three products, GB-1, GB-2 and kolaflavanone, in unspecified amount was reported. Furthermore, no details concerning the spectral characterization of the compounds was presented.

Acknowledgements

This study was supported by an USAID grant DAN-5053-G-00-1071-00. The authors wish to thank Drs. Y. Ito and R.J. Highet, Laboratory of Biophysical Chemistry, National Heart, Blood and Lung Institute, National Institutes of Health, Bethesda, MD, USA and Dr. Edward Chou, Pharma-Tech Research, Baltimore, MD, USA for helpful discussions.

References

[1] M.M. Iwu and O.A. Igboko, *J. Nat. Prod.*, 45 (1982) 650.
[2] P.J. Cotterill, F. Scheinmann and I.A. Stenhouse, *J. Chem. Soc., Perkin Trans. 1*, (1978) 532–539.
[3] H.D. Locksley, *Fortschr. Chem. Org. Naturst.*, 30 (1973) 207–312.
[4] R.A. Hussain, A.G. Owegby, P. Parimoo and P.G. Waterman, *Planta Med.*, 44 (1982) 78.
[5] M.M. Iwu, *Experientia*, 41 (1985) 699.
[6] M.M. Iwu, O.A.Igboko, U.A. Onwuchekwa and C.O. Okunji, *J. Ethnopharmacol.*, 21 (1987) 1237.
[7] M.M. Iwu, *Prog. Clin. Biol. Res.*, 213 (1986) 485.
[8] M.M. Iwu, O.A. Igboko and M.M. Tempesta, *J. Pharm. Pharmacol.*, 42 (1990) 290.
[9] B. Oguntimein and G.J. Kapadia, unpublished results.
[10] Y. Ito, *Crit. Rev. Anal. Chem.*, 17 (1986) 65–143.

Journal of Chromatography A

Request for Manuscripts

Susumu Honda will edit a special, thematic issue of the *Journal of Chromatography A* entitled

Chromatographic and Electrophoretic Analyses of Carbohydrates

Both reviews and research articles will be included.
Topics such as the following will be covered:

- Gas chromatography and gas chromatography–mass spectrometry of carbohydrates
- Supercritical fluid chromatography of carbohydrates
- Thin-layer chromatography of carbohydrates
- Liquid chromatography of carbohydrates
  - Separations based on various modes including adsorption, hydrophilic interaction, hydrophobic interaction, ion exchange, ligand exchange, size exclusion, bioaffinity, etc.
  - Derivatization
  - Preparative liquid chromatography
  - High-performance liquid chromatography–mass spectrometry
- Electrophoresis of carbohydrates
  - Gel electrophoresis
  - Capillary zone electrophoresis
  - Micellar electrokinetic capillary chromatography
  - Ultrasensitive detection
  - Derivatization
  - Capillary electrophoresis–mass spectrometry
- Chromatography and electrophoresis in glycobiology
  - Release of carbohydrates from glycoconjugates
  - Monosaccharide composition analysis
  - Oligosaccharide mapping
  - Oligosaccharide sequencing
  - Automated analysis of carbohydrates

Potential authors of reviews should contact Roger Giese, Editor, prior to any submission. Address: Mugar Building Rm 122, Northeastern University, Boston, MA 02115, USA; tel.: (+1-617) 373-3227; fax: (+1-617) 373-8720.

The deadline for receipt of submissions is **November 15, 1994**. Manuscripts submitted after this date can still be published in the Journal, but then there is no guarantee that an accepted article will appear in this special, thematic issue. Four copies of the manuscript, citing this issue, should be submitted to the Editorial Office, *Journal of Chromatography A*, P.O. Box 681, NL-1000 AR Amsterdam, The Netherlands. All manuscripts will be reviewed and acceptance will be based on the usual criteria for publishing in the *Journal of Chromatography A*.

Vol. 673, No. 1

Journal of Chromatography A

NEWS SECTION

ANNOUNCEMENT

WORKSHOP ON CHROMATOGRAPHY, ELECTROKINETICS, AND SEPARATIONS IN POROUS MEDIA, GAITHERSBURG, MD, USA, AUGUST 4–5, 1994

The workshop, organized by the National Institute of Standards and Technology, will explore fundamental and practical aspects of separation technologies such as chromatography, electrokinetics and molecular recognition, all in porous media. Particular emphasis will be placed on processes that combine these separate technologies into new and enhanced separation schemes, such as electrochromatography and electrodialysis. Applications of all these technologies to separation of biological molecules, chemical processing and environmental remediation will be explored

Invited speakers have been selected according to their area of expertise in both applied and fundamental topics relevant to separations. The applied topics were chosen based on high potential for practical use, while the fundamental topics were chosen on wide applicability.

The workshop objectives are:

- to promote technological progress in chromatography, electrokinetic and other separation processes;
- to identify industrial needs in these areas, particularly where the application of chromatography, electrokinetic phenomena, molecular recognition, or other techniques to a specific problem may have significant impact.

Workshop sessions are designed for scientists and engineers with interest in biological separations, chemical processing and environmental remediation

A poster session, open to all participants, but focused on industrial applications and needs, will be held on Thursday, August 4.

Location: The conference will be held at National Institute of Standards and Technology (NIST), Administration Building, Green Auditorium, in Gaithersburg, MD. NIST is about 25 miles northwest of Washington, DC.

Registration: Registration will begin at 8.00 a.m. August 4, The registration fee of $160 covers conference materials, coffee break, lunch and a banquet. The conference registration does not include your hotel reservation. For pre-registration, the registration form must be mailed to NIST, Office of the Comptroller, or faxed to Tammie Grice (address, see below)

Accommodation: A block of rooms (rates US$ 70

single or double + 15% taxes, if booked before July 8, 1994) has been reserved at the Gaithersburg Hilton, 620 Perry Parkway, Gaithersburg, MD 20877; telephone: (301) 977-8900.

Program

Thursday, August 4

8.00 a.m.	Registration and Coffee
8.45 a.m.	Opening Remarks
9.00 a.m.	An Overview of Industrial Chromatographic Separations (G. Sofer)
9.50 a.m.	Macrotransport Theory of Chromatographic Separation (H. Brenner)
10.40 a.m.	Coffee break
11.00 a.m	Design of Chromatographic Separations (E.N. Lightfoot)
11.50 a.m.	Large Scale Chromatographic Separations of Proteins (S.R. Rudge)
12.45 p.m.	Lunch
2.00 p.m.	Discussion on Chromatographic Separations
2.50 p.m.	Fundamentals of Electrokinetic Phenomena (D.A. Saville)
3.40 p.m.	Optimization of Buffers for Electrokinetics Separations (M. Bier)
4.30 p.m.	Poster Session and Reception
7.00 p.m.	Banquet

Friday, August 5

9.00 a.m.	Electrochromatographic Separations (M.R. Ladisch)
9.50 a.m.	Electrodialysis Separation Processes (H. Strathmann)
10.40 a.m.	Coffee Break
11.00 a.m.	Molecular Recognition and Bioseparations (I. Chaiken)
11.50 a.m.	Environmental Applications of Electrokinetic Phenomena (R.F. Probstein)
12.45 p.m.	Lunch
1.45 p.m.	Discussion on Electrokinetics and Molecular Recognition
2.30 p.m.	Closing Remarks
2.40 p.m.	End

For technical information contact Dr. Heribeto Cabezas, Jr., Dr. Kenneth D. Cole or Dr. Joseph B. Hubbard at NIST, Bldg. 222, Rm A353, Gaithersburg, MD 20899-0001, USA. Telephone: (301) 975-4265, Fax: (301) 330-3447. For registration questions contact Tammie Grice, NIST, Bldg. 101, Rm B116, Gaitherburg, MD 20899-0001, USA. Telephone: (301) 975-3883, Fax: (301) 948-2067

PUBLICATION SCHEDULE FOR THE 1994 SUBSCRIPTION

Journal of Chromatography A and *Journal of Chromatography B: Biomedical Applications*

MONTH	1993	J	F	M	A	M	J	
Journal of Chromatography A	652–657	658/1 658/2 659/1 659/2	660/1 + 2 661/1 + 2 662/1 662/2	663/1 663/2 664/1	664/2 665/1 665/2 666/1 + 2 667/1 + 2	668/1 668/2 669/1 + 2	670/1 + 2 671/1 + 2 672/1	The publication schedule for further issues will be published later.
Bibliography Section				681/1			681/2	
Journal of Chromatography B: Biomedical Applications		652/1	652/2 653/1	653/2 654/1	654/2 655/1	655/2	656/1 656/2	

INFORMATION FOR AUTHORS

(Detailed *Instructions to Authors* were published in *J. Chromatogr. A*, Vol. 657, pp. 463–469. A free reprint can be obtained by application to the publisher, Elsevier Science B.V., P.O. Box 330, 1000 AH Amsterdam, Netherlands.)

Types of Contributions. The following types of papers are published: Regular research papers (full-length papers), Review articles, Short Communications and Discussions. Short Communications are usually descriptions of short investigations, or they can report minor technical improvements of previously published procedures; they reflect the same quality of research as full-length papers, but should preferably not exceed five printed pages. Discussions (one or two pages) should explain, amplify, correct or otherwise comment substantively upon an article recently published in the journal. For Review articles, see inside front cover under Submission of Papers.

Submission. Every paper must be accompanied by a letter from the senior author, stating that he/she is submitting the paper for publication in the *Journal of Chromatography A* or *B*.

Manuscripts. Manuscripts should be typed in **double spacing** on consecutively numbered pages of uniform size. The manuscript should be preceded by a sheet of manuscript paper carrying the title of the paper and the name and full postal address of the person to whom the proofs are to be sent. As a rule, papers should be divided into sections, headed by a caption (*e.g.*, Abstract, Introduction, Experimental, Results, Discussion, etc.). All illustrations, photographs, tables, etc., should be on separate sheets.

Abstract. All articles should have an abstract of 50–100 words which clearly and briefly indicates what is new, different and significant. No references should be given.

Introduction. Every paper must have a concise introduction mentioning what has been done before on the topic described, and stating clearly what is new in the paper now submitted.

Experimental conditions should preferably be given on a *separate* sheet, headed "Conditions". These conditions will, if appropriate, be printed in a block, directly following the heading "Experimental".

Illustrations. The figures should be submitted in a form suitable for reproduction, drawn in Indian ink on drawing or tracing paper. Each illustration should have a caption, all the *captions* being typed (with double spacing) together on a *separate sheet*. If structures are given in the text, the original drawings should be provided. Coloured illustrations are reproduced at the author's expense, the cost being determined by the number of pages and by the number of colours needed. The written permission of the author and publisher must be obtained for the use of any figure already published. Its source must be indicated in the legend.

References. References should be numbered in the order in which they are cited in the text, and listed in numerical sequence on a separate sheet at the end of the article. Please check a recent issue for the layout of the reference list. Abbreviations for the titles of journals should follow the system used by *Chemical Abstracts*. Articles not yet published should be given as "in press" (journal should be specified), "submitted for publication" (journal should be specified), "in preparation" or "personal communication".

Vols. 1–651 of the *Journal of Chromatography*; *Journal of Chromatography, Biomedical Applications* and *Journal of Chromatography, Symposium Volumes* should be cited as *J. Chromatogr.* From Vol. 652 on, *Journal of Chromatography A* (incl. Symposium Volumes) should be cited as *J. Chromatogr. A* and *Journal of Chromatography B: Biomedical Applications* as *J. Chromatogr. B*.

Dispatch. Before sending the manuscript to the Editor please check that the envelope contains four copies of the paper complete with references, captions and figures. One of the sets of figures must be the originals suitable for direct reproduction. Please also ensure that permission to publish has been obtained from your institute.

Proofs. One set of proofs will be sent to the author to be carefully checked for printer's errors. Corrections must be restricted to instances in which the proof is at variance with the manuscript.

Reprints. Fifty reprints will be supplied free of charge. Additional reprints can be ordered by the authors. An order form containing price quotations will be sent to the authors together with the proofs of their article.

Advertisements. The Editors of the journal accept no responsibility for the contents of the advertisements. Advertisement rates are available on request. Advertising orders and enquiries can be sent to the Advertising Manager, Elsevier Science B.V., Advertising Department, P.O. Box 211, 1000 AE Amsterdam, Netherlands; courier shipments to: Van de Sande Bakhuyzen-straat 4, 1061 AG Amsterdam, Netherlands; Tel. (+31-20) 515 3220/515 3222, Telefax (+31-20) 6833 041, Telex 16479 els vi nl. *UK*: T.G. Scott & Son Ltd., Tim Blake, Portland House, 21 Narborough Road, Cosby, Leics. LE9 5TA, UK; Tel. (+44-533) 753 333, Telefax (+44-533) 750 522. *USA and Canada*: Weston Media Associates, Daniel S. Lipner, P.O. Box 1110, Greens Farms, CT 06436-1110, USA; Tel. (+1-203) 261 2500, Telefax (+1-203) 261 0101.

0021-9673(19940701)673:1;1-V